THE DEVELOPMENT OF CONTROLLED POLYMERIZATION PROCESSES AND THEIR APPLICATION TOWARDS THE SYNTHESIS OF TAILOR-MADE MATERIALS

A Dissertation

Presented to the Faculty of the Graduate School

of Cornell University

In Partial Fulfillment of the Requirements for the Degree of

Doctor of Philosophy

by

Veronika Kottisch

December 2019

THE DEVELOPMENT OF CONTROLLED POLYMERIZATION PROCESSES AND THEIR APPLICATION TOWARDS THE SYNTHESIS OF TAILOR-MADE MATERIALS

Veronika Kottisch, Ph.D.

Cornell University 2019

Abstract

Over the last century, synthetic polymers have become highly abundant in everyday life and have therefore drastically changed the way we live. Due to the need for intricate polymer architectures in high-end applications, polymer chemists are posed with the challenge of developing new methods of synthesizing polymers. Specifically, mild polymerization conditions have become increasingly important and the potential to regulate chain growth via external stimuli has recently become a powerful tool for the development of well-defined polymers. Herein, we describe the development of a photocontrolled cationic polymerizations of vinyl ethers (chapter 2 and 5). This method employs unique chain-transfer agents that have the ability to switch between cationic and radical intermediates. We were therefore able to combine our photocontrolled cationic polymerization with photocontrolled radical polymerization in one pot and mediate the two polymerization mechanisms with different light sources to produce vinyl ether-acrylate copolymers (chapter 3). Using a single-electron oxidant rather than photoredox chemistry to mediate cationic polymerization,

allowed us to gain absolute control over polymerization mechanism by switching between chemical and photochemical stimuli (chapter 4).

Additionally, we describe the development of a novel, organic acid-mediated cationic polymerization, which proceeds under ambient atmosphere while maintaining excellent control. This simple, single-component system enables the polymerization of a large suite of vinyl ethers without the need for rigorous purification or inert atmosphere (chapter 6).

Lastly, we take advantage of the living characteristics of anionic polymerization of styrene and create skewed molecular weight distributions (MWD) through temporally-regulated initiation. We demonstrate that the shape of the MWD has a profound influence on material properties by measuring the Young's Modulus of poly(styrene-*block*-isoprene) samples with altered polystyrene MWDs (chapter 7).

BIOGRAPHICAL SKETCH

Veronika Kottisch was born in Cologne, Germany, in 1993. She attended the Paul-Klee-Gymnasium in Overath, Germany, and received her Abitur (German high school diploma) in 2012. She went on to study chemistry at Jacobs University Bremen and graduated with a Bachelor of Science in 2015. Following this, Veronika moved to Ithaca, NY, to pursue her graduate studies at Cornell University. In the laboratory of Professor Brett Fors, she worked on photocontrolled cationic and radical polymerizations and their application to stimuli-controlled copolymer synthesis. Additionally, she developed a novel cationic polymerization using bench-stable organic acids under mild conditions and utilized anionic polymerization to tailor the molecular weight distribution of polystyrene. In December 2019, Veronika will continue her journey as a postdoc in Boston at the Massachusetts Institute of Technology in the laboratory of Professor Stephen Buchwald.

ACKNOWLEDGMENTS

Throughout my high school education, I always dreamt about pursuing my higher education in the US. For the fact that this has become reality, I have some people to thank.

First and foremost, I would like to thank my parents, Petra and Frank Kottisch. I would have never been able to make it this far without their support throughout high school, my undergraduate studies at Jacobs University, and my Ph.D. at Cornell University. They have always believed in me and my abilities and, more often than not, also told me that it is okay to take a break. They always listened to me when I was panicking over a B+ or had a hard time writing an essay. To this date, despite being more than 6000 kilometers away, my parents are available if I need vent about my failed experiments or if I just need to talk. So once again, vielen, vielen Dank, Mama und Papa!

I was always interested in STEM education and if it was for my dad, I probably would have gone into mathematics, but it really was a fantastic high school teacher who inspired me to study chemistry: Dr. Daniel Schiffbauer, thank you for sparking my curiosity and love for chemistry.

Additionally, I would like to thank my professors, lecturers, and graduate student mentors at Jacobs University Bremen for a great undergraduate education in the classroom and lab. The three years of undergraduate studies were some of the most stressful years of my education, but a wonderful group

of friends made every day worth it. Thank you, and I am so very glad that we are still in contact up to today.

After my time in Bremen, I moved to Ithaca, NY, and decided to join the lab of Professor Brett Fors, who was just starting his second year at Cornell University. Therefore, the lab was small, and I was the first female graduate student. I am very thankful for having had the opportunity to shape a lab environment and culture. I have learned so much throughout graduate school and I owe this largely to Brett and his great mentorship. Thank you for your continued support, for creating such a positive atmosphere in the lab, and for giving me the freedom to explore my own project ideas (even if they did not work out). Thank you for always being understanding, empathetic, and believing in my abilities. I know that I made the right decision about joining your lab.

I would also like to thank the whole Fors group, former and current grad students and postdocs. Dillon, thanks for being a great lab and office mate; I always enjoyed our talks. Quentin, my European mate, thank you for teaching me some valuable lab and writing skills. Jacob, Parker, and Brian, your idiosyncrasies were always able to brighten up a day in lab. Erin, you are fantastic researcher and I am glad that I was able to work with you. I believe that you will do incredible things in your independent career. Liz, we have only spent a few months together in lab, but it's been a lot of fun and I feel like we have known each other for much longer. I am sure you will be a fantastic PI.

I have also made some very valuable friendships during graduate school and every single one was important. Specifically, I would like to thank Aran

Hubbell and Arianna Gagnon. Your friendship, support, and advice throughout graduate school has been invaluable and I can't thank you enough for always being there for me.

I would also like to thank my committee Professor Dave Collum and Geoffrey Coates and collaborator Professor Tristan Lambert for their great ideas, experiment suggestions, and support.

TABLE OF CONTENTS

LIST OF FIGURES AND SCHEMES

LIST OF TABLES

PREFACE

This thesis was largely adapted from the following published articles co-written by the author:

Chapter 1 was reprinted with permission from: Michaudel, Q.; Kottisch, V.; Fors, B. P. Cationic Polymerization: From Photoinitiation to Photocontrol. *Angew. Chem. Int. Ed.* **2017**, *56*, 9670. © 2017 Wiley-VCH Verlag GmbH & Co. KGaA, Weinheim.

Chapter 2 was reprinted with permission from: Kottisch, V.; Michaudel, Q.; Fors, B. P. Cationic Polymerization of Vinyl Ethers Controlled by Visible Light. *J. Am. Chem. Soc.* **2016**, *138*, 15535. © 2016 American Chemical Society

Chapter 3 was reprinted with permission from: Kottisch, V.; Michaudel, Q.; Fors, B. P. Photocontrolled Interconversion of Cationic and Radical Polymerizations. *J. Am. Chem. Soc.* **2017**, *139*, 10665. © 2017 American Chemical Society

Chapter 4 was reprinted with permission from: Peterson, B. M.; Kottisch, V.; Supej, M. J.; Fors, B.P. On Demand Switching of Polymerization Mechanism and Monomer Selectivity with Orthogonal Stimuli. *ACS Cent. Sci.* **2018**, *4*, 1228. Link: https://pubs.acs.org/doi/10.1021/acscentsci.8b00401

CHAPTER 1

CATIONIC POLYMERIZATION: FROM PHOTOINITIATION TO PHOTOCONTROL

1.1 Abstract

During the last 40 years, researchers investigating photoinitiated cationic polymerizations have delivered tremendous success in both industrial and academic settings. A myriad of photoinitiating systems have been developed, thus allowing polymerization of a broad array of monomers (e.g., epoxides, vinyl ethers, alkenes, cyclic ethers, and lactones) under practical, inexpensive, and environmentally benign conditions. More recently, owing to progress in photoredox catalysis, photocontrolled cationic polymerization has emerged as a means to precisely regulate polymer chain growth. This review provides a concise historical perspective on cationic polymerization induced by light and discusses the latest advances in both photoinitiated and photocontrolled processes. The latter are exciting new directions for the field that will likely impact industries ranging from micro-patterning to the synthesis of complex biomaterials and sequence-controlled polymers.

1.2 Introduction

With the development of living chain-growth polymerizations came the unprecedented ability to design polymers with complex molecular compositions and three-dimensional architectures. Living processes such as ionic, radical, ring-opening metathesis, and chain-walking coordination polymerizations have

afforded well-defined polymers with predictable molar mass (M_n), narrow dispersity ($Đ$), and functional chain-ends. This ever-expanding synthetic toolbox has enabled the preparation of macromolecules with structures that slowly but steadily approach the intricacy of biopolymers such as proteins and DNA. In the pursuit of emulating nature, one of the next key challenges is the control of polymer chain growth by external stimuli.[1,2] Among the stimuli being explored (e.g. , mechanical, electrochemical), light boasts several inherent advantages: it is inexpensive, green, and non-invasive.[1] Light also confers both temporal and spatial control, and can potentially act as an actual on/off switch for polymerization.[1,2]

Using light as a stimulus for polymerization is not a new strategy. Several decades of research have led to the discovery of almost countless photoinitiated processes.[3] Applications for these techniques encompass conventional industries such as coating, inks, and adhesives as well as high-end technologies including photolithography, laser imaging, and biomaterials.[4] Photoinitiation (also called photoinduction) relies on the activation of either a photoinitiator or photoinitiating system through light irradiation. The excited species then initiates the radical or ionic polymerization (Figure 1.1 a). As expected, once irradiation has started, the practitioner has no control over chain growth. A complementary approach based on reversible initiation and termination regulated by light has recently emerged. In this approach, control over chain growth is mediated by periods of light (activation) and dark (deactivation), and the rate of

polymerization can be controlled by the intensity of the light (Figure 1.1 b). Several strategies have been pursued in the development of such systems, including photoactivation of the polymer chain-end, the monomer, or a catalyst.[1] A major breakthrough occurred with the application of photoredox catalysis, a process which has enabled the development of a number of elegant photocontrolled polymerizations.[5–8] However, photocontrolled polymerizations have largely been limited to radical processes[5–7] and have only recently been implemented in cationic reactions. The success of photoinitiated cationic polymerizations provided a glimpse into the outcomes which may result from gaining full control over cationic chain growth with light. In a short span, a diverse set of mechanistically distinct cationic polymerizations regulated by light were uncovered and applied to a vast array of monomers.[9–11] This review highlights how research on photoinitiated cationic polymerizations has impacted polymer science and set the stage for the discovery of photocontrolled cationic polymerizations. Cationic processes are exciting new directions in photocontrolled polymerization and should find many applications, as well as allow the synthesis of high-value macromolecules with defined sequences and architectures.

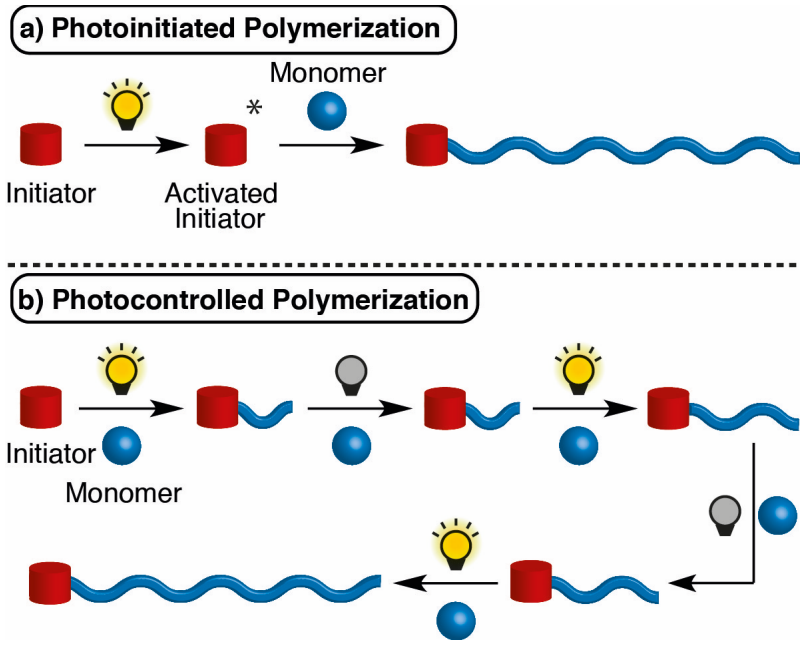

Figure 1.1. Schematic depiction of a) photoinitiated and b) photocontrolled polymerizations.

1.3 Photoinitiated Cationic Polymerizations

Direct Initiation with Onium Salts

Reactions that rely on photoinitiation have garnered much interest in the polymer community owing in part to the pressing needs of the coating industry.[12] Early efforts focused on the photoinitiation of radical polymerizations, as very few cationic photoinitiators were known. However, the high oxygen sensitivity of radical polymerizations made large-scale implementation cost prohibitive. The discovery of onium salt cationic photoinitiators (Figure 1.2) in the early 1970s by Crivello and others opened new avenues of research,[13] and photoinitiated cationic polymerizations were indeed found to be rapid, tolerant of ambient oxygen and water, and applicable to a wide variety of monomers.[12–16] Virtually all cationic polymerizations, including those of alkenes, epoxides, lactones, and

oxazolines, can be photoinitiated by onium salts.[12] Dozens of onium initiators have been synthesized and studied, and the relationship between cation structure and the photophysical properties of these compounds is well documented.[12]

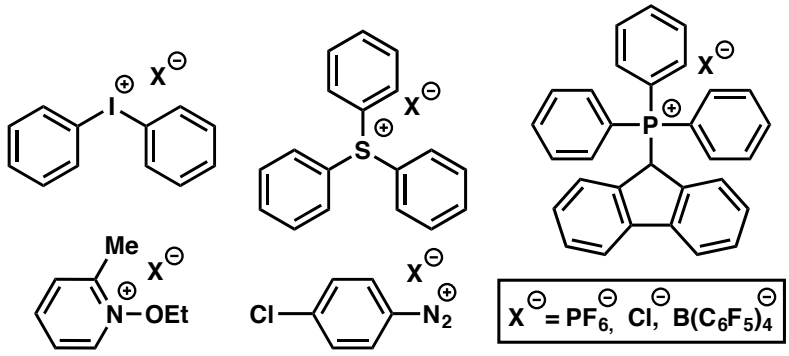

Figure 1.2. Common onium salts used for photoinitiated cationic polymerization. A few representative anions are shown.

A typical mechanism of onium salt photoinitiation is shown in Figure 1.3. Upon UV irradiation, diphenyliodonium undergoes either homo- or heterolytic cleavage, thus generating a radical cation/aryl radical pair or an aryl cation, respectively. These highly reactive species can initiate radical or cationic polymerization directly, but generally react further with hydrogen donors such as the solvent, monomer, or impurities to give rise to Brønsted acids, which in turn initiate the polymerization.[12]

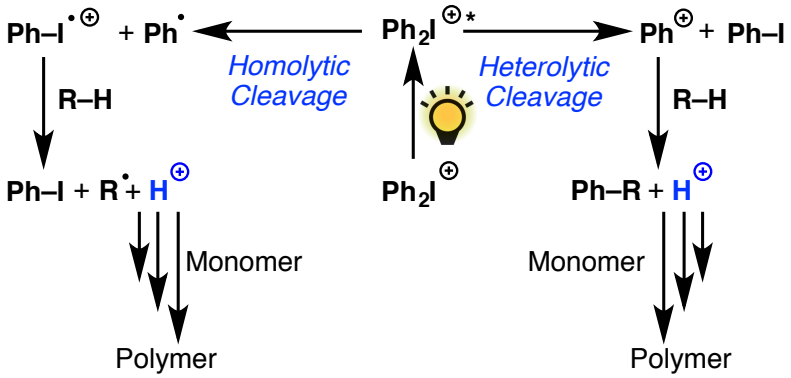

Figure 1.3. Mechanism of direct activation of onium salts with light.

This robust transformation remains key in various industrial processes, particularly for those in which a spatially controlled initiation is required, including the UV curing of epoxy resins and silicones, stereolithography, and synthesis of photoresists for microcircuits.[12] Although originally developed for specific industrial applications, cationic polymerization initiated by the irradiation of onium salts achieved universal success and is now a textbook methodology.[17]

Multicomponent Photoinitiating System: Photosensitizers and Free Radicals

Direct photolysis of onium salts requires high-energy UV light, which introduces safety concerns and increases costs because of its higher energy consumption and the need for expensive reaction plants. These limitations were recognized early,[18] and various strategies have been devised to adapt the approaches to use near-UV and even visible light. Several reviews have covered these topics exhaustively,[3,19–24] and only a few representative

examples are discussed herein. A common way to achieve softer irradiations in chemical reactions is to use photosensitizing dyes that absorb in the near UV/visible region. Upon excitation, these dyes activate onium initiators by energy transfer,[25] and then induce the fragmentation cascade and cationic polymerization depicted in Figure 1.3.[18,26] However, efficient photosensitizers with desirable solubility profiles remain to be identified.[27] Therefore, free-radical-promoted cationic photopolymerization has emerged as an enticing strategy which circumvents some of these issues.[3,19–24,27] In these reactions, free radicals arise from the irradiation of a photoinitiator (with or without a photosensitizer) by two pathways: direct homolytic bond cleavage for type I photoinitiators or hydrogen abstraction (or photoinduced electron transfer [PET]) with an adequate donor species for type II photoinitiators. An example of a type I photoinitiating system is shown in Figure 1.4.[28–30] The photolysis of the benzoin **1** produces the benzoyl radical **2** and radical **3**. The latter likely undergoes oxidation from diphenyliodonium, and leads to the formation of the cation **4** to initiate the polymerization of various monomers, such as the ring-opening polymerization of cyclohexene oxide (**5**).[30]

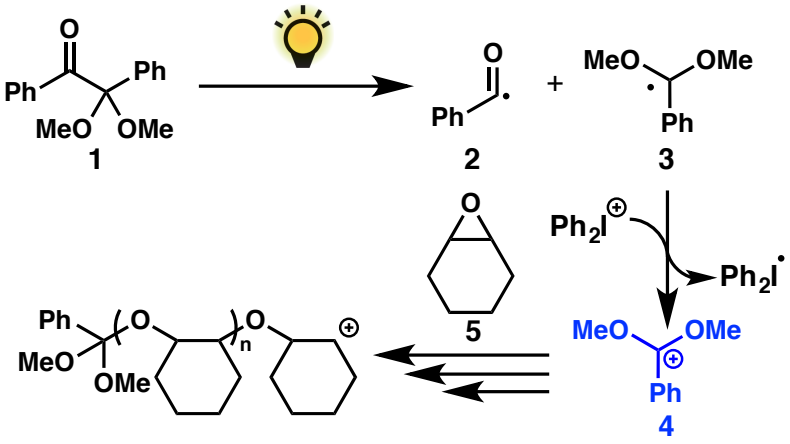

Figure 1.4. Mechanism of free-radical-promoted cationic polymerization using the type I photoinitiator **1**.

As demonstrated by Yagci and co-workers, the thioxanthone derivative **6** acts as a typical type II initiator (Figure 1.5).[31] Excited **6*** engages in a hydrogen abstraction reaction with either ethanol or tetrahydrofuran (THF). The resulting ketyl radical (**7**) undergoes oxidation followed by the loss of a proton, a process concomitant with the regeneration of **6**. Then, the acid-catalyzed polymerization of either **5**, isobutyl vinyl ether (IBVE; **9**), or *N*-vinylcarbazole takes place with modest to high conversion depending on the monomer.

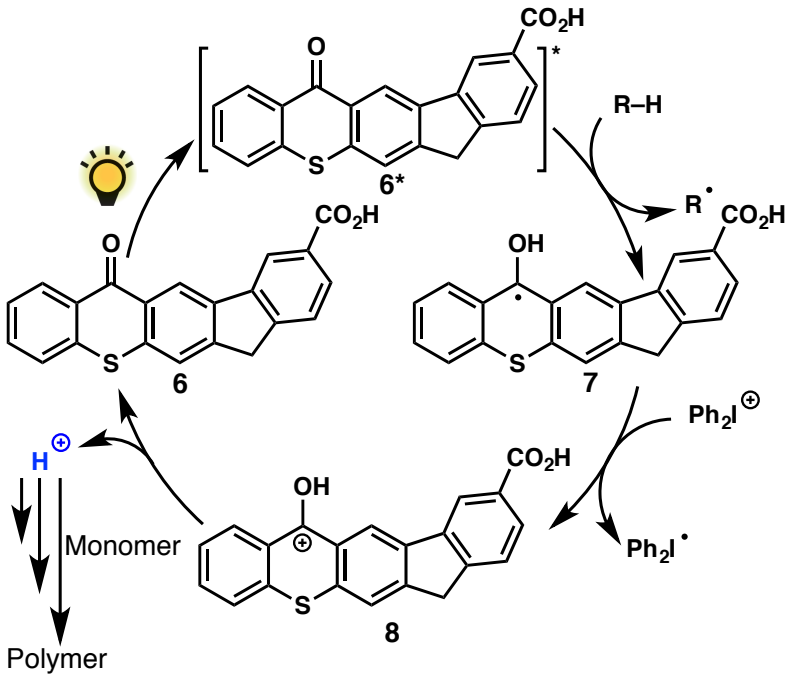

Figure 1.5. Mechanism of free-radical-promoted cationic polymerization using the type II photoinitiator **6** and hydrogen-donating additives.

Many multicomponent photoinitiating systems based on a variety of photoactive and radical species have been developed. Recently, Lalevée, Fouassier, and co-workers[23,32–39] pioneered the use of photoredox catalysis to promote cationic polymerizations in which the photosensitizer is regenerated and can therefore be used at very low loading. In this vein, an elegant three-component system comprising a photocatalyst, a silane co-initiator, and diphenyliodonium was designed for cationic polymerization (Figure 1.6). Oxidative quenching of the photocatalyst by diphenyliodonium leads to the formation of both iodobenzene and a phenyl radical which can abstract a hydrogen from the silane. The oxidation of the newly created silyl radical by either diphenyliodonium or the oxidized photocatalyst delivers a silylium species

while turning over the photocatalyst. Polymerization is then triggered by the silylium species. Numerous transition-metal or organic photocatalysts have demonstrated competency in this photoinitiating system (Figure 1.7), and this wealth of options has fostered the emergence of systems with specific photophysical and chemical properties.[36] Specifically, some ruthenium[32] and iridium[33] complexes have high molar extinction coefficients in the visible region that allow activation with inexpensive fluorescent light bulbs. Additionally, *N*-vinylcarbazole can be substituted for silanes as the co-initiator.[37]

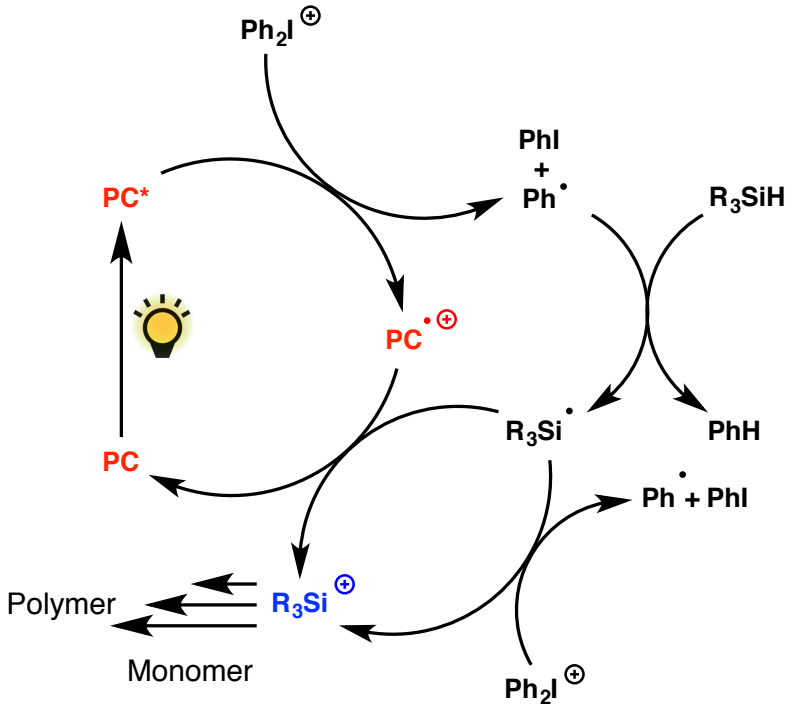

Figure 1.6. General scheme of a three-component photoinitiating system based on silane co-initiators. PC = photocatalyst.

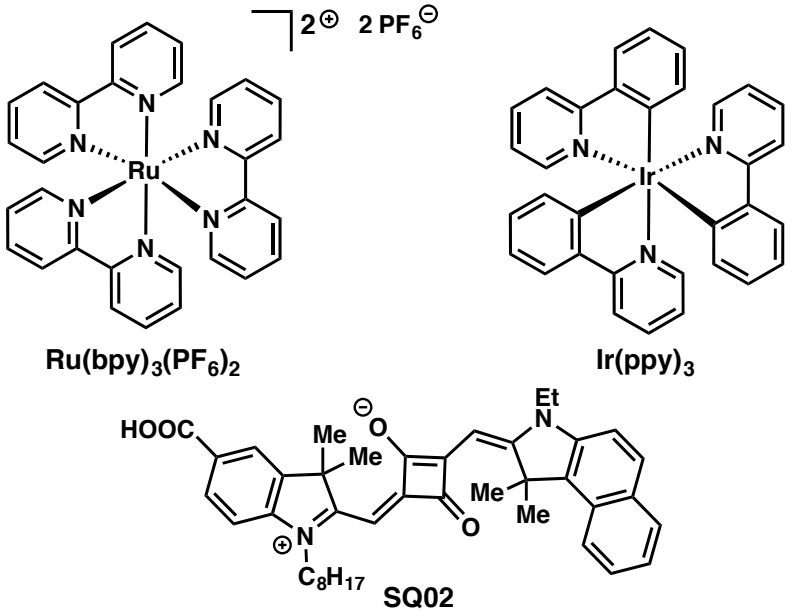

Figure 1.7. Representative transition-metal and organic photocatalysts for three-component photoinitiating systems. bpy = 2,2′-bipyridine, ppy = phenylpyridine.

The development of many ingenious multicomponent photoinitiating systems offers safer, greener, and more energy efficient alternatives to the early photoinitiated cationic polymerizations. Moreover, because both radical and cationic intermediates are generated during these processes, radical and cationic polymerization can be performed concurrently in one vessel.[32,38] Unfortunately, these new methods often suffer from both oxygen inhibition, because of the presence of radical species, and slow polymerization rates. However, several photoredox catalysts have shown improved kinetics and low oxygen sensitivity, particularly when combined with silanes which can act as oxygen scavengers.[27,34,39] These observations should serve as a blueprint for future photoinitiating systems.

Light-Initiated Cationic Polymerizations with Living Characteristics

Chain transfer and termination by nucleophilic attack commonly occur during the cationic polymerization of linear monomers and hamper the development of processes with living characteristics. Lewis acids such as boron[40] or zinc[41] halides have been used with hydrohalic acid initiators to stabilize the propagating carbocations by coordination to the halogen adduct end groups, and thus allows good control over the polymerization. This general strategy has been successfully implemented with various photoinitiated polymerization methodologies.[42–44]

Yagci and co-workers recently reported an alternative living polymerization of vinyl ethers under photoinduction using dimanganese dicarbonyl (Figure 1.8).[45] Under visible-light irradiation (λ = 400–500 nm), $Mn_2(CO)_{10}$ and benzyl bromide produce benzyl radicals through homolytic cleavage of the manganese–manganese bond followed by bromide abstraction. In the presence of diphenyliodonium bromide, benzyl radicals are oxidized to benzyl cations, which can then initiate the polymerization of IBVE (**9**). The authors postulate that nucleophilic attack by the bromide anion deactivates the chain-end, and the combined actions of $Mn_2(CO)_{10}$, Ph_2IBr, and light reactivate the polymerization. Although this process has not been shown to be turned on and off by light, its strategy has the potential to afford photocontrol over polymer chain growth and has laid the groundwork for future discoveries.

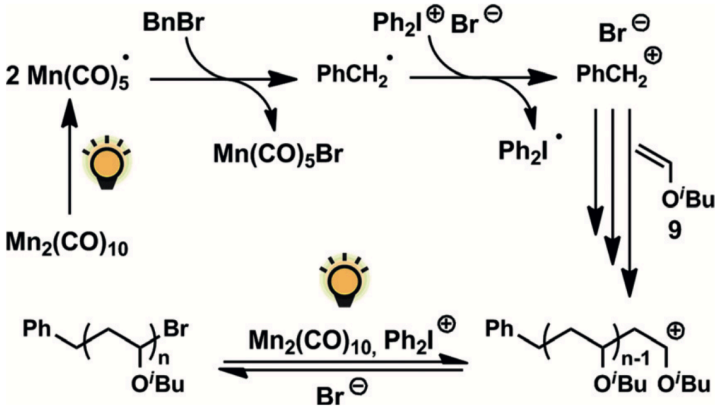

Figure 1.8. Living polymerization by a photoinduced radical oxidation/activation/deactivation mechanism.

While early termination, chain transfer, and backbiting have been observed for ring-opening polymerizations, the cationic ring-opening polymerization (CROP) of cyclic ethers is generally considered living when appropriate temperatures and monomer concentrations are chosen.[46] Living behavior has also been described for the photoinitiated cationic polymerization of lactones by Dove and Barker.[47]

New Modes of Direct Photoinitiation

The vast majority of cationic photoinitiation systems are based on irreversible reduction of onium salts, but a few conceptually different systems have been described recently. For example, Nicewicz and co-workers[48] described an innovative living polymerization of 4-methoxystyrene (**10**) with the photoredox catalyst **11** (Figure 1.9). In combination with methanol, **11** induces the polymerization of **10** using blue LEDs (λ = 450 nm). Methanol proved critical

to obtaining a living system with a narrow *Đ* value (<1.3) and linear growth of M_n with monomer conversion.

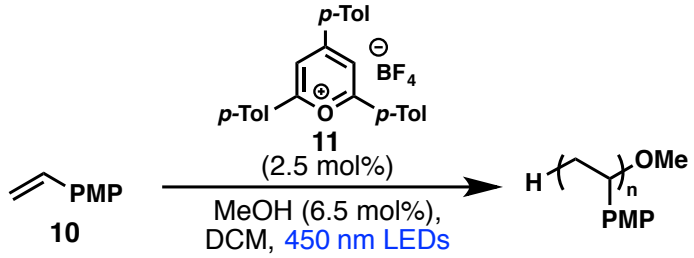

Figure 1.9. Polymerization of 4-methoxystyrene (**10**) initiated by light in the presence of the pyrylium **11**. DCM = dichloromethane, PMP = 4-(OMe)C_6H_4, *p*-Tol = 4-Me-C_6H_4.

The following mechanism was proposed on the basis of experimental data (Figure 1.10). 1) Oxidation of **10** by the excited photocatalyst **11*** forms radical cation **12** and is followed by anti-Markovnikov addition of methanol. The resulting adduct (**13**) protonates a molecule of **10** to initiate chain propagation while 2) the radical **14** is oxidized by **11** to form another reactive cation (**15**). 3) Rapid chain transfer by nucleophilic addition of methanol and protonation of **10** continues until the methanol is completely consumed. The authors hypothesize that control over chain growth is achieved through a process reminiscent of reversible addition-fragmentation chain transfer (RAFT), in which methanol functions as a chain-transfer agent (CTA). 4) The chain shuttle between active and dormant chains occurs through the nucleophilic capture of a propagating cation by a methyl ether end group. Subsequent heterolytic cleavage of the oxygen–carbon bond regenerates both an active and a dormant species.

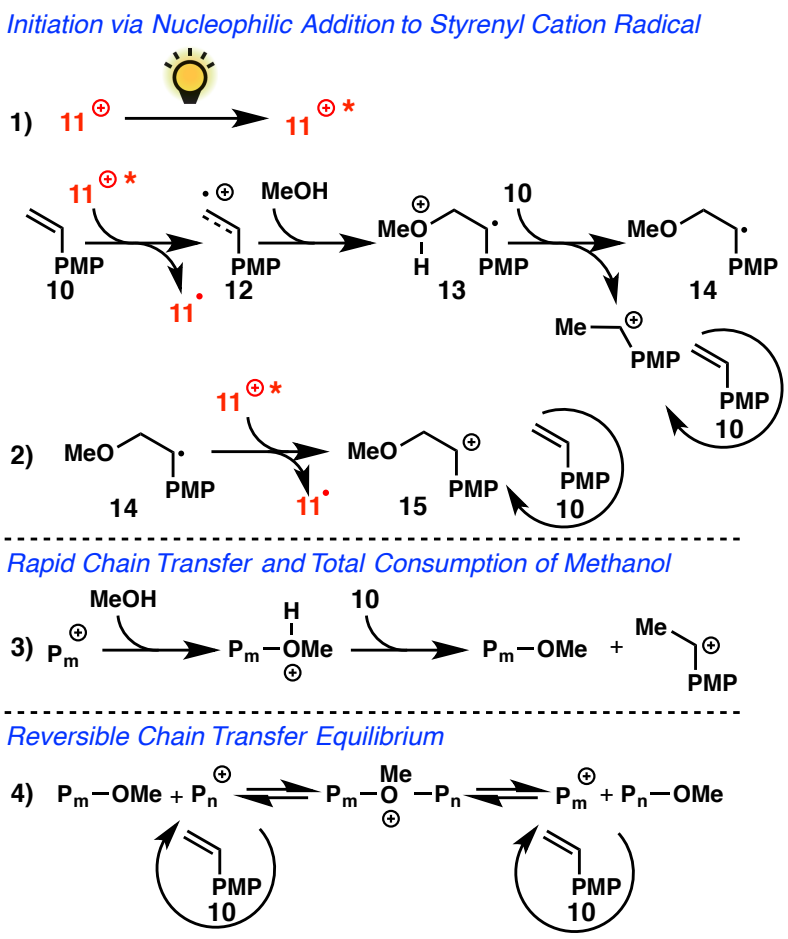

Figure 1.10. Living polymerization of **10** photoinitiated by **11** and methanol. Adapted with permission from Ref. 48 (*J. Am. Chem. Soc*. **2015**, *137*, 7580). Copyright 2017 American Chemical Society.

In a similar approach, Spokoyny and co-workers showcased the polymerization of styrene derivatives (**17**) and isobutylene (**18**) using the fluoroaromatic boron-rich cluster **16** (Figure 1.11).[49] The electron-withdrawing effect of the fluoro-substituted benzyl groups increased the redox potential of the excited state of **16** (E^* vs. SCE = 2.98 V), and enabled direct photooxidation of non-activated styrene monomers (**17**) as well as **18**. Although nonliving, this system is the first example of a photoinitiated polymerization of **18** under metal-

free conditions and is attributable to the extremely high redox potential of the excited cluster. These two complementary systems will pave the way for the development of novel cationic photoinitiation methods beyond the classic use of onium salts.

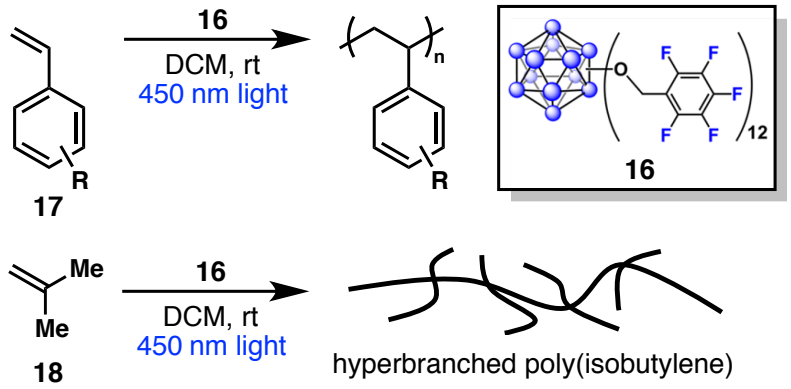

Figure 1.11. Cationic polymerization of styrene derivatives (**17**) or isobutylene (**18**) induced by the aromatic boron-cluster photooxidant **16**. Adapted with permission from Ref. 49 (*J. Am. Chem. Soc*. **2016**, *138*, 6952). Copyright 2017 American Chemical Society.

1.3 Photocontrolled Cationic Polymerizations

Recent developments have enabled cationic polymerization to go beyond photoinitiation and made possible photocontrol over polymer chain growth. This section highlights cationic processes which have explicitly demonstrated the reversible activation and deactivation of polymer chain growth with light.

Photocontrolled Ring-Opening Metathesis Polymerization (ROMP)

Although the previously examined processes developed by the groups of Lalevée,[32,33] Nicewicz,[48] Spokoyny,[49] and Yagci[45] are clear milestones towards

photocontrol, to the best of our knowledge, the ROMP reported by Boydston and co-workers[9] in 2015 is the first example of a truly photocontrolled polymerization with a cationic mechanism. Traditional transition-metal-catalyzed ROMP has enabled the production of well-defined polymers with applications in high-performance plastics,[50] photovoltaics,[51] drug delivery, and biomedical engineering,[52] but it often suffers from metal contamination, which can impair the properties of the materials.[53] In search of a metal-free alternative, Boydston and co-workers designed a ROMP process based on an organocatalyzed photoredox transformation.[9] Inspired by the studies of Chiba on electrochemical [2+2] cycloadditions[54] and the emergence of photocontrolled polymerization,[5–8] they combined the vinyl ether initiator **19**, an organic photocatalyst [2,4,6-tri(4-methoxyphenyl)pyrylium tetrafluoroborate (**20**)], and blue-light irradiation to promote the polymerization of norbornene (**21**), an archetypal ROMP monomer (Figure 1.12a).

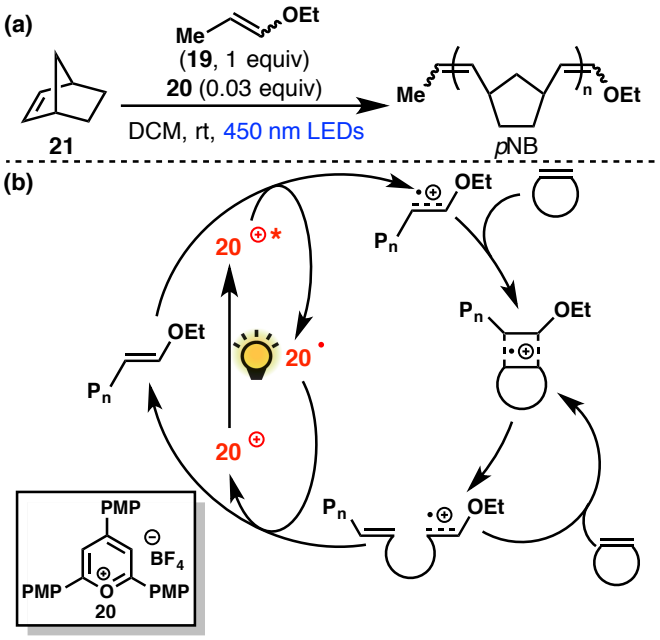

Figure 1.12. Metal-free ring-opening metathesis polymerization (ROMP). a) Polymerization conditions for norbornene (**21**) with the initiator **19** and photocatalyst **20**. b) Postulated catalytic cycle for the photocontrolled ROMP. pNB = poly(norbornene), RT = room temperature.

Although its mechanism differs from that of classic ROMP, this photoredox approach delivers the same types of polymeric structures. The authors propose that reversible single-electron oxidation of the vinyl ether (initiator **19** or polymer chain-end) by the excited photocatalyst **20*** leads to the formation of a highly reactive radical cation (Figure 1.12b). This radical cation end group then undergoes [2+2] cycloaddition with **21** followed by rapid ring opening to extend the polymer chain and regenerate a radical cation. Importantly, the reversibility of the electron transfer between **20** and the vinyl ether group equates to reversible activation/deactivation of the chain-end. The

mechanism provides a “regulation loop” mediated by light and affords photocontrol over chain growth.

A reasonably linear relationship was observed between M_n and monomer conversion, particularly for polymers with high M_n values (ca. 60 kg mol^{-1}). Polymers with narrow $Đ$ values ($1.3 \leq Đ \leq 1.7$) and predictable M_n values can be obtained by manipulating the initiator-to-monomer ratio. As expected from the mechanistic hypothesis, temporal control of polymer chain growth was demonstrated through intermittent exposure of the reactions to visible light. No monomer consumption occurred in the dark (off periods), but the polymerization could be reinitiated by re-exposure to light (Figure 1.13).

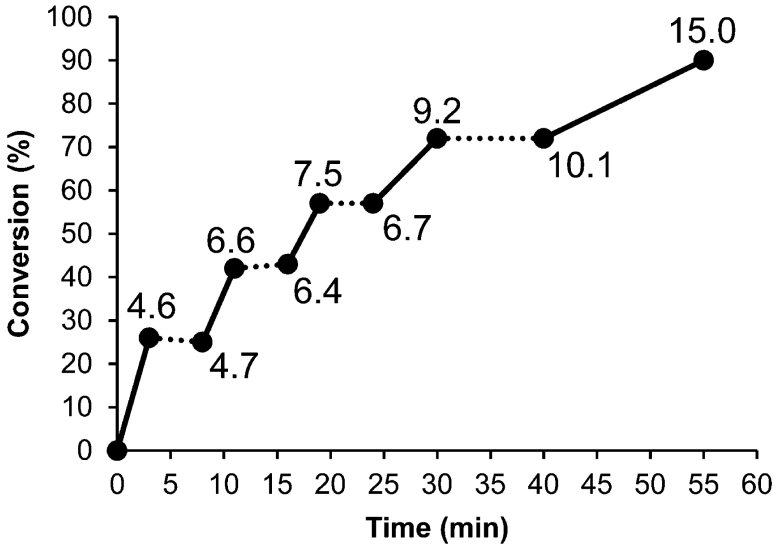

Figure 1.13. Conversion of **21** vs. time while alternating between periods of light exposure (solid lines) and dark (dotted lines). Data point labels indicate molecular weight (M_n; kg mol^{-1}). Adapted with permission from Ref. 9 (*J. Am. Chem. Soc*. **2015**, *137*, 1400). Copyright 2017 American Chemical Society.

The method was expanded to several norbornene derivatives (**22**–**26**), including the polar monomers **23** and **24 a**–**d** (Figure 1.14a).[55] These

functionalized analogues were either homo- or copolymerized with **21**, which should allow for the synthesis of complex polymeric materials. Dicyclopentadiene (DCPD; **27**) also proved susceptible to polymerization under reaction conditions, albeit only for low-M_n polymers (Figure 1.14b). Poly(DCPD) was then successfully crosslinked by thiol-ene chemistry using **28**.

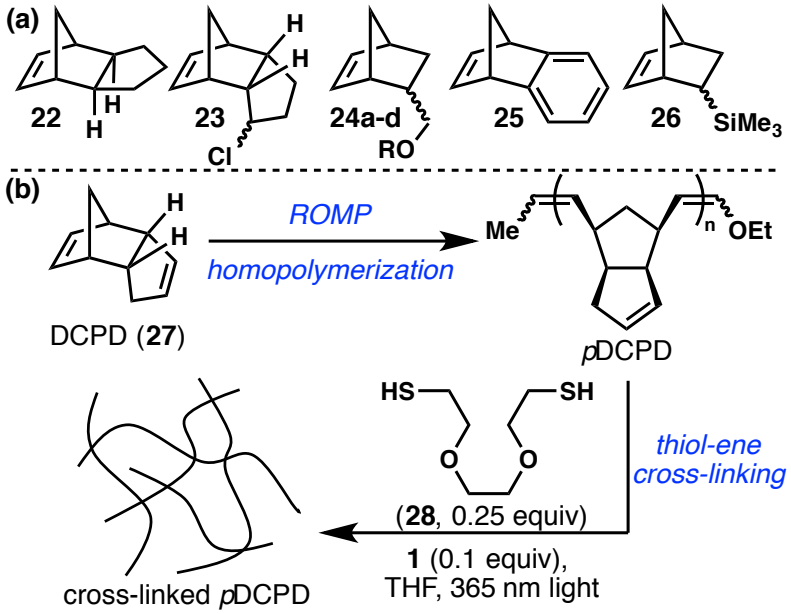

Figure 1.14. Metal-free ROMP with functionalized monomers: a) Library of norbornene derivatives. R = Me, Boc, Piv, or TBS. b) Synthesis of poly(dicyclopentadiene). Boc = *tert*-butyloxycarbonyl, Piv = pivaloyl, TBS = *tert*-butyldimethylsilyl.

An investigation of a small library of photocatalysts (Figure 1.15) showed that compared with **20**, pyryliums with higher excited-state redox potentials showed decreased conversion of **21** (E^* = 1.89 V vs. SCE) and, specifically, triphenylpyrylium tetrafluoroborate (**29**; E^* = 2.46 V vs. SCE) did not yield polymer.[57] On the contrary, 2,4,6-tri-(4-methoxyphenyl)thiopyrylium (**30**) performed slightly better than its oxygen counterpart. To date, few clear correlations between the physical properties of catalysts and the various

features of this polymerization have been identified, and should prompt investigations aimed at improving the overall process.[57] The robust and versatile nature of metal-free ROMP makes it an extraordinarily promising synthetic method for many fields.

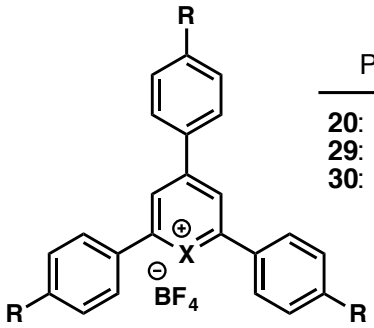

Photocatalysts	E^*_{red} (vs SCE)
20: R = OMe, X = O	1.89 V
29: R = H, X = O	2.46 V
30: R = OMe, X = S	1.86 V

Figure 1.15. Representative examples of the photocatalyst investigation for metal-free ROMP.

Photocontrolled Cationic Polymerization of Vinyl Ethers

As discussed above, the 1970s marked the beginning of an ever-expanding body of work on the photoinitiated polymerization of vinyl ethers.[12,13] Dozens of elegant methods that rely on UV or visible light have been published, and many have found direct industrial applications. However, unlike those for acrylate or styrene derivatives, photocontrolled processes for this family of monomers have been unavailable until recently. The lack of existing living radical homopolymerizations for common vinyl ethers[58] accounts for this discrepancy, as early photocontrolled polymerizations were based on radical mechanisms.[5–7] To overcome this challenge and gain photocontrol in the polymerization of vinyl ethers, Fors and co-workers recently developed a

method which allows for the reversible formation of a propagating cation mediated by visible light.[10]

In 2015, the groups of Kamigaito[59,60] and Sugihara[61] independently reported the cationic RAFT polymerization of vinyl ethers using a combination of unique CTAs and strong acids as initiators. These new methods paved the way for the development of a photocontrolled cationic polymerization. The group of Fors postulated that these CTAs could be oxidized with an appropriate photocatalyst, subsequently yielding a carbocation after mesolytic cleavage, a carbocation which could participate in the RAFT process (Figure 1.16a). Similar mesolytic cleavages, which produce concurrent cation and radical species, have been previously used in small-molecule transformations.[62,63] This hypothesis relied on the inherent reversibility of photomediated cation formation which would allow control of the activation and deactivation of the polymer chain-end by light irradiation. The reduction of the persistent radical would turn over the pyrylium catalyst, whereas the resulting anion would cap the chain-end and generate a dormant species, thus creating a “regulation loop” similar to that of metal-free ROMP.

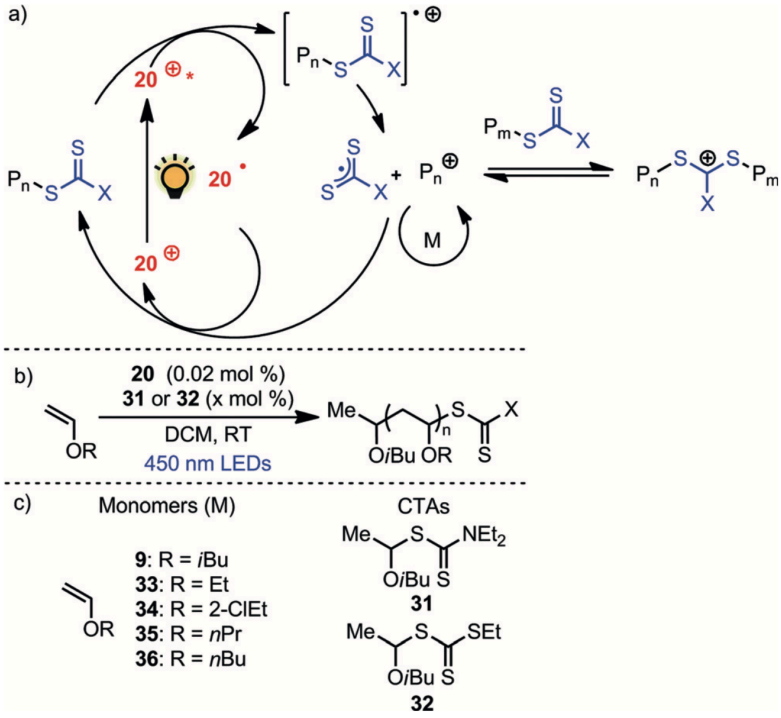

Figure 1.16. Cationic polymerization of vinyl ethers regulated by light: a) mechanism, b) reaction conditions, c) monomers and chain-transfer agents (CTAs).

Indeed, an investigation of oxidizing photocatalysts showed that 2,4,6-tri-(4-methoxyphenyl)pyrylium tetrafluoroborate (**20**) catalyzed the polymerization of **9** under blue LED irradiation (Figure 1.16b). Very low catalyst loading (0.02 mol %) combined with the CTA **31** were required to prepare poly(IBVE) with a narrow *Đ* value. During the reaction, M_n increased linearly as *Đ* steadily decreased, and corroborates a controlled polymerization mechanism. Adjusting the CTA-to-monomer ratio predictively tuned M_n while maintaining low catalyst loading. Several other vinyl ethers (**33**–**36**) were successfully polymerized using CTA **32** (Figure 1.16c), which allowed for higher rates of polymerization while broadening the chain-length distribution only slightly. The high chain-end fidelity

of this chain growth process was further substantiated by chain-extending poly(ethyl vinyl ether) with **9** to yield a poly(EVE-*b*-IBVE) diblock polymer (Figure 1.17).

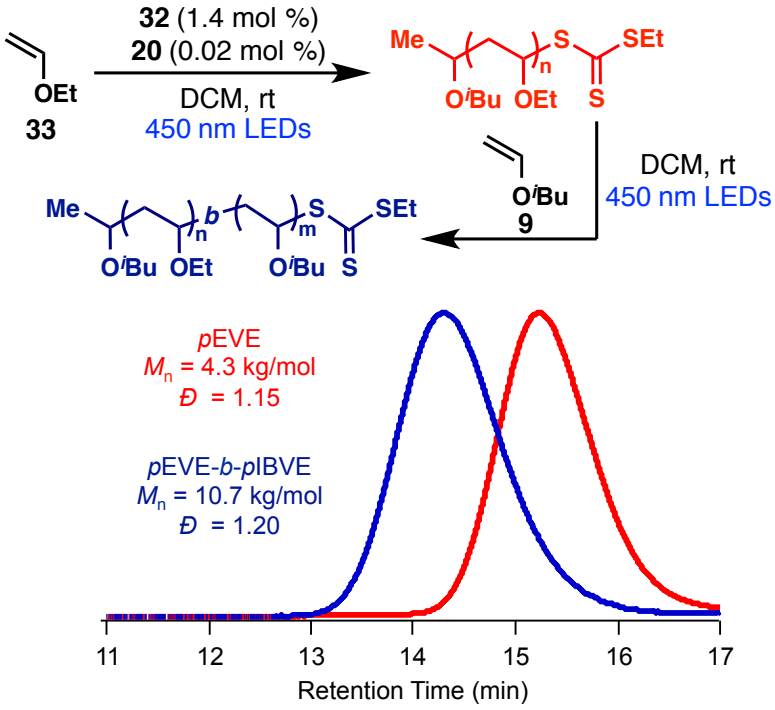

Figure 1.17. Synthesis of poly(ethyl vinyl ether) (pEVE) and poly(ethyl vinyl ether-block-isobutyl vinyl ether) (pEVE-*b*-pIBVE). Adapted with permission from Ref. 10 (*J. Am. Chem. Soc.* **2016**, *138*, 15535). Copyright 2017 American Chemical Society.

The reversibility of this new transformation was probed by halting and restarting chain propagation through alternating periods of light and dark (Figure 1.18a). The system allowed excellent control over chain growth with no conversion of the monomer in the dark. Moreover, it displayed first-order kinetics in light intensity, as shown by determining the initial rates of polymerization for various intensities (Figure 1.18b). This feature indicates the capacity for

spatiotemporal control over polymer chain growth, which holds great promise in patterning applications.

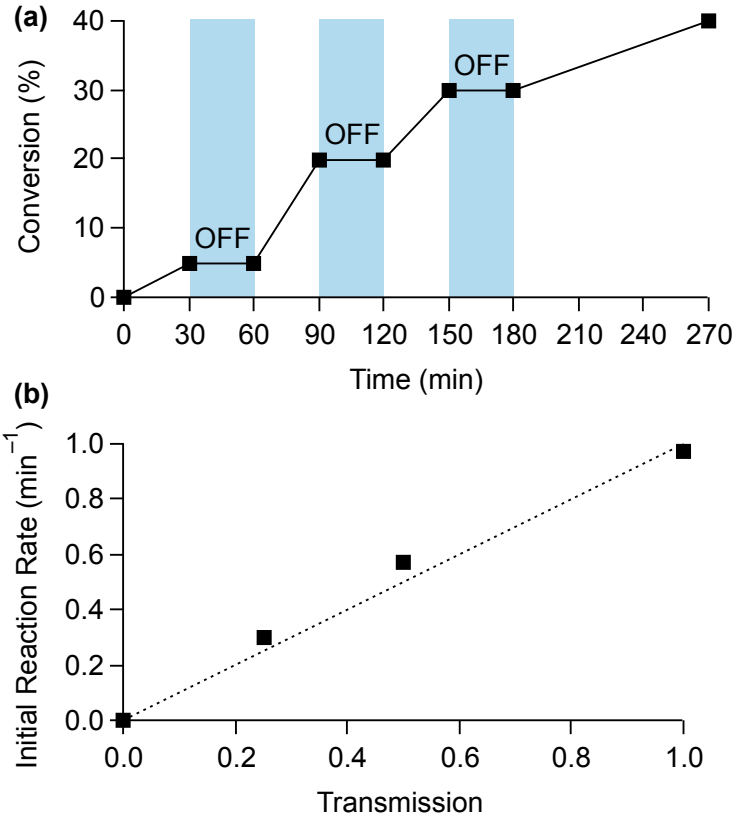

Figure 1.18. Temporal control of polymerization: a) monomer conversion vs. time with intermittent light exposure; b) influence of light intensity on initial reaction rate. Adapted with permission from Ref. 10 (*J. Am. Chem. Soc*. **2016**, *138*, 15535). Copyright 2017 American Chemical Society.

Photocontrolled Cationic Ring Opening of Lactones

Capitalizing on the photochromic properties of merocyanines,[64–66] Boyer and Xu developed a photocontrolled CROP.[11] This redox-neutral approach is, mechanistically speaking, quite different from the two transformations covered above, but it illustrates the diversity in the photocontrolled reactions which can

be designed. After the seminal reports of photoinitiated CROP by Dove and co-workers,[47] the merocyanine-based photoacid (PAH) **37** was used to mediate the polymerization of δ-valerolactone (δ-VL; **38**) and ϵ-caprolactone (ϵ-CL; **39**; Figure 1.19a). Upon blue-light irradiation, alkene isomerization followed by cyclization induces the formation of the dissociated pair PA−/H+. Inversely, **37** adopts the more-stable, open-form PAH in the dark. Thus, **37** can be considered a strong acid under light excitation and a weak acid in the dark. This unique feature was exploited to develop a novel light-regulated CROP for lactones (Figure 1.19 b). With benzyl alcohol as an initiator and **37** (25 mol % relative to BnOH), a typical polymerization of δ-VL (**38**) in propylene carbonate reaches 90 % conversion after 22 hours under blue LEDs. As expected for a controlled system, plots of Mn versus monomer conversion and $\ln([M]_0/[M]_t)$ versus time showed linear relationships. Additionally, experimental M_n values were in good agreement with theoretical M_n values, and a low $Đ$ of 1.14 was measured.

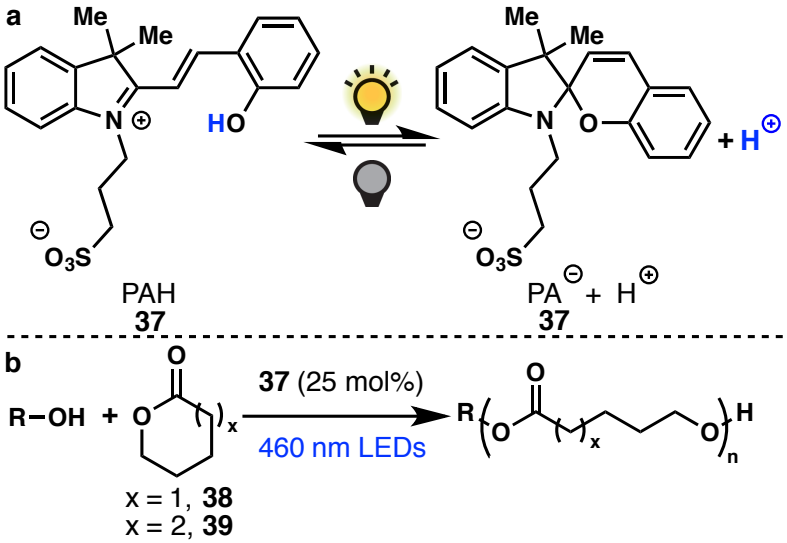

Figure 1.19. a) The photoswitchable acid **37**. b) Cationic ring-opening polymerization of lactones **38** and **39** regulated by light.

The reversibility of the proton release was examined through intermittent cycles of light and dark. Although the rate of dissociation of PAH to PA−/H+ under blue light is fast compared with that of chain propagation (ca. 1 min), the rate of recombination is significantly slower (65 % recombination after 8 h in propylene carbonate). Consequently, the rate of monomer conversion was clearly attenuated in the absence of light. However, dark polymerization could not be fully avoided. Finally, an elegant illustration of the power of photocontrolled polymerization was achieved by coupling this novel CROP with PET-RAFT, a radical process regulated by light. The experimental conditions were judiciously chosen to enable switching between both polymerizations. The hydroxy-containing CTA **40** was selected as a dual initiator and ZnTPP (**41**) as a PET-RAFT photocatalyst with a light-absorption window that differed from that of **37** (Figure 1.20). A mixture of δ-VL (**38**), methylacrylate (MA, **42**),

photocatalysts **37** and **41**, and CTA **40** was irradiated with blue light, thus resulting in the consumption of δ-VL by CROP without MA polymerization. They then observed that upon red-light irradiation, MA polymerization started while the rate of δ-VL consumption slowed. CROP and PET-RAFT were alternated by simply switching the wavelength of the light source. A block copolymer poly(VL-*b*-MA) and a graft copolymer poly(VL-*g*-MA) were synthesized in one pot with this strategy.

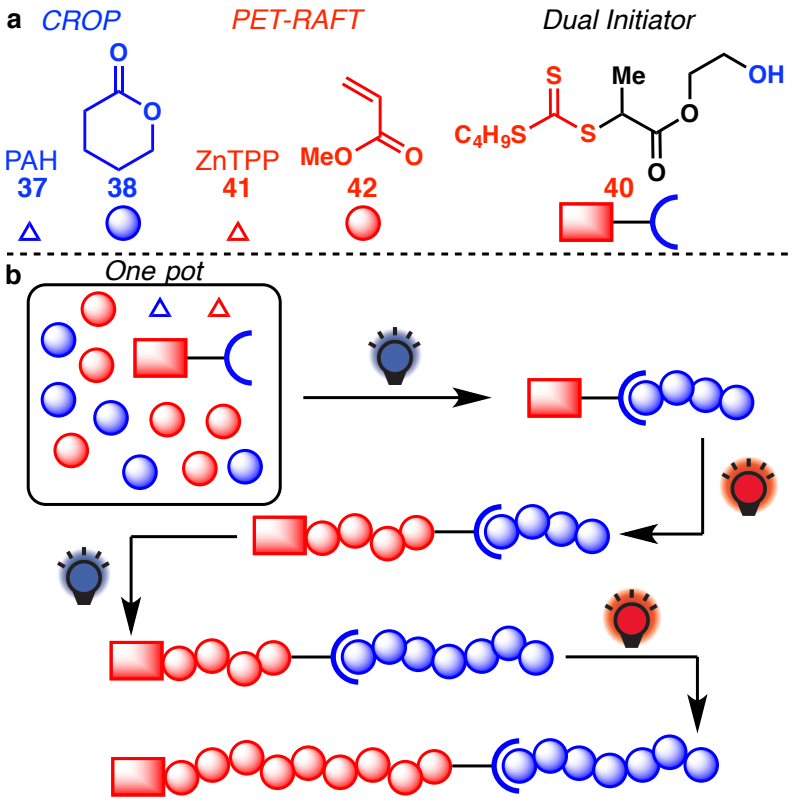

Figure 1.20. Schematic illustration of a dual polymerization system regulated by two different wavelengths of light for the synthesis of poly(δ-valerolactone-*block*-methyl acrylate) block copolymer by alternating blue- and red-light irradiation.

1.4 Conclusion and Outlook

Since its inception four decades ago, photoinduced cationic polymerization has blossomed into a dynamic field with broad influence in both academic and industrial settings. With their milder, greener, and less expensive characteristics, these systems can now trigger the cationic polymerization of either alkene, epoxide, or lactone monomers. The degree of control that can be exerted during these polymerizations has also dramatically increased with the development of living cationic polymerizations and, more recently, photocontrolled polymerizations in which chain growth is directly regulated by light. Although still scarce, such modern methods have already been implemented in three types of polymerizations: ROMP, vinyl ether polymerization, and CROP. To increase the currently limited scope of these photocontrolled cationic processes new methods to reversibly form cations with light are still needed. With that goal in mind, precise understanding of the often complex underlying mechanisms, as well as the careful design of photocatalysts and experimental conditions, will be instrumental in the further development of novel photocontrolled polymerizations. This burgeoning area of research will undoubtedly expand the applications of cationic polymerizations, applications which range from UV curing and three-dimensional printing to the synthesis of highly complex architectures and intricate surface patterning for biomedical and electronic devices.

1.5 References

(1) F. A. Leibfarth, K. M. Mattson, B. P. Fors, H. A. Collins, C. J. Hawker, *Angew. Chem. Int. Ed.* **2013**, *52*, 199; *Angew. Chem.* **2013**, *125*, 210.

(2) A. J. Teator, D. N. Lastovickova, C. W. Bielawski, *Chem. Rev.* **2016**, *116*, 1969.

(3) "Reactivity and Efficiency of Radical Photoinitiators": J.-P. Fouassier, J. Lalevée in Photoinitiators for Polymer Synthesis: Scope, Reactivity and Efficiency, Wiley-VCH, Weinheim, **2012**.

(4) Y. Yagci, S. Jockusch, N. J. Turro, *Macromolecules* **2010**, *43*, 6245.

(5) M. Chen, M. Zhong, J. A. Johnson, *Chem. Rev.* **2016**, *116*, 10167.

(6) N. Corrigan, S. Shanmugam, J. Xu, C. Boyer, *Chem. Soc. Rev.* **2016**, *45*, 6165.

(7) J. T. Trotta, B. P. Fors, *Synlett* **2016**, *27*, 702.

(8) T. G. McKenzie, Q. Fu, M. Uchiyama, K. Satoh, J. Xu, C. Boyer, M. Kamigaito, G. G. Qiao, *Adv. Sci.* **2016**, *3*, 1500394.

(9) K. A. Ogawa, A. E. Goetz, A. J. Boydston, *J. Am. Chem. Soc.* **2015**, *137*, 1400.

(10) V. Kottisch, Q. Michaudel, B. P. Fors, *J. Am. Chem. Soc.* **2016**, *138*, 15535.

(11) C. Fu, J. Xu, C. Boyer, *Chem. Commun.* **2016**, *52*, 7126.

(12) J. V. Crivello, *J. Polym. Sci. Part A* **1999**, *37*, 4241.

(13) J. V. Crivello, J. H. W. Lam, *Macromolecules* **1977**, *10*, 1307.

(14) “The Photoinitiated Cationic Polymerization of Epoxy Resins”: J. V. Crivello, J. H. W. Lam in Epoxy Resin Chemistry, ACS Symposium Series, 114 (Eds.: R. S. Bauer), American Chemical Society, Washington, DC, **1979**.

(15) J. V. Crivello, *Adv. Polym. Sci.* **1984**, *62*, 1.

(16) M. Shirai, M. Tsunooka, *Prog. Polym. Sci.* **1996**, *21*, 1.

(17) “Poly(vinyl ether)s, Poly(vinyl ester)s, Poly(vinyl halogenide)s”: O. Nuyken, H. Braun, J. Crivello in Handbook of Polymer Synthesis, 2nd ed. (Eds.: H. R. Kricheldorf, O. Nuyken, G. Swift), Marcel Dekker, New York, **2004**.

(18) J. V. Crivello, J. H. W. Lam, *J. Polym. Sci. Polym. Chem. Ed.* **1978**, *16*, 2441.

(19) J.-P. Fouassier, F. Morlet-Savary, J. Lalevée, X. Allonas, C. Ley, *Materials* **2010**, *3*, 5130.

(20) M. Sangermano, *Pure Appl. Chem.* **2012**, *84*, 2089.

(21) S. Dadashi-Silab, C. Aydogan, Y. Yagci, *Polym. Chem.* **2015**, *6*, 6595.

(22) “Sensitization of Cationic Photopolymerizations”: J. Crivello in Dyes and Chromophores in Polymer Science (Eds.: J. Lalevée, J.-P. Fouassier), Wiley, Hoboken, **2015**.

(23) P. Xiao, J. Zhang, F. Dumur, M.-A. Tehfe, F. Morlet-Savary, B. Graff, D. Gigmes, J.-P. Fouassier, J. Lalevée, *Prog. Polym. Sci.* **2015**, *41*, 32.

(24) [24] S. Dadashi-Silab, S. Doran, Y. Yagci, *Chem. Rev.* **2016**, *116*, 10212.

(25) Photosensitization can also occur by a PET pathway leading to the generation of cationic species that subsequently initiate polymerization. See Ref. 3, 21–23.

(26) G. Manivannan, J.-P. Fouassier, J. V. Crivello, *J. Polym. Sci. Part A* **1992**, *30*, 1999.

(27) M.-A. Tehfe, F. Louradour, J. Lalevée, J.-P. Fouassier, *Appl. Sci.* **2013**, *3*, 490.

(28) A. Ledwith, *Makromol. Chem.* **1979**, *3*, 348.

(29) Y. Yagci, A. Ledwith, *J. Polym. Sci. Part A* **1988**, *26*, 1911.

(30) M. Degirmenci, Y. Hepuzer, Y. Yagci, *J. Appl. Polym. Sci.* **2002**, *85*, 2389.

(31) G. Yilmaz, S. Beyazit, Y. Yagci, *J. Polym. Sci. Part A* **2011**, *49*,1591.

(32) J. Lalevée, N. Blanchard, M.-A. Tehfe, F. Morlet-Savary, J.-P. Fouassier, *Macromolecules* **2010**, *43*, 10191.

(33) J. Lalevée, N. Blanchard, M.-A. Tehfe, M. Peter, F. Morlet-Savary, J.-P. Fouassier, *Macromol. Rapid Commun.* **2011**, *32*, 917.

(34) J. Lalevée, H. Mokbel, J.-P. Fouassier, *Molecules* **2015**, *20*, 7201.

(35) N. Zivic, M. Bouzrati-Zerelli, A. Kermagoret, F. Dumur, J.-P. Fouassier, D. Gigmes, J. Lalevée, *ChemCatChem* **2016**, *8*, 1617.

(36) F. Dumur, D. Gigmes, J.-P. Fouassier, J. Lalevée, *Acc. Chem. Res.* **2016**, *49*, 1980.

(37) J. Lalevée, M.-A. Tehfe, A. Zein-Fakih, B. Ball, S. Telitel, F. Morlet-Savary, B. Graff, J.-P. Fouassier, *ACS Macro Lett.* **2012**, *1*, 802.

(38) S. Telitel, J. Lalevée, N. Blanchard, T. Kavalli, M.-A. Tehfe, S. Schweizer, F. Morlet-Savary, B. Graff, J.-P. Fouassier, *Macromolecules* **2012**, *45*, 6864.

(39) J. Lalevée, J.-P. Fouassier, *Polym. Chem.* **2011**, *2*, 1107.

(40) R. Faust, J. P. Kennedy, *Polym. Bull.* **1986**, *15*, 317.

(41) M. Sawamoto, C. Okamoto, T. Higashimura, *Macromolecules* **1987**, *20*, 2693.

(42) S. Kwon, H. Chun, S. Mah, *Fibers Polym.* **2004**, *5*, 253.

(43) M. U. Kahveci, Y. Yagci, *Macromolecules* **2011**, *44*, 5569.

(44) M. U. Kahveci, F. Oytun, Y. Yagci, *Polymer* **2013**, *54*, 4798.

(45) M. Ciftci, Y. Yoshikawa, Y. Yagci, *Angew. Chem. Int. Ed.* **2016**, *55*, 519; *Angew. Chem.* **2016**, *128*, 529.

(46) O. Nuyken, S. D. Pask, *Polymer* **2013**, *5*, 361.

(47) I. A. Barker, A. P. Dove, *Chem. Commun.* **2013**, *49*, 1205.

(48) A. J. Perkowski, W. You, D. A. Nicewicz, *J. Am. Chem. Soc.* **2015**, *137*, 7580.

(49) M. S. Messina, J. C. Axtell, Y. Wang, P. Chong, A. I. Wixtrom, K. O. Kirlikovali, B. M. Upton, B. M.; Hunter, O. S. Shafaat, S. I. Khan, J. R. Winkler, H. B. Gray, A. N. Alexandrova, H. D. Maynard, A. M. Spokoyny, J. Am. Chem. Soc. 2016, 138, 6952; Hunter, O. S. Shafaat, S. I. Khan, J. R. Winkler, H. B. Gray, A. N. Alexandrova, H. D. Maynard, A. M. Spokoyny, *J. Am. Chem. Soc.* **2016**, *138*, 6952.

(50) J. C. Mol, *J. Mol. Catal. A* **2004**, *213*, 39.

(51) M. Horie, I.-W. Shen, S. M. Tuladhar, H. Leventis, S. A. Haque, J. Nelson, B. R. Saunders, M. L. Turner, *Polymer* **2010**, *51*, 1541.

(52) S. Sutthasupa, M. Shiotsuki, F. Sanda, *Polym. J.* **2010**, *42*, 905.

(53) K. A. Ogawa, A. E. Goetz, A. J. Boydston, *Synlett* **2016**, *27*, 203.

(54) T. Miura, S. Kim, Y. Kitano, M. Tada, K. Chiba, *Angew. Chem. Int. Ed.* **2006**, *45*, 1461; *Angew. Chem.* **2006**, *118*, 1489.

(55) A. E. Goetz, L. M. M. Pascual, D. G. Dunford, K. A. Ogawa, D. B. Knorr, Jr., A. J. Boydston, *ACS Macro Lett.* **2016**, *5*, 579.

(56) A. E. Goetz, A. J. Boydston, *J. Am. Chem. Soc.* **2015**, *137*, 7572.

(57) L. M. M. Pascual, D. G. Dunford, A. E. Goetz, K. A. Ogawa, A. J. Boydston, *Synlett* **2016**, *27*, 759.

(58) S. Sugihara, Y. Kawamoto, Y. Maeda, *Macromolecules* **2016**, *49*, 1563.

(59) M. Uchiyama, K. Satoh, M. Kamigaito, *Angew. Chem. Int. Ed.* **2015**, *54*, 1924; *Angew. Chem.* **2015**, *127*, 1944.

(60) M. Uchiyama, K. Satoh, M. Kamigaito, *Macromolecules* **2015**, *48*, 5533.

(61) S. Sugihara, N. Konegawa, Y. Maeda, *Macromolecules* **2015**, *48*, 5120.

(62) P. Maslak, J. N. Narvaez, *Angew. Chem. Int. Ed. Engl.* **1990**, *29*, 283; *Angew. Chem.* **1990**, *102*, 302.

(63) Q. Zhu, E. C. Gentry, R. R. Knowles, *Angew. Chem. Int. Ed.* **2016**, *55*, 9969; *Angew. Chem.* **2016**, *128*, 10123.

(64) Z. Shi, P. Peng, D. Strohecker, Y. Liao, *J. Am. Chem. Soc.* **2011**, *133*, 14699.

(65) V. K. Johns, Z. Wang, X. Li, Y. Liao, *J. Phys. Chem. A* **2013**, *117*, 13101.

(66) H. Chen, Y. Liao, *J. Photochem. Photobiol. A* **2015**, *300*, 22.

CHAPTER 2

CATIONIC POLYMERIZATION OF VINYL ETHERS CONTROLLED BY VISIBLE LIGHT

2.1 Abstract

Photoinitiated cationic polymerizations are widely used in industrial processes; however, gaining photocontrol over chain growth would expand the utility of these methods and facilitate the design of novel complex architectures. We report herein a cationic polymerization regulated by visible light. This polymerization proceeds under mild conditions: a combination of a metal-free photocatalyst, a chain-transfer agent, and light irradiation enables the synthesis of various poly(vinyl ether)s with good control over molecular weight and dispersity as well as excellent chain-end fidelity. Significantly, photoreversible cation formation in this system enables efficient control over polymer chain growth with light.

2.2 Introduction

Applications for polymers are constantly expanding, in part because of the increasing degree of control that can be exerted during the synthesis of these complex macromolecules. The recent merging of photoredox chemistry and controlled radical polymerizations has led to the development of novel reactions that produce polymers with precise average molar masses and narrow dispersities ($Đ$) and, most interestingly, afford spatiotemporal control over chain

growth.[1] The implementation of these reactions for patterning has delivered a bottom-up alternative to classic top-down photolithography techniques and has the potential to provide unique polymer architectures.[2] Consequently, it remains highly desirable to broaden the scope of polymerizations that allow photoregulation over chain growth and increase the number of polymeric architectures that can be created with these methods.

The vast majority of the photocontrolled polymerizations developed to date are based on radical processes. Several elegant photocontrolled atom transfer radical polymerizations (ATRP),[3] photoinduced organotellurium-mediated radical polymerizations (TERP),[4] and photoinduced electron transfer reversible addition–fragmentation chain transfer (PET-RAFT)[5] polymerizations have enabled the polymerization of a variety of acrylate, methacrylate, and styrenic derivatives. In a different approach, Boydston and co-workers disclosed a metal-free ring opening metathesis polymerization (ROMP) based on photoredox catalysis.[6] Through light irradiation, these reactions can be turned on or off at will, paving the way for applications requiring spatiotemporal control.

Photocontrolled cationic polymerizations have yet to receive the attention of their radical counterparts despite an impressive body of work on the photoinitiation of cationic transformations. Photoinitiated cationic polymerizations of vinyl ethers and oxiranes are indeed industrially relevant, and such systems commonly rely on the generation of acids or reactive cations through light irradiation.[7] More recently, Nicewicz[8a] and Spokoyny[8b] have separately reported new systems for photoinitiated cationic polymerizations.

However, these methods provide control only over polymer chain initiation, and the regulation of chain growth with light remains a notable challenge. Herein we address this unmet need and report the discovery of a photocontrolled “living” cationic polymerization of vinyl ethers (Scheme 2.1). The ability to form carbocations reversibly in situ with light is the key to achieving photoregulation in cationic polymerizations. In 2015, Kamigaito and co-workers and Sugihara and co-workers independently disclosed controlled cationic RAFT polymerizations that used unique chain-transfer agents (CTAs) initiated with strong acids.[1c,9] We postulated that the oxidation of these CTAs with an appropriate photocatalyst followed by mesolytic cleavage would photoreversibly yield a carbocation that could participate in the RAFT process.[10] Significantly, this reaction would give rise to a “living” cationic polymerization process in which chain growth is regulated by light (Scheme 2.1).

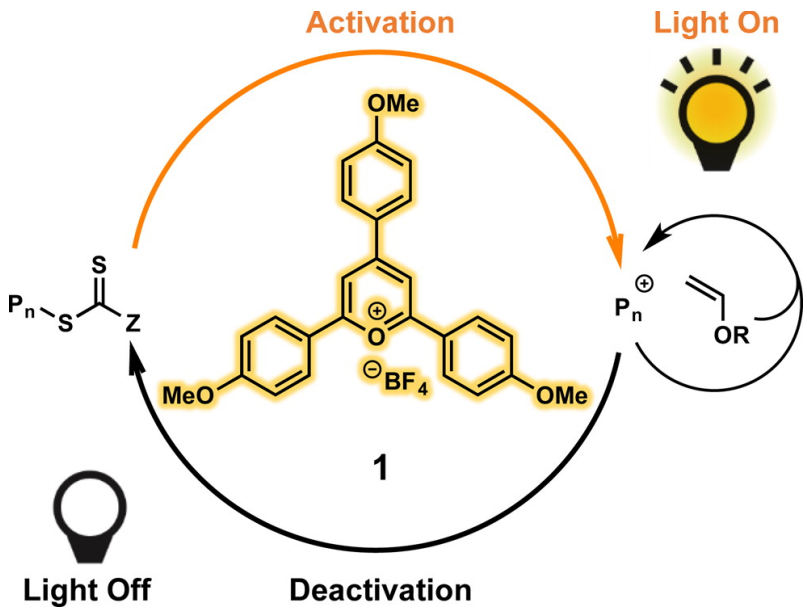

Scheme 2.1. Design of a Photoreversible Cationic Polymerization of Vinyl Ethers

2.3 Results and Discussion

To test our hypothesis, we investigated the polymerization of isobutyl vinyl ether (IBVE) with **2a** as the CTA (Table 2.1). An examination of strongly oxidizing photocatalysts showed that 0.01 mol % 2,4,6-tris(p-methoxyphenyl)pyrylium tetrafluoroborate (**1**)[11] converted 47% of the monomer after exposure to visible light for 3 h to yield a 2.6 kg/mol poly(IBVE) with a *Đ* of 1.29 (Table 2.1, entry 1). Increasing the concentration of **1** to 0.02 mol % led to full conversion and yielded 5.6 kg/mol polymer with a narrower *Đ* of 1.19 (Table 2.1, entry 2). These results demonstrate that a controlled cationic polymerization process promoted by light takes place. In further support of a controlled process, modulation of the CTA-to-monomer ratio enabled the synthesis of polymers with controlled number-average molecular weight (M_n)

and narrow *Đ* values (Table 2.1, entries 2–5). Notably, all of the reactions were run to full conversion and showed excellent agreement between the theoretical and experimental molar masses. Furthermore, better control was observed at lower catalyst loadings when larger M_n values were targeted (Table 2.1, entries 5 and 6). Control experiments without light or **1** (Table 2.1, entries 7 and 8) did not yield any polymer. Additionally, reactions in the absence of **2a** led to uncontrolled polymerization, which we attributed to photoinitiation by direct oxidation of the monomer (Table 2.1, entry 9).[6,8a,12]

Table 2.1. Photocontrolled Cationic Polymerization of Isobutyl Vinyl Ether

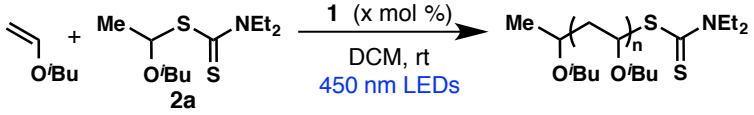

Entry[a]	1 (mol %)	$M_{n,\,exp}$ (kg/mol)	$M_{n,\,theo}$(kg/mol)	*Đ*
1	0.01	2.6	2.3	1.29
2	0.02	5.6	5.0	1.19
3	0.02	10.0	10.0	1.21
4	0.02	17.5	20.0	1.21
5	0.01	35.0	40.0	1.30
6	0.02	26.0	40.0	1.37
7b	0.02	—	5.0	—
8c	—	—	5.0	—
9d	0.02	52.2	—	3.96

[a]Reaction conditions: IBVE (1 equiv), **1** (0.01–0.02 mol %), and **2a** (0.0025–0.02 equiv) at room temperature (rt) in DCM with blue light-emitting diode (LED) irradiation. [b]Carried out in the absence of light. [c]Carried out in the absence of **1**. [d]Carried out in the absence of **2a**.

Monitoring the polymerization of IBVE under the optimized reaction conditions revealed a small induction period followed by fast monomer consumption to give full conversion after 2 h (Figure 2.1a). As expected for a system with living characteristics, M_n grew linearly with conversion and $Đ$ steadily decreased from 1.41 to 1.19 as the reaction proceeded (Figure 2.1b). These data further corroborate the involvement of a controlled chain-growth process.

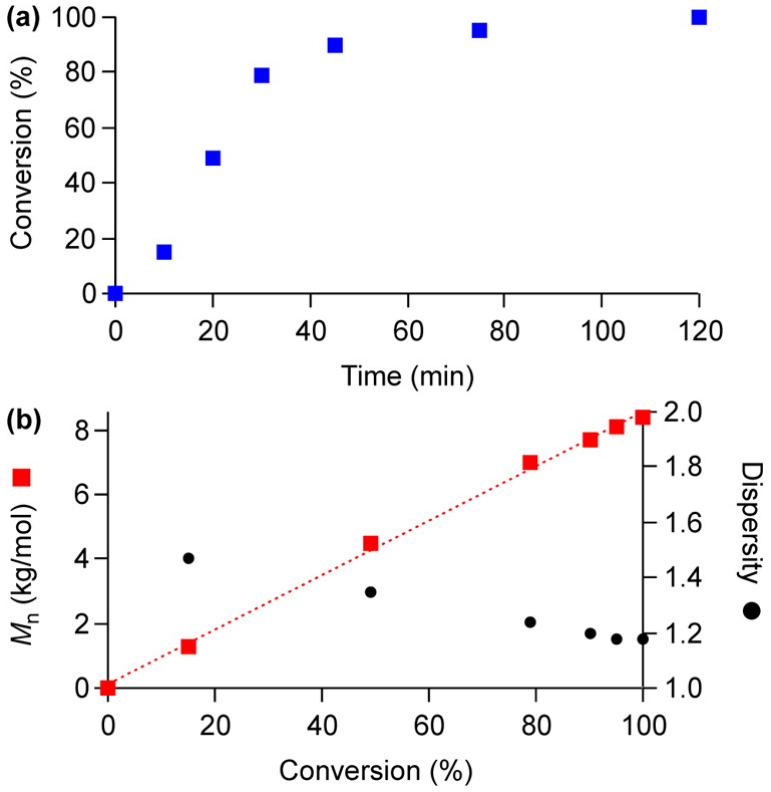

Figure 2.1. Polymerization of IBVE: (a) conversion vs time; (b) M_n and $Đ$ vs conversion.

We next investigated our hypothesis that cation photoactivation is reversible, which would provide temporal control over the chain-growth process.

A reaction mixture containing monomer, catalyst, and a CTA was exposed to light for 30 min and then stirred in the dark for the same time period. This cycle was repeated three times, and aliquots were obtained at each switching point for analysis by NMR spectroscopy and size-exclusion chromatography (SEC). The plot representing conversion versus time (Figure 2.1a) clearly shows that polymerization proceeded only under visible-light irradiation. Moreover, these results demonstrate that the reaction was arrested by removing the external stimulus and efficiently reinitiated by re-exposure to light. The SEC traces further support these data and show that the polymers grew only during periods of light exposure (Figure 2.16). These data illustrate that the catalyst system provides photocontrol over polymer chain growth and that we have developed a truly photoregulated cationic polymerization process.[13]

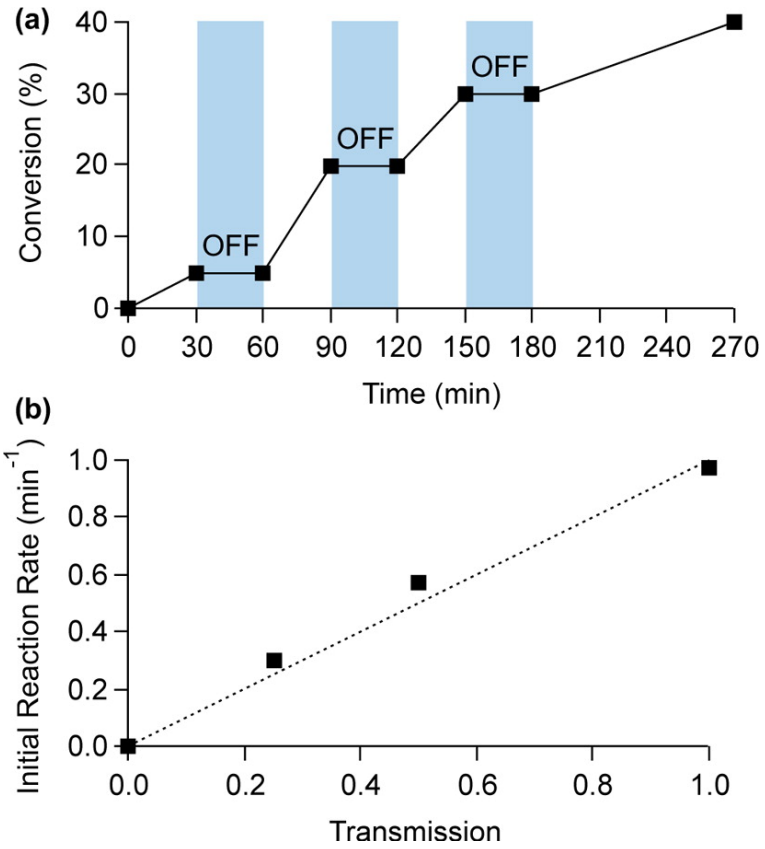

Figure 2.2. Temporal control of polymerization: (a) monomer conversion vs time with intermittent light exposure; (b) influence of light intensity on initial reaction rate.

To further demonstrate the temporal control of these polymerizations, we investigated the influence of the light intensity on the polymerization rate. Using neutral density filters, we observed a linear relationship between transmission and the initial reaction rate (Figure 2.2b), which shows that light intensity can be used to control the rate of polymer chain growth.

We then sought to apply this new methodology to other vinyl monomers. Interestingly, CTA **2a** yielded no polymer when used with other vinyl ethers. We therefore decided to use CTA **2b**, from which we expected to obtain a more active propagating cation.[9a] Gratifyingly, the use of **2b** under our standard

conditions and low catalyst loadings of **1** led to the polymerization of ethyl vinyl ether (EVE), 2-chloroethyl vinyl ether (Cl-EVE), *n*-propyl vinyl ether (PVE), and *n*-butyl vinyl ether (BVE). In all cases, good agreement between the experimental and theoretical M_n and narrow $Đ$ values were observed (Table 2.2).

Table 2.2. Optimized Polymerization Conditions for Other Vinyl Ethers with Photocatalyst **1** and CTA **2b**

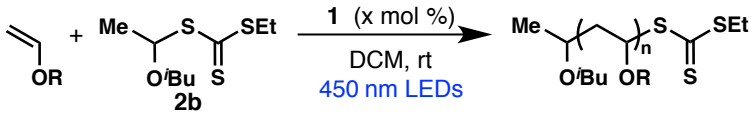

Entry	Monomer	1 (mol %)	$M_{n,\,exp}$ (kg/mol)	$M_{n,\,theo}$(kg/mol)	$Đ$
1	EVE	0.02	5.4	5.0	1.16
2	EVE	0.01	9.6	10.0	1.20
3	Cl-EVE	0.02	5.0	5.0	1.28
4	Cl-EVE	0.02	8.8	10.0	1.30
5	PVE	0.01	4.8	5.0	1.27
6	BVE	0.02	5.8	5.0	1.23

[a]Reaction conditions: vinyl ether (1 equiv), **1** (0.01–0.02 mol %), and **2b** (0.01–0.02 equiv) at room temperature (rt) in DCM with blue light-emitting diode (LED) irradiation. Reactions were run to full conversion.

With conditions in hand that provide well-controlled vinyl ether homopolymers, we probed the chain-end fidelity of these materials through the synthesis of block copolymers. Using our standard conditions with **2b** as the CTA, we synthesized 4.3 kg/mol poly(EVE) followed by the addition of IBVE to yield a 10.7 kg/mol poly(EVE-*b*-IBVE) diblock copolymer (Figure 2.3). The SEC trace shows a monomodal distribution with low $Đ$ (1.20) and little to no tailing. This result demonstrates that our method can be used for the one-pot synthesis of block polymers and that the products maintain excellent chain-end fidelity even at full conversion.

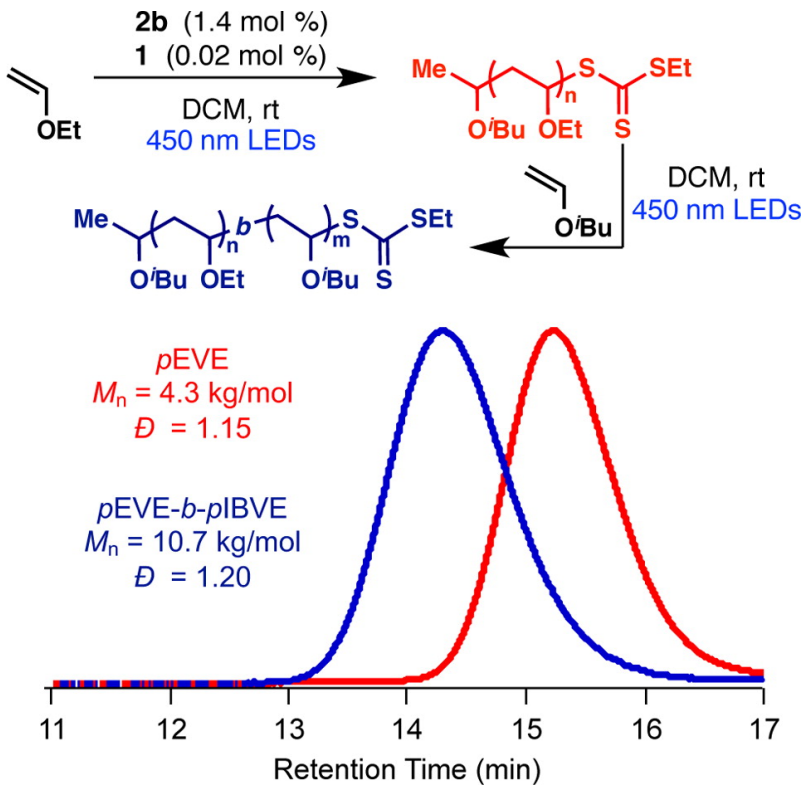

Figure 2.3. Synthesis of poly(ethyl vinyl ether) and poly(ethyl vinyl ether-*block*-isobutyl vinyl ether).

Finally, photoluminescence quenching experiments were conducted to gain a better understanding of the polymerization mechanism. Strong quenching of **1*** by **2a** was observed at millimolar concentrations, and significant quenching by IBVE was measured at molar concentrations similar to those of the polymerization conditions (Figures 2.19–2.23). These observations suggest that **1*** may oxidize either the CTA or IBVE as previously reported by Nicewicz[8a] and Boydston.[6] Given these experimental data and literature precedents, we postulate that polymerization is activated by either direct oxidation of the CTA[14] with the excited catalyst or oxidation of the monomer[6,8a,12] followed by electron transfer from the CTA (Figure 2.4). Mesolytic fragmentation of the oxidized

CTA[10] would then result in a carbocation that would polymerize via a degenerative chain-transfer mechanism, thereby allowing for narrow *Đ* and controlled M_n values. Reduction of the radical CTA with the reduced photocatalyst to the dithiocarbamate (for **2a**) or trithiocarbonate (for **2b**) anion would allow for the regeneration of **1** and concomitant chain capping. This final step closes the catalytic cycle and enables the photoreversible formation of a cation, which gives rise to temporal control over polymer chain growth.[15]

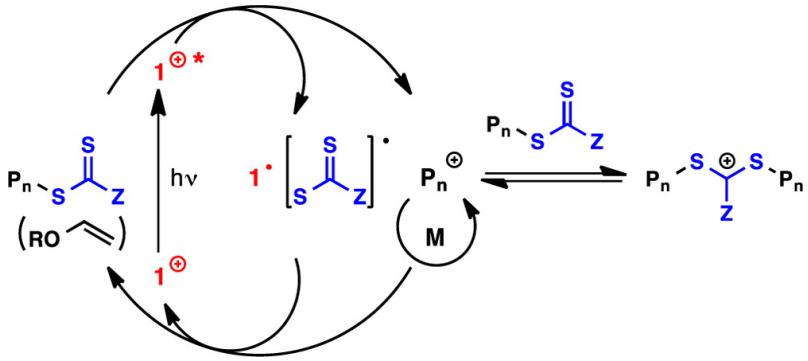

Figure 2.4. Postulated catalytic cycle for the photocontrolled polymerization of vinyl ethers.

2.4 Conclusion

In summary, we have developed a cationic polymerization regulated by visible light that requires mild reaction conditions, parts per million concentrations of a metal-free photocatalyst,[16] and inexpensive blue light-emitting diodes. Narrow *Đ* and predictable M_n values can be obtained for a variety of vinyl ether monomers, and block copolymers can be synthesized because of the high chain-end fidelity. Linear responses to light intensity and

reversible photoactivation of the chain end allow temporal control over chain growth. This methodology therefore opens the field of photocontrolled reactions to a brand new class of monomers and should find numerous applications for the synthesis of complex polymeric architectures.

2.5 References

(1) (a) Chen, M.; Zhong, M.; Johnson, J. A. *Chem. Rev.* **2016**, *116*, 10167. (b) Corrigan, N.; Shanmugam, S.; Xu, J.; Boyer, C. *Chem. Soc. Rev.* **2016**, *45*, 6165. (c) McKenzie, T. G.; Fu, Q.; Uchiyama, M.; Satoh, K.; Xu, J.; Boyer, C.; Kamigaito, M.; Qiao, G. G. *Adv. Sci.* **2016**, *3*, 1500394.

(2) (a) Poelma, J. E.; Fors, B. P.; Meyers, G. F.; Kramer, J. W.; Hawker, C. J. *Angew. Chem., Int. Ed.* **2013**, *52*, 6844. (b) Discekici, E. H.; Pester, C. W.; Treat, N. J.; Lawrence, J.; Mattson, K. M.; Narupai, B.; Toumayan, E. P.; Luo, Y.; McGrath, A. J.; Clark, P. G.; Read de Alaniz, J.; Hawker, C. J. *ACS Macro Lett.* **2016**, *5*, 258. (c) Yan, J.; Pan, X.; Schmitt, M.; Wang, Z.; Bockstaller, M. R.; Matyjaszewski, K. *ACS Macro Lett.* **2016**, *5*, 661. (d) Pester, C. W.; Narupai, B.; Mattson, K. M.; Bothman, D. P.; Klinger, D.; Lee, K. W.; Discekici, E. H.; Hawker, C. J. *Adv. Mater.* **2016**, *28*, 9292.

(3) (a) Fors, B. P.; Hawker, C. J. *Angew. Chem., Int. Ed.* **2012**, *51*, 8850. (b) Konkolewicz, D.; Schroder, K.; Buback, J.; Bernhard, S.; Matyjaszewski, K. *ACS Macro Lett.* **2012**, *1*, 1219. (c) Anastasaki, A.; Nikolaou, V.; Zhang, Q.; Burns, J.; Samanta, S. R.; Waldron, C.;

Haddleton, A. J.; McHale, R.; Fox, D.; Percec, V.; Wilson, P.; Haddleton, D. M. *J. Am. Chem. Soc.* **2014**, *136*, 1141. (d) Treat, N. J.; Sprafke, H.; Kramer, J. W.; Clark, P. G.; Barton, B. E.; Read de Alaniz, J.; Fors, B. P.; Hawker, C. J. *J. Am. Chem. Soc.* **2014**, *136*, 16096. (e) Pan, X.; Malhotra, N.; Simakova, A.; Wang, Z.; Konkolewicz, D.; Matyjaszewski, K. *J. Am. Chem. Soc.* **2015**, *137*, 15430. (f) Jones, G. R.; Whitfield, R.; Anastasaki, A.; Haddleton, D. M. *J. Am. Chem. Soc.* **2016**, *138*, 7346. (g) Theriot, J. C.; Lim, C.-H.; Yang, H.; Ryan, M. D.; Musgrave, C. B.; Miyake, G. M. *Science* **2016**, *352*, 1082. (h) Pearson, R. M.; Lim, C.-H.; McCarthy, B. G.; Musgrave, C. B.; Miyake, G. M. *J. Am. Chem. Soc.* **2016**, *138*, 11399.

(4) For selected examples, see: (a) Yamago, S.; Ukai, Y.; Matsumoto, A.; Nakamura, Y. *J. Am. Chem. Soc.* **2009**, *131*, 2100. (b) Nakamura, Y.; Arima, T.; Tomita, S.; Yamago, S. *J. Am. Chem. Soc*. **2012**, *134*, 5536.

(5) For selected examples, see: (a) Xu, J.; Jung, K.; Atme, A.; Shanmugam, S.; Boyer, C. *J. Am. Chem. Soc.* **2014**, *136*, 5508. (b) Chen, M.; MacLeod, M. J.; Johnson, J. A. *ACS Macro Lett.* **2015**, *4*, 566. (c) Shanmugam, S.; Xu, J.; Boyer, C. *J. Am. Chem. Soc.* **2015**, *137*, 9174. (d) Xu, J.; Shanmugam, S.; Duong, H. T.; Boyer, C. *Polym. Chem.* **2015**, *6*, 5615. (e) Shanmugam, S.; Xu, J.; Boyer, C. *Chem. Sci.* **2015**, *6*, 1341. (f) Shanmugam, S.; Xu, J.; Boyer, C. *Angew. Chem., Int. Ed.* **2016**, *55*, 1036. (g) Xu, J.; Shanmugam, S.; Fu, C.; Aguey-Zinsou, K.; Boyer, C. *J. Am. Chem. Soc.* **2016**, *138*, 3094.

(6) (a) Ogawa, K. A.; Goetz, A. E.; Boydston, A. J. *J. Am. Chem. Soc.* **2015**, *137*, 1400. (b) Goetz, A. E.; Boydston, A. J. *J. Am. Chem. Soc.* **2015**, *137*, 7572. (c) Pascual, L. M. M.; Dunford, D. G.; Goetz, A. E.; Ogawa, K. A.; Boydston, A. J. *Synlett* **2016**, *27*, 759. (d) Goetz, A. E.; Pascual, L. M. M.; Dunford, D. G.; Ogawa, K. A.; Knorr, D. B., Jr.; Boydston, A. J. *ACS Macro Lett.* **2016**, *5*, 579.

(7) (a) Crivello, J. V.; Lam, J. H. W. *Macromolecules* **1977**, *10*, 1307. (b) Crivello, J. V. *J. Polym. Sci., Part A: Polym. Chem.* **1999**, *37*, 4241. (c) Dumur, F.; Gigmes, D.; Fouassier, J.-P.; Lalevée, J. *Acc. Chem. Res.* **2016**, *49*, 1980.

(8) (a) Perkowski, A. J.; You, W.; Nicewicz, D. A. *J. Am. Chem. Soc.* **2015**, *137*, 7580. (b) Messina, M. S.; Axtell, J. C.; Wang, Y.; Chong, P.; Wixtrom, A. I.; Kirlikovali, K. O.; Upton, B. M.; Hunter, B. M.; Shafaat, O. S.; Khan, S. I.; Winkler, J. R.; Gray, H. B.; Alexandrova, A. N.; Maynard, H. D.; Spokoyny, A. M. *J. Am. Chem. Soc.* **2016**, *138*, 6952.

(9) (a) Uchiyama, M.; Satoh, K.; Kamigaito, M. *Angew. Chem., Int. Ed.* **2015**, *54*, 1924. (b) Sugihara, S.; Konegawa, N.; Maeda, Y. *Macromolecules* **2015**, *48*, 5120. (c) Uchiyama, M.; Satoh, K.; Kamigaito, M. *Macromolecules* **2015**, *48*, 5533.

(10) (a) Maslak, P.; Narvaez, J. N. *Angew. Chem., Int. Ed. Engl.* **1990**, *29*, 283. (b) Zhu, Q.; Gentry, E. C.; Knowles, R. R. *Angew. Chem., Int. Ed.* **2016**, *55*, 9969.

(11) Miranda, M. A.; García, H. *Chem. Rev.* **1994**, *94*, 1063.

(12) Cationic polymerization of vinyl ethers via anodic oxidation has been reported. See: Nuyken, O.; Braun, H.; Crivello, J. In *Handbook of Polymer Synthesis, 2nd ed.*; Kricheldorf, H. R.; Nuyken, O.; Swift, G., Eds.; Marcel Dekker: New York, 2004.

(13) Leibfarth, F. A.; Mattson, K. M.; Fors, B. P.; Collins, H. A.; Hawker, C. J. *Angew. Chem., Int. Ed.* **2013**, *52*, 199.

(14) Batanero, B.; Picazo, O.; Barba, F. *J. Org. Chem.* **2001**, *66*, 320.

(15) The proposed mechanism has similarities to PET-RAFT—see ref 5d.

(16) Trotta, J. T.; Fors, B. P. *Synlett* **2016**, *27*, 702.

2.6 Appendix

General Reagent Information

All polymerizations were set up in an Unilab MBraun glovebox with a nitrogen atmosphere and irradiated with blue LED light under nitrogen atmosphere outside the glovebox. Isobutyl vinyl ether (IBVE) (99%, TCI), ethyl vinyl ether (EVE) (99%, Sigma Aldrich), 2-chloroethyl vinyl ether (Cl-EVE) (97%, TCI), *n*-propyl vinyl ether (PVE) (99%, Sigma Aldrich), and *n*-butyl vinyl ether (BVE) (98%, Sigma Aldrich) were dried over calcium hydride (CaH_2) (ACROS organics, 93% extra pure, 0–2 mm grain size) for 12 h and distilled under nitrogen and degassed by vigorously sparging with nitrogen for 30 minutes. Ethanethiol (97%, Alfa Aesar) and carbon disulfide (99.9+%, Alfa Aesar) were distilled before use. 2.0 M HCl in Et_2O (Sigma Aldrich) and sodium hydride (60%, dispersion in mineral oil, Sigma Aldrich) were used as received. Sodium *N,N*-diethylcarbamate trihydrate (98%, Alfa Aesar) was azeotropically dried with toluene. Dichloromethane (DCM) and diethylether (Et_2O) were purchased from J.T. Baker and were purified by vigorous purging with argon for 2 h, followed by passing through two packed columns of neutral alumina under argon pressure. 2,4,6-tri-(*p*-methoxyphenyl)pyrylium tetrafluoroborate was synthesized according to literature procedures.[1]

General Analytical Information

All polymer samples were analyzed using a Tosoh EcoSec HLC 8320GPC system with two SuperHM-M columns in series at a flow rate of 0.350

mL/min. THF was used as the eluent and all number-average molecular weights (M_n), weight-average molecular weights (M_w), and dispersities ($Đ$) for poly(isobutyl vinyl ether) were calculated from refractive index chromatograms against TSKgel polystyrene standards. Number-average molecular weights (M_n), weight-average molecular weights (M_w), and dispersities ($Đ$) for all other polymers were determined by light scattering using a Wyatt miniDawn Treos multi-angle light scattering detector. The *dn/dc* values were calculated from light scattering in THF for poly(ethyl vinyl ether), poly(2-chloroethyl vinyl ether), poly(*n*-propyl vinyl ether), poly(*n*-butyl vinyl ether) and block copolymers in THF. Nuclear magnetic resonance (NMR) spectra were recorded on a Mercury 300 MHz, a Varian 400 MHz or a Varian 600 MHz instrument.

General Reaction Setup

Irradiation of photochemical reactions was done using blue diode led® BLAZE™ lights (450 nm, 2.88 W/ft) or a 9W Kobi Electric (460–470 nm) bulb. Green LEDs (540 nm) can also be used and give similar polymerization results. For light intensity modulation, Rangers® CLARITY series full neutral density filters ND2 and ND4 were used.

Synthesis of *S*-1-isobutoxyethyl *N,N*-diethyl dithiocarbamate (2a)

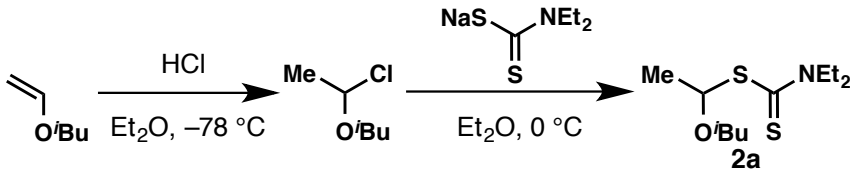

In a flame dried flask, a solution of HCl in Et_2O (5.15 mL, 2.0 M, 10.3 mmol, 1.2 equiv) was added dropwise to a solution of isobutyl vinyl ether (1.15 mL, 8.8 mmol, 1.0 equiv) in Et_2O (10 mL) over 10 minutes at –78 °C and stirred for 1.5 hours under nitrogen. This solution was then added dropwise to a solution of *N,N*-diethyl dithiocarbamate (11.7 mmol, 1.3 equiv) in Et_2O (30 mL) over 30 min at 0 °C. Stirring was continued for one hour at 0 °C, followed by 1.5 hours at room temperature. The reaction was diluted with Et_2O (30 mL) and saturated aqueous sodium bicarbonate solution (30 mL) was added. The layers were separated, and the aqueous layer was extracted with Et_2O (2 × 20 mL). The combined organic phases were washed with water (10 mL), brine (10 mL), then diluted with hexanes (40 mL), dried over Na_2SO_4 and evaporated to dryness *in vacuo*. The brown oil was further purified by column chromatography (SiO_2, gradient from 10:0 to 8.0:0.5 hexanes:ethyl acetate) to yield a pale yellow oil (1.34 g, 61% yield). The spectroscopic data for this compound were identical to those reported in the literature.[2]

^{1}H NMR ($CDCl_3$, 600 MHz) δ: 5.88 (q, *J* = 6.2 Hz, 1 H), 4.02 (q, *J* = 7.2 Hz, 2 H), 3.80–3.70 (m, 2 H), 3.46 (dd, *J* = 9.0, 6.6 Hz, 1 H), 3.34 (dd, *J* = 9.0, 6.6 Hz, 1 H), 1.91 – 1.78 (m, 1 H), 1.73 (d, *J* = 6.3 Hz, 3 H), 1.28 (dt, *J* = 11,4, 7.2 Hz, 6 H), 0.90 (d, *J* = 6.7 Hz, 6 H) ppm.

^{13}C NMR ($CDCl_3$, 150 MHz) δ: 195.1, 91.7, 76.2, 48.9, 47.0, 28.5, 23.6, 19.5, 12.7, 11.8 ppm.

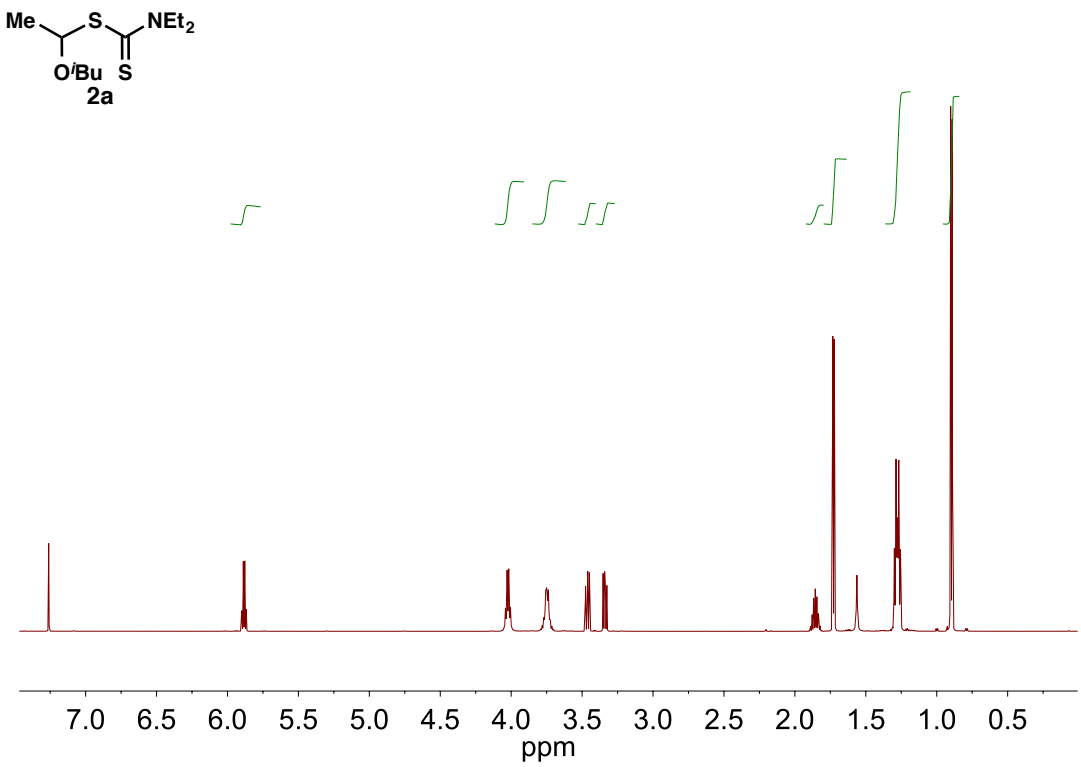

Figure 2.5. ^{1}H NMR of *S*-1-isobutoxyethyl *N,N*-diethyl dithiocarbamate (**2a**).

Synthesis of S-1-isobutoxylethyl S′-ethyl trithiocarbonate (2b)

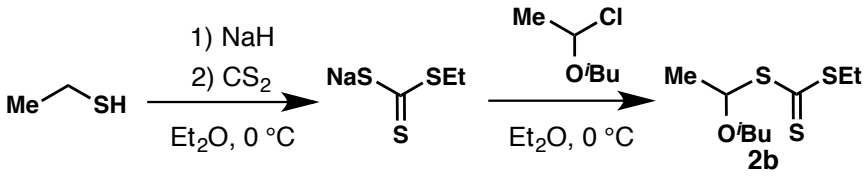

2b was synthesized according to a slightly modified literature procedure.[3] Sodium hydride (60%, 1.00 g, 25.0 mmol, 1.0 equiv) was placed in a flame-dried flask under nitrogen and then washed with anhydrous hexanes, also under

nitrogen. Anhydrous Et_2O (10 mL) was added and the reaction mixture was cooled to 0 °C. Freshly distilled ethanethiol (1.85 mL, 25.0 mmol, 1.0 equiv) was added dropwise over 10 minutes at 0 °C. The suspension was stirred at room temperature for 10 minutes, then cooled again to 0 °C before freshly distilled carbon disulfide (1.65 mL, 27.5 mmol, 1.1 equiv) was added dropwise over 10 minutes at 0 °C. The resulting thick yellow suspension was stirred at room temperature for 2 hours. A separate flame-dried flask containing a solution of HCl in Et_2O (13.8 mL, 2.0 M, 27.5 mmol, 1.1 equiv) was cooled to –78 °C and distilled isobutyl vinyl ether (3.26 mL, 25.0 mmol, 1.0 equiv) was added dropwise. The pale yellow solution was stirred at –78 °C for 1 hour, then warmed to 0 °C over 30 minutes. Subsequently, the cold solution was added dropwise to the suspension of sodium ethyl trithiocarbonate over 30 minutes. The resulting mixture was stirred at room temperature for 2 hours, then diluted with Et_2O (10 mL) and quenched with sat. $NaHCO_3$ (10 mL). The layers were separated, and the aqueous layer was extracted with Et_2O (2 $\times$ 20 mL). The combined organic phases were washed with water (10 mL), brine (10 mL), then diluted with hexanes (40 mL), dried over Na_2SO_4 and evaporated to dryness in vacuo. Column chromatography (SiO_2, hexanes) provided **2b** as a yellow oil (3.59 g, 59%).

The spectroscopic data for this compound were consistent with those reported in the literature.[3]

^{1}H NMR ($CDCl_3$, 600 MHz,) δ: 5.97 (q, *J* = 6.3 Hz, 1 H), 3.43 (dd, *J* = 10.2, 6.6 Hz, 1 H), 3.39 – 3.29 (m, 2 H), 3.27 (dd, *J* = 10.2, 6.6 Hz, 1 H), 1.87 – 1.81 (m, 1 H), 1.71 (d, *J* = 6.3 Hz, 3 H), 1.35 (t, *J* = 7.4 Hz, 3 H), 0.90 – 0.87 (m, 6 H). ^{13}C NMR ($CDCl_3$, 150 MHz) δ: 224.9, 89.1, 76.5, 31.0, 28.4, 22.9, 19.4, 13.1 ppm.

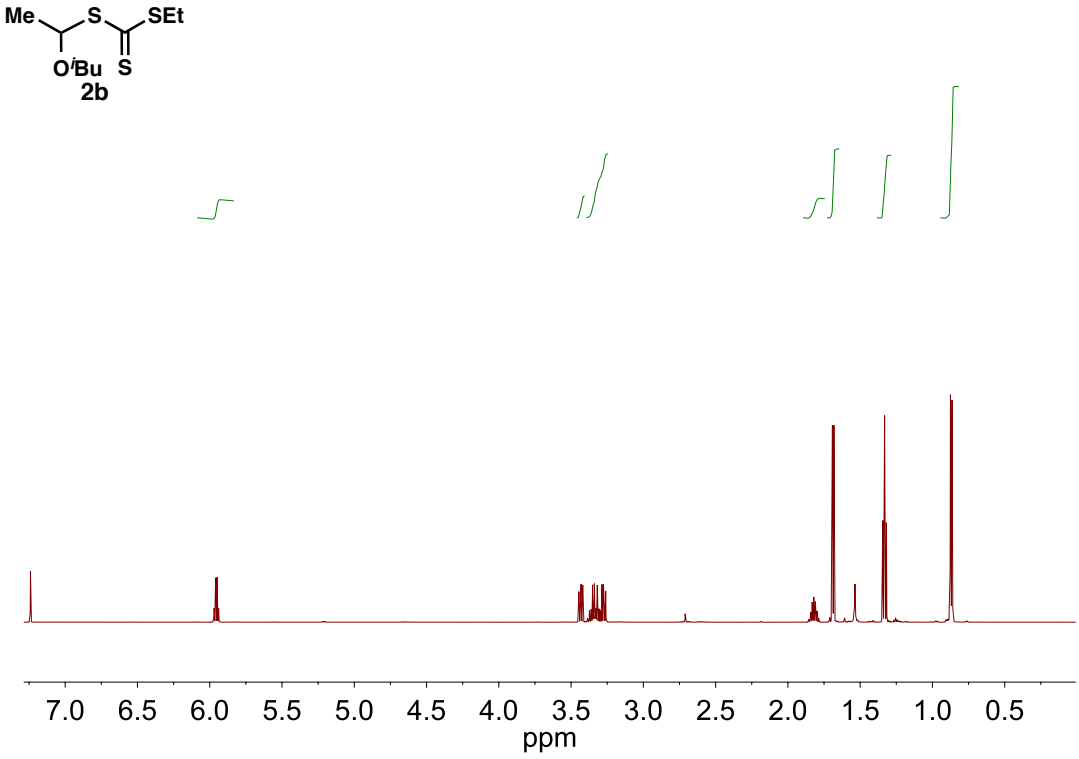

Figure 2.6. ^{1}H NMR of *S*-1-isobutoxylethyl *S′*-ethyl trithiocarbonate (**2b**).

General Procedure for Photocontrolled Cationic Polymerization of Isobutyl Vinyl Ether

In a nitrogen filled glove box, an oven-dried one-dram vial was equipped with a stir bar and charged with isobutyl vinyl ether (0.26 mL, 2.00 mmol, 50 equiv), 0.2 mL of a stock solution of 2,4,6-tri-(*p*-methoxyphenyl)pyrylium

tetrafluoroborate (**1**) in DCM (2.0 mM, 0.40 μmol, 0.02 mol % relative to IBVE), and 0.04 mL of a stock solution of **2a** or **2b** in DCM (1 M, 0.04 mmol, 1 equiv). The vial was sealed with a septum cap under an atmosphere of nitrogen, placed next to blue LED strips (~450 nm) outside of the glove box, and stirred while cooling by blowing compressed air over the reaction vial. Following the desired amount of reaction time, benzene (89 μL, 1.0 mmol, 25 equiv) was added as an internal standard for NMR, and aliquots for NMR and GPC analysis were taken. Full conversion was generally reached after 3–5 hours. The solvent was removed under *vacuo* to yield the pure polymer. A typical ^{1}H NMR for poly(isobutyl vinyl ether) is shown in Figure 2.7a,b. For a picture of the experimental setup, see Figure 2.8.

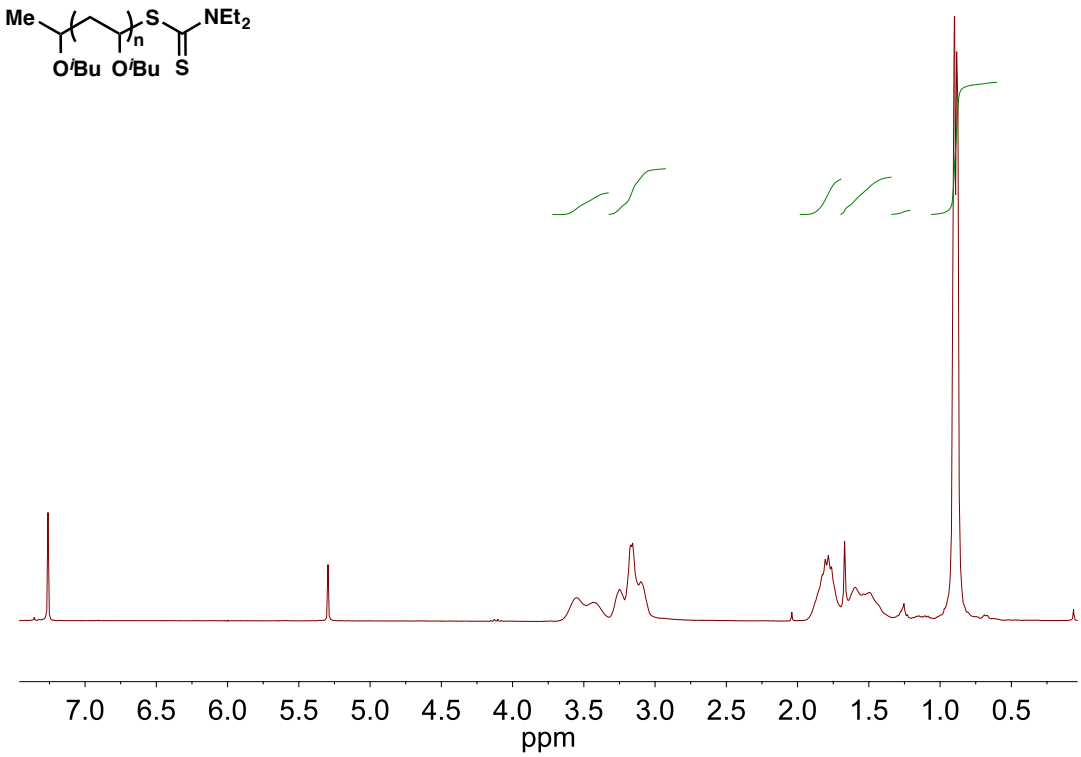

Figure 2.7a. ^{1}H NMR of poly(isobutyl vinyl ether); M_n = 35.0 kg/mol, $Đ$ = 1.30 (Table 2.1, entry 5).

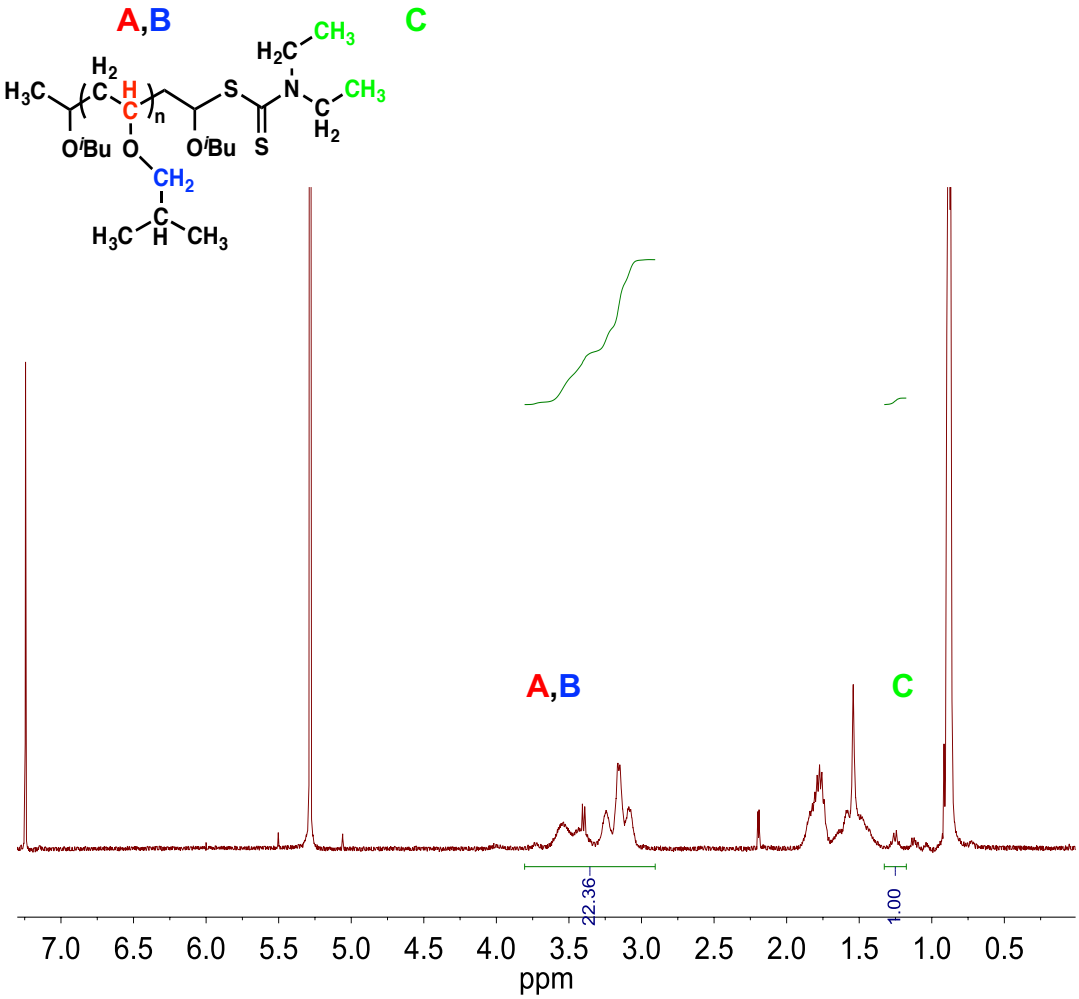

Figure 2.7b. ^{1}H NMR of poly(isobutyl vinyl ether); ratios of chain-end and backbone integrations can be used to calculate M_n and show good chain-end fidelity; M_n (NMR) = 4.4 kg/mol (M_n (GPC) = 5.6 kg/mol, $M_{n,theo}$ = 5.0 kg/mol).

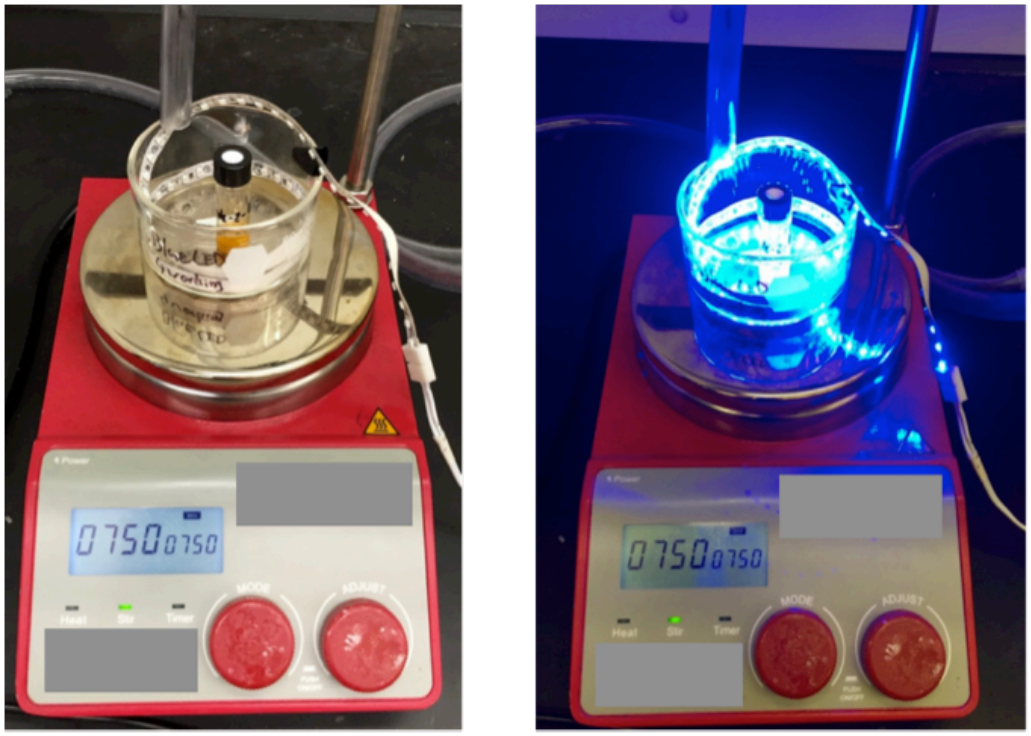

Figure 2.8. Polymerization setup.

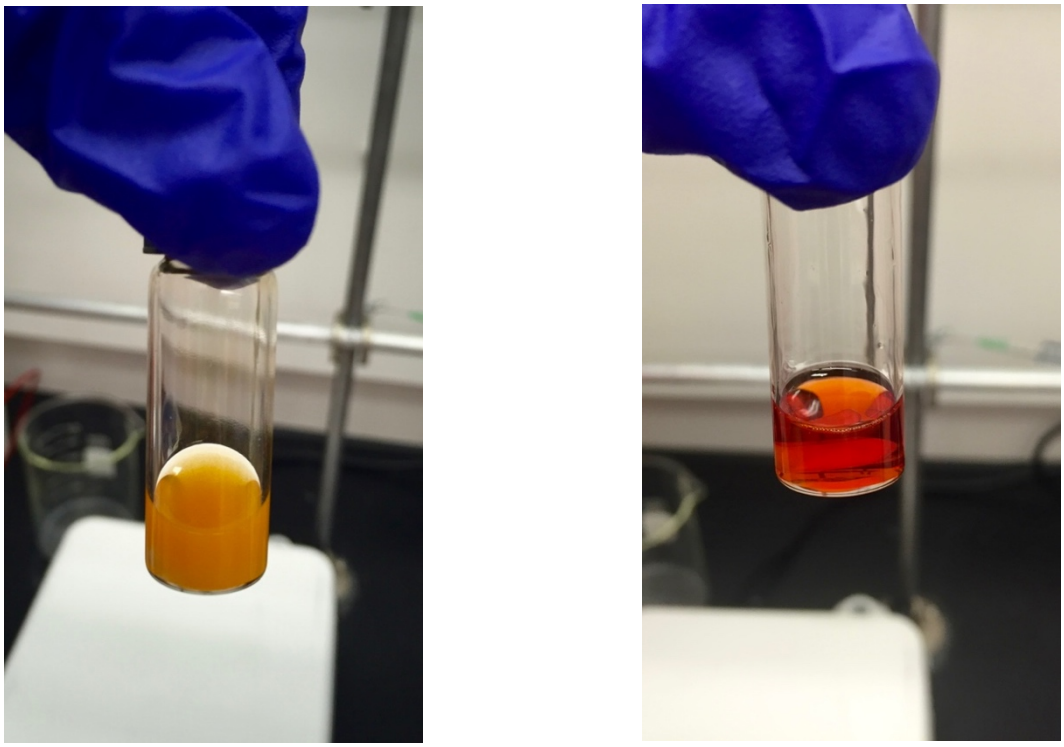

Figure 2.9. Reaction before (left) and after (right) irradiation.

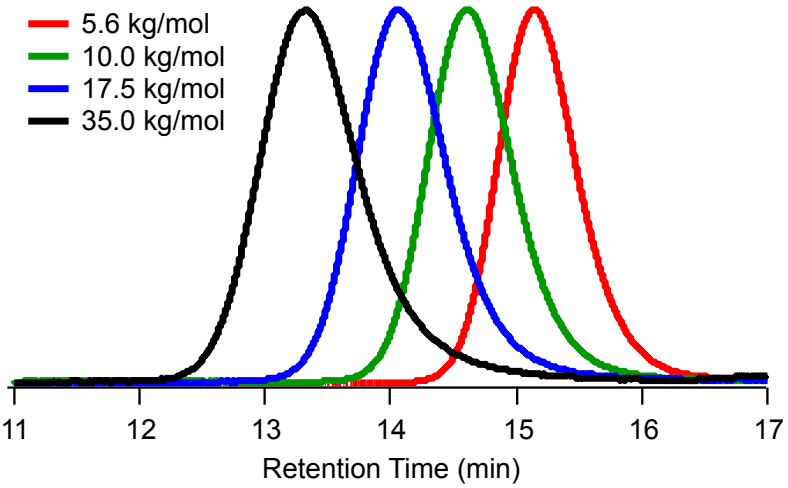

Figure 2.10. GPC traces of polymers in Table 2.1, entries 2–5.

General Procedure for Photocontrolled Cationic Polymerization of Ethyl Vinyl Ether ($M_{n,theo}$ = 10.0 kg/mol) (Table 2.2, entry 2).

In a nitrogen filled glove box, an oven-dried one-dram vial was equipped with a stir bar and charged with ethyl vinyl ether (0.27 mL, 2.78 mmol, 140 equiv) 0.2 mL of a stock solution of 2,4,6-tri-(*p*-methoxyphenyl)pyrylium tetrafluoroborate (**1**) in DCM (2.0 mM, 0.40 μmol, 0.02 mol % relative to EVE), and 0.02 mL of a stock solution of **2b** in DCM (1 M, 0.02 mmol, 1 equiv). The vial was sealed with a septum cap under an atmosphere of nitrogen, placed next to blue LED strips (~450 nm) outside of the glove box, and stirred while cooling by blowing compressed air over the reaction vial. Following the desired amount of reaction time, benzene (89 μL, 1.0 mmol, 50 equiv) was added as an internal standard for NMR, and aliquots for NMR and GPC analysis were taken. Full conversion was generally reached after 2–3 hours. The solvent was removed

under *vacuo* to yield the pure polymer. A typical ^{1}H NMR for poly(ethyl vinyl ether) is shown in Figure 2.11.

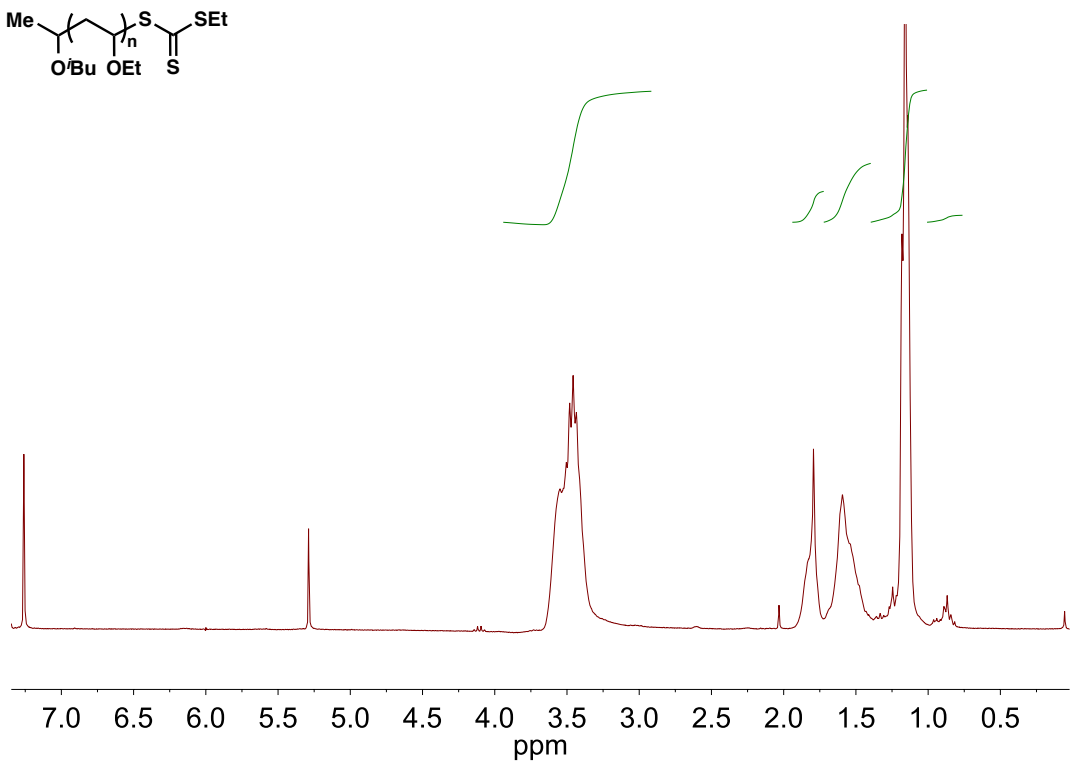

Figure 2.11. ^{1}H NMR of poly(ethyl vinyl ether); M_n = 9.6 kg/mol, $Đ$ = 1.20 (Table 2.2, entry 2).

General Procedure for Photocontrolled Cationic Polymerization of 2-chloroethyl Vinyl Ether ($M_{n,theo}$ = 10.0 kg/mol) (Table 2.2, entry 4).

In a nitrogen filled glove box, an oven-dried one-dram vial was equipped with a stir bar and charged with 2-chloroethyl vinyl ether (0.18 mL, 1.8 mmol, 90 equiv relative to **2b**), 0.2 mL of a stock solution of 2,4,6-tri-(*p*-methoxyphenyl)pyrylium tetrafluoroborate (**1**) in DCM (2.0 mM, 0.40 μmol, 0.02 mol % relative to Cl-EVE), and 0.02 mL of a stock solution of **2b** in DCM (1 M,

0.02 mmol, 1.0 equiv). The vial was sealed with a septum cap under an atmosphere of nitrogen, placed next to blue LED strips (~450 nm) outside of the glove box, and stirred while cooling by blowing compressed air over the reaction vial. Following the desired amount of reaction time, benzene (89 μL, 1.0 mmol, 50 equiv) was added as an internal standard for NMR, and aliquots for NMR and GPC analysis were taken. Full conversion was generally reached after 18 hours. The solvent was removed under *vacuo* to yield the pure polymer. A typical ^{1}H NMR for poly(2-chloroethyl vinyl ether) is shown in Figure 2.12.

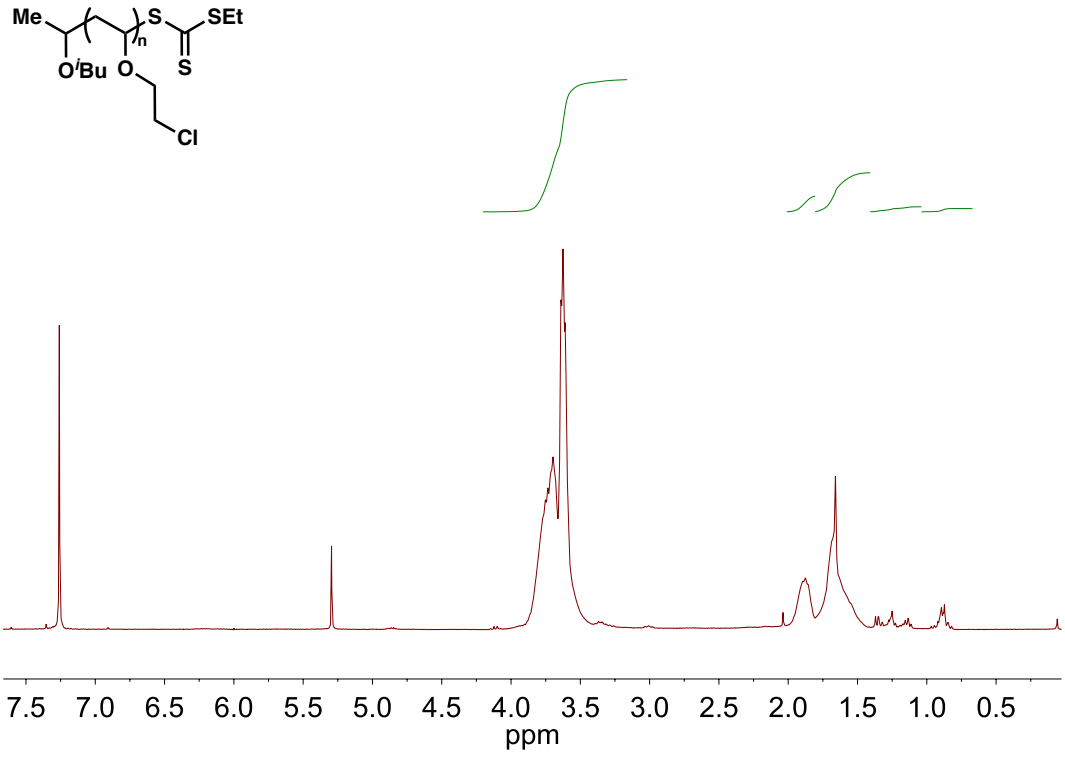

Figure 2.12. ^{1}H NMR of poly(2-chloroethyl vinyl ether); M_n = 8.8 kg/mol, $Đ$ = 1.30 (Table 2.2, entry 4).

Procedure for Photocontrolled Cationic Polymerization of *n*-Propyl Vinyl Ether ($M_{n,theo}$ = 5.0 kg/mol) (Table 2.2, entry 5).

In a nitrogen filled glove box, an oven-dried one-dram vial was equipped with a stir bar and charged with *n*-propyl vinyl ether (0.26 mL, 2.32 mmol, 60 equiv relative to **2b**), 0.12 mL of a stock solution of 2,4,6-tri-(*p*-methoxyphenyl)pyrylium tetrafluoroborate (**1**) in DCM (2.0 mM, 0.25 μmol, 0.01 mol % relative to PVE), and 0.02 mL of a stock solution of **2b** in DCM (1 M, 0.02 mmol, 1.0 equiv). The vial was sealed with a septum cap under an atmosphere of nitrogen, placed next to blue LED strips (~450 nm) outside of the glove box, and stirred while cooling by blowing compressed air over the reaction vial. Following the desired amount of reaction time, benzene (89 μL, 1.0 mmol, 50 equiv) was added as an internal standard for NMR, and aliquots for NMR and GPC analysis were taken. Full conversion was generally reached after 2–3 hours. The solvent was removed under *vacuo* to yield the pure polymer. A typical ^{1}H NMR for poly(*n*-propyl vinyl ether) is shown in Figure 2.13.

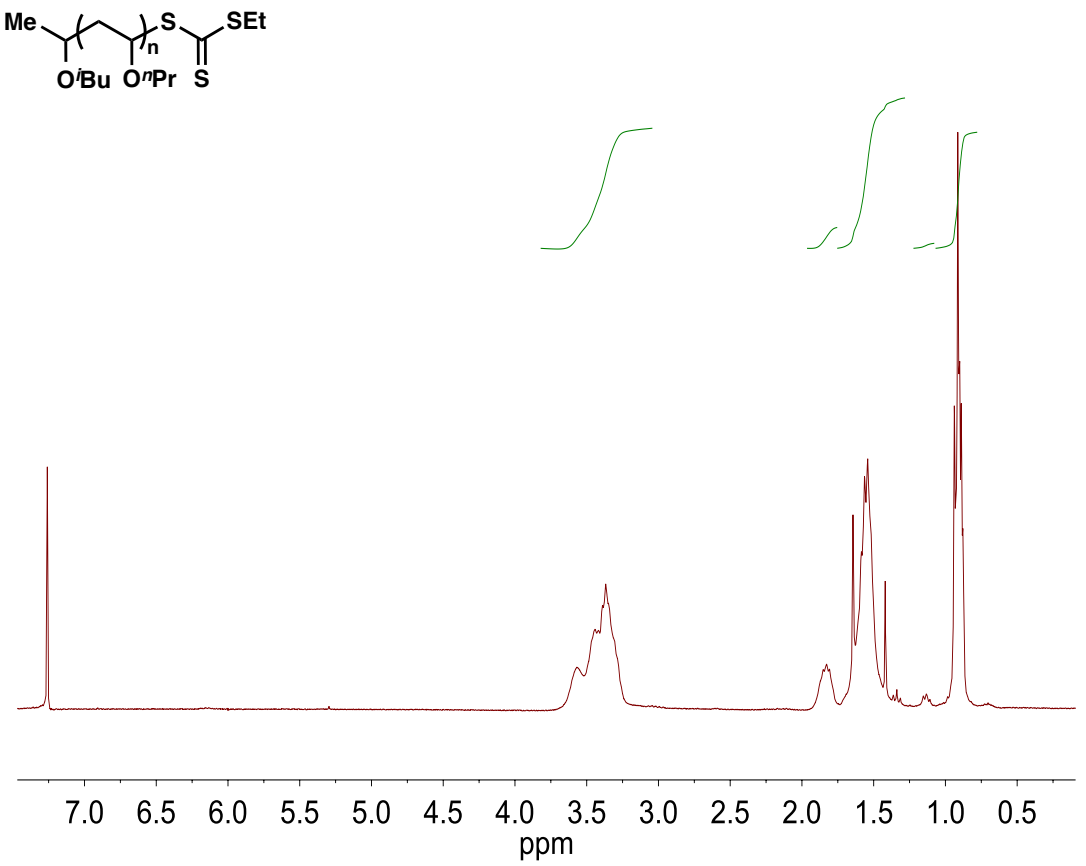

Figure 2.13. ^{1}H NMR of poly(*n*-propyl vinyl ether); M_n = 4.8 kg/mol, $Đ$ = 1.27 (Table 2.2, entry 5).

Procedure for Photocontrolled Cationic Polymerization of *n*-Butyl Vinyl Ether ($M_{n,theo}$ = 5.0 kg/mol) (Table 2.2, entry 6).

In a nitrogen filled glove box, an oven-dried one-dram vial was equipped with a stir bar and charged with *n*-butyl vinyl ether (0.26 mL, 2.00 mmol, 50 equiv relative to **2b**), 0.2 mL of a stock solution of 2,4,6-tri-(*p*-methoxyphenyl)pyrylium tetrafluoroborate (**1**) in DCM (2.0 mM, 0.40 μmol, 0.02 mol % relative to BVE), and 0.02 mL of a stock solution of **2b** in DCM (1 M, 0.02 mmol, 1.0 equiv). The vial was sealed with a septum cap under an atmosphere of nitrogen, placed next

to blue LED strips (~450 nm) outside of the glove box, and stirred while cooling by blowing compressed air over the reaction vial. Following the desired amount of reaction time, benzene (89 µL, 1.0 mmol, 50 equiv) was added as an internal standard for NMR, and aliquots for NMR and GPC analysis were taken. Full conversion was generally reached after 2–3 hours. The solvent was removed under *vacuo* to yield the pure polymer. A typical ^{1}H NMR for poly(*n*-butyl vinyl ether) is shown in Figure 2.14a,b.

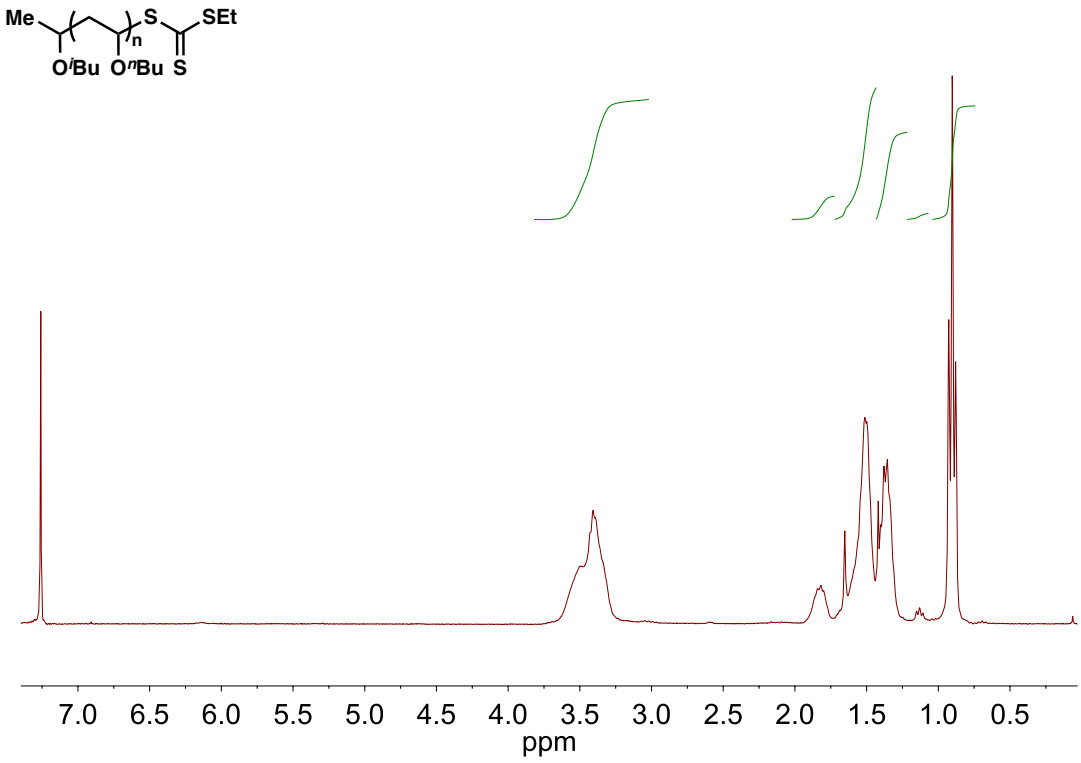

Figure 2.14a. ^{1}H NMR of poly(*n*-butyl vinyl ether); M_n = 5.8 kg/mol, $Đ$ = 1.23 (Table 2.2, entry 6).

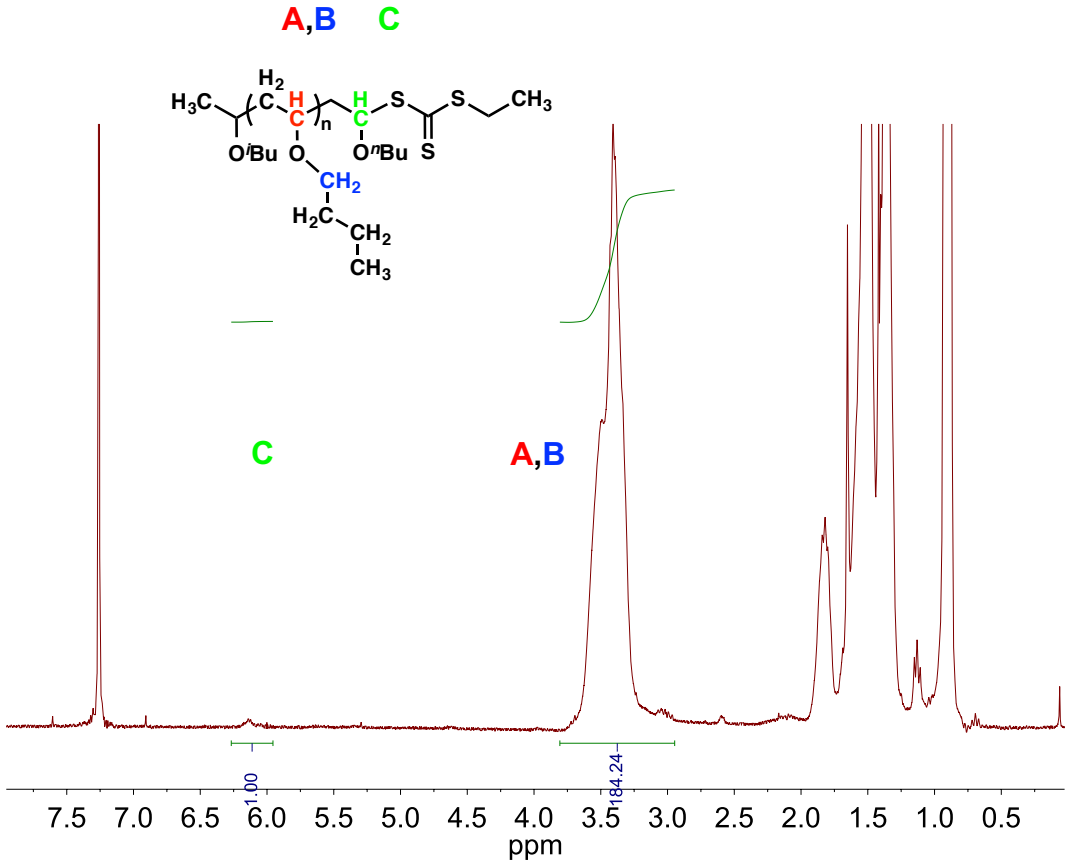

Figure 2.14b. ^{1}H NMR of poly(*n*-butyl vinyl ether); ratios of chain-end and backbone integrations can be used to calculate M_n and show good chain-end fidelity; M_n (NMR) = 6.1 kg/mol (M_n (GPC) = 5.8 kg/mol, $M_{n,theo}$ = 5.0 kg/mol).

Procedure for Photocontrolled Synthesis of Diblock Copolymer (Figure 2.3)

In a nitrogen filled glove box, an oven-dried one-dram vial was equipped with a stir bar and charged with ethyl vinyl ether (0.27 mL, 2.78 mmol, 70 equiv relative to **2**), 0.2 mL of a stock solution of 2,4,6-tri-(*p*-methoxyphenyl)pyrylium tetrafluoroborate (**1**) in DCM (2.0 mM, 0.40 μmol, 0.02 mol % relative to EVE) and 0.02 mL of a stock solution of **2b** in DCM (1 M, 0.02 mmol, 1.0 equiv). The vial was sealed with a septum cap under an atmosphere of nitrogen, placed next to blue LED strips (~450 nm) outside of the glove box, and stirred while cooling

by blowing compressed air over the reaction vial. The reaction was run to full conversion (1 hour). The vial was brought back in the glove box and an aliquot for ^{1}H NMR and GPC analysis was taken prior to the addition of isobutyl vinyl ether (0.52 mL, 4 mmol, 100 equiv relative to **2b**). The vial was sealed with a septum cap under an atmosphere of nitrogen, placed next to blue LED strips (~450 nm) outside of the glove box, and stirred while cooling by blowing compressed air over the reaction vial until the reaction reached full conversion (14 hours). The solvent was removed under *vacuo* to yield the pure polymer.

The ^{1}H NMR for poly(ethyl vinyl ether-*block*-isobutyl vinyl ether) is shown in Figure 2.15.

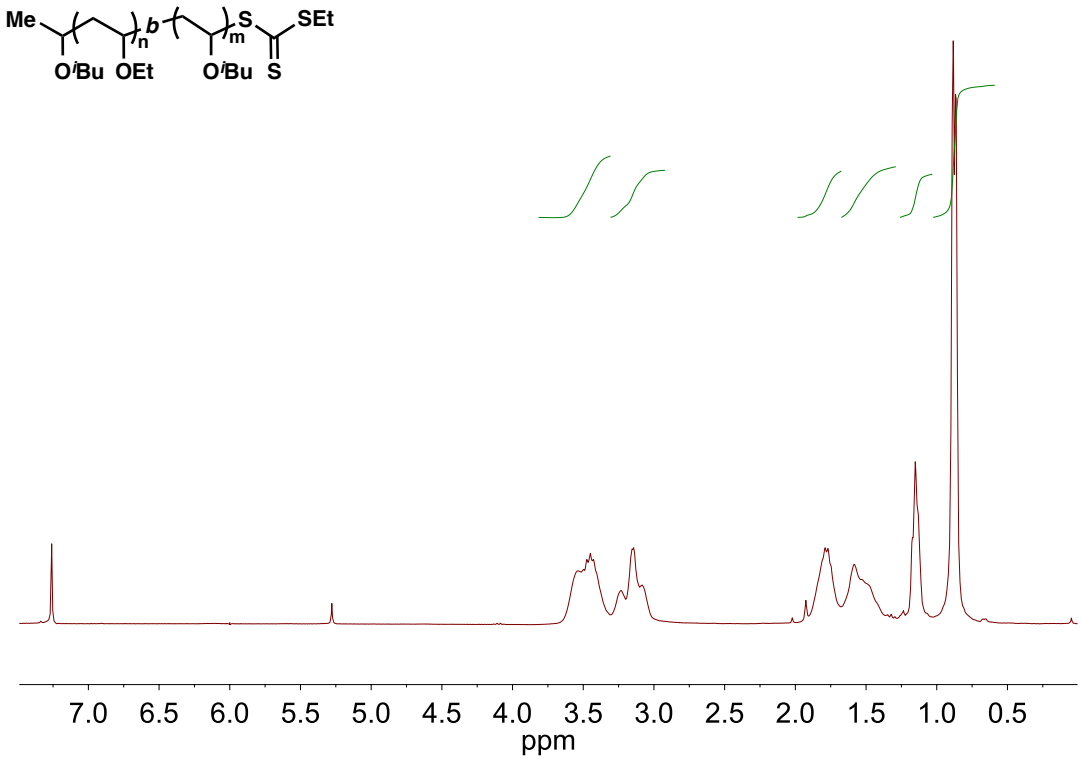

Figure 2.15. ^{1}H NMR of poly(ethyl vinyl ether-*block*-isobutyl vinyl ether); M_n = 10.7 kg/mol, $Đ$ = 1.20 (Figure 2.3).

Procedure for On/Off Photocontrolled Cationic Polymerization of Isobutyl Vinyl Ether (Figure 2.2a)

In a nitrogen filled glove box, an oven-dried 20 mL scintillation vial was equipped with a stir bar and charged with isobutyl vinyl ether (1.3 mL, 10 mmol, 50 equiv), 0.5 mL of a stock solution of 2,4,6-tri-(*p*-methoxyphenyl)pyrylium tetrafluoroborate (**1**) in DCM (2.0 mM, 1.0 μmol, 0.01 mol % relative to IBVE), 0.2 mL of a stock solution of **2a** in DCM (1 M, 0.2 mmol, 1.0 equiv), and benzene (89 μL, 1.0 mmol, 50 equiv) as an internal standard for NMR. The vial was sealed with a septum cap under an atmosphere of nitrogen, placed next to blue LED strips (~450 nm) outside of the glove box, and stirred while cooling by blowing compressed air over the reaction vial. Aliquots were taken after 30 min intervals under positive nitrogen pressure and subjected to ^{1}H NMR and GPC analysis. The vial was covered in aluminum foil during “off” periods. The GPC traces of all aliquots and the development of M_n vs. time are depicted in Figure 2.16.

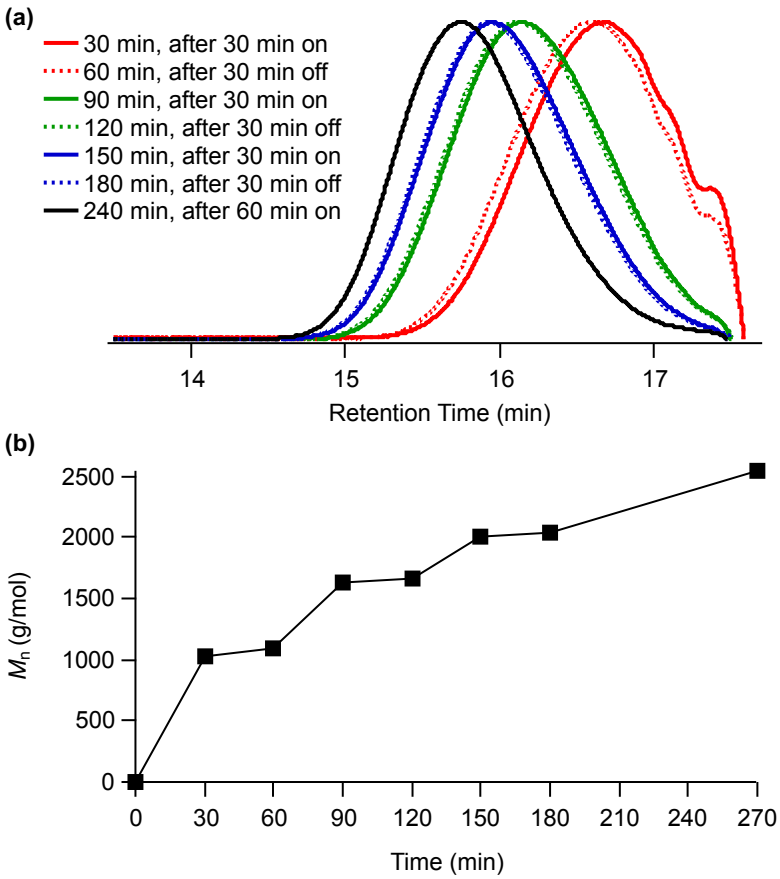

Figure 2.16. (a) GPC traces of aliquots and (b) M_n vs. time development of On/Off-Experiment (Figure 2.2a).

Procedure for Kinetic Investigation of Photocontrolled Cationic Isobutyl Vinyl Ether Polymerization (Figure 2.2a and 2.2b)

In a nitrogen filled glove box, an oven-dried 20 mL scintillation vial was equipped with a stir bar and charged with isobutyl vinyl ether (1.3 mL, 10 mmol, 100 equiv), 0.5 mL of a stock solution of 2,4,6-tri-(*p*-methoxyphenyl)pyrylium tetrafluoroborate (**1**) in DCM (2.0 mM, 1.0 μmol, 0.01 mol % relative to IBVE), 0.1 mL of a stock solution of **2a** in DCM (1 M, 0.1 mmol, 1.0 equiv), and benzene (89 μL, 1.0 mmol, 100 equiv) as an internal standard for NMR. The vial was

sealed with a septum cap under an atmosphere of nitrogen, placed next to blue LED strips (~450 nm) outside of the glove box, and stirred while cooling by blowing compressed air over the reaction vial. Aliquots were taken after 10 min, 20 min, 30 min, 45 min, 75 min and 120 min under positive nitrogen pressure and subjected to ^{1}H NMR and GPC analysis.

Procedure for Photocontrolled Cationic Isobutyl Vinyl Ether Polymerizations Using Neutral Density Filters to Modulate Light Intensity (Figure 2.2b)

In a nitrogen filled glove box, an oven-dried one-dram vial was equipped with a stir bar and charged with isobutyl vinyl ether (0.52 mL, 4 mmol, 100 equiv), 0.2 mL of a stock solution of 2,4,6-tri-(*p*-methoxyphenyl)pyrylium tetrafluoroborate (**1**) in DCM (2.0 mM, 0.40 μmol, 0.01 mol % relative to IBVE), 0.04 mL of a stock solution of **2a** in DCM (1 M, 0.04 mmol, 1.0 equiv), and benzene (30 μL, 0.34 mmol, 8.5 equiv) as an internal standard for NMR. The vial was sealed with a septum cap under an atmosphere of nitrogen, taken outside of the glove box, and placed about 2 cm away from a 9W Kobi Electric (460–470nm) bulb. The reaction was stirred while cooling by blowing compressed air over the reaction vial and aliquots for ^{1}H NMR and GPC were taken at specified time points (Figure S2.17). The reaction was repeated three times with different light intensities: 1) 100% transmission, 2) 50% transmission, and 3) 25% transmission. In order to achieve 50% and 25% light transmission, a Rangers® CLARITY series full neutral density filter was intercalated between

the light bulb and the reaction vial, touching the latter. A ND2 filter (50%) and a ND4 filter (25%) were used. For a picture of the experimental setup, see Figure 2.18.

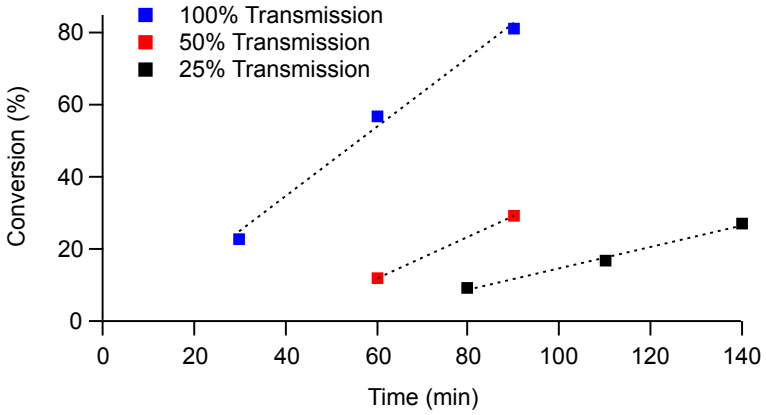

Figure 2.17. Monomer conversion (%) at specified time point during the reaction at 100% transmission (blue), 50% transmission (red), and 25% transmission (black) of light. The slope represents the initial reaction rates used for Figure 2.2b.

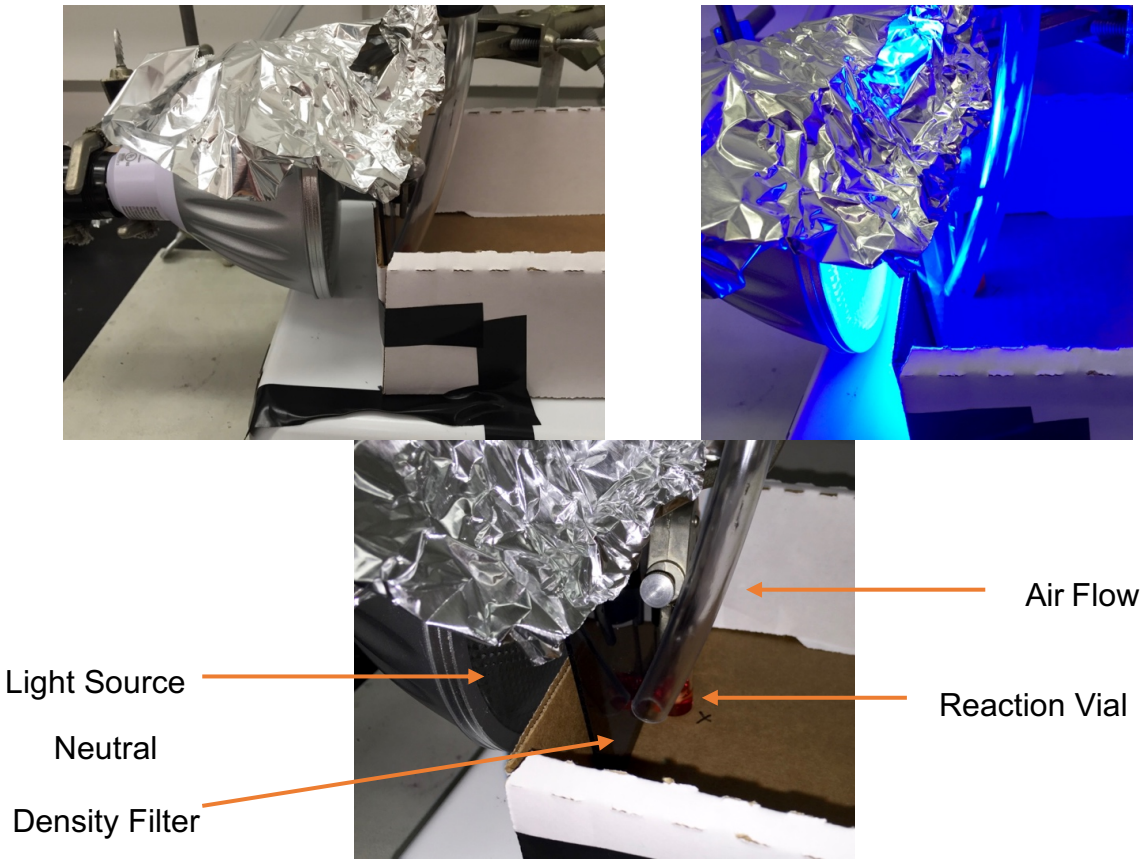

Figure 2.18. Setup with neutral density filters.

Procedure for Fluorescence Quenching Studies

A Varian Cary Eclipse Fluorescence Spectrophotometer was used for the quenching studies. The solutions of 2,4,6-tri-(*p*-methoxyphenyl)pyrylium tetrafluoroborate (**1**) were excited at 475 nm and the fluorescence spectra were recorded between 480 and 700 nm. The emission of a 0.21 mM solution of **1** in DCM was measured at varying concentrations of *S*-1-isobutoxyethyl *N*,*N*-diethyl dithiocarbamate (**2a**) (0 – 26 mM). As shown in Figures 2.19, 2.10, 2.21 and 2.22 a concentration dependent fluorescence quenching was observed. The

emission of a 0.21 mM solution of **1** in DCM was also measured at varying low concentrations of IBVE (0 – 260 mM) then at higher concentrations (0.67 – 1.3 M). As shown in Figures 2.21–2.23 no quenching of the emission of **1** was observed at low concentrations of IBVE, but a concentration dependent fluorescence quenching was observed at molar concentrations.

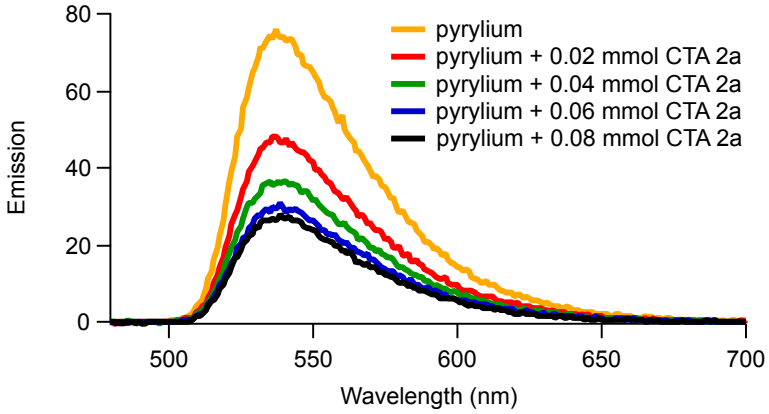

Figure 2.19. Fluorescence quenching of 2,4,6-tri-(*p*-methoxyphenyl)pyrylium tetrafluoroborate by CTA **2a** (λ_{ex} = 475 nm).

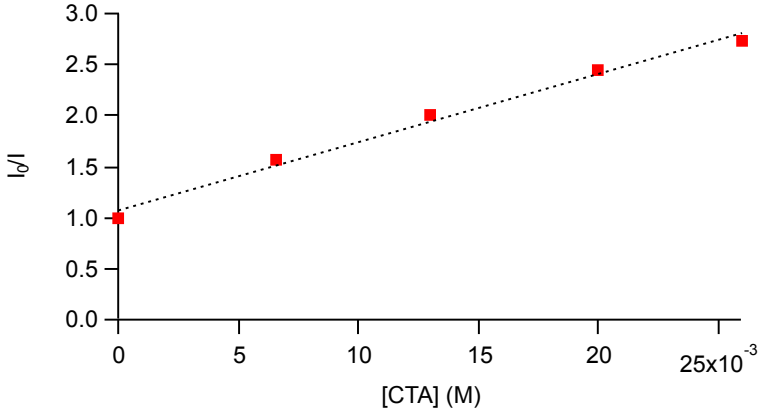

Figure 2.20. Stern-Volmer plot for the fluorescence quenching of 2,4,6-tri-(*p*-methoxyphenyl)pyrylium tetrafluoroborate by CTA **2a**.

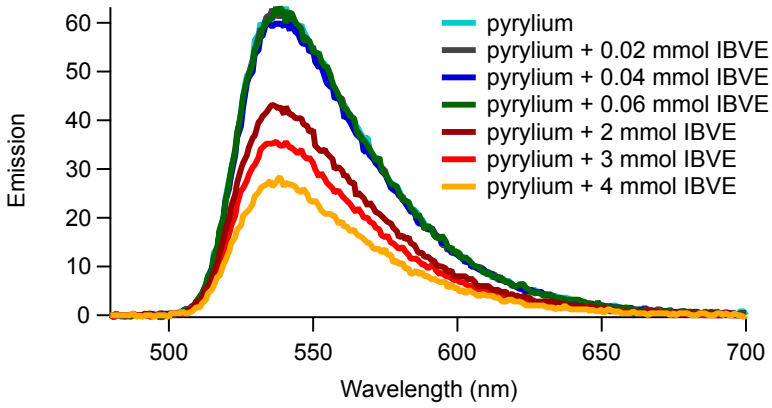

Figure 2.21. Fluorescence quenching of 2,4,6-tri-(*p*-methoxyphenyl)pyrylium tetrafluoroborate by IBVE (λ_{ex} = 475 nm).

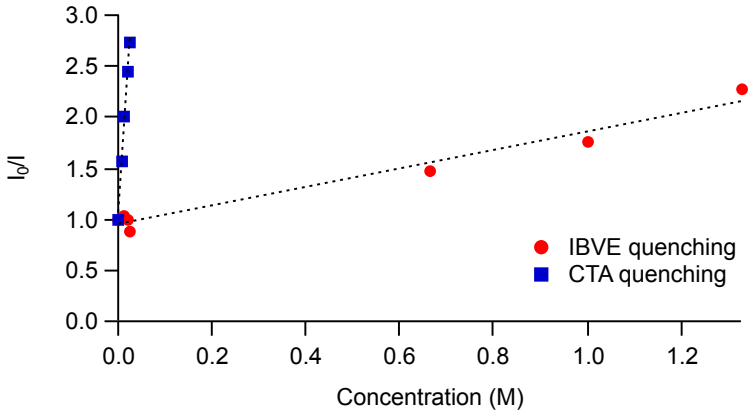

Figure 2.22. Stern-Volmer plot for the fluorescence quenching of 2,4,6-tri-(*p*-methoxyphenyl)pyrylium tetrafluoroborate by IBVE and CTA **2a**.

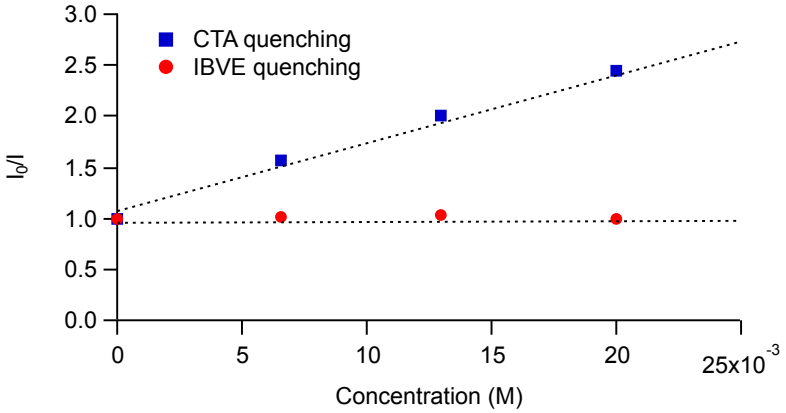

Figure 2.23. Stern-Volmer plot for the fluorescence quenching of 2,4,6-tri-(*p*-methoxyphenyl)pyrylium tetrafluoroborate by IBVE and CTA **2a** (low concentration section of Figure 2.22) .

Table 2.3. Results of initial photocatalyst screening

Catalyst	**mol %***	**reaction time**	**Conv.**
$Ru(bpy)_3(PF_6)_2$	0.02	12 h	–
$Ru(bpz)_3(PF_6)_2$	0.02	12 h	–
$(Ir[dF(CF_3)ppy]_2(dtbpy))PF_6$	0.02	12 h	–
9-(2,6-diisopropylphenyl)-10-methylacridinium perchlorate	0.01	12 h	–
9-(mesityl)-10-methylacridinium tetrafluoroborate	0.01	12 h	–
9-(mesityl)-10-methylacridinium perchlorate	0.02	12 h	–
2,4,6-tri-(*p*-methoxyphenyl)pyrylium tetrafluoroborate	0.01	12 h	100%

*Catalyst loading is reported with respect to monomer concentration

Attempts of 4-Methoxystyrene Polymerizations

4-methoxystyrene can be polymerized with this catalytic system, however, the reaction proceeds only very slowly and does not reach full conversion even after several days. Polymerization typically produced only short polymers (M_n = 1.7 kg/mol) with moderate control ($Đ$ = 1.7). Higher catalyst loading improved the conversion but was detrimental to the control of the chain-length.

Appendix References

(1) Martiny, M.; Steckhan, E.; Esch, T. *Chem. Ber.* **1993**, *126*, 1671.

(2) Uchiyama, M.; Satoh, K.; Kamigaito, M. *Angew. Chem., Int. Ed.* **2015**, *54*, 1924.

(3) Kumagai, S.; Nagai, K.; Satoh, K.; Kamigaito, M. *Macromolecules* **2010**, *43*, 7523.

CHAPTER 3

PHOTOCONTROLLED INTERCONVERSION OF CATIONIC AND RADICAL POLYMERIZATIONS

3.1 Abstract

The ability to combine two polymerization mechanisms in a one-pot setup and switch the monomer selectivity via an external stimulus provides an excellent opportunity to control polymer sequence and structure. We report a strategy that enables monomer incorporation to be determined via the selection of the wavelength of light through selective activation of either cationic or radical processes. This method enables the synthesis of varying polymeric structures under identical solution conditions but with simple modulation of the external stimulus. Additionally, changes in the ratios of the two photocatalysts afford complementary chemical control over these reactions to design elaborated polymeric structures. Our strategy takes advantage of the unique regulation that can be accessed through light.

3.2 Introduction

During the past two decades, advances in polymer chemistry have enabled the synthesis of macromolecules with well-defined structures. However, an opportunity remains to develop strategies that offer precise control over polymer structure in a single efficient process. Specifically, the ability to switch the polymerization mechanism and hence the monomer selectivity *in situ*

by using an external stimulus is a grand challenge. Achieving such a breakthrough would streamline the synthesis of functional materials.

Light is one of the most powerful external stimuli and may be the key to addressing this challenge.[1] A renaissance of photochemistry has recently taken place in materials science, and a wide range of polymerization techniques that enable precise control of polymer chain growth with light have been developed.[2] The majority of these processes have been applied to radical polymerizations,[3,4] but recent advances have extended light regulation to cationic polymerizations.[5] Using these photopolymerizations, Boyer[6] as well as Goto and Kaji[7] have promoted two in situ polymerization processes with various wavelengths of light using a bifunctional initiator to form diblock copolymers. However, these methods do not allow conversion between polymerization mechanisms or monomer selectivity at a single propagating chain end. The ability to change the monomer selectivity in situ with light would provide a major opportunity to control polymer structure. Our group recently developed a photocontrolled cationic polymerization of vinyl ethers. The oxidation of a trithiocarbonate chain-transfer agent (CTA) with a photocatalyst yielded a cation that could promote the controlled polymerization of vinyl ethers in a reversible addition–fragmentation chain transfer (RAFT) polymerization process.[5a] Notably, using a reducing photocatalyst, Boyer[4a–4h] and others[4i,4j] have shown that similar trithiocarbonates can be used for the photocontrolled radical polymerization of acrylates.

We hypothesized that a combination of these photocontrolled cationic and radical processes would enable switching of the monomer selectivity in situ with light. Specifically, excitation of an oxidizing photocatalyst would generate a propagating cation and allow the selective polymerization of vinyl ethers. Conversely, excitation of a reducing photocatalyst would induce a radical mechanism selective for the polymerization of acrylates (Scheme 3.1). This mechanism would enable monomer incorporation to be determined via the selection of the wavelength of light and give precise control of the polymer structure through the use of an external stimulus. Beyond photocontrolled polymerizations, Satoh and Kamigaito[8] independently developed systems in which both radical and cationic polymerizations are concurrently active to allow copolymerizations of vinyl ethers and acrylates. Under these conditions, the trithiocarbonate chain end efficiently interconverts between cationic and radical mechanisms to yield multiblock structures. The data obtained with this system provide support for our hypothesis that we could efficiently switch the polymer chain growth from a cationic to a radical mechanism using the photocontrolled polymerizations discussed above.

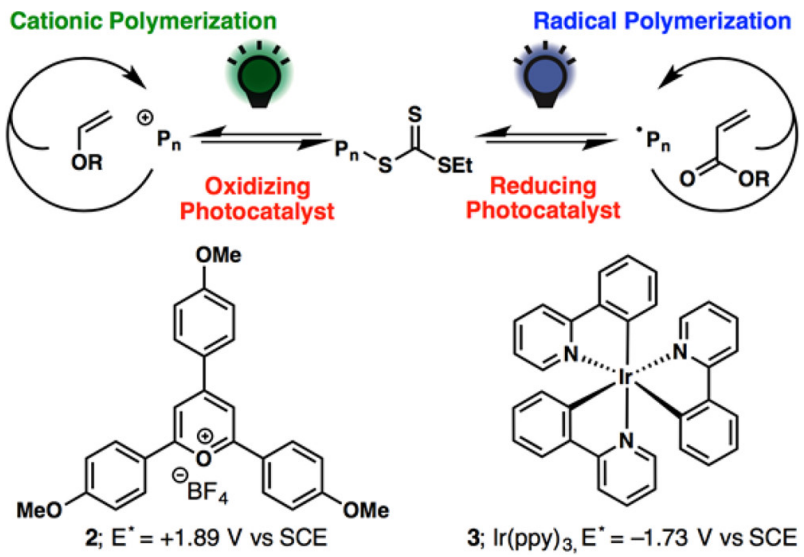

Scheme 3.1. Switching the Polymerization Mechanism and Monomer Selectivity by Changing the Wavelength of Light Irradiation

3.3 Results and Discussion

Our initial studies investigated the monomer selectivity under our cationic polymerization conditions. Using trithiocarbonate **1** as the CTA and 2,4,6-tri-(*p*-methoxyphenyl)pyrylium tetrafluoroborate (**2**) as the oxidizing photocatalyst, we irradiated an equimolar reaction mixture of isobutyl vinyl ether (IBVE) and methyl acrylate (MA) with blue light-emitting diodes (LEDs). After 2 h, a well-controlled poly(IBVE) homopolymer was formed, and no polymerization of MA was observed (Figure 3.1a). Notably, negligible conversion of MA was detected even after several days under these conditions. These results both clearly demonstrate that our photocontrolled cationic polymerization conditions using catalyst **2** lead to the selective polymerization of IBVE in the presence of MA

and, critically, establish that the putative radical species[5a] formed under these conditions do not initiate the polymerization of MA.

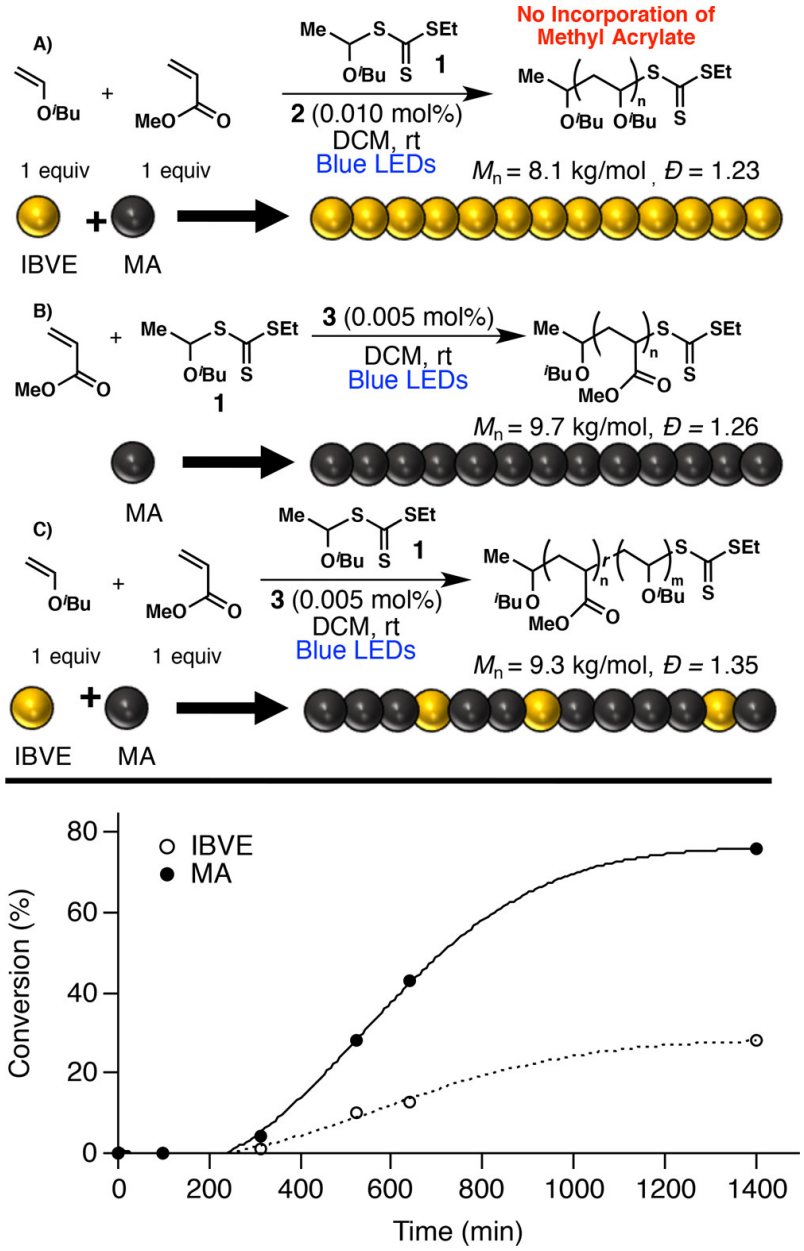

Figure 3.1. (a) Homopolymerization of IBVE in the presence of MA under standard oxidizing conditions. (b) Radical polymerization of MA in the presence of CTA **1** and $Ir(ppy)_3$ (**3**). (c) Statistical copolymerization of IBVE and MA under blue light during radical copolymerization.

Further studies probed photocontrolled radical polymerizations of MA with **1** as the CTA and $Ir(ppy)_3$ (**3**) as the reducing catalyst. Complex **3** has been used previously in photoinduced electron transfer RAFT (PET-RAFT)[4a] and photocontrolled atom transfer radical polymerization (ATRP)[3a] processes. Irradiation with blue light produced poly(methyl acrylate) with a number-average molar mass (M_n) of 9.7 kg/mol and a dispersity ($Đ$) of 1.26 within 23 h (Figure 3.1b). Notably, this result illustrates that radical polymerization can be efficiently initiated from the poly(IBVE) chain ends grown under our cationic polymerization conditions on the basis of their structural similarity with trithiocarbonate **1**, which is imperative for switching between cationic and radical polymerizations.

The radical polymerization with both IBVE and MA was probed using conditions analogous to those in the experiment in Figure 3.1a but substituting **2** with the reducing photocatalyst **3**. Exposure to blue light yielded a 9.3 kg/mol poly(IBVE-*r*-MA) random copolymer with ~30% incorporation of IBVE (Figure 3.1c). ^{13}C and ^{1}H NMR analyses showed that all of the IBVE units within the copolymer chain were flanked by two MA monomers. This result is consistent with other radical copolymerizations of these two monomers.[8]

With an understanding of the cationic and radical photopolymerizations with both IBVE and MA, we next investigated the use of light to switch between polymerization mechanisms. For these experiments, we used a combination of photocatalysts **2** and **3** with an equimolar mixture of IBVE and MA.[9] On the basis of the absorption windows of the two catalysts, we hypothesized that we could

selectively excite the oxidizing photocatalyst **2** in the presence of **3** with 520 nm light, which would result in the exclusive cationic polymerization of IBVE (Figure 3.2).[4a]

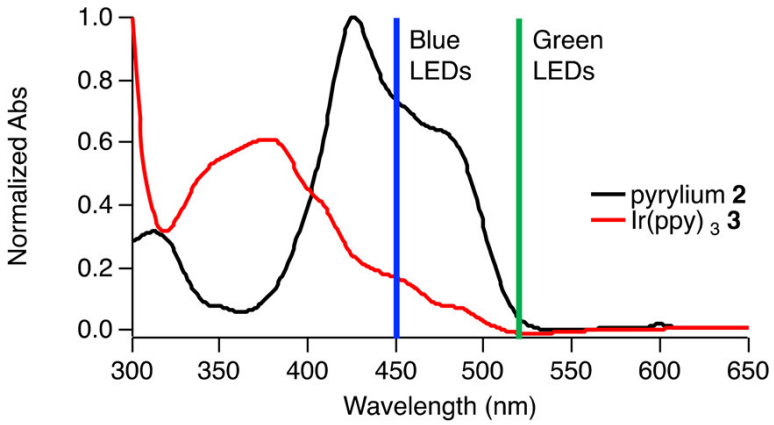

Figure 3.2. UV–vis absorption spectra of **2** and **3**.

In support of this hypothesis, the use of green LEDs yielded a well-controlled IBVE homopolymer with no evident MA conversion even after irradiation for several hours (Figure 3.3a(i)).[10] Under the same conditions, the light source was then switched to blue LEDs after almost 80% consumption of IBVE, which led to the excitation of **3** and initiated the radical polymerization of MA to give a poly(IBVE-*b*-MA) tapered diblock copolymer (Figure 3.3a(ii) and Figure 3.3b). This result shows that the polymerization mechanism can indeed be switched *in situ* from cationic to radical by changing the wavelength of the light.[11]

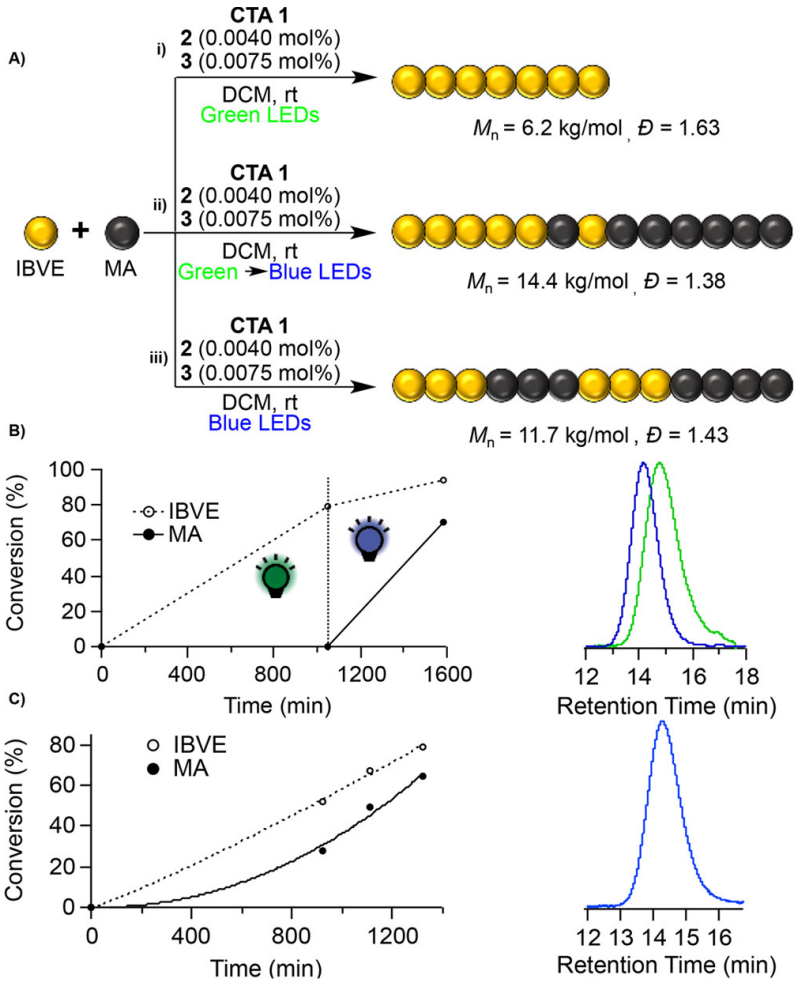

Figure 3.3. (a) Exposing an equimolar mixture of MA and IBVE (i) to green light selectively induces cationic polymerization, whereas (ii) exposure to green and then blue light creates a tapered diblock copolymer and (iii) exposure to blue light yields a multiblock copolymer. (b) Gel permeation chromatography (GPC) traces and monomer conversion of the diblock copolymer. (c) GPC traces and monomer conversion of in situ multiblock copolymer formation.

Notably, using the same reaction conditions with only blue-light irradiation yields a multiblock copolymer with M_n = 11.7 kg/mol and $Đ$ = 1.43 (Figure 3.3a(iii) and Figure 3.3c). Because both photocatalysts are excited by 450 nm light, the radical and cationic polymerizations are concurrently active under such conditions, which causes the polymer chain end to switch between

the two polymerization types (Figure 3.2). Data obtained by monitoring the conversion over the course of the reaction highlight the copolymerization of the two monomers (Figure 3.3c). Crossover peaks from the poly(IBVE) block to a poly(methyl acrylate) block and vice versa were clearly observed in the ^{13}C NMR spectrum and showed that these conditions led to a pentablock copolymer.[8b] Similar experiments were performed with chloroethyl vinyl ether and a variety of acrylates with comparable levels of control (see Appendix).

The three experiments in Figure 3.3 illustrate that we can tune the polymer structure with light using photocontrolled polymerizations. These experiments were performed under identical conditions in solution and varied only in the exposure to external light stimuli. With this variation, we can selectively induce one polymerization mechanism over the other with light and accordingly manipulate the final polymer structure. This new level of control brings us another step closer to light-mediated sequence control of polymers.[12] Along with light, the catalyst ratio can also be varied to control the polymer structure. Using double the amount of **2** with respect to **3** changed the polymer from a multiblock copolymer, as seen in Figure 3.3c, to a tapered diblock copolymer (Figure 3.4a(i)). Monitoring the conversion of both monomers over time revealed that the polymerization of IBVE started immediately upon irradiation, whereas the polymerization of MA had a large induction period and commenced only after the conversion of IBVE had reached 80% (Figure 3.4b). By further increasing the amount of **2**, we created a nontapered diblock

copolymer (Figure 3.4a(ii)). Under these conditions, the consumption of IBVE reached 100% before MA polymerization started (Figure 3.4c).

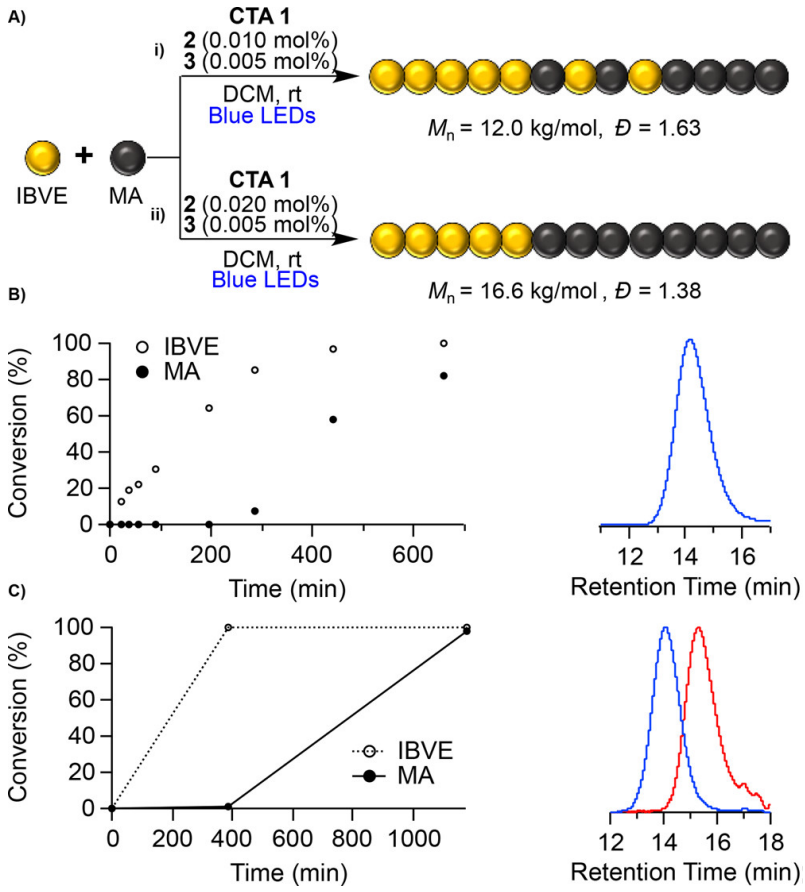

Figure 3.4. (a) Reaction conditions for diblock copolymer synthesis under blue light. (b) Conversion and GPC trace of in situ tapered diblock copolymer formation. (c) Conversion and GPC trace of *in situ* nontapered diblock copolymer formation.

3.4 Conclusion

In conclusion, we have successfully coupled photocontrolled cationic and radical polymerization processes to enable switching of the polymerization mechanism and monomer selectivity by changing the wavelength of light. Under

identical solution conditions, we could discriminatorily synthesize a homo-, diblock, or multiblock polymer by adjusting our external stimulus, light. The ability to use light as a tool to manipulate the identity of propagating chain ends can simplify a multistep synthesis to a one-pot procedure and, importantly, enable the synthesis of novel polymeric materials. Notably, facile switching from cationic to radical polymerization with light still remains a difficult challenge in this system. However, we expect this study to lay the groundwork for a new strategy to control polymer structure and architecture with light.

3.5 References

(1) Prier, C. K.; Rankic, D. A.; MacMillan, D. W. C. *Chem. Rev.* **2013**, *113*, 5322.

(2) (a) Chen, M.; Zhong, M.; Johnson, J. A. *Chem. Rev.* **2016**, *116*, 10167. (b) Corrigan, N.; Shanmugam, S.; Xu, J.; Boyer, C. *Chem. Soc. Rev.* **2016**, *45*, 6165. (c) Dadashi-Silab, S.; Doran, S.; Yagci, Y. *Chem. Rev*. **2016**, *116*, 10212.

(3) (a) Fors, B. P.; Hawker, C. J. *Angew. Chem., Int. Ed.* **2012**, *51*, 8850. (b) Konkolewicz, D.; Schroder, K.; Buback, J.; Bernhard, S.; Matyjaszewski, K. *ACS Macro Lett.* **2012**, *1*, 1219. (c) Anastasaki, A.; Nikolaou, V.; Zhang, Q.; Burns, J.; Samanta, S. R.; Waldron, C.; Haddleton, A. J.; McHale, R.; Fox, D.; Percec, V.; Wilson, P.; Haddleton, D. M. *J. Am. Chem. Soc.* **2014**, *136*, 1141. (d) Treat, N. J.; Sprafke, H.; Kramer, J. W.; Clark, P. G.; Barton, B. E.; Read de Alaniz, J.; Fors, B. P.; Hawker, C. J.

J. Am. Chem. Soc. **2014**, *136*, 16096. (e) Pan, X.; Malhotra, N.; Simakova, A.; Wang, Z.; Konkolewicz, D.; Matyjaszewski, K. *J. Am. Chem. Soc.* **2015**, *137*, 15430. (f) Jones, G. R.; Whitfield, R.; Anastasaki, A.; Haddleton, D. M. *J. Am. Chem. Soc.* **2016**, *138*, 7346. (g) Theriot, J. C.; Lim, C.-H.; Yang, H.; Ryan, M. D.; Musgrave, C. B.; Miyake, G. M. *Science* **2016**, *352*, 1082. (h) Pearson, R. M.; Lim, C.-H.; McCarthy, B. G.; Musgrave, C. B.; Miyake, G. M. *J. Am. Chem. Soc.* **2016**, *138*, 11399. (i) Ramsey, B. L.; Pearson, R. M.; Beck, L. R.; Miyake, G. M. *Macromolecules* **2017**, *50*, 2668. (j) Koumura, K.; Satoh, K.; Kamigaito, M. *Macromolecules* **2008**, *41*, 7359.

(4) (a) Xu, J.; Jung, K.; Atme, A.; Shanmugam, S.; Boyer, C. *J. Am. Chem. Soc.* **2014**, *136*, 5508. (b) Shanmugam, S.; Xu, J.; Boyer, C. *J. Am. Chem. Soc.* **2015**, *137*, 9174. (c) Xu, J.; Shanmugam, S.; Duong, H. T.; Boyer, C. *Polym. Chem.* **2015**, *6*, 5615. (d) Shanmugam, S.; Xu, J.; Boyer, C. *Chem. Sci.* **2015**, *6*, 1341. (e) Shanmugam, S.; Xu, J.; Boyer, C. *Angew. Chem., Int. Ed.* **2016**, *55*, 1036. (f) Xu, J.; Shanmugam, S.; Fu, C.; Aguey-Zinsou, K.; Boyer, C. *J. Am. Chem. Soc.* **2016**, *138*, 3094. (g) Xu, J.; Fu, C.; Shanmugam, S.; Hawker, C. J.; Moad, G.; Boyer, C. *Angew. Chem., Int. Ed.* **2017**, *56*, 8376. (h) Shanmugam, S.; Boyer, C. *J. Am. Chem. Soc.* **2015**, *137*, 9988. (i) Chen, M.; MacLeod, M. J.; Johnson, J. A. *ACS Macro Lett.* **2015**, *4*, 566. (j) Chen, M.; Deng, S.; Gu, Y.; Lin, J.; MacLeod, M. J.; Johnson, J. A. *J. Am. Chem. Soc.* **2017**, *139*, 2257.

(5) (a) Kottisch, V.; Michaudel, Q.; Fors, B. P. *J. Am. Chem. Soc.* **2016**, *138*, 15535. (b) Ogawa, K. A.; Goetz, A. E.; Boydston, A. J. *J. Am. Chem. Soc.* **2015**, *137*, 1400. (c) Goetz, A. E.; Boydston, A. J. *J. Am. Chem. Soc.* **2015**, *137*, 7572. (d) Pascual, L. M. M.; Dunford, D. G.; Goetz, A. E.; Ogawa, K. A.; Boydston, A. J. *Synlett* **2016**, 27, 759. (e) Goetz, A. E.; Pascual, L. M. M.; Dunford, D. G.; Ogawa, K. A.; Knorr, D. B., Jr.; Boydston, A. J. *ACS Macro Lett.* **2016**, *5*, 579. (f) Perkowski, A. J.; You, W.; Nicewicz, D. A. *J. Am. Chem. Soc.* **2015**, *137*, 7580. (g) Messina, M. S.; Axtell, J. C.; Wang, Y.; Chong, P.; Wixtrom, A. I.; Kirlikovali, K. O.; Upton, B. M.; Hunter, B. M.; Shafaat, O. S.; Khan, S. I.; Winkler, J. R.; Gray, H. B.; Alexandrova, A. N.; Maynard, H. D.; Spokoyny, A. M. *J. Am. Chem. Soc.* **2016**, *138*, 6952. (h) Michaudel, Q.; Kottisch, V.; Fors, B. P. *Angew. Chem., Int. Ed.* **2017**, *56*, 2.

(6) Fu, C.; Xu, J.; Boyer, C. *Chem. Commun.* **2016**, *52*, 7126.

(7) Ohtsuki, A.; Lei, L.; Tanishima, M.; Goto, A.; Kaji, H. *J. Am. Chem. Soc.* **2015**, *137*, 5610.

(8) (a) Satoh, K.; Hashimoto, H.; Kumagai, S.; Aoshima, H.; Uchiyama, M.; Ishibashi, R.; Fujiki, Y.; Kamigaito, M. *Polym. Chem.* **2017**, *8*, 5002. (b) Aoshima, H.; Uchiyama, M.; Satoh, K.; Kamigaito, M. *Angew. Chem., Int. Ed.* **2014**, *53*, 10932.

(9) In this system, electron transfer between the two catalysts could be occurring; future studies will investigate the mechanism and possible influence of this electron transfer on these polymerizations.

(10) During irradiation with green LEDs it is important to exclude all other light sources to avoid any radical polymerization.

(11) Switching from radical to cationic polymerization by changing the wavelength of light remains difficult because formation of the cation at the acrylate chain end is unfavorable.

(12) Lutz, J.-F.; Ouchi, M.; Liu, D. R.; Sawamoto, M. *Science* **2013**, *341*, 1238149.

3.6 Appendix

General Reagent Information

All polymerizations were set up in an Unilab MBraun glovebox with a nitrogen atmosphere and irradiated with blue LED light or green LED light under nitrogen atmosphere outside the glovebox. Isobutyl vinyl ether (IBVE) (99%, TCI), 2-chloroethyl vinyl ether (Cl-EVE) (97%, TCI), methyl acrylate (MA) (>99%, TCI), ethyl acrylate (EA) (Sigma Aldrich, 99%) and *tert*-butyl acrylate (tBA) (Sigma Aldrich, 98%) were dried over calcium hydride (CaH_2) (ACROS organics, 93% extra pure, 0-2 mm grain size) for 12 h and distilled under nitrogen and degassed by vigorously sparging with nitrogen for 30 minutes. Ethanethiol (97%, Alfa Aesar) and carbon disulfide (99.9+%, Alfa Aesar) were distilled before use. 2.0M HCl in Et_2O (Sigma Aldrich), Tris[2-phenylpyridinato-C2,N]iridium(III) ($Ir(ppy)_3$, **3**) (Ark Pharm) and sodium hydride (60%, dispersion in mineral oil, Sigma Aldrich) were used as received. Dichloromethane (DCM) and diethylether (Et_2O) were purchased from J.T. Baker and were purified by vigorous purging with argon for 2 h, followed by passing through two packed columns of neutral alumina under argon pressure. 2,4,6-tri-(*p*-methoxyphenyl)pyrylium tetrafluoroborate[1] (**2**) and S-1-isobutoxylethyl S'-ethyl trithiocarbonate[2] (**1**) were synthesized according to literature procedures.

General Analytical Information

All polymer samples were analyzed using a Tosoh EcoSec HLC 8320GPC system with two SuperHM-M columns in series at a flow rate of 0.350

mL/min. THF was used as the eluent and all number-average molecular weights (M_n), weight-average molecular weights (M_w), and dispersities ($Đ$) for all copolymers were calculated from refractive index chromatograms against TSKgel polystyrene standards. Number-average molecular weights (M_n), weight-average molecular weights (M_w), and dispersities ($Đ$) for homopolymers in Figure 3.1 were determined by light scattering using a Wyatt miniDawn Treos multi-angle light scattering detector. Nuclear magnetic resonance (NMR) spectra were recorded on a Varian 400 MHz, Bruker 500 MHz, or a Varian 600 MHz instrument at room temperature using $CDCl_3$ as a solvent. UV-vis spectra in DCM were recorded on a Varian Cary 50 Bio UV-Visible Spectrophotometer.

General Reaction Setup

Irradiation of photochemical reactions was done using blue diode led® BLAZETM lights (450 nm, 2.88 W/ft) or green LED strip lights (FlexTec®, 520 nm, 4.5W/ft). The inside of a crystallization dish was lined with led strips to irradiate the reaction vessel uniformly. The reaction was cooled by blowing compressed air over the reaction vial. It is important to remove any other light source from the vicinity of the reaction when irradiating with green LEDs. Already small amounts of higher energy light or heat can induce polymerization of MA.

General Procedure for Tapered Block Copolymer Formation from Isobutyl Vinyl Ether and Methyl Acrylate

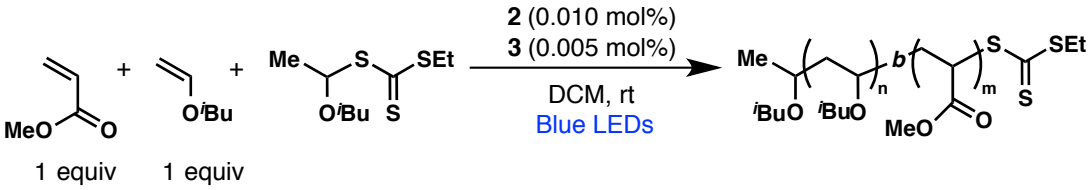

In a nitrogen filled glove box, an oven-dried one-dram vial was equipped with a stir bar and charged with IBVE (0.26 mL, 2.00 mmol, 100 equiv), MA (0.18 mL, 2.00 mmol, 100 equiv), 0.1 mL of a stock solution of 2,4,6-tri-(*p*-methoxyphenyl)pyrylium tetrafluoroborate (**2**) in DCM (2.0 mM, 0.20 μmol, 0.01 mol % relative to IBVE), 0.065 mL of a stock solution of $Ir(ppy)_3$ (**3**) in DCM (1.5 mM, 0.10 μmol, 0.005 mol % relative to MA), 0.02 mL of a stock solution of **1** in DCM (1 M, 0.02 mmol, 1 equiv), and additional 0.17 mL of DCM. Benzene (89 μL, 1.0 mmol, 25 equiv) was added as an internal standard for NMR. The vial was sealed with a septum cap under an atmosphere of nitrogen, placed next to blue LED strips (~450 nm) outside of the glove box, and stirred while cooling by blowing compressed air over the reaction vial. Aliquots for NMR and GPC analysis were taken at designated time points. Full conversion was generally reached after 10–12 hours. The solvent was removed under *vacuo*. The polymer can be purified by precipitation in cold isopropanol to remove residual pIBVE homopolymer. A typical ^{1}H NMR for poly(isobutyl vinyl ether-*b*-methyl acrylate) is shown in Figure 3.5.

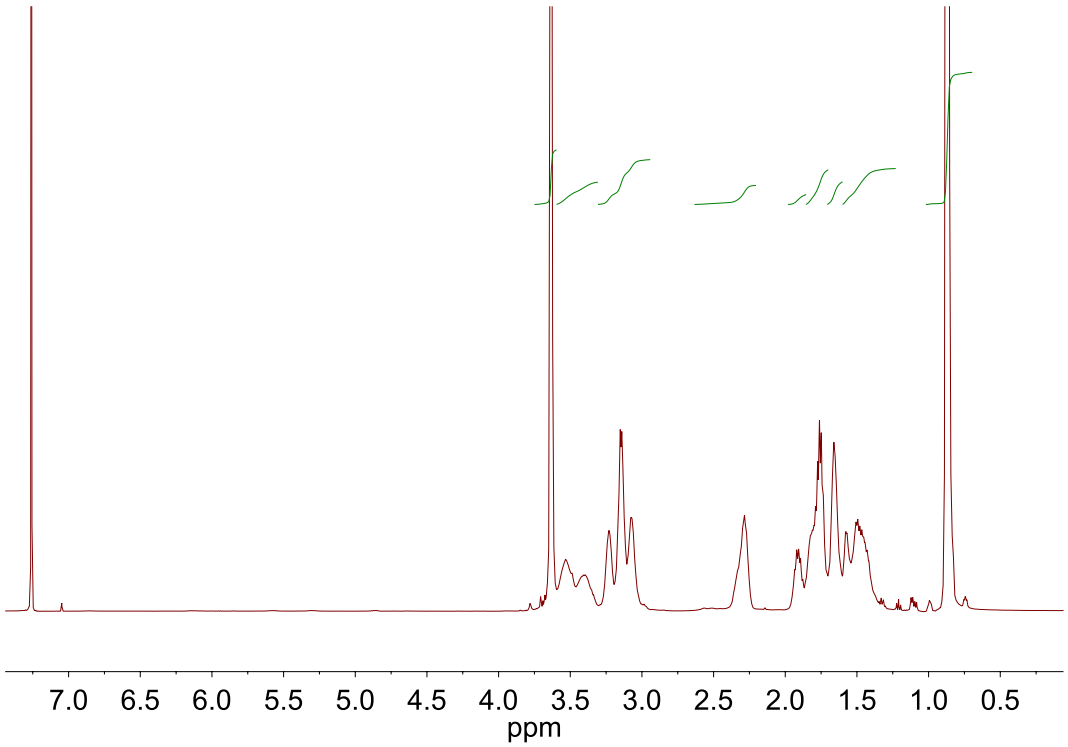

Figure 3.5. ^{1}H NMR of poly(isobutyl vinyl ether-*b*-methyl acrylate) (M_n = 12.0 kg/mol, $Đ$ = 1.63, $M_{n,theo}$ = 17.1 kg/mol).

General Procedure for Multiblock Copolymer Formation from Isobutyl Vinyl Ether and Methyl Acrylate

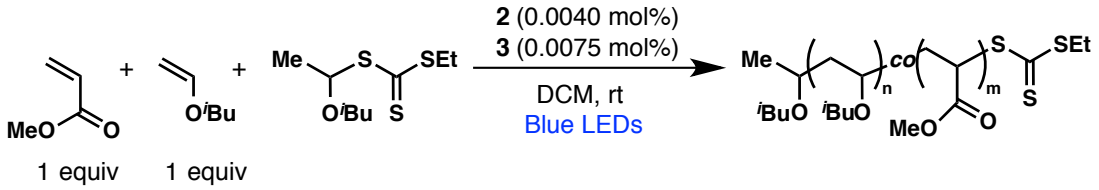

In a nitrogen filled glove box, an oven-dried one-dram vial was equipped with a stir bar and charged with IBVE (0.26 mL, 2.00 mmol, 100 equiv), MA (0.18 mL, 2.00 mmol, 100 equiv), 0.040 mL of a stock solution of 2,4,6-tri-(*p*-methoxyphenyl)pyrylium tetrafluoroborate (**2**) in DCM (2.0 mM, 0.04 μmol,

0.004 mol % relative to IBVE), 0.10 mL of a stock solution of $Ir(ppy)_3$ (**3**) in DCM (1.5 mM, 0.15 μmol, 0.0075 mol % relative to MA), 0.02 mL of a stock solution of **1** in DCM (1 M, 0.02 mmol, 1 equiv), and additional 0.19 mL of DCM. Benzene (89 μL, 1.0 mmol, 25 equiv) was added as an internal standard for NMR. The vial was sealed with a septum cap under an atmosphere of nitrogen, placed next to blue LED strips (~450 nm) outside of the glove box, and stirred while cooling by blowing compressed air over the reaction vial. Aliquots for NMR and GPC analysis were taken at designated time points. Conversion of 80% was generally reached after 24 hours. The solvent was removed under *vacuo* to yield the pure polymer. A typical ^{1}H NMR and ^{13}C NMR for poly(isobutyl vinyl ether-*co*-methyl acrylate) are shown in Figure 3.6 and 3.7, respectively. The number of crossovers was determined from the ratio of the methine carbon signal of *p*IBVE (73.8 ppm) and crossover peak (74.6 ppm). The integrations of five identical experiments were averaged.

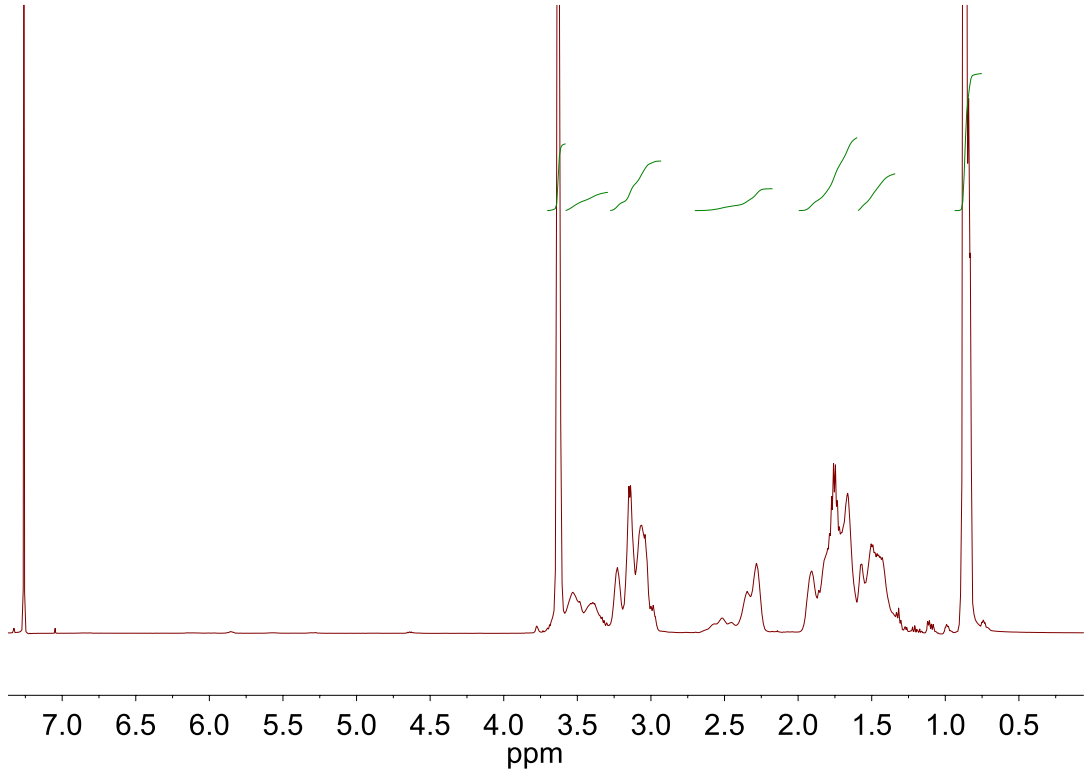

Figure 3.6. ^{1}H NMR of poly(isobutyl vinyl ether-*co*-methyl acrylate) (M_n = 11.7 kg/mol, $Đ$ = 1.43, $M_{n,theo}$ = 14.1 kg/mol).

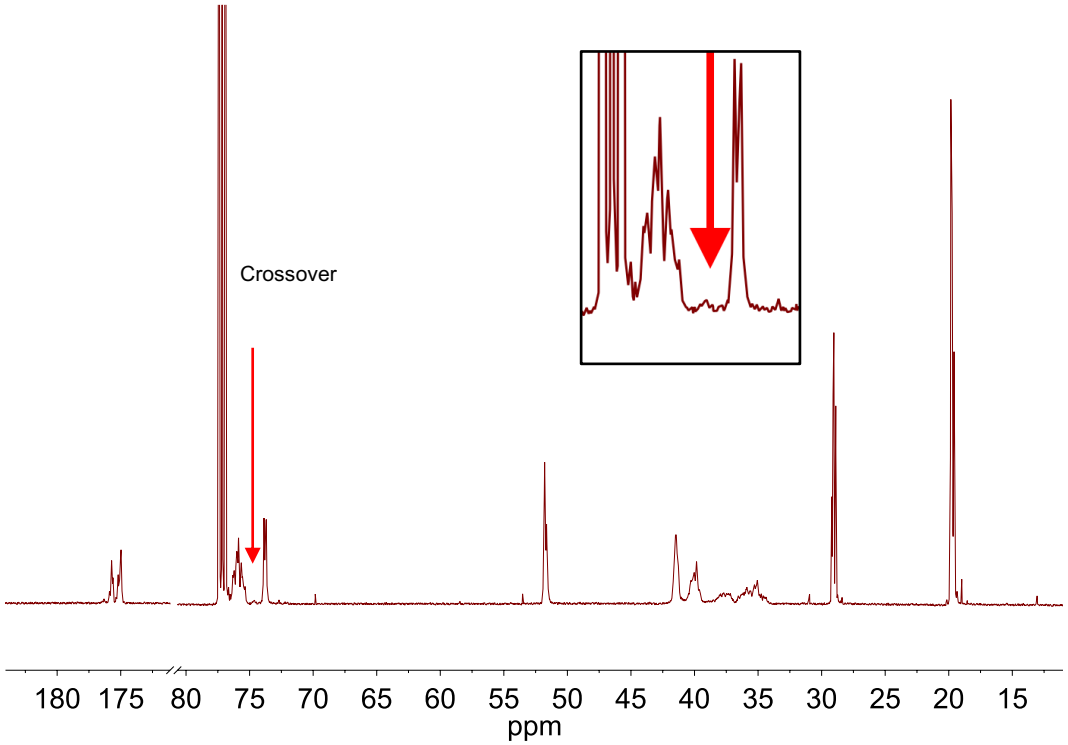

Figure 3.7. ^{13}C NMR of poly(isobutyl vinyl ether-*co*-methyl acrylate).

General Procedure for Random Copolymer Formation from Isobutyl Vinyl Ether and Methyl Acrylate via a Radical Mechanism

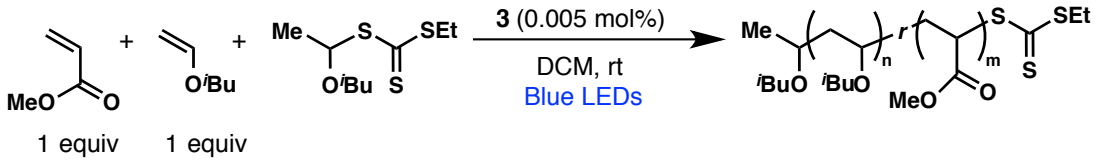

In a nitrogen filled glove box, an oven-dried one-dram vial was equipped with a stir bar and charged with IBVE (0.26 mL, 2.00 mmol, 100 equiv), MA (0.18 mL, 2.00 mmol, 100 equiv), 0.065 mL of a stock solution of $Ir(ppy)_3$ (**3**) in DCM (1.5 mM, 0.10 μmol, 0.005 mol % relative to MA), 0.02 mL of a stock solution of

1 in DCM (1 M, 0.02 mmol, 1 equiv), and additional 0.22 mL of DCM. Benzene (89 μL, 1.0 mmol, 25 equiv) was added as an internal standard for NMR. The vial was sealed with a septum cap under an atmosphere of nitrogen, placed next to blue LED strips (~450 nm) outside of the glove box, and stirred while cooling by blowing compressed air over the reaction vial. Aliquots for NMR and GPC analysis were taken at designated time points. Conversion of 80% of MA was generally reached after 24 hours. The solvent was removed under *vacuo* to yield the pure polymer. A typical ^{1}H NMR and ^{13}C NMR for poly(isobutyl vinyl ether-*r*-methyl acrylate) are shown in Figure 3.8 and 3.9, respectively.

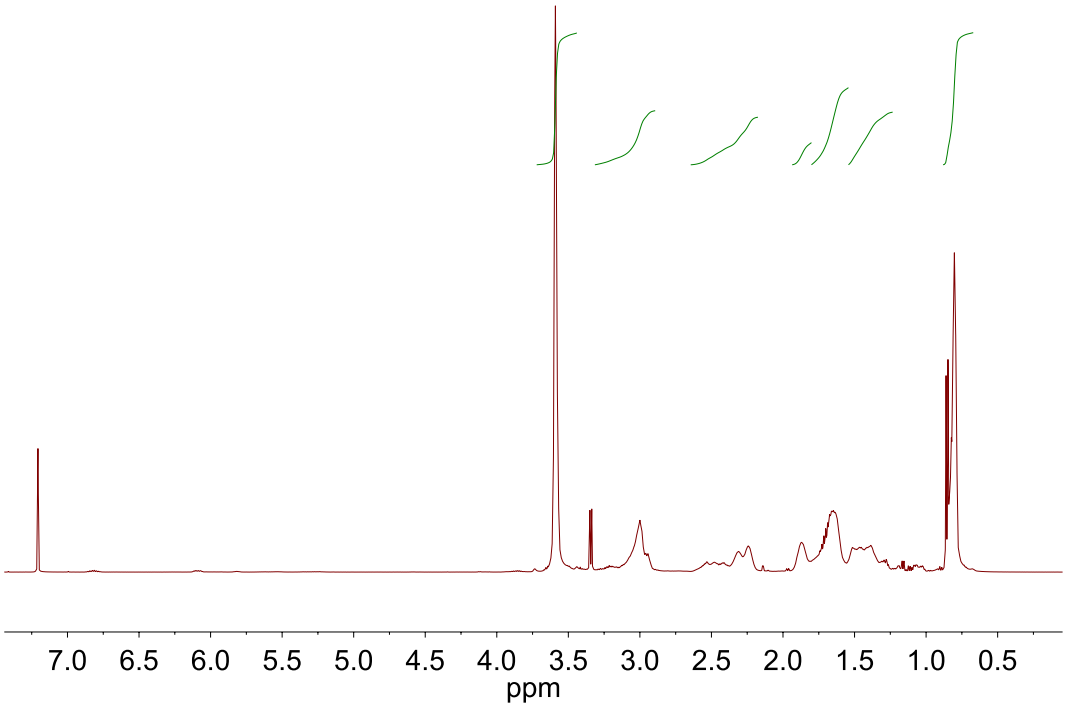

Figure 3.8. ^{1}H NMR of poly(isobutyl vinyl ether-*r*-methyl acrylate) *(*M_n = 9.3 kg/mol, $Đ$ = 1.35*,* $M_{n,theo}$ = 9.3 kg/mol*)*.

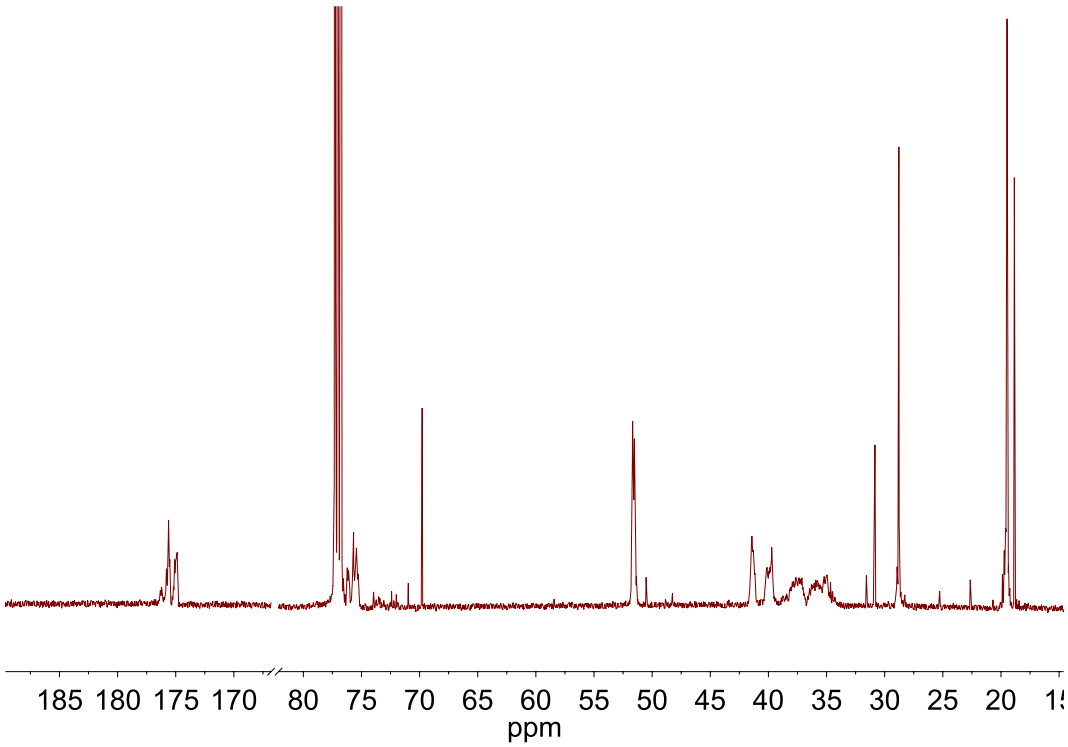

Figure 3.9. ^{13}C NMR of poly(isobutyl vinyl ether-*r*-methyl acrylate).

General Procedure for Diblock Copolymer from Isobutyl Vinyl Ether and Methyl Acrylate via Consecutive Exposure to Green and Blue Light

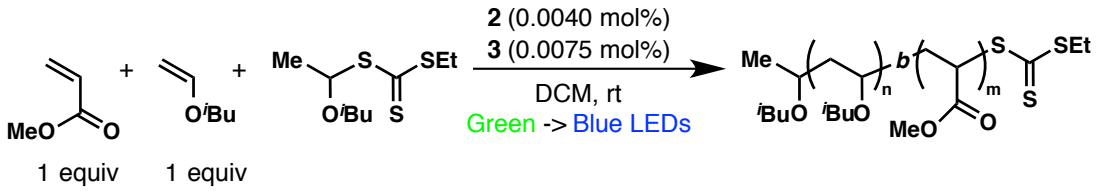

The reaction conditions were identical to the *General Procedure for Multiblock Copolymer Formation*. Two identical vials were prepared, then sealed with a septum cap under an atmosphere of nitrogen, placed next to green LED strips (~540 nm) outside of the glove box, and stirred while cooling by

blowing compressed air over the reaction vial. One of the reactions was typically stopped after 18 hours and analyzed by NMR and GPC. Conversion of IBVE 80% (MA = 0% conversion) was generally reached after 18 hours. The second vial was then placed next to blue LED strips (~540 nm) and stirred while cooling by blowing compressed air over the reaction vial. The crude reaction mixture was analysed by NMR and GPC (IBVE: 94% conv, MA: 70% conv., M_n = 9.6 kg/mol, $Đ$ = 1.70). The diblock copolymer was purified by precipitation from cold isopropanol to remove terminated *p*IBVE homopolymer. ^{1}H NMR of the crude and purified diblock copolymer are shown in Figure 3.10 and 3.11, respectively.

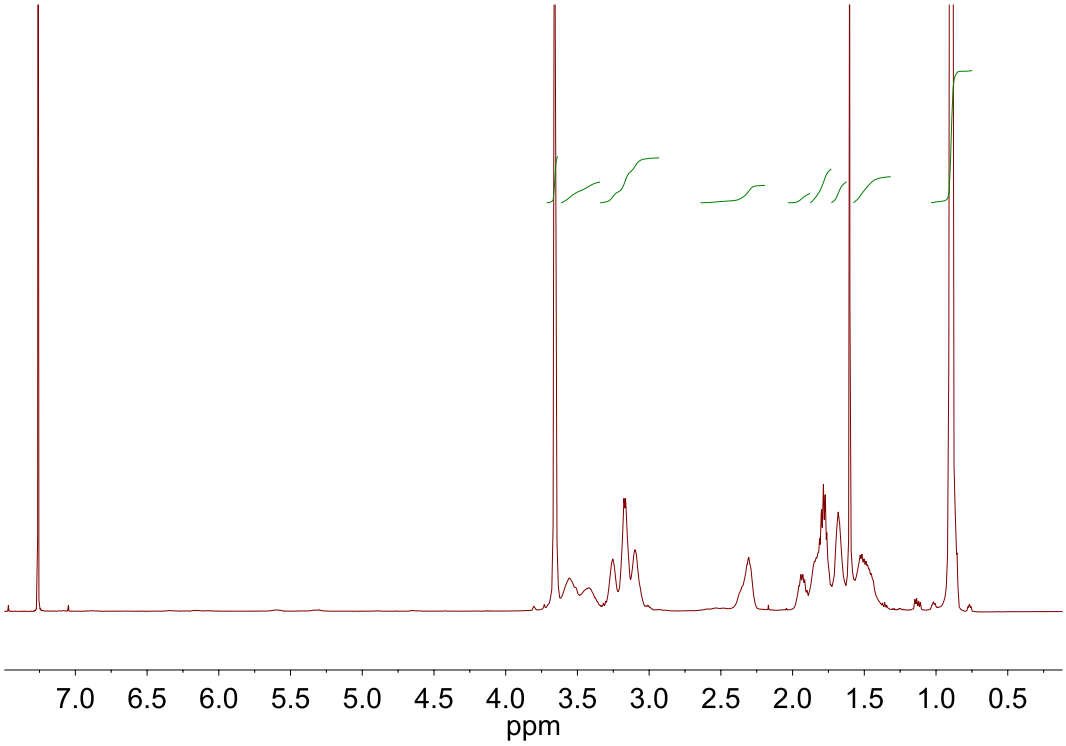

Figure 3.10. ^{1}H NMR of poly(isobutyl vinyl ether-*b*-methyl acrylate) (before purification) (M_n = 9.6 kg/mol, $Đ$ = 1.70).

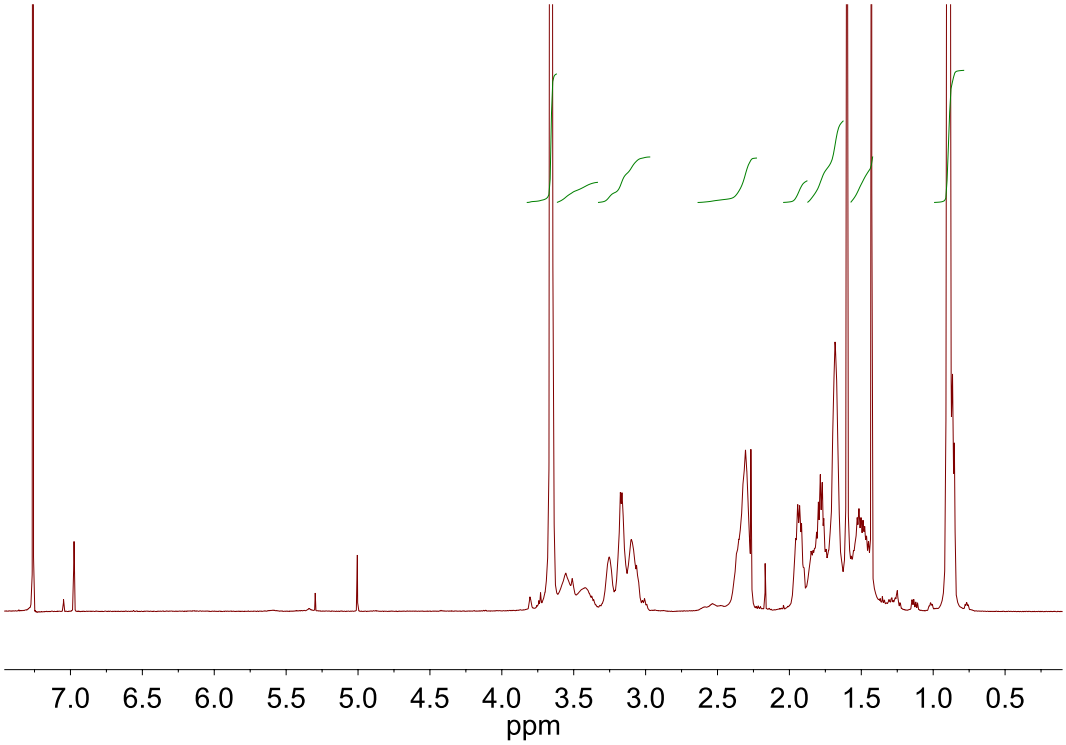

Figure 3.11. ^{1}H NMR of poly(isobutyl vinyl ether-*b*-methyl acrylate) (after purification) (M_n = 14.4 kg/mol, $Đ$ = 1.38, $M_{n,theo}$ = 13.9 kg/mol).

General Procedure for Diblock Copolymer from Isobutyl Vinyl Ether and Methyl Acrylate

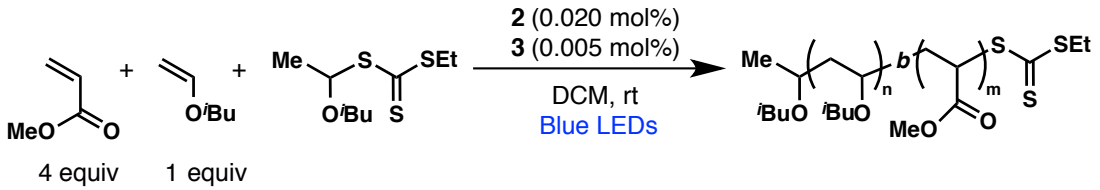

In a nitrogen filled glove box, an oven-dried one-dram vial was equipped with a stir bar and charged with IBVE (0.08 mL, 0.6 mmol, 30 equiv), MA (0.21 mL, 2.33 mmol, 117 equiv), 0.060 mL of a stock solution of 2,4,6-tri-(*p*-methoxyphenyl)pyrylium tetrafluoroborate (**2**) in DCM (2.0 mM, 0.12 μmol, 0.02 mol % relative to IBVE), 0.080 mL of a stock solution of $Ir(ppy)_3$ (**3**) in DCM (1.5

mM, 0.12 μmol, 0.005 mol % relative to MA), and 0.02 mL of a stock solution of **1** in DCM (1 M, 0.02 mmol, 1 equiv). The vial was sealed with a septum cap under an atmosphere of nitrogen, placed next to blue LED strips (~450 nm) outside of the glove box, and stirred while cooling by blowing compressed air over the reaction vial. Full conversion of *p*IBVE was generally reached after 7 hours. The reaction was stopped after 20 hours. The diblock copolymer was purified twice by precipitation from cold isopropanol. ^{1}H NMR of the crude and purified diblock copolymer are shown in Figure 3.12 and 3.13, respectively.

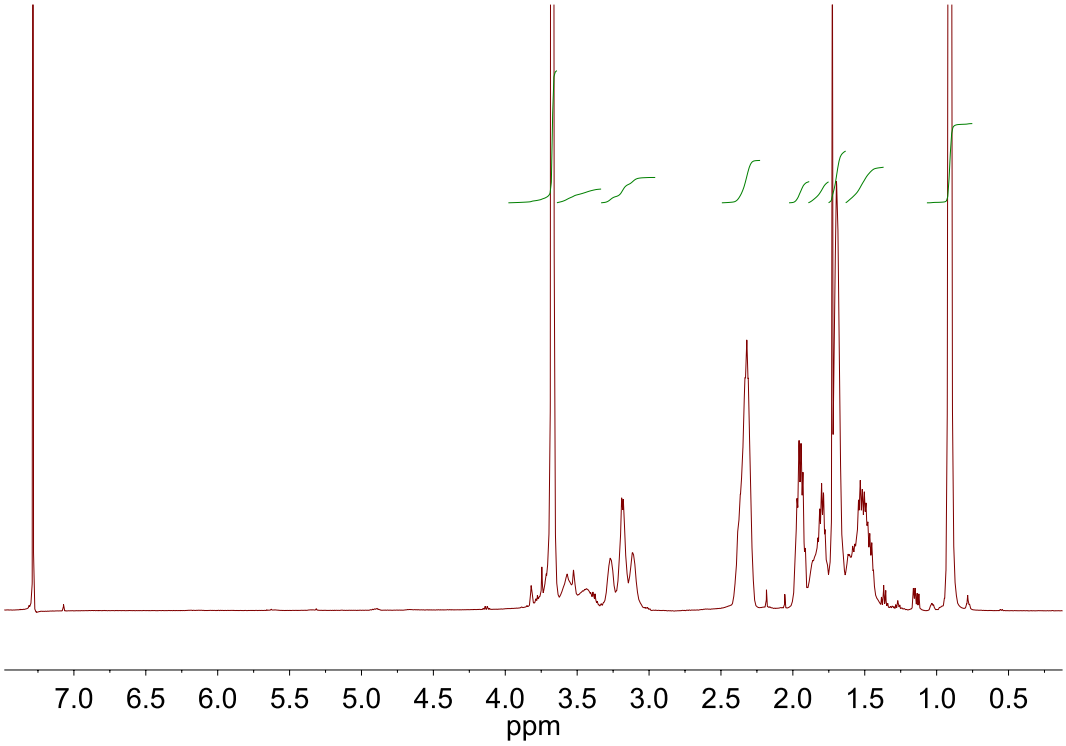

Figure 3.12. ^{1}H NMR of poly(isobutyl vinyl ether-*b*-methyl acrylate) (before purification) (M_n = 10.9 kg/mol, $Đ$ = 1.83).

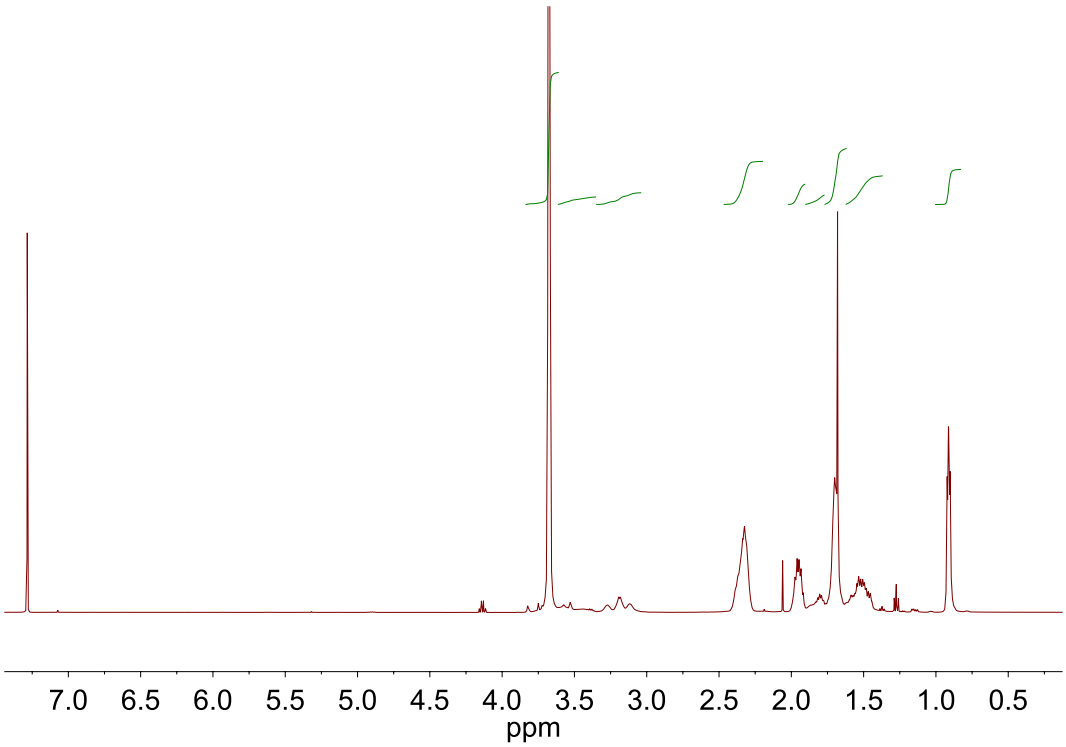

Figure 3.13. ^{1}H NMR of poly(isobutyl vinyl ether-*b*-methyl acrylate) (after purification) (M_n = 16.6 kg/mol, $Đ$ = 1.38, $M_{n,theo}$ = 12.8 kg/mol).

General Procedure for Isobutyl Vinyl Ether Polymerization in the Presence of Methyl Acrylate

In a nitrogen filled glove box, an oven-dried one-dram vial was equipped with a stir bar and charged with IBVE (0.26 mL, 2.00 mmol, 100 equiv), MA (0.18 mL, 2.00 mmol, 100 equiv), 0.01 mL of a stock solution of 2,4,6-tri-(*p*-methoxyphenyl)pyrylium tetrafluoroborate (**2**) in DCM (2.0 mM, 0.02 μmol, 0.01 mol % relative to IBVE), 0.02 mL of a stock solution of **1** in DCM (1 M, 0.02 mmol, 1 equiv), and additional 0.13 mL of DCM. Benzene (89 μL, 1.0 mmol, 25 equiv) was added as an internal standard for NMR. The vial was sealed with a septum cap under an atmosphere of nitrogen, placed next to blue LED strips

(~450 nm) outside of the glove box, and stirred while cooling by blowing compressed air over the reaction vial. The reaction was stopped after three days and subjected to GPC and NMR analysis (IBVE = 100% conv., MA = 6% conv., M_n = 8.1 kg/mol, $Đ$ = 1.23). A standard reaction for IBVE polymerizations can be stopped after a few hours, after which no MA polymerization has typically occurred.

Reactions with 2-Chloroethyl Vinyl Ether:

General Procedure for Radical Copolymerization of 2-Chloroethyl Vinyl Ether and Acrylates (MA, EA, tBA)

In a nitrogen filled glove box, an oven-dried one-dram vial was equipped with a stir bar and charged with Cl-EVE (0.21 mL, 2.00 mmol, 100 equiv), the desired acrylate (2.00 mmol, 100 equiv), 0.13 mL of a stock solution of $Ir(ppy)_3$ (**3**) in DCM (1.5 mM, 0.20 μmol, 0.01 mol % relative to MA), 0.02 mL of a stock solution of **1** in DCM (1 M, 0.02 mmol, 1 equiv), and additional 0.20 mL of DCM. Benzene (30 μL, 0.34 mmol, 8 equiv) was added as an internal standard for NMR. The vial was sealed with a septum cap under an atmosphere of nitrogen, placed next to blue LED strips (~450 nm) outside of the glove box, and stirred while cooling by blowing compressed air over the reaction vial. Aliquots for NMR and GPC analysis were taken at designated time points. Acrylate generally reached 80% conversion after 30–45 hours. The solvent and unreacted

monomer were removed under *vacuo* to yield the pure polymer. NMR spectra for poly(2-chloroethyl vinyl ether-*r*-acrylate) are shown in Figure 3.14–3.17. The results of Cl-EVE-acrylate radical copolymerizations can be seen in Table 3.1.

Table 3.1. Radical copolymerizations of a variety of acrylates with Cl-EVE.

Acrylate	**Conv.$_{Acrylate}$ (%)**	**Conv.$_{VE}$ (%)**	**Time (h)**	**M_n (kg/mol)**	**$M_{n,theo}$ (kg/mol)**	**$Đ$**
MA	79	33	26	6.5	10.3	1.41
EA	82	28	48	9.0	11.2	1.37
tBA	76	22	48	13.8	12.1	1.42

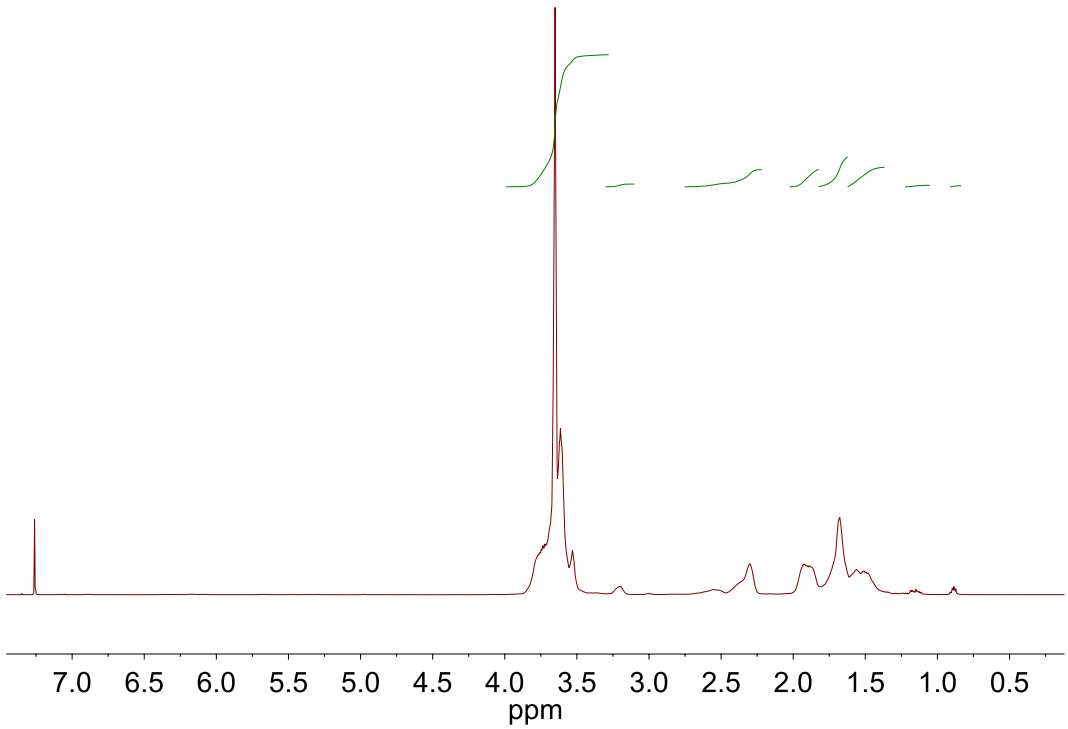

Figure 3.14. ^{1}H NMR of poly(2-chloroethyl vinyl ether-*r*-methyl acrylate)(M_n = 6.5 kg/mol, $Đ$ = 1.41, $M_{n,theo}$ = 10.3 kg/mol).

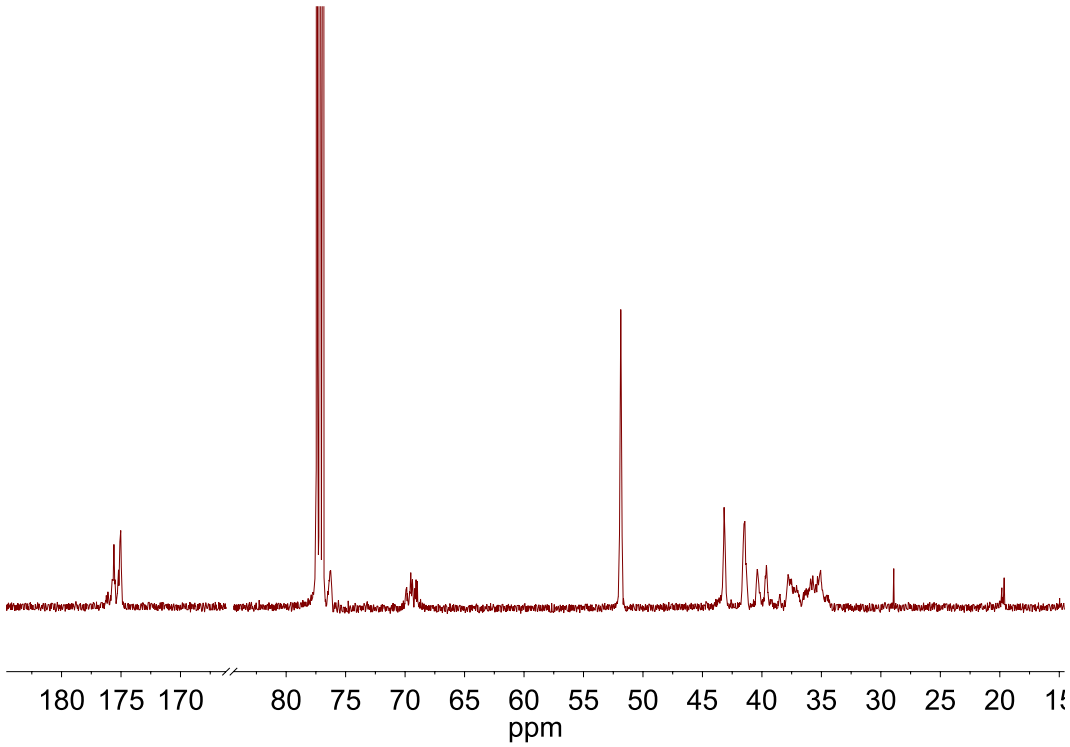

Figure 3.15. ^{13}C NMR of poly(2-chloroethyl vinyl ether-*r*-methyl acrylate) (M_n = 6.5 kg/mol, Đ = 1.41, $M_{n,theo}$ = 10.3 kg/mol).

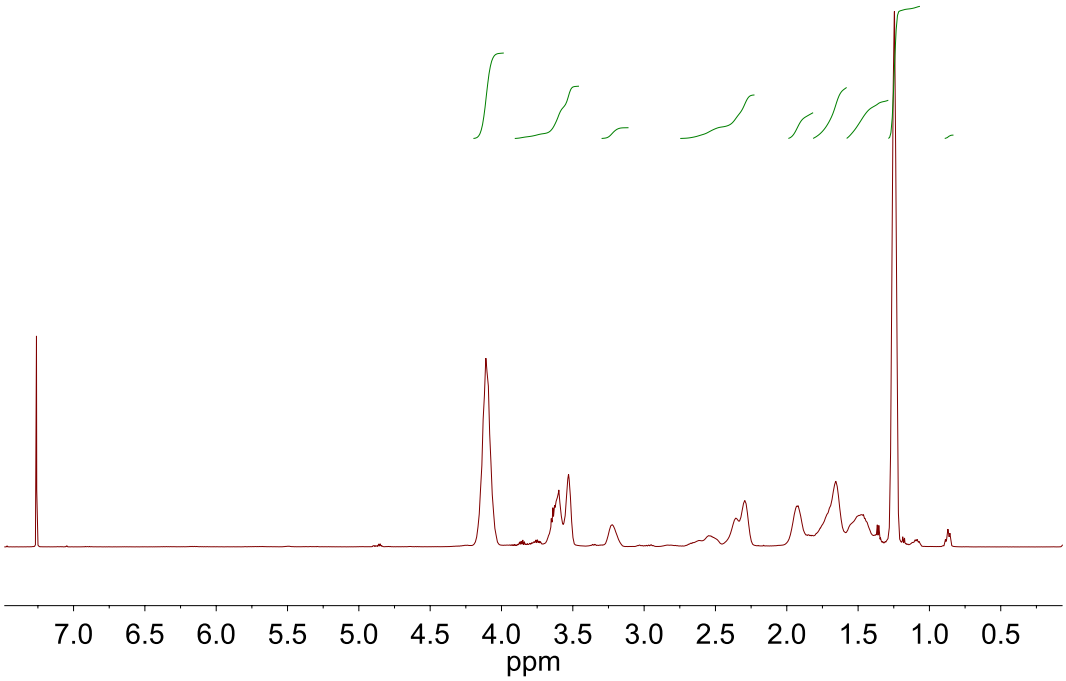

Figure 3.16. ^{1}H NMR of poly(2-chloroethyl vinyl ether-*r*-ethyl acrylate) (M_n = 9.0 kg/mol, $Đ$ = 1.37, $M_{n,theo}$ = 11.2 kg/mol).

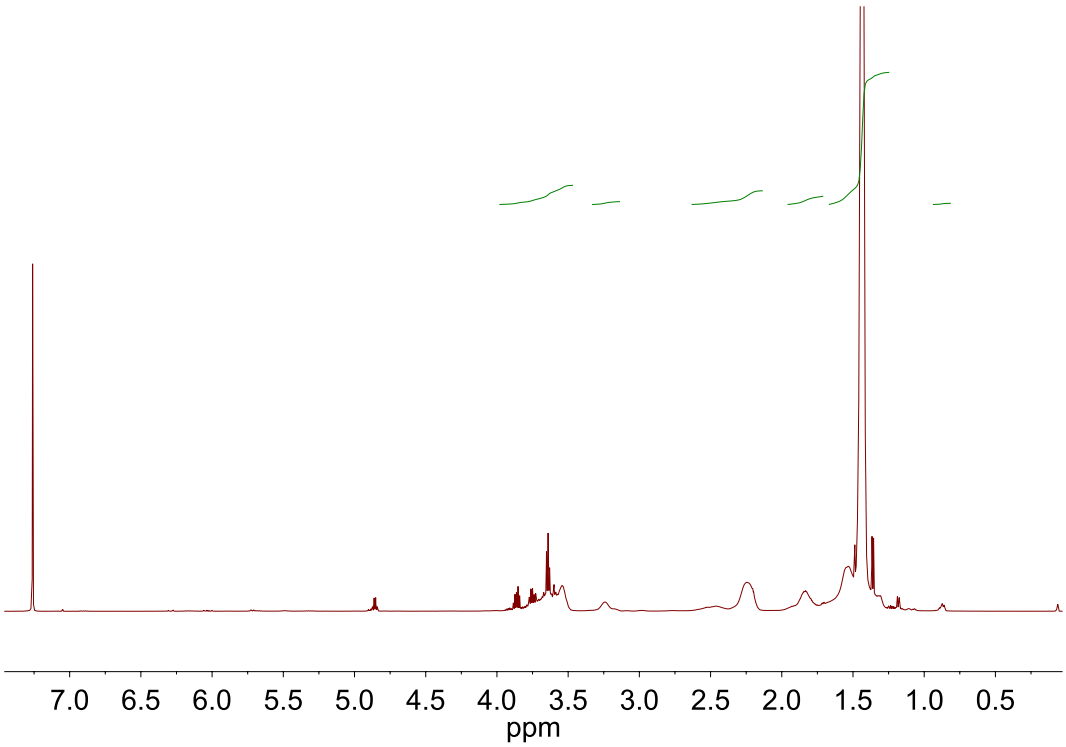

Figure 3.17. ^{1}H NMR of poly(2-chloroethyl vinyl ether-*r*-tert-butyl acrylate) (M_n = 13.8 kg/mol, $Đ$ = 1.42, $M_{n,theo}$ = 12.1 kg/mol).

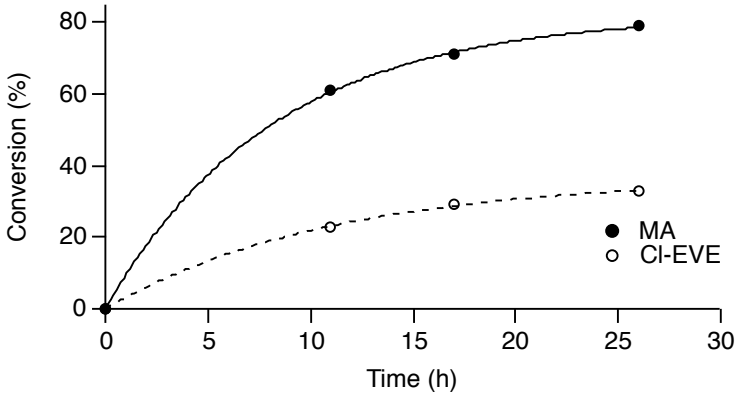

Figure 3.18. Radical copolymerization of methyl acrylate and 2-chloroethyl vinyl ether with $Ir(ppy)_3$.

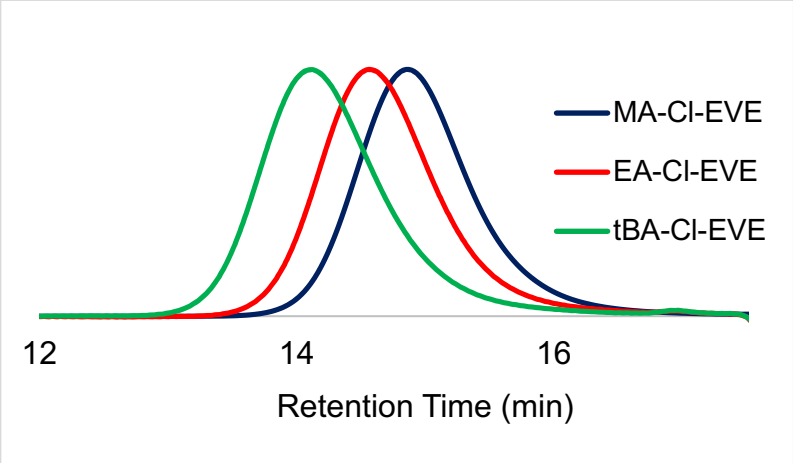

Figure 3.19. GPC traces of acrylate-2-chloroethyl vinyl ether copolymers (data from Table 3.1).

General Procedure for Multiblock Copolymerization of 2-Chloroethyl Vinyl Ether and Methyl Acrylate

In a nitrogen filled glove box, an oven-dried one-dram vial was equipped with a stir bar and charged with Cl-EVE (0.21 mL, 2.00 mmol, 100 equiv), MA (0.18 mL, 2.00 mmol, 100 equiv), 0.13 mL of a stock solution of $Ir(ppy)_3$ (**3**) in DCM (1.5 mM, 0.20 μmol, 0.01 mol % relative to MA), 0.18 mL of a stock solution of 2,4,6-tri-(*p*-methoxyphenyl)pyrylium tetrafluoroborate (**2**) in DCM (2.0 mM, 0.36 μmol, 0.018 mol % relative to Cl-EVE), 0.02 mL of a stock solution of **1** in DCM (1 M, 0.02 mmol, 1 equiv) and 0.02 mL of DCM. Benzene (30 μL, 0.34 mmol, 8 equiv) was added as an internal standard for NMR. The vial was sealed with a septum cap under an atmosphere of nitrogen, placed next to blue LED strips (~450 nm) outside of the glove box, and stirred while cooling by blowing compressed air over the reaction vial. Aliquots for NMR and GPC analysis were taken at designated time points. Full conversion of both monomers was

generally reached conversion after 44 hours. The solvent and unreacted monomer were removed under *vacuo* to yield the pure polymer. A typical ^{1}H NMR and ^{13}C NMR for poly(2-chloroethyl vinyl ether-*co*-methyl acrylate) are shown in Figure 3.20 and 3.21, respectively.

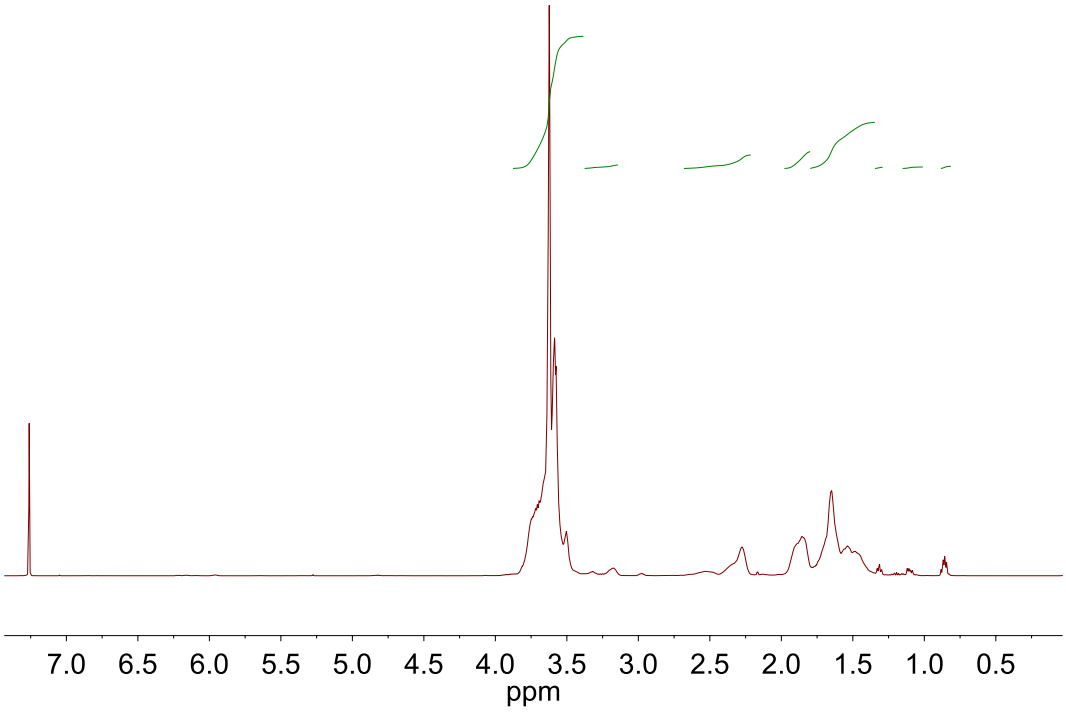

Figure 3.20. ^{1}H NMR of poly(2-chloroethyl vinyl ether-*co*-methyl acrylate) (M_n = 6.6 kg/mol, $Đ$ = 1.48, $M_{n,theo}$ = 9.8 kg/mol).

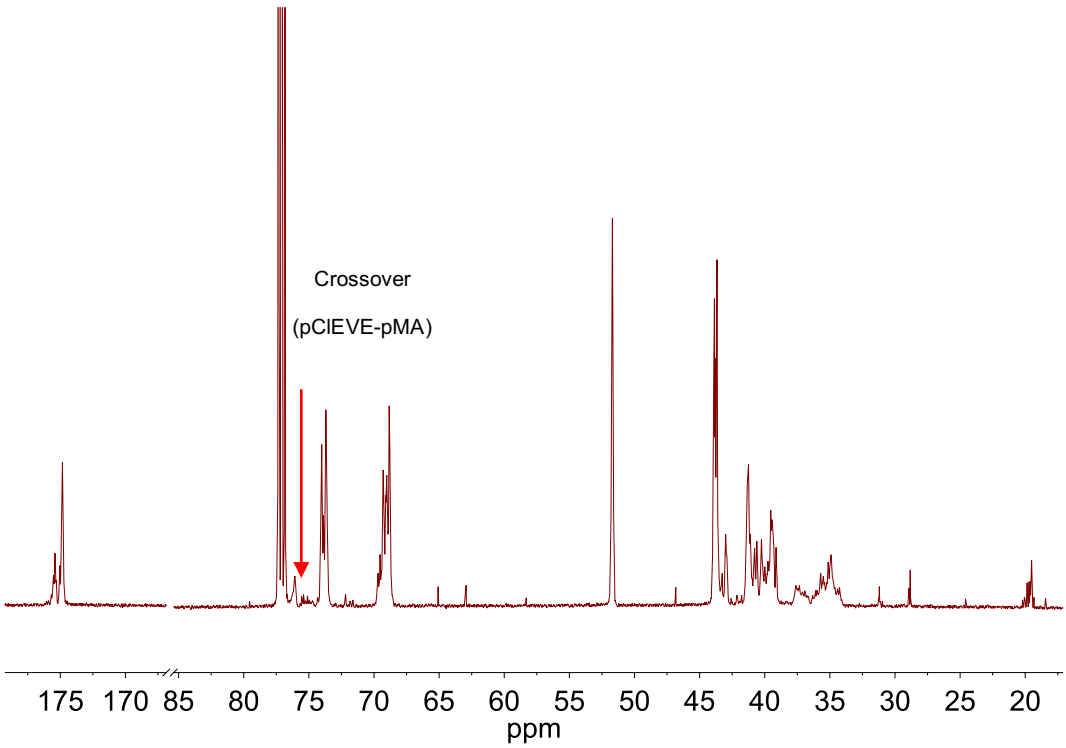

Figure 3.21. ^{13}C NMR of poly(2-chloroethyl vinyl ether-*co*-methyl acrylate) (M_n = 6.6 kg/mol, $Đ$ = 1.48, $M_{n,theo}$ = 9.8 kg/mol).

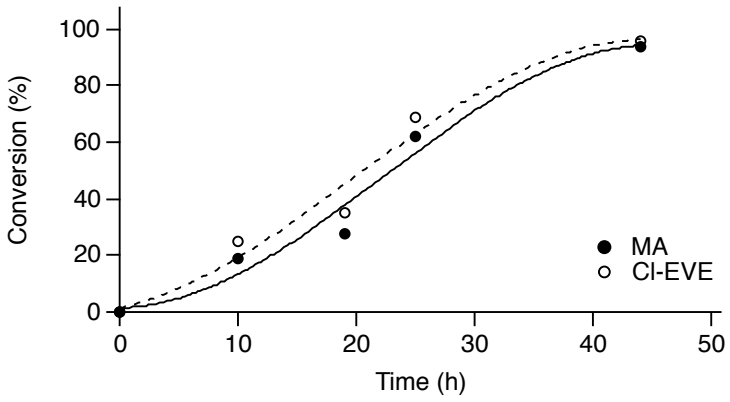

Figure 3.22. Multiblock copolymerization of methyl acrylate and 2-chloroethyl vinyl ether with $Ir(ppy)_3$ and pyrylium.

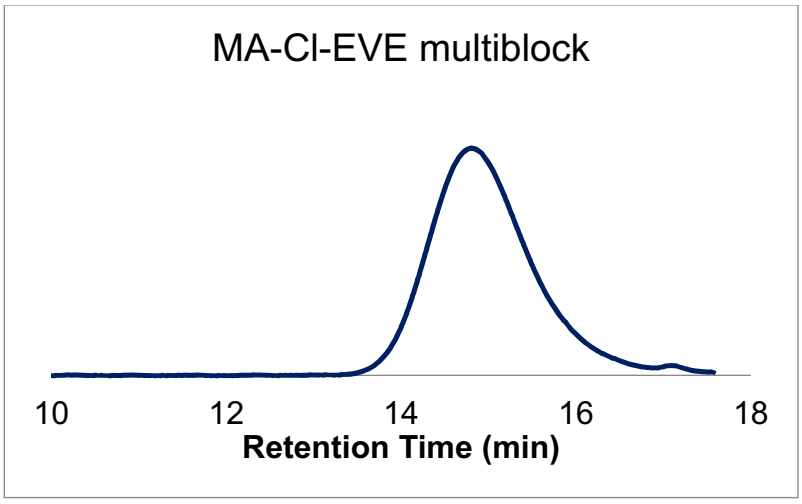

Figure 3.23. GPC trace of methyl acrylate-2-chloroethyl vinyl ether multiblock copolymer.

Appendix References

(1) Martiny, M.; Steckhan, E.; Esch, T. *Chem. Ber.* **1993**, *126*, 1671.

(2) Kottisch, V.; Michaudel, Q.; Fors, B. P. *J. Am. Chem. Soc.* **2016**, *138*, 15535.

CHAPTER 4

ON DEMAND SWITCHING OF POLYMERIZATION MECHANISM AND MONOMER SELECTIVITY WITH ORTHOGONAL STIMULI

4.1 Abstract

The development of next-generation materials is coupled with the ability to predictably and precisely synthesize polymers with well-defined structures and architectures. In this regard, the discovery of synthetic strategies that allow on demand control over monomer connectivity during polymerization would provide access to complex structures in a modular fashion and remains a grand challenge in polymer chemistry. In this Article, we report a method where monomer selectivity is controlled during the polymerization by the application of two orthogonal stimuli. Specifically, we developed a cationic polymerization where polymer chain growth is controlled by a chemical stimulus and paired it with a compatible photocontrolled radical polymerization. By alternating the application of the chemical and photochemical stimuli the incorporation of vinyl ethers and acrylates could be dictated by switching between cationic and radical polymerization mechanisms, respectively. This enables the synthesis of multiblock copolymers where each block length is governed by the amount of time a stimulus is applied, and the quantity of blocks is determined by the number of times the two stimuli are toggled. This new method allows on demand control over polymer structure with external influences and highlights the potential for using stimuli-controlled polymerizations to access novel materials.

4.2 Introduction

Macromolecular properties are inherently influenced by polymer molar mass, monomer sequence, and architecture, as made evident by the diversity of functions observed among bio-macromolecules derived from a limited library of molecular building blocks. Therefore, the discovery of synthetic techniques that give increased control over monomer connectivity and structure in a polymer will broaden the range of applications of these materials. Chemists have made significant progress in making well-defined materials with the development of "living" polymerizations that enable the formation of macromolecules with predictable molar masses (M_n) and narrow molar mass distributions (dispersity, $Đ$) with high chain-end fidelity capable of postpolymerization modification.[1,2] Even greater control over polymerization processes has recently been achieved through regulation of chain growth with various external stimuli[3,4] (i.e., thermal,[5−7] chemical,[8−13] mechanochemical,[14−17] electrochemical,[18,19] and photochemical[20−45]). However, the ability to precisely control monomer connectivity during a polymerization remains a grand challenge.

Temporal control of polymer chain growth in externally regulated polymerizations provides an excellent opportunity to precisely control macromolecular structure and function. To exploit this unique level of control, we envisioned a system where monomer selectivity at a given polymer chain-end could be switched on demand with two different stimuli.[46,47] This strategy would enable the one-pot synthesis of polymers where the monomer

connectivity would be precisely dictated by external influences and would be a step closer to nature's ability to perfectly control polymer sequence.

To achieve this goal, we were inspired by systems developed by Kamigaito and co-workers where both radical and cationic polymerization processes are active in a single reaction, allowing blocks of two monomers that react via different mechanisms to be randomly incorporated into the same polymer chain.[48−52] We reasoned that temporal control over the cationic and radical mechanisms via two stimuli would allow on demand switching of polymerization mechanism in situ and lead to precise control over the block structure of the final polymer.

Taking a step toward this challenge, our group recently developed a two-photocatalyst system that took advantage of photocontrolled cationic and radical reversible addition–fragmentation chain transfer (RAFT) polymerizations (Figure 4.1a).[53,54] Irradiating our system with green light led to promotion of the cationic polymerization of isobutyl vinyl ether (IBVE) through selective excitation of an oxidizing photocatalyst.[55,56] Alternatively, irradiation with blue light excited both the reducing and oxidizing photocatalysts in solution leading to simultaneous radical polymerization of methyl acrylate (MA) and cationic polymerization of IBVE (Figure 4.1a). Although this two-photocatalyst system demonstrated that the polymerization mechanism could be changed in situ, selective promotion of the radical mechanism was not possible due to the overlap of the absorption spectra of the two catalysts. In order to overcome this limitation, polymerization processes where chain growth is regulated by two

orthogonal and compatible stimuli are necessary to allow selective promotion of either the radical or cationic pathways (Figure 4.1b). Herein, we report the development of a new chemically controlled cationic polymerization of vinyl ether monomers. Combining this cationic polymerization with a photocontrolled radical process enables completely orthogonal switching of polymerization mechanism at a single chain-end in situ. This increased level of control is successfully applied to the one-pot synthesis of multiblock copolymers of IBVE and MA, without the need for subsequent polymer isolation, purification, or chain-end modification (Figure 4.1c).

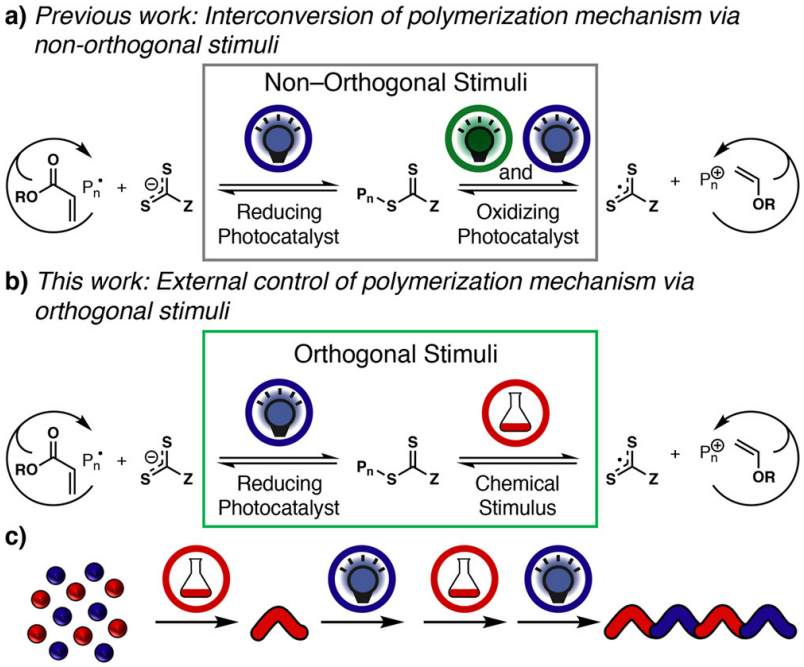

Figure 4.1. (a) Interconversion of polymerization mechanisms via nonorthogonal photoirradiation of two photocatalysts with blue and green light. (b) Generation of cations and radicals at polymer chain-ends via two orthogonal stimuli. (c) Synthesis of tetrablock vinyl ether-*b*-methyl acrylate copolymers via a chemical–photochemical gated mechanistic switch.

4.3 Results and Discussion

To gain precise control over polymerization mechanism in situ, we set out to develop a cationic polymerization regulated by a stimulus orthogonal and compatible with the photocontrolled radical polymerization process. In recent years, chemists have investigated a number of stimuli compatible with light to induce polymerization, including mechanical force, electricity, redox events triggered by chemical additives, and temperature. Among those, we opted for a chemical stimulus that could be used to initiate and reversibly terminate the propagating cation. We hypothesized that the cationic polymerization could be initiated with a mild single electron oxidant (Figure 4.2a).

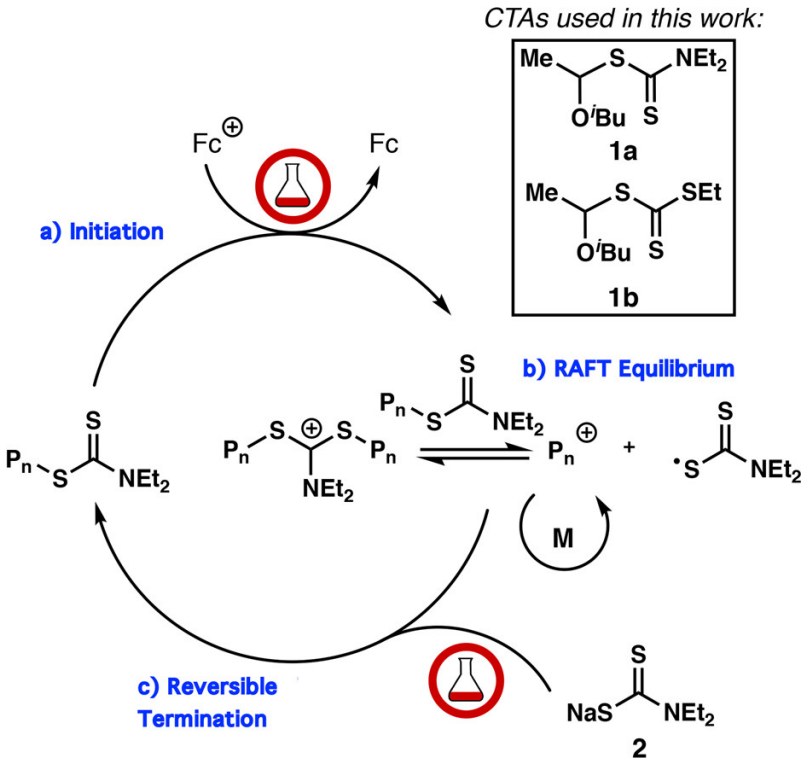

Figure 4.2. Proposed mechanism including (a) initiation, (b) reversible addition–fragmentation chain transfer (RAFT) equilibrium, and (c) termination of the chemically (red flask) gated cationic polymerization of vinyl ether monomers (M = monomer).

Specifically, we reasoned that the addition of ferrocenium salts (FcX) should selectively oxidize the chain transfer agents (CTA) **1a** or **1b** and, consequently, shuttle a predictable amount of an oxocarbenium ion into the RAFT mechanism (Figure 4.2b).[57] Importantly, temporal control over chain growth could be achieved through the addition of a dithiocarbamate anion, **2**, to recap propagating cations as well as reduce any remaining ferrocenium to ferrocene, completely halting the polymerization (Figure 4.2c). This process would provide a cationic polymerization that could be reversibly activated/deactivated through the addition of two chemical species. Moreover, the rate of polymerization could be dictated by the concentration of FcX added.

To test our hypothesis, we examined the use of ferrocenium tetrafluoroborate ($FcBF_4$) to initiate the cationic polymerization of vinyl ethers. Treating a solution of IBVE and **1a** with $FcBF_4$ in dichloromethane (DCM) gave a 10.3 kg/mol polymer with a narrow $Đ$ of 1.11 (Table 4.1, entry 1). Importantly, the experimental molar mass aligned well with the theoretical value, demonstrating that this system has excellent initiator efficiency. Control experiments demonstrated that performing the reaction in the absence of $FcBF_4$ gave no polymerization (Table 4.1, entry 2), while removal of **1a** gave a broad dispersity, high molecular weight polymer (Table 4.1, entry 3). At higher loadings of $FcBF_4$ (5 mol % relative to IBVE), experimental M_n's deviated from theoretical values (Table 4.1, entry 4), through promotion of uncontrolled polymerization pathways like those observed in the absence of **1a**. Additionally, at very low

concentrations of $FcBF_4$ (0.0025 mol %), no conversion of monomer is observed (Table 4.1, entry 5), unless the more active CTA **1b** is used (Table 4.1, entry 6).

Table 4.1. Optimization of the Cationic Polymerization of IBVE Using $FcBF_4$

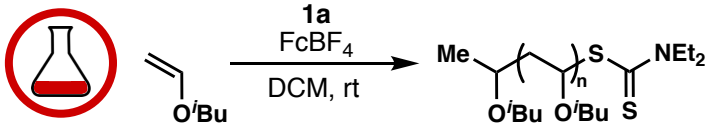

Entry[a]	[IBVE]:[CTA]:[Fc$^+$]	Conv. (%)	$M_{n,theo}$[b] (kg/mol)	$M_{n,exp}$[c] (kg/mol)	$Đ$
1	100:1:0.01	>99	10.2	10.3	1.11
2	100:1:0	0	0	0	0
3	100:0:0.01	89		243	2.35
4	100:1:5.0	>99	10.2	14.7	1.14
5	100:1:0.0025	0	0	0	0
6[d]	100:1:0.0025	>99	10.2	11.1	1.45
7	100:1:1.0	>99	10.2	10.6	1.10
8	200:1:0.01	>99	20.2	19.0	1.11
9	400:1:0.02	>99	40.2	35.1	1.16
10	600:1:0.04	>99	60.5	54.6	1.28
11	800:1:0.04	>99	80.5	65.3	1.24
12[e]	100:1:0.01	>99	10.2	10.1	1.25

[a][IBVE] = 3.1 M (in DCM); reaction volume = 0.65 mL. [b]$M_{n,theo}$ = [M]/[CTA] × $MW_{monomer}$ × conversion + MW_{CTA}. [c]$M_{n,exp}$ determined by gel permeation chromatography with a multiangle light scattering detector. [d]CTA = **1b**. [e]Open to air.

Interestingly, initiating the polymerization with $FcBF_4$ proved to be effective at synthesizing high molecular weight poly(IBVE) up to 65 kg/mol with narrow $Đ$ values (Table 4.1, entries 7–11). This is a significant advantage over our previously reported photocontrolled cationic polymerizations where we

observed a loss in control when targeting molar masses above 20 kg/mol. We attribute this increased efficiency to the lower oxidation potential of ferrocene (Fc) relative to **1a**, creating milder polymerization conditions that limit the generation of new chains via direct oxidation of IBVE, a previously observed undesired pathway.[55] Under the reported reaction conditions, high degrees of polymerization were achieved within 3 h. Additionally, these conditions provide a polymerization robust enough to proceed under ambient atmosphere while maintaining low *Đ* and excellent control over the final polymer M_n (Table 4.1, entry 12).[58] This result demonstrates the practicality of the polymerization and avoids the requirement of advanced air and water free techniques.

Importantly, the new $FcBF_4$-initiated process delivered effective cationic polymerization of a range of vinyl ether monomers that had varied steric and electronic characteristics, along with *para*-methoxystyrene. In each case, excellent agreement between theoretical and experimental M_n's was observed while maintaining narrow *Đ* values (Figure 4.3).

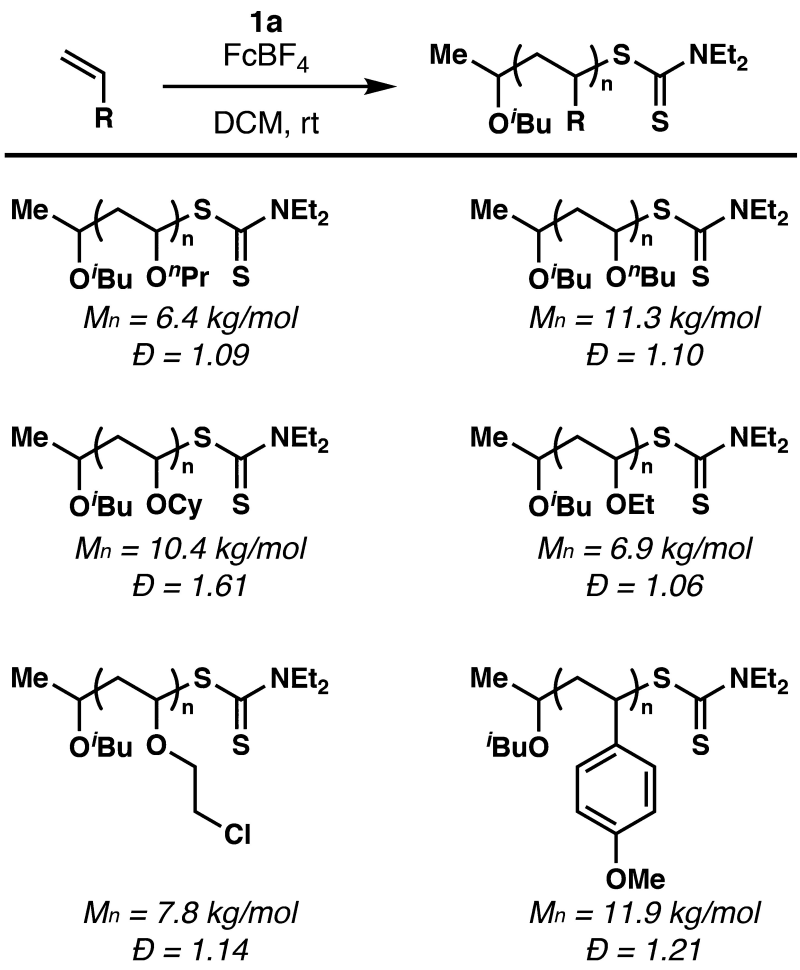

Figure 4.3. Substrate scope of vinyl monomers that can be polymerized via ferrocenium-mediated cationic RAFT polymerization.

To grow multiblock copolymers employing this method excellent chain-end fidelity is essential. To demonstrate that active chain-ends are maintained in these polymerizations, we synthesized a poly(IBVE) macroinitiator under our standard conditions and then chain-extended it with ethyl vinyl ether (EVE) to give a well-defined poly(IBVE-*b*-EVE) diblock copolymer (see the Appendix, Figures 4.13–4.15). Importantly, we observed a clear shift in the size exclusion

chromatography trace to higher molar mass with no tailing, demonstrating that the dithiocarbamate chain-ends are intact after the polymerization.

Thus far, we have shown that ferrocenium is an effective mediator of the cationic polymerization vinyl ethers. However, the ability to temporally control chain growth on demand is required to pair this system with a photocontrolled radical polymerization and enable switching of polymerization mechanism. We hypothesized that the chemically controlled polymerization could be reversibly terminated through the addition of 1 equiv of the dithiocarbamate anion **2** relative to the amount of $FcBF_4$ added to initiate polymerization (Figure 4.2c). Theoretically, the anion should cap propagating cations to generate a dormant chain-end, while reducing unreacted Fc^+ to Fc, preventing the generation of new propagating cations. To test this hypothesis, polymerization of IBVE was initiated through the addition of $FcBF_4$ under our standard conditions (Figure 4.4). After 25 min, **2** was added, and conversion of the monomer immediately halted. Importantly, the subsequent addition of $FcBF_4$ once again initiated the cationic polymerization. This process was repeated multiple times, demonstrating excellent temporal control over the polymerization with a chemical stimulus.

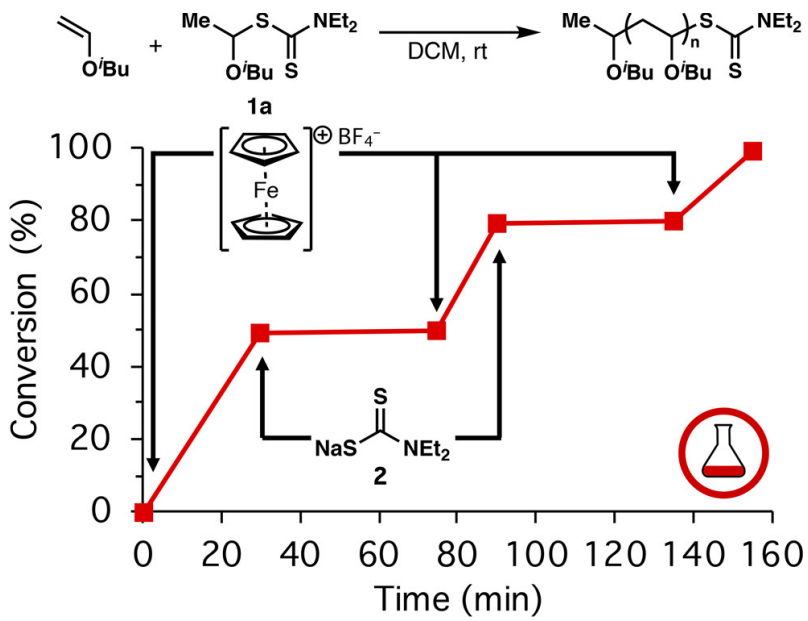

Figure 4.4. Temporal control over polymer initiation and reversible termination via the addition of $FcBF_4$ and **2**, respectively.

Significantly, our new chemically regulated cationic polymerization method is orthogonal to visible light and should be compatible with the radical photoinduced electron transfer-RAFT (PET-RAFT) polymerizations employing $Ir(ppy)_3$ as the photocatalyst. Therefore, combining these two polymerizations in one pot should enable switching of polymerization mechanisms through modulation of the two stimuli, although consideration must be given to the mechanism of switching. We have previously demonstrated efficient initiation of the radical polymerization of MA from a poly(IBVE) macroinitiator due to the favorable formation of an α–oxy radical, which will enable efficient chain extension of MA from poly(IBVE). Conversely, initiation of the polymerization of IBVE from the poly(MA) chain-end could be problematic because it requires the formation of a high energy α–acyl cation. However, we proposed that we could

circumvent this issue by taking advantage of the small amounts of incorporation of IBVE during the radical copolymerization with MA. As previously shown by Kamigaito, the majority of dormant chain-ends are thioacetals derived from vinyl ether monomers due to the radical RAFT fragmentation kinetics.[59] These thioacetals are effective at generating a cation and can promote vinyl ether homopolymerization.

Indeed, when exposing **1b**, equimolar amounts of MA and IBVE, and 0.02 mol % $Ir(ppy)_3$ to blue light, poly(MA) is synthesized with 20–30% incorporation of IBVE (Figure 4.5a). Chain-end analysis by ^1H NMR of the final polymer revealed the presence of greater than 90% thioacetal chain-ends (Figure 4.5b). Gratifyingly, upon removal of blue light irradiation and addition of $FcBF_4$ to the crude reaction mixture, the polymer was successfully chain-extended via cationic polymerization to give a well-defined poly(MA-*b*-IBVE) block polymer (Figure 4.5a). This result demonstrates successful switching from radical to cationic polymerization in situ through modulation of the external stimuli, which is a key requirement for the controlled synthesis of multiblock copolymers. This approach represents a significant advance over our previously reported photocontrolled switching method, due to the orthogonal stimuli that enable us to selectively invoke the radical mechanism.

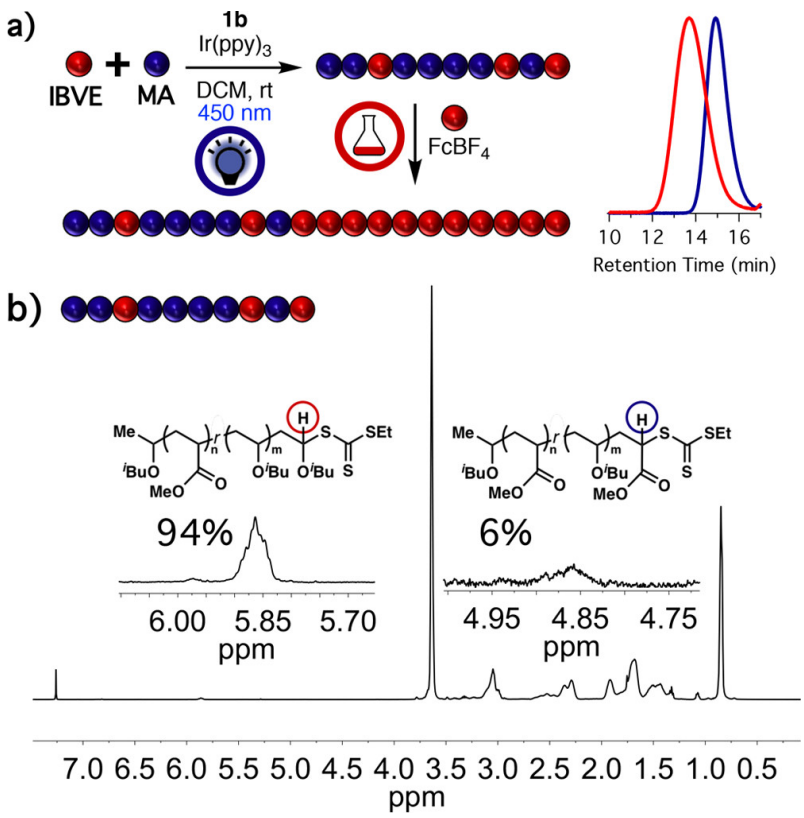

Figure 4.5. (a) A random copolymer of MA and IBVE can act as a macroinitiator for poly(MA-*b*-IBVE). (b) ^{1}H NMR chain-end analysis of the random copolymer revealed >90% thioacetal chain-ends.

With the ability to switch polymerization mechanism on demand, we set out to explore the range of copolymer sequences that can be targeted through modulation of the order of applied stimuli. Figure 4.6a shows the monomer conversion over time for the synthesis of poly(MA-*b*-IBVE) diblock copolymer, where we first promoted the radical polymerization with light followed by the chemically controlled cationic polymerization. This can be extended to triblock copolymers under the same conditions by adding an additional switching event. After the first mechanistic switch from radical to cationic polymerization to generate poly(MA-*b*-IBVE), vinyl ether polymerization can be successfully

halted by the addition of **2**. Subsequent re-exposure to blue light initiates radical polymerization of MA resulting in poly(MA-*b*-IBVE-*b*-MA) triblock with predictable molar mass and narrow dispersity (Figure 4.6b).

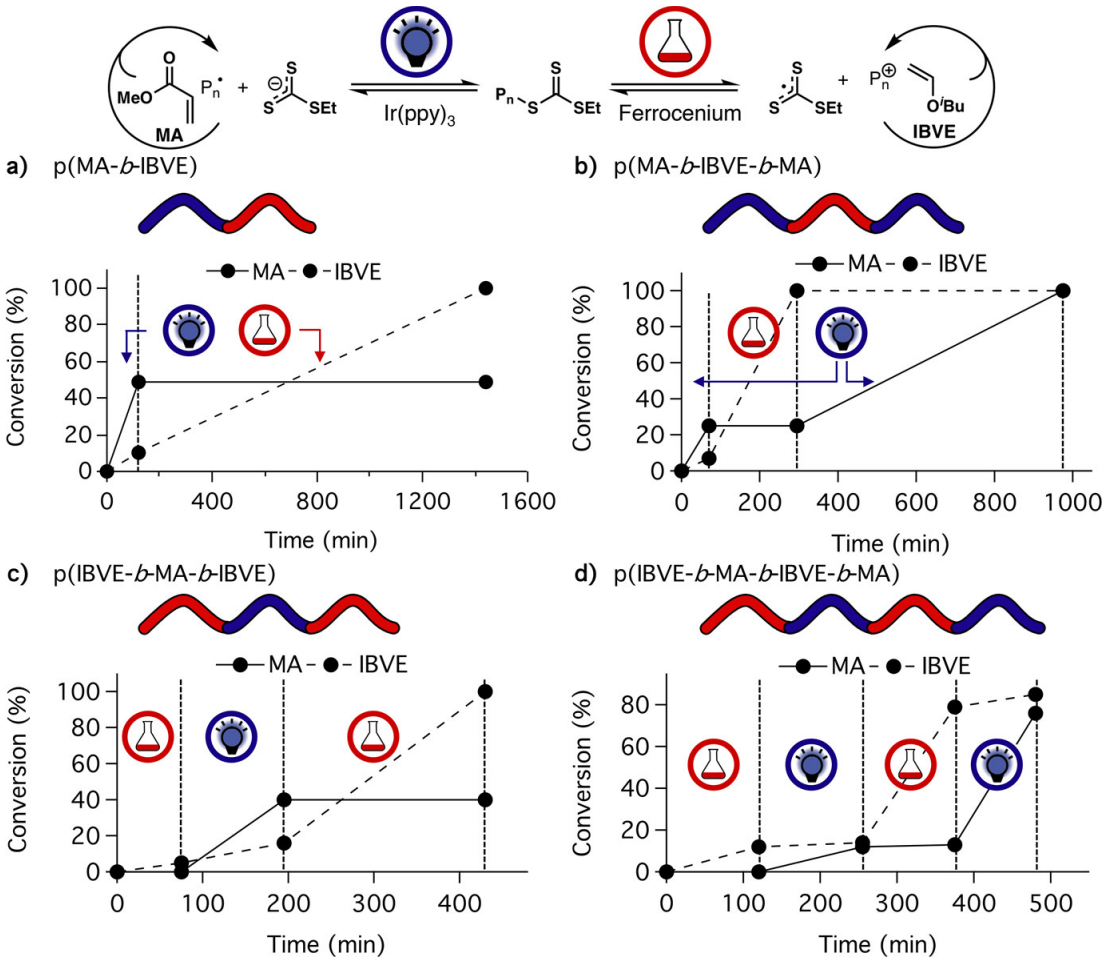

Figure 4.6. Conversion of MA (solid line) and IBVE (dashed line) over time upon applying chemically controlled cationic and photochemically controlled radical polymerization. (a) Conversion plot for poly(MA-*b*-IBVE). (b) Conversion plot for poly(MA-*b*-IBVE-*b*-MA). (c) Conversion plot for poly(IBVE-*b*-MA-*b*-IBVE). (d) Conversion plot for poly(IBVE-*b*-MA-*b*-IBVE-*b*-MA).

Interestingly, from the same solution conditions the inverse triblock copolymer can be synthesized by simply altering the sequence of the two applied stimuli. Specifically, initiating polymerization of IBVE, in the presence of

MA and $Ir(ppy)_3$, by treatment with $FcBF_4$ in the absence of blue light (Figure 4.6c), we observed solely conversion of IBVE over the first hour. Addition of **2** resulted in termination of the cationic polymerization, followed by irradiation with blue light for 2 h to promote radical polymerization of the acrylate. Turning the light off and treating the reaction with 0.05 mol % $FcBF_4$ resulted in a clean mechanistic switch from radical polymerization of MA to the cationic polymerization of vinyl ethers, generating a well-defined poly(IBVE-*b*-MA-*b*-IBVE) triblock. This can be taken a step further, generating a poly(IBVE-*b*-MA-*b*-IBVE-*b*-MA) tetrablock copolymer (Figure 4.6d) by adding one additional switching event to the last triblock copolymer. It is worth noting that the length of each block can be controlled by the length of time the stimulus is applied, and the number of blocks can be dictated by the number of times the stimuli are toggled. These data clearly show that pairing orthogonal stimuli to control polymerization mechanism and monomer selectivity is a powerful approach toward the synthesis of advanced polymeric structures.

4.4 Conclusion

In conclusion, we have developed a system that enables switching of polymerization mechanism and monomer selectivity in situ with two external stimuli. The identification of a cationic polymerization controlled by a chemical stimulus that was both orthogonal and compatible with the photocontrolled radical polymerization was key to achieving efficient switching. We demonstrated that ferrocenium salts were highly efficient initiators for the

cationic RAFT polymerization of vinyl ethers and showed that reversible termination could be achieved through the addition of a dithiocarbamate anion. By pairing this new chemically controlled cationic polymerization with a photocontrolled RAFT polymerization, we were able to selectively and reversibly promote the polymerization of vinyl ethers or acrylates. Under identical solution conditions, this enabled the synthesis of an array of well-defined multiblock copolymers where the final structure was dictated by the two stimuli; the length of each block was controlled by the amount of time the stimulus was applied, and the number of blocks was governed by the alternating application of the two stimuli. These results demonstrate the power of combining controlled polymerization processes that are regulated by different external stimuli and lay the groundwork for developing systems where polymer sequence, structure, and architecture are controlled on demand via external influences.

4.5 References

(1) Szwarc, M. *Nature* **1956**, *178*, 1168.

(2) Lunn, D. J.; Discekici, E. H.; de Alaniz, J. R.; Guntekunst, W. R.; Hawker, C. J. J. *Polym. Sci., Part A: Polym. Chem.* **2017**, *55*, 2903.

(3) Leibfarth, F. A.; Mattson, K. M.; Fors, B. P.; Collins, H. A.; Hawker, C. J. *Angew. Chem., Int. Ed.* **2013**, *52*, 199.

(4) Teator, A. J.; Lastovickova, D. N.; Bielawski, C. W. *Chem. Rev.* **2016**, *116*, 1969.

(5) Yağci, Y.; Reetz, I. *Prog. Polym. Sci.* **1998**, *23*, 1485.

(6) Naumann, S.; Buchmeiser, M. R. *Catal. Sci. Technol.* **2014**, *4*, 2466.

(7) Naumann, S.; Buchmeiser, M. R. *Macromol. Rapid Commun.* **2014**, *35*, 682.

(8) Gregson, C. K. A.; Gibson, V. C.; Long, N. J.; Marshall, E. L.; Oxford, P. J.; White, A. J. P. *J. Am. Chem. Soc.* **2006**, *128*, 7410.

(9) Gregson, C. K. A.; Blackmore, I. J.; Gibson, V. C.; Long, N. J.; Marshall, E. L.; White, A. J. P. *Dalton Trans.* **2006**, *0*, 3134.

(10) Broderick, E. M.; Guo, N.; Vogel, C. S.; Xu, C.; Sutter, J.; Miller, J. T.; Meyer, K.; Mehrkhodavandi, P.; Diaconescu, P. L. *J. Am. Chem. Soc.* **2011**, *133*, 9278.

(11) Broderick, E. M.; Guo, N.; Wu, T.; Vogel, C. S.; Xu, C.; Sutter, J.; Miller, J. T.; Meyer, K.; Cantat, T.; Diaconescu, P. L. *Chem. Commun.* **2011**, *47*, 9897.

(12) Wang, X.; Thevenon, A.; Brosmer, J. L.; Yu, I.; Khan, S. I.; Mehrkhodavandi, P.; Diaconescu, P. L. *J. Am. Chem. Soc.* **2014**, *136*, 11264.

(13) Biernesser, A. B.; Li, B.; Byers, J. A. *J. Am. Chem. Soc.* **2013**, *135*, 16553.

(14) Mohapatra, H.; Kleiman, M.; Esser-Kahn, A. P. *Nat. Chem.* **2017**, *9*, 135.

(15) Wang, Z.; Pan, X.; Li, L.; Fantin, M.; Yan, J.; Wang, Z.; Wang, Z.; Xia, H.; Matyjaszewski, K. *Macromolecules* **2017**, *50*, 7940.

(16) McKenzie, T. G.; Colombo, E.; Fu, Q.; Ashokkumar, M.; Qiao, G. G. *Angew. Chem., Int. Ed.* **2017**, *56*, 12302.

(17) Wang, Z.; Pan, X.; Yan, J.; Dadashi-Silab, S.; Xie, G.; Zhang, J.; Wang, Z.; Xia, H.; Matyjaszewski, K. *ACS Macro Lett.* **2017**, *6*, 546.

(18) Chmielarz, P.; Fantin, M.; Park, S.; Isse, A. A.; Gennaro, A.; Magenau, A. J. D.; Sobkowiak, A.; Matyjaszewski, K. *Prog. Polym. Sci.* **2017**, *69*, 47.

(19) Peterson, B. M.; Lin, S.; Fors, B. P. *J. Am. Chem. Soc.* **2018**, *140*, 2076.

(20) Murata, K.; Saito, K.; Kikuchi, S.; Akita, M.; Inagaki, A. *Chem. Commun.* **2015**, *51*, 5717.

(21) Chen, M.; Zhong, M.; Johnson, J. A. *Chem. Rev.* **2016**, *116*, 10167.

(22) Corrigan, N.; Shanmugam, S.; Xu, J.; Boyer, C. *Chem. Soc. Rev.* **2016**, *45*, 6165.

(23) Ciftci, M.; Yoshikawa, Y.; Yagci, Y. *Angew. Chem., Int. Ed.* **2017**, *56*, 519.

(24) Kütahya, C.; Schmitz, C.; Strehmel, V.; Yagci, Y.; Strehmel, B. *Angew. Chem., Int. Ed.* **2018**, *57*, 7898.

(25) Dadashi-Silab, S.; Doran, S.; Yagci, Y. *Chem. Rev.* **2016**, *116*, 10212.

(26) Trotta, J. T.; Fors, B. P. *Synlett* **2016**, *27*, 702.

(27) McKenzie, T. G.; Fu, Q.; Uchiyama, M.; Satoh, K.; Xu, J.; Boyer, C.; Kamigaito, M.; Qiao, G. G. *Adv. Sci.* **2016**, *3*, 1500394.

(28) Fors, B. P.; Hawker, C. J. *Angew. Chem., Int. Ed.* **2012**, *51*, 8850.

(29) Konkolewicz, D.; Schröder, K.; Buback, J.; Bernhard, S.; Matyjaszewski, K. *ACS Macro Lett.* **2012**, *1*, 1219.

(30) Anastasaki, A.; Nikolaou, V.; Zhang, Q.; Burns, J.; Samanta, S. R.; Waldron, C.; Haddleton, A. J.; McHale, R.; Fox, D.; Percec, V. *J. Am. Chem. Soc.* **2014**, *136*, 1141.

(31) Treat, N. J.; Sprafke, H.; Kramer, J. W.; Clark, P. G.; Barton, B. E.; Read de Alaniz, J.; Fors, B. P.; Hawker, C. J. *J. Am. Chem. Soc.* **2014**, *136*, 16096.

(32) Pan, X.; Malhotra, N.; Simakova, A.; Wang, Z.; Konkolewicz, D.; Matyjaszewski, K. *J. Am. Chem. Soc.* **2015**, *137*, 15430.

(33) Jones, G. R.; Whitfield, R.; Anastasaki, A.; Haddleton, D. M. *J. Am. Chem. Soc.* **2016**, *138*, 7346.

(34) Theriot, J. C.; Lim, C.-H.; Yang, H.; Ryan, M. D.; Musgrave, C. B.; Miyake, G. M. *Science* **2016**, *352*, 108.

(35) Pearson, R. M.; Lim, C.-H.; McCarthy, B. G.; Musgrave, C. B.; Miyake, G. M. *J. Am. Chem. Soc.* **2016**, *138*, 11399.

(36) Ramsey, B. L.; Pearson, R. M.; Beck, L. R.; Miyake, G. M. *Macromolecules* **2017**, *50*, 2668.

(37) Koumura, K.; Satoh, K.; Kamigaito, M. *Macromolecules* **2008**, *41*, 7359.

(38) Xu, J.; Jung, K.; Atme, A.; Shanmugam, S.; Boyer, C. A J. *Am. Chem. Soc.* **2014**, *136*, 5508.

(39) Shanmugam, S.; Xu, J.; Boyer, C. *J. Am. Chem. Soc.* **2015**, *137*, 9174.

(40) Shanmugam, S.; Xu, J.; Boyer, C. *Chem. Sci.* **2015**, *6*, 1341.

(41) Shanmugam, S.; Xu, J.; Boyer, C. *Angew. Chem., Int. Ed.* **2016**, *55*, 1036.

(42) Xu, J.; Shanmugam, S.; Fu, C.; Aguey-Zinsou, K.-F.; Boyer, C. *J. Am. Chem. Soc.* **2016**, *138*, 3094.

(43) Shanmugam, S.; Boyer, C. *J. Am. Chem. Soc.* **2015**, *137*, 9988.

(44) Chen, M.; MacLeod, M. J.; Johnson, J. A. *ACS Macro Lett.* **2015**, *4*, 566.

(45) Theriot, J. C.; Miyake, G. M.; Boyer, C. A. *ACS Macro Lett.* **2018**, *7*, 662.

(46) Qi, M.; Dong, Q.; Wang, D.; Byers, J. A. *J. Am. Chem. Soc.* **2018**, *140*, 5686.

(47) Kikuchi, S.; Saito, K.; Akita, M.; Inagaki, A. *Organometallics* **2018**, *37*, 359.

(48) Guerre, M.; Uchiyama, M.; Lopez, G.; Améduri, B.; Satoh, K.; Kamigaito, M.; Ladmiral, V. *Polym. Chem.* **2018**, *9*, 352.

(49) Satoh, K.; Hashimoto, H.; Kumagai, S.; Aoshima, H.; Uchiyama, M.; Ishibashi, R.; Fujiki, Y.; Kamigaito, M. *Polym. Chem.* **2017**, *8*, 5002.

(50) Guerre, M.; Uchiyama, M.; Folgado, E.; Semsarilar, M.; Améduri, B.; Satoh, K.; Kamigaito, M.; Ladmiral, V. *ACS Macro Lett.* **2017**, *6*, 393.

(51) Uchiyama, M.; Satoh, K.; Kamigaito, M. *Angew. Chem., Int. Ed.* **2015**, *54*, 1924.

(52) Aoshima, H.; Uchiyama, M.; Satoh, K.; Kamigaito, M. *Angew. Chem., Int. Ed.* **2014**, *53*, 10932.

(53) Kottisch, V.; Michaudel, Q.; Fors, B. P. *J. Am. Chem. Soc.* **2017**, *139*, 10665.

(54) Previous work employing two wavelengths of light to promote PET-RAFT and ROP polymerization mechanisms from two different chain-ends can be found. Fu, C.; Xu, J.; Boyer, C. *Chem. Commun.* **2016**, *52*, 7126.

(55) Kottisch, V.; Michaudel, Q.; Fors, B. P. *J. Am. Chem. Soc.* **2016**, *138*, 15535.

(56) Michaudel, Q.; Chauviré, T.; Kottisch, V.; Supej, M. J.; Stawiasz, K. J.; Shen, L.; Zipfel, W. R.; Abruña, H. D.; Freed, J. H.; Fors, B. P. *J. Am. Chem. Soc.* **2017**, *139*, 15530.

(57) CTAs **1a** and **1b** were selected due to the control provided in cationic polymerizations and their potential to function in radical polymerizations: See ref (49).

(58) Yeow, J.; Chapman, R.; Gormley, A. J.; Boyer, C. *Chem. Soc. Rev.* **2018**, *47*, 4357.

(59) Kumagai, S.; Nagai, K.; Satoh, K.; Kamigaito, M. *Macromolecules* **2010**, *43*, 7523.

4.6 Appendix

General Reagent Information

Isobutyl vinyl ether (IBVE) (99%, TCI), ethyl vinyl ether (EVE) (99%, Sigma Aldrich), 2-chloroethyl vinyl ether (Cl-EVE) (97%, TCI), *n*-propyl vinyl ether (nPrVE) (99%, Sigma Aldrich), and *n*-butyl vinyl ether (nBuVE) (98%, Sigma Aldrich), cyclohexyl vinyl ether (CyVE) (98%, Sigma Aldrich) and methyl acrylate (MA) (>99%, TCI) were dried over calcium hydride (CaH_2) (ACROS organics, 93% extra pure, 0–2 mm grain size) for 12 hours, distilled under nitrogen, and degassed by three freeze-pump-thaw cycles. 4-Methoxystyrene (97%, Sigma Aldrich) was dried over CaH_2 for 12 hours, distilled under vacuum, and degassed by three freeze-pump-thaw cycles. Sodium *N,N*-diethyldithiocarbamate trihydrate (**2**) (98%, Alfa Aesar) was azeotropically dried with toluene. Ethanethiol (97%, Alfa Aesar) and carbon disulfide (99.9+%, Alfa Aesar) were distilled before use. Ferrocenium tetrafluoroborate ($FcBF_4$) (97%, Sigma Aldrich), HCl in Et_2O (2.0 M, Sigma Aldrich), Tris[2-phenylpyridinatoC2,N]iridium(III) ($Ir(ppy)_3$) (Ark Pharm) and sodium hydride (60%, dispersion in mineral oil, Sigma Aldrich) were used as received. Dichloromethane (DCM), acetonitrile (MeCN), and diethylether (Et_2O) were purchased from J.T. Baker and were purified by vigorous purging with argon for 2 hours, followed by passing through two packed columns of neutral alumina under argon pressure. Hexanes and ethyl acetate were purchased from Fischer Scientific and used as received. Ethanol (anhydrous, 200 proof) was purchased from Koptec. Alumina (1.0, 0.3, 0.05 μm pore size) was purchased from Extec.

S-1-isobutoxyethyl *N,N*-diethyl dithiocarbamate (**1a**)[1] and *S*-1-isobutoxylethyl *S′*-ethyl trithiocarbonate (**1b**)[1] were synthesized according to literature procedures.

General Analytical Information

All polymer samples were analyzed using a Tosoh EcoSec HLC 8320GPC system with two SuperHM-M columns in series at a flow rate of 0.350 mL/min. THF was used as the eluent and all number-average molecular weights (M_n), weight-average molecular weights (M_w), and dispersities ($Đ$) were determined by light scattering using a Wyatt miniDawn Treos multi-angle light scattering detector. Nuclear magnetic resonance (NMR) spectra were recorded on a Varian 400 MHz, a Varian 600 MHz, or a Bruker 500 MHz instrument.

Experimental Procedures

General Procedure for Chemically Controlled Polymerization

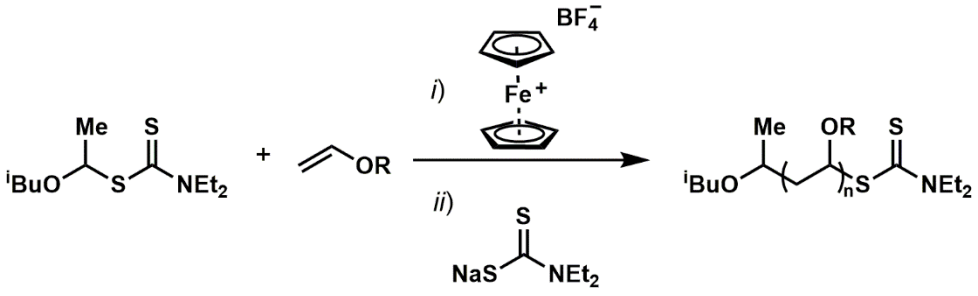

In a nitrogen filled glove box, an oven-dried one-dram vial was equipped with a stir bar and charged with IBVE (0.13 mL, 1.00 mmol, 100 equiv), 0.02 mL of a stock solution of **1a** in DCM (0.5 M, 0.01 mmol, 1 equiv), 0.13 mL of DCM, and then 0.05 mL of a stock solution of $FcBF_4$ in DCM (2.0 mM, 0.1 μmol, 0.01

mol % relative to IBVE). The vial was sealed with a cap equipped with a Teflon septum under an atmosphere of nitrogen and left to stir. After the desired reaction time (2–3 hours), the reaction was quenched by addition of 0.05 mL of a stock solution of sodium *N,N*-diethyl dithiocarbamate in MeCN (0.03 M, 0.15 mmol) and aliquots were taken for GPC and ^{1}H NMR.

Table 4.2. Breadth of Polymerizable Monomers

Monomer[a]	**Conv. (%)**	$M_{n,theo}$ **(kg/mol)**	$M_{n,exp}$ **(kg/mol)**	$Đ$
*n*BuVE	> 99	9.9	11.3	1.10
*n*PrVE	> 99	8.7	6.4	1.09
EVE	> 99	7.4	6.9	1.06
Cl-EVE[b]	93	10	7.8	1.14
CyVE[c]	> 99	12.7	10.4	1.61
p-OMe-Styrene[c]	96	13.3	11.9	1.21

[a]Standard Reaction Conditions: Vinyl Monomer (100 equiv), **1a** (0.01 equiv), and $FcBF_4$ (0.01 mol %) at room temperature in dichloromethane. [b]Using 0.04 mol % $FcBF_4$. [c]Using 0.10 mol % $FcBF_4$.

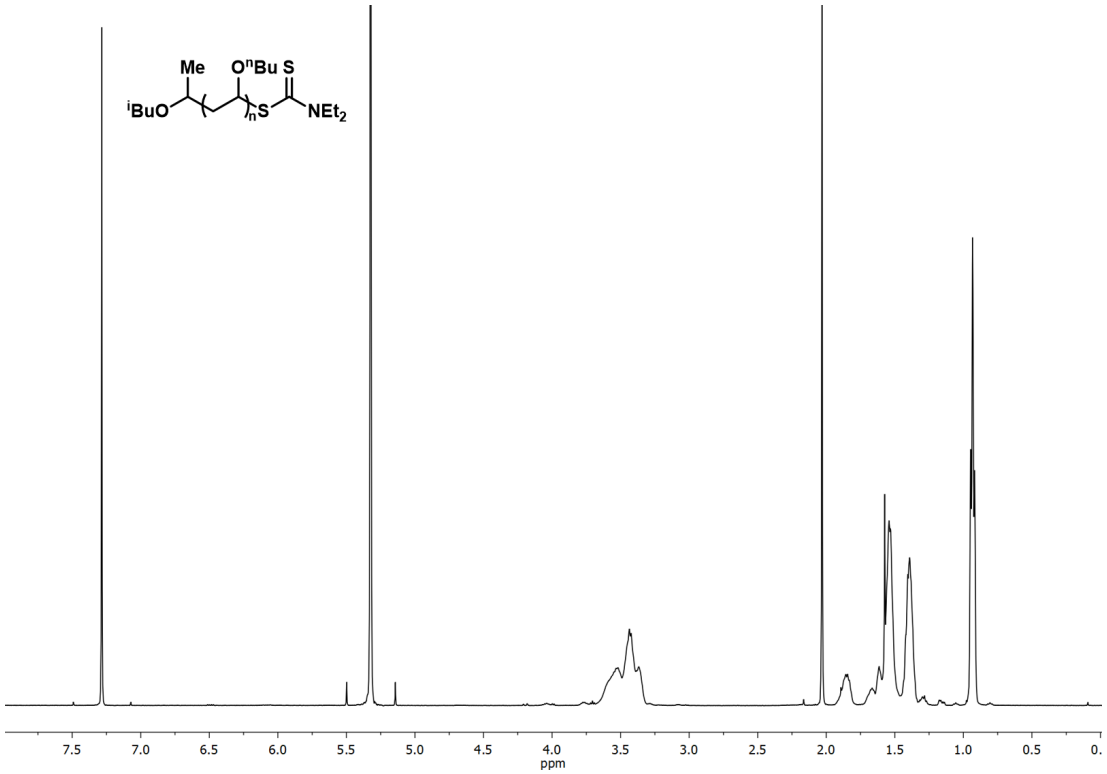

Figure 4.7. ^{1}H NMR of poly(*n*-butyl vinyl ether), M_n = 11.3 kg/mol, $Đ$ = 1.10 (Table 4.2, entry 1).

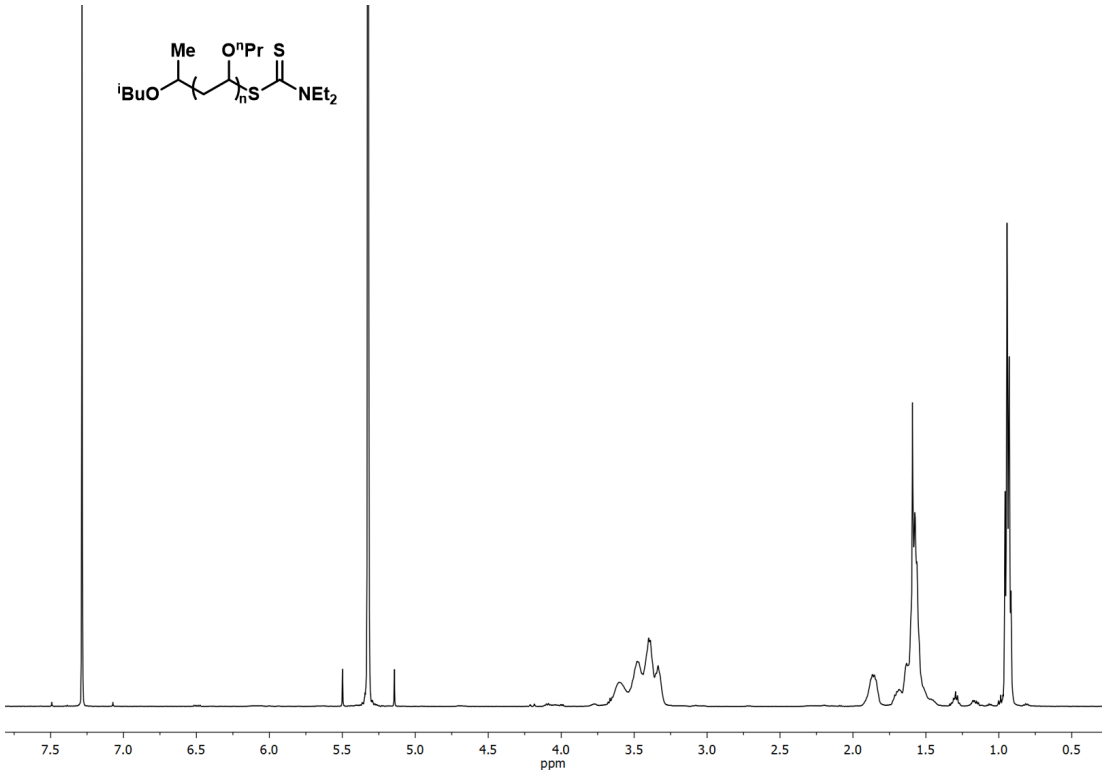

Figure 4.8. ^{1}H NMR of poly(*n*-propyl vinyl ether), M_n = 6.4 kg/mol, $Đ$ = 1.09 (Table 4.2, entry 2).

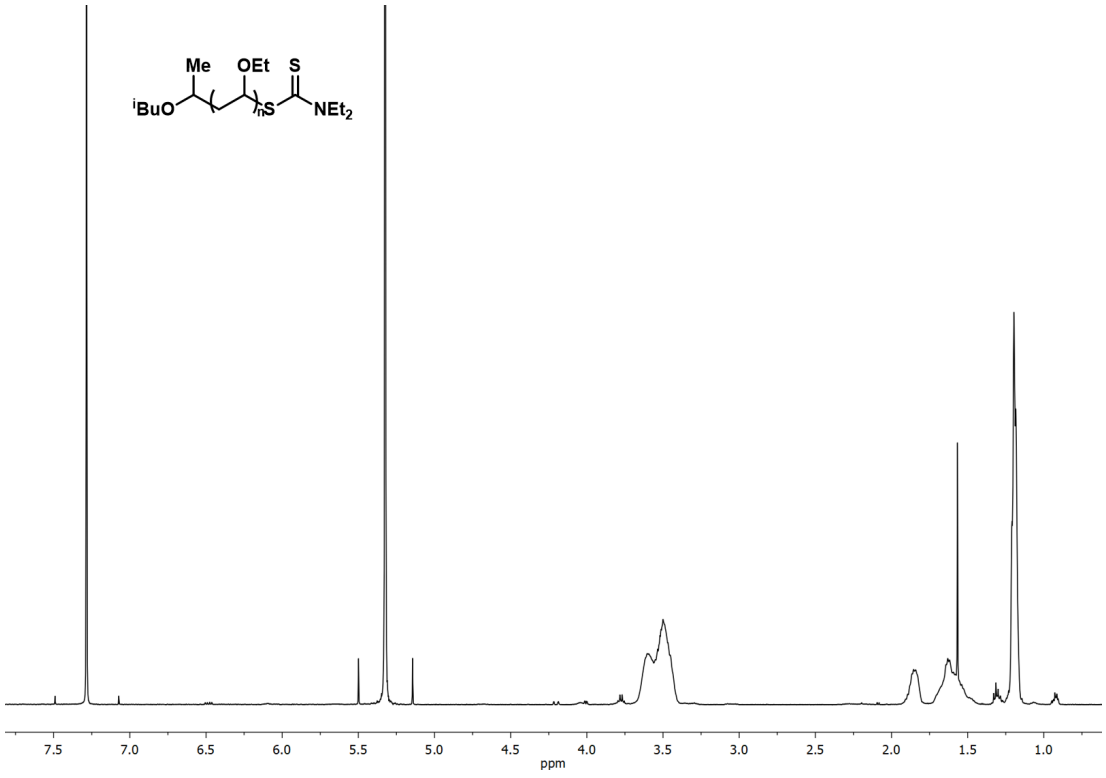

Figure 4.9. ^{1}H NMR of poly(ethyl vinyl ether), M_n = 6.9 kg/mol, $Đ$ = 1.06 (Table 4.2, entry 3).

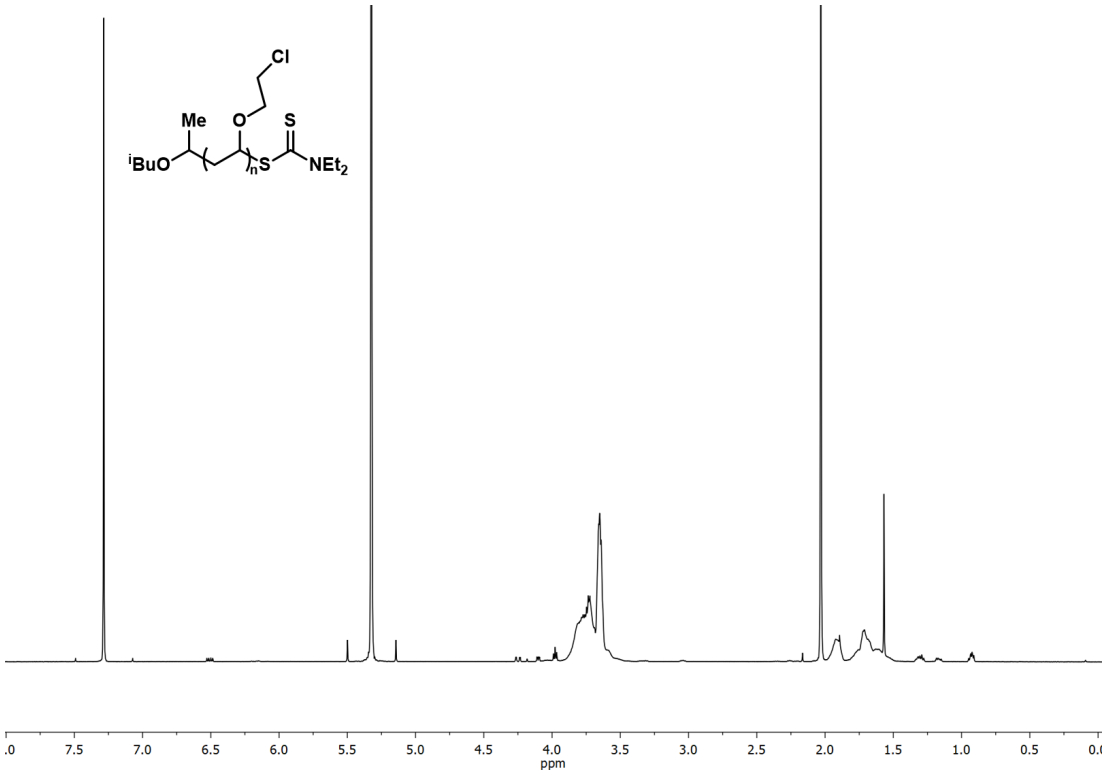

Figure 4.10. ^{1}H NMR of poly(2-chloroethyl vinyl ether), M_n = 7.8 kg/mol, $Đ$ = 1.14 (Table 4.2, entry 4).

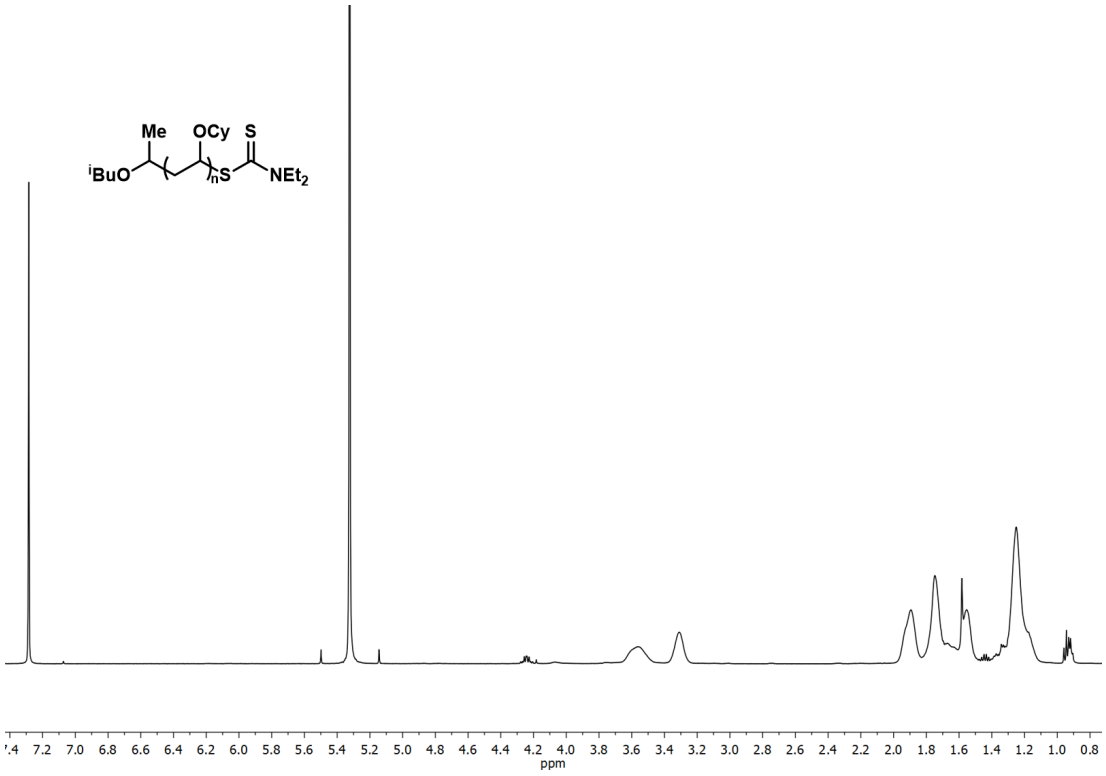

Figure 4.11. ^{1}H NMR of poly(cyclohexyl vinyl ether), M_n = 10.4 kg/mol, $Đ$ = 1.61 (Table 4.2, entry 5).

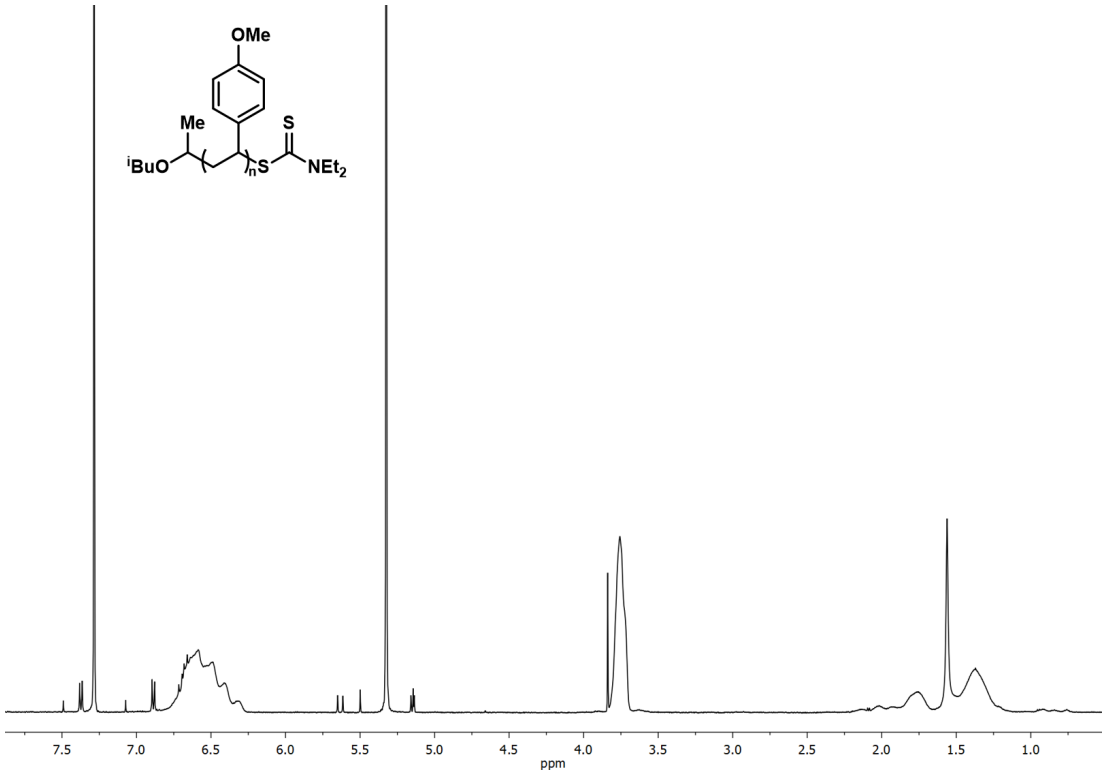

Figure 4.12. ^{1}H NMR of poly(*p*-methoxystyrene), M_n = 11.9 kg/mol, $Đ$ = 1.21 (Table 4.2, entry 6).

Procedure for Chemical Synthesis of Diblock Copolymer

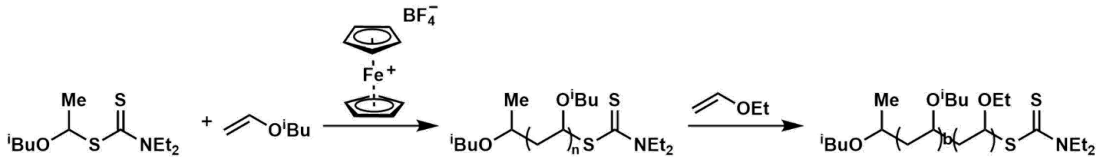

In a nitrogen filled glove box, an oven-dried one-dram vial was equipped with a stir bar and charged with IBVE (0.26 mL, 2.00 mmol, 100 equiv), 0.04 mL of a stock solution of **1a** in DCM (0.5 M, 0.01 mmol, 1 equiv), 0.25 mL of DCM, and then 0.10 mL of a stock solution of $FcBF_4$ in DCM (2.0 mM, 0.2 μmol, 0.01 mol % relative to IBVE). The vial was sealed with a cap equipped with a Teflon septum under an atmosphere of nitrogen and left to stir. The reaction was run to full conversion (5 hours) and an aliquot was taken and quenched by addition of sodium N,N-diethyl dithiocarbamate for GPC (M_n = 8.5 kg/mol, $Đ$ = 1.14) and ^{1}H NMR analysis prior to the addition of EVE (0.20 mL, 2.00 mmol, 100 equiv). After reaching full conversion (16 hours), the reaction was quenched by addition of sodium *N,N*-diethyl dithiocarbamate and aliquots were taken for GPC and ^{1}H NMR. M_n(GPC) = 13.4 kg/mol, $Đ$ = 1.09.

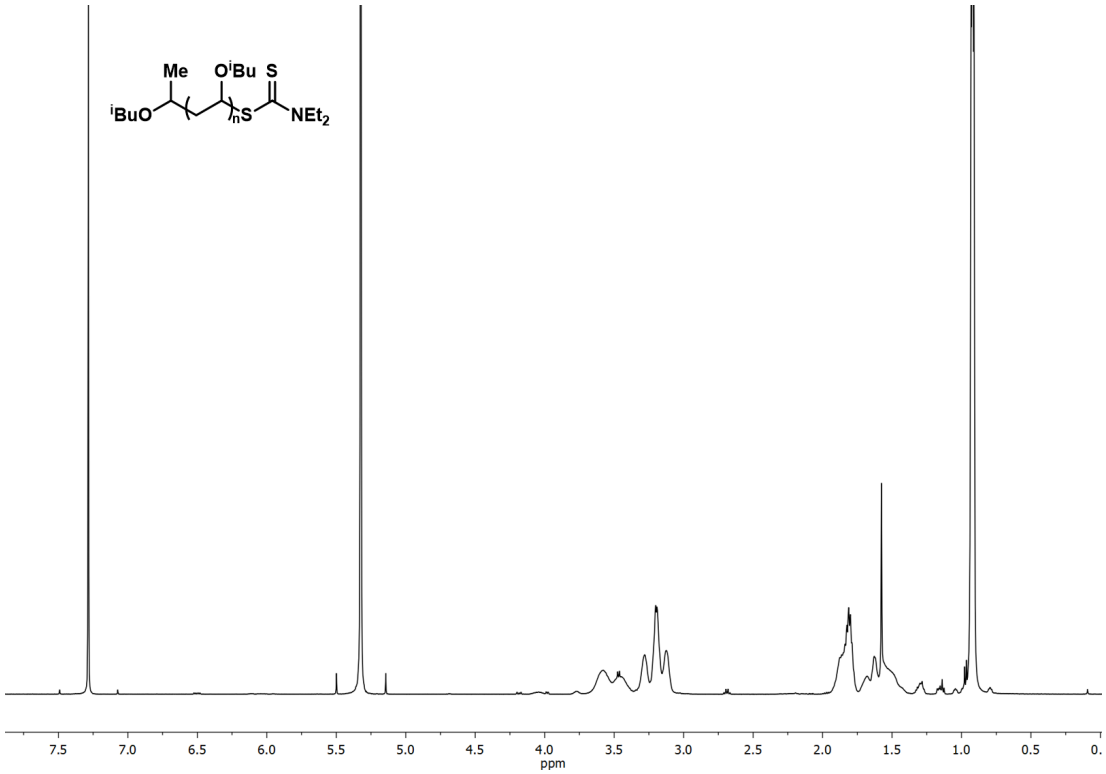

Figure 4.13. ^{1}H NMR of poly(isobutyl vinyl ether), M_n = 8.5 kg/mol, $Đ$ = 1.14.

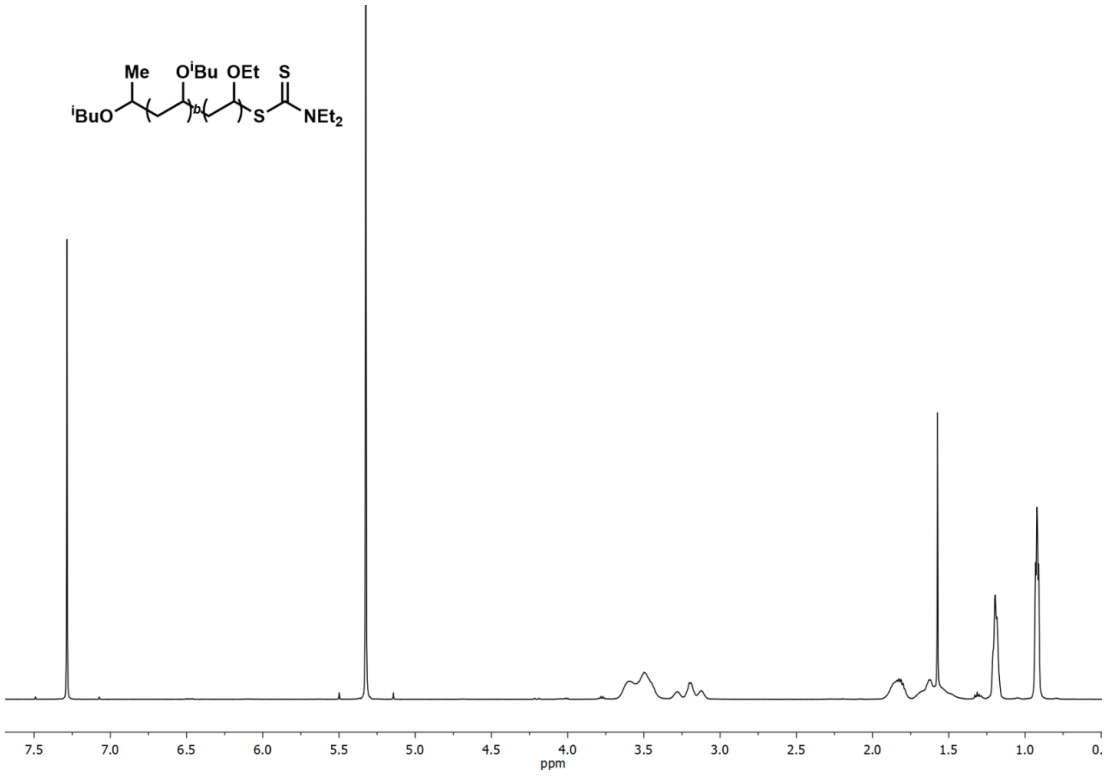

Figure 4.14. ^{1}H NMR of poly(isobutyl vinyl ether-*block*-ethyl vinyl ether), M_n = 13.4 kg/mol, $Đ$ = 1.09.

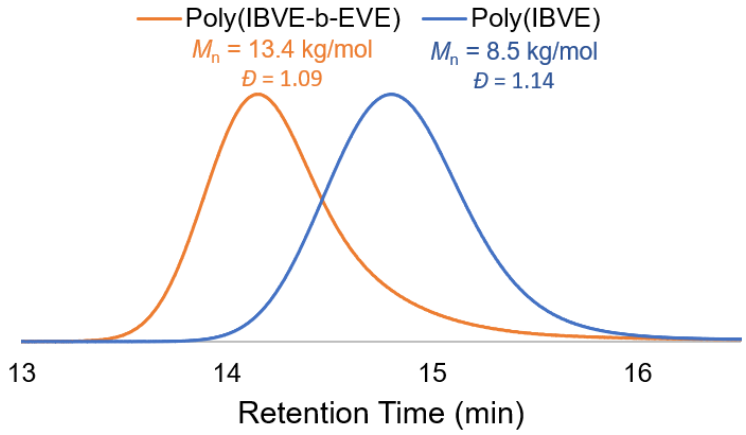

Figure 4.15. GPC traces of poly(isobutyl vinyl ether) and poly(isobutyl vinyl ether-*block*-ethyl vinyl ether)

Procedure for Chemical Initiation and Termination of the Polymerization of Isobutyl Vinyl Ether

In a nitrogen filled glove box, an oven-dried one-dram vial was equipped with a stir bar and charged with IBVE (0.260 mL, 2.00 mmol, 100 equiv), **1a** (0.040 mL of a 0.55 mM solution in DCM, 0.022 mmol, 1 equiv), $FcBF_4$ (0.100 mL, 2 μmol, 0.01 equiv), and 0.25 mL DCM. The vial was sealed with a cap equipped with a Teflon septum under an atmosphere of nitrogen. After 30 min (total time = 30 min), sodium *N,N*-diethyl dithiocarbamate (0.040 mL of a 5.8 mM solution in 1:1 DCM: MeCN, 2 μmol, 0.01 equiv) was added to terminate the polymerization. After a 45 min "off" period (total time = 75 min), $FcBF_4$ (0.04 mL of a 7.3 mM solution in DCM, 2 μmol, 0.01 equiv) was added to reinitiate polymerization. After a 15 min "on" period (total time = 90 min), sodium *N,N*-diethyl dithiocarbamate (0.040 mL of a 5.8 mM solution in 1:1 DCM: MeCN, 2 μmol, .01 equiv) was added to the reaction. After a 45 min "off" period (total time = 135 min), $FcBF_4$ (0.04 mL of a 7.3 mM solution in DCM, 2 μmol, 0.01 equiv) was added to reinitiate polymerization. Aliquots were taken after each addition of $FcBF_4$ and *N,N*-diethyl dithiocarbamate and the end of reaction (time = 155 min) for ^1H NMR and GPC analysis.

Procedure for Diblock Copolymer Synthesis of Methyl Acrylate and Isobutyl Vinyl Ether (p(MA-*b*-IBVE), Figure 4.5a and 4.6a)

In a nitrogen filled glove box, an oven-dried one-dram vial was equipped with a stir bar and charged with IBVE (0.26 mL, 2.00 mmol, 100 equiv), MA (0.18

mL, 2.00 mmol, 100 equiv), 0.13 mL of a stock solution of $Ir(ppy)_3$ in DCM (3 mM, 0.40 μmol, 0.02 mol % relative to MA), and 0.02 mL of a stock solution of **1b** in DCM (1 M, 0.02 mmol, 1 equiv). The vial was sealed with a cap equipped with a Teflon septum under an atmosphere of nitrogen, placed next to blue KESSIL lamps (~460 nm) outside of the glove box, and stirred while cooling by blowing compressed air over the reaction vial. After 2 hours of reaction time, the vial was transferred back into the glove box. Under inert atmosphere, an aliquot for ^1H NMR and GPC analysis was taken prior to the addition of additional IBVE (0.13 mL, 1.00 mmol, 50 equiv) and 0.045 mL of a stock solution of $FcBF_4$ in DCM (22 mM, 1 μmol, 0.033 mol % relative to IBVE). The reaction was quenched with **2** after 24 hours. The solvent was removed under *vacuo* to yield the pure polymer. GPC traces of the polymers before and after chain extension are shown in Figure 4.5aii.

Chain Extension from poly(Methyl Acrylate) Synthesized in the Absence of IBVE (Figure 4.5a)

In a nitrogen filled glove box, an oven-dried one-dram vial was equipped with a stir bar and charged with MA (0.18 mL, 2.00 mmol, 100 equiv), 0.13 mL of a stock solution of $Ir(ppy)_3$ in DCM (3 mM, 0.40 μmol, 0.02 mol % relative to MA), and 0.02 mL of a stock solution of **1b** in DCM (1 M, 0.02 mmol, 1 equiv). The vial was sealed with a cap equipped with a Teflon septum under an atmosphere of nitrogen, placed next to blue KESSIL lamps (~460 nm) outside of the glove box, and stirred while cooling by blowing compressed air over the

reaction vial. After 2 hours of reaction time, the vial was transferred back into the glove box. Under inert atmosphere, an aliquot for ^{1}H NMR NMR and GPC analysis was taken prior to the addition of IBVE (0.26 mL, 2.00 mmol, 100 equiv) and 0.045 mL of a stock solution of $FcBF_4$ in DCM (22 mM, 1 μmol, 0.05 mol % relative to IBVE). The reaction was quenched with **2** after 24 hours. The solvent was removed under *vacuo* to yield pMA and pIBVE resulting from uncontrolled cationic polymerization. GPC traces of the first aliquot and final polymer are displayed in Figure 4.16.

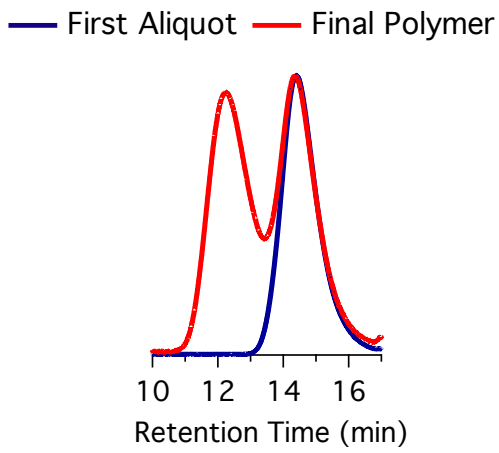

Figure 4.16. GPC Traces of Chain Extension from p(MA) Synthesized in the absence of IBVE.

The GPC trace of the first aliquot (poly(methyl acrylate) and final polymer (homopolymers of poly(methyl acrylate) and poly(isobutyl vinyl ether)) demonstrate that chain extension does not occur when methyl acrylate block is synthesized in the absence of a vinyl ether.

Procedure for Triblock Copolymer Synthesis of Methyl Acrylate and Isobutyl Vinyl Ether (p(MA-*b*-IBVE-*b*-MA), Figure 4.6b)

In a nitrogen filled glove box, an oven-dried one-dram vial was equipped with a stir bar and charged with IBVE (0.26 mL, 2.00 mmol, 100 equiv), MA (0.18 mL, 2.00 mmol, 100 equiv), 0.13 mL of a stock solution of $Ir(ppy)_3$ in DCM (3 mM, 0.40 μmol, 0.02 mol % relative to MA), and 0.02 mL of a stock solution of **1b** in DCM (1 M, 0.02 mmol, 1 equiv). The vial was sealed with a cap equipped with a Teflon septum under an atmosphere of nitrogen, placed next to blue KESSIL lamps (~460 nm) outside of the glove box, and stirred while cooling by blowing compressed air over the reaction vial. After 1 hour of reaction time, the vial was transferred back into the glove box. Under inert atmosphere, an aliquot for ^1H NMR and GPC analysis was taken prior to the addition of 0.045 mL of a stock solution of $FcBF_4$ in DCM (22 mM, 1 μmol, 0.05 mol % relative to IBVE). The reaction was stirred at room temperature for 2 hours, followed by the addition of **2** (1 μmol) to halt the cationic polymerization. Under inert atmosphere, aliquots for NMR and GPC analysis were taken at designated time points prior to a change in stimuli. The reaction was stopped after 11 hours of blue light irradiation. The solvent was removed in *vacuo* to yield the final polymer. GPC traces of the polymer are shown in Figure 4.17. ($M_{n,Theo}$ (kg/mol) = 18.9*,* $M_{n,Exp}$ (kg/mol) = 15.7, $Đ$ = 1.68)

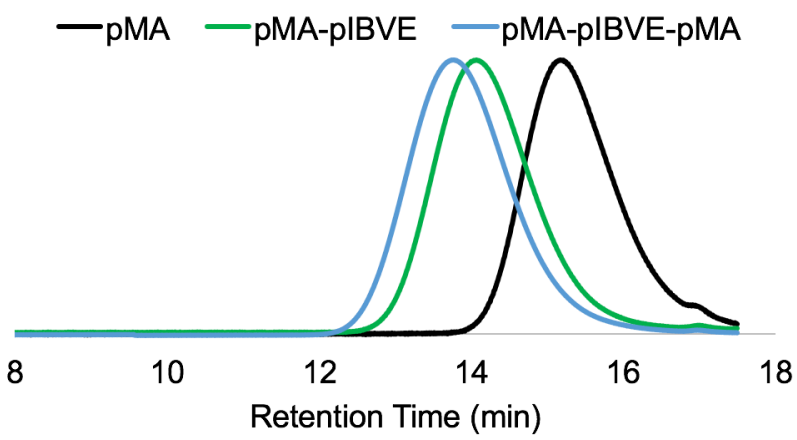

Figure 4.17. GPC traces of p(MA-*b*-IBVE-*b*-MA) (Figure 6b)

Procedure for Triblock Copolymer Synthesis of Methyl Acrylate and Isobutyl Viny Ether (p(IBVE-*b*-MA-*b*-IBVE), Figure 4.6c)

In a nitrogen filled glove box, an oven-dried one-dram vial was equipped with a stir bar and charged with IBVE (0.26 mL, 2.00 mmol, 100 equiv), MA (0.18 mL, 2.00 mmol, 100 equiv), 0.13 mL of a stock solution of $Ir(ppy)_3$ in DCM (3 mM, 0.40 μmol, 0.02 mol % relative to MA), 0.07 mL of a stock solution of $FcBF_4$ in DCM (4 mM, 0.50 μmol, 0.025 mol % relative to IBVE) and 0.02 mL of a stock solution of **1b** in DCM (1 M, 0.02 mmol, 1 equiv). The vial was sealed with a cap equipped with a Teflon septum under an atmosphere of nitrogen and stirred at room temperature for 1 hour before the addition of **2** (0.4 μmol). The vial was irradiated with blue KESSIL lamps (~460 nm) outside of the glove box, and stirred while cooling by blowing compressed air over the reaction vial. After 2 hours of irradiation, the vial was transferred back into the glove box. The addition of 0.03 mL of a stock solution of $FcBF_4$ in DCM (22 mM, 0.67 μmol, 0.033 mol % relative to IBVE) reinitiated cationic polymerization. Under inert

atmosphere, aliquots for NMR and GPC analysis were taken at designated time points prior to a change in stimulus. The reaction was quenched with **2** after 8 hours. The solvent was removed in *vacuo* to yield the pure polymer. GPC traces of the polymer are shown in Figure 4.18. ($M_{n,Theo}$ (kg/mol) = 13.6, $M_{n,Exp}$ (kg/mol) = 10.6, $Đ$ = 1.20)

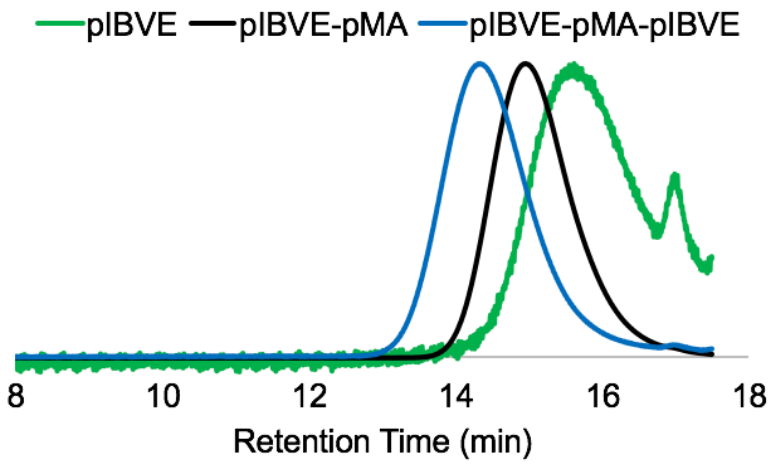

Figure 4.18. GPC traces of p(IBVE-*b*-MA-*b*-IBVE) (Figure 4.6c)

Procedure for Tetrablock Copolymer Synthesis of Methyl Acrylate and Isobutyl Vinyl Ether (p(IBVE-*b*-MA-*b*-IBVE-*b*-MA), Figure 4.6d)

In a nitrogen filled glove box, an oven-dried one-dram vial was equipped with a stir bar and charged with IBVE (0.26 mL, 2.00 mmol, 100 equiv), MA (0.18 mL, 2.00 mmol, 100 equiv), 0.13 mL of a stock solution of $Ir(ppy)_3$ in DCM (3 mM, 0.40 µmol, 0.02 mol % relative to MA), 0.07 mL of a stock solution of $FcBF_4$ in DCM (4 mM, 0.50 µmol, 0.025 mol % relative to IBVE) and 0.02 mL of a stock solution of **1b** in DCM (1 M, 0.02 mmol, 1 equiv). The vial was sealed with a cap equipped with a Teflon septum under an atmosphere of nitrogen and stirred at

room temperature for 2 hours before the addition of **2** (0.4 μmol). The vial was then placed next to blue KESSIL lamps (~460 nm) outside of the glove box, and stirred while cooling by blowing compressed air over the reaction vial. After 2 hours of irradiation, the vial was transferred back into the glove box. The addition of 0.045 mL of a stock solution of $FcBF_4$ in DCM (22 mM, 1 μmol, 0.05 mol % relative to IBVE) reinitiated cationic polymerization. The reaction was stirred for 2 hours at room temperature before the addition of **2** (1 μmol) halted the cationic polymerization. The vial was then re-exposed to blue light. Under inert atmosphere, aliquots for NMR and GPC analysis were taken at designated time points prior to a change in stimuli. The reaction was stopped after 2 hours of irradiation. The solvent was removed *in vacuo* to yield the pure polymer. GPC traces of the polymer are shown in Figure 4.19. ($M_{n,Theo}$ (kg/mol) = 15.1, $M_{n,Exp}$ (kg/mol) = 18.2, $Đ$ = 1.41)

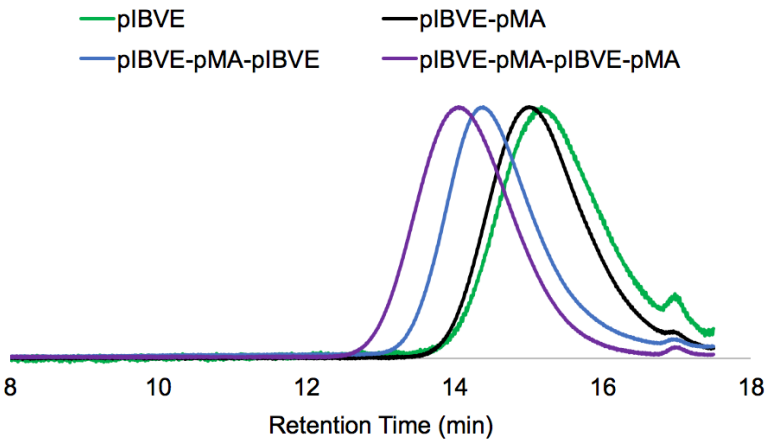

Figure 4.19. GPC traces of p(IBVE-*b*-MA-*b*-IBVE-*b*-MA) (Figure 6d)

Generation of Tetraethylthiuram Disulfide Through the Oxidation of CTA by Ferrocenium Tetrafluoroborate

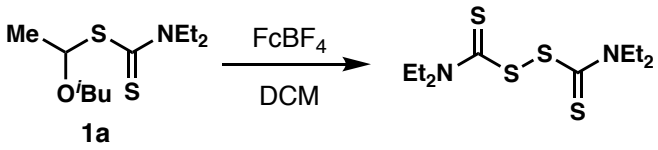

1a

In a nitrogen-filled glove box, an oven-dried one-dram vial was equipped with a stir bar and charged with $FcBF_4$ (273mg, 1.00 mmol, 5 equiv) and CTA **1a** (0.4 mL (0.5 M in DCM), 0.2 mmol, 1 equiv). After 2 hours, the reaction was passed through a silica plug with ethyl acetate. Tetraethylthiuram disulfide was observed in the ^1H NMR of the filtrate.[2]

Radical Copolymerization of Methyl Acrylate and Isobutyl Vinyl Ether with Different Feed Ratios

In a nitrogen filled glove box, an oven-dried one-dram vial was equipped with a stir bar and charged with IBVE, MA, 0.13 mL of a stock solution of $Ir(ppy)_3$ in DCM (3 mM, 0.40 μmol, 0.02 mol % relative to monomers), and 0.02 mL of a stock solution of 1b in DCM (1 M, 0.02 mmol, 1 equiv). The ratio of MA to IBVE was varied as shown in Table 4.3, while maintaining the total amount of monomers at 2 mmol. The vial was sealed with a cap equipped with a Teflon septum under an atmosphere of nitrogen, placed next to blue KESSIL lamps (~460 nm) outside of the glove box, and stirred while cooling by blowing compressed air over the reaction vial. Aliquots for GPC and NMR were taken after the reaction time of 13 hours. The solvent was removed in vacuo to yield

the pure polymers. The amount of thioacetal chain end was determined by ^{1}H NMR.

Table 4.3. Amount of Thioacetal Chain End in Copolymers of Methyl Acrylate and Isobutyl Vinyl Ether.

Entry	**MA : IBVE (feed ratio)**	**MA : IBVE (polymer comp.)**	M_n **(kg/mol)**	$Đ$	**Thioacetal Chain End (%)**
1	2:1	4:1	9.6	1.3.9	>95
2	10:1	14:1	11.0	1.58	>95
3	1:2	2:1	6.8	1.2.6	>95

Appendix References

(1) Kottisch, V.; Michaudel, Q.; Fors, B. P. *J. Am. Chem. Soc.* **2016**, *138*, 15535.

(2) Michaudel, Q.; Chauviré, T.; Kottisch, V.; Supej, M. J.; Stawiasz, K. J.; Shen, L.; Zipfel, W. R.; Abruña, H. D.; Freed, J. H.; Fors, B. P. *J. Am. Chem. Soc.* **2017**, *139*, 15530.

(3) Peterson, B. M.; Lin, S.; Fors, B. P. *J. Am. Chem. Soc.* **2018**, *140*, 2076.

CHAPTER 5

ENHANCING TEMPORAL CONTROL AND ENABLING CHAIN-END MODIFICATION IN PHOTOREGULATED CATIONIC POLYMERIZATIONS BY USING IRIDIUM-BASED PHOTOCATALYSTS

5.1 Abstract

Gaining temporal control over chain growth is a key challenge in the enhancement of controlled living polymerizations. Though research on photocontrolled polymerizations is still in its infancy, it has already proven useful in the development of previously inaccessible materials. Photocontrol has now been extended to cationic polymerizations using 2,4,6-triarylpyrylium salts as photocatalysts. Despite the ability to stop polymerization for a short time, monomer conversion was observed over long dark periods. Improved catalyst systems based on Ir complexes give optimal temporal control over chain growth. The excellent stability of these complexes and the ability to tune the excited and ground state redox potentials to regulate the number of monomer additions per cation formed allows polymerization to be halted for more than 20 hours. The excellent stability of these iridium catalysts in the presence of more nucleophilic species enables chain-end functionalization of these polymers.

5.2 Introduction

The advent of controlled living polymerizations has allowed for the facile synthesis of macromolecules with predictable molecular weights (M_n), narrow

dispersities (*Đ*), and complex architectures.[1] Recently, chemists have developed systems that gain spatiotemporal control over polymer chain growth with various external stimuli, adding to the repertoire of methods to control macromolecular structure.[2–9] These techniques have proven useful in a variety of applications such as biological assays, photoresponsive materials, and surface patterning based on the ability to externally regulate chain-growth. Light is arguably one of the most powerful external stimuli used for polymerizations and new developments in this area will enable the synthesis of new functional materials.[10]

In 2016, we reported a photocontrolled cationic polymerization of vinyl ethers using pyrylium-based dyes as the oxidizing photocatalyst (Figure 5.1 a,b).[11,12] The foundation for temporal control in these polymerizations is based on two major aspects: 1) the stability of the photocatalyst and 2) the delicate interplay between the oxidation of the trithiocarbonate chain end with the excited state photocatalyst to generate carbocations (Figure 5.1 c, step I) and the recapping of the propagating carbocations by the reduced photocatalyst (Figure 5.1 c, step II).[13] The balance required for these two steps leads to large differences in the temporal control observed in these polymerizations when small changes are made to the catalyst structure. For example, triphenylpyrylium tetrafluoroborate (**1 a**) gives fast polymerization but poor temporal control owing to the high number of monomer additions per photon absorbed (approx. 35). Its highly oxidizing excited state potential (E^* = +2.55 V vs. SCE) gives fast chain-end oxidation; however, the ground-state potential

($E_{1/2}$ = −0.31 V vs. SCE) is too weakly reducing to enable facile recapping of the propagating cation, leading to a system that has control over only initiation and not chain growth. Interestingly, switching to the 4-methoxyphenyl congener of the pyrylium catalyst, **1 b**, provides excellent photocontrol over chain-growth (6 monomer additions per photon absorbed). The lower excited state potential (E^* = +1.84 V vs. SCE) of **1 b** still gives efficient oxidation of the trithiocarbonate and, importantly, the more reducing ground state potential ($E_{1/2}$ = −0.50 V vs. SCE) enables facile capping of the chain end, thereby giving temporal control.[13] Although the use of **1 b** gave the first photocontrolled cationic polymerization of vinyl ethers, further studies showed monomer conversion occurred after dark periods of several hours or in dark periods at high conversion. We attributed this background reaction to small amounts of catalyst decomposition.[13,14] We therefore sought other photocatalysts for these polymerizations that had increased stability compared to the pyryliums but similar redox potentials to **1 b** to give enhanced temporal control. We postulated that polypyridyl Ir complexes, which have been extensively used as photosensitizers and catalysts in photomediated small-molecule transformations, would provide the additional catalyst stability that was needed in these reactions.[15,16] Moreover, modification of the ligand structure in these complexes permits precise tuning of both the excited state and ground state redox potentials, allowing us to predictably control chain-end oxidation and recapping (Figure 5.1c, steps I and II). Based on our previous work, we reasoned that we needed photocatalysts with excited state potentials around +1.50 V vs. SCE to give chain-end oxidation

and ground state redox potentials of at least −0.5 V vs. SCE to enable efficient chain-end recapping. We decided to synthesize Ir complexes **2 a**, **2 b**, and **2 c**, which all had similar excited state potentials above +1.60 V but ground state redox potentials of −0.69 V, −0.79 V, and −1.16 V vs. SCE, respectively (Figure 5.2).[17]

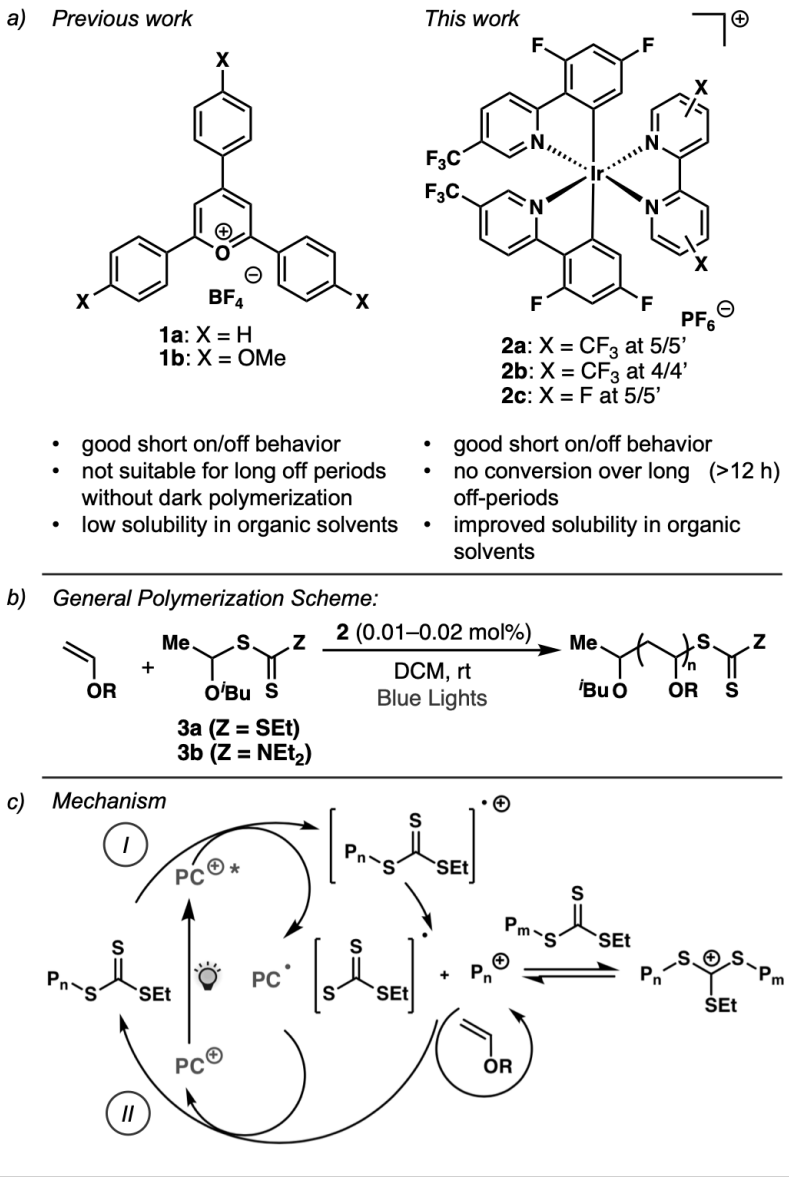

Figure 5.1. Advances in the photocontrolled cationic polymerization of vinyl ethers. a) Photocatalysts (PCs) employed in this and previous work. b) General polymerization scheme. c) Mechanism of photocontrolled cationic polymerization.

5.3 Results and Discussion

We began our studies by looking at the polymerization of isobutyl vinyl ether (IBVE) with Ir complexes **2 a**, **2 b**, and **2 c**. First, using 0.02 mol % of **2 a** in the presence of IBVE and chain-transfer agent (CTA) **3 a**, a 6.3 kg mol^{-1} polymer

was obtained after irradiation with blue LEDs for 16 hours (Table 5.1 entry 1). This reaction went to 97 % conversion and good agreement between theoretical and experimental molecular weights was observed. This initial result demonstrated that these complexes were viable catalysts for photocontrolled cationic polymerizations of vinyl ethers. By modulating the ratio of IBVE to CTA, higher molar mass polymers could be successfully synthesized with good control (Table 5.1 entries 2 and 3). Significantly, good agreement between experimental and theoretical molar masses was maintained for polymers above 30 kg mol^{-1}. This is a marked improvement from the pyrylium-based catalyst systems, where experimental M_n values were significantly lower than the theoretical M_n values when targeting molar masses above 20 kg mol^{-1}.[11] We hypothesize that direct oxidation of the vinyl ether is less competitive to oxidation of **3 a** with **2 a**, allowing the synthesis of higher molar mass polymers.

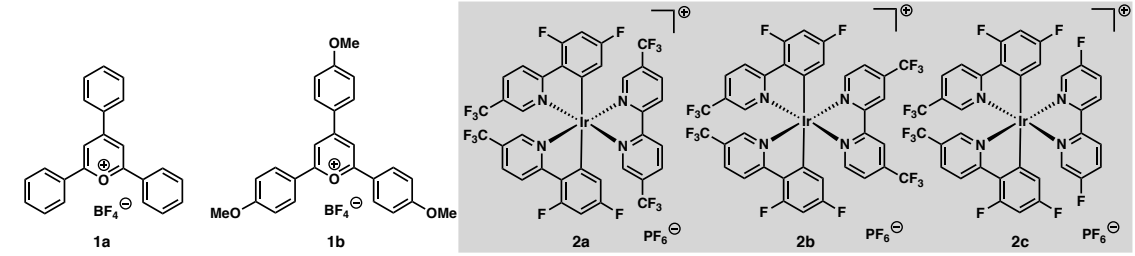

Figure 5.2. Comparison of excited-state oxidation potentials, ground-state reduction potentials, and quantum efficiencies for PCs **1 a**–**2 c**. Ir complexes **2 a**–**c** are subject of this report (gray region).

Under identical conditions, catalyst **2 b** also gave well-controlled polymerizations for targeted molar masses up to about 20 kg mol^{-1} (Table 5.1, entries 4–6). However, when targeting a molar mass above 30 kg mol^{-1}, a polymer with a lower than predicted M_n and broad $Đ$ was obtained (Table 5.1, entry 7). Finally, switching to catalyst **2 c** resulted in an incredibly slow polymerization. After 16 hours, only 9 % of the IBVE had been consumed (Table 5.1, entry 8). We reasoned that the more reducing ground-state potential of **2 c** increases the rate of polymer recapping relative to propagation, slowing the rate of polymerization. This result suggests that there is a lower limit for the ground state redox potential of these catalysts for efficient polymerization to occur.[18] Compared to the pyrylium-based systems, catalysts **2 a** and **2 b** gave reduced rates of polymerization at the same catalyst concentrations and with the same irradiation intensities. UV/Vis spectroscopy of the Ir complexes revealed extinction coefficients 100 times lower than **1 b**, giving rise to the reduced activity. Gratifyingly, the reaction proceeded much faster under higher intensity lights and reached full conversion after 1.5 and 3 hours for catalysts **2 a** and **2 b**, respectively (Table 5.1, entries 9 and 10). Trithiocarbonate CTA **3 a** was mainly used for this work because it gives increased rates of reaction and is a versatile CTA but it does produce polymers with slightly broadened $Đ$.[10] However, when using dithiocarbamate **3 b** under our standard conditions, polymers with narrower $Đ$ values were produced (Table 5.1, entries 11 and 12), albeit with slower rates of polymerization. Importantly, excellent control was maintained for both **3 a** and **3 b** under higher-intensity lights.

Table 5.1. Polymerization of IBVE using **2 a**, **2 b**, and **2 c**.

Entry[a]	Catalyst	Conv. (%)	$M_{n,theo}$ (kg/mol)	M_n (kg/mol)	$Đ$
1	2a	97	4.9	6.3	1.40
2	2a	96	9.6	8.9	1.35
3[b]	2a	86	34.6	32.6	1.45
4	2b	87	4.3	6.5	1.21
5	2b	89	8.9	10.3	1.37
6	2b	89	17.8	19.4	1.37
7[b]	2b	84	33.6	26.0	1.71
8	2c	9	1.0	2.7	1.33
9[b,c]	2a	99	9.9	8.4	1.37
10[c]	2b	90	9.0	9.3	1.39
11[d]	2a	53	5.3	5.0	1.24
12[d]	2b	51	5.1	5.1	1.24

[a]IBVE (1 equiv), **3 a** (0.01–0.0025 equiv), and 0.02 mol % of **2** were irradiated with blue LEDs (455 nm) for 16 h. [b]0.01 mol % of **2** was used. [c]Entries 9 and 10 were irradiated with higher intensity light for 1.5 h and 3 h, respectively. [d]IBVE (1 equiv), **3 b** (0.01 equiv), and 0.02 mol % of **2** were irradiated with higher intensity lights for 8 h.

Therefore, we set out to test our hypothesis that the increased stability of the Ir complexes will allow efficient photogating at high conversions and for long off periods. Using catalyst **2 a** under the standard conditions, the reaction was exposed to intermittent blue light exposure. After only 2 minutes of irradiation, the polymerization reached 55 % conversion. The reaction tube was then placed in the dark for about 1 hour and this process was repeated two more times (Figure 5.3 a). The conversion was measured by NMR spectroscopy before and

after exposure to light. Significantly, we observed no monomer consumption during off periods and efficient polymerization when the reaction was re-exposed to light. Furthermore, all dark periods were performed above 50 % conversion; at these high conversions the pyrylium-based catalyst systems showed some polymerization in the dark. We then performed the same reaction with an off period for >20 hours (Figure 5.3 b). Again, no monomer conversion was observed during the dark period, which is a significant improvement over previous catalyst systems. These same experiments were repeated with catalyst **2 b**, and similar levels of temporal control were observed (Appendix, Figure 5.4).

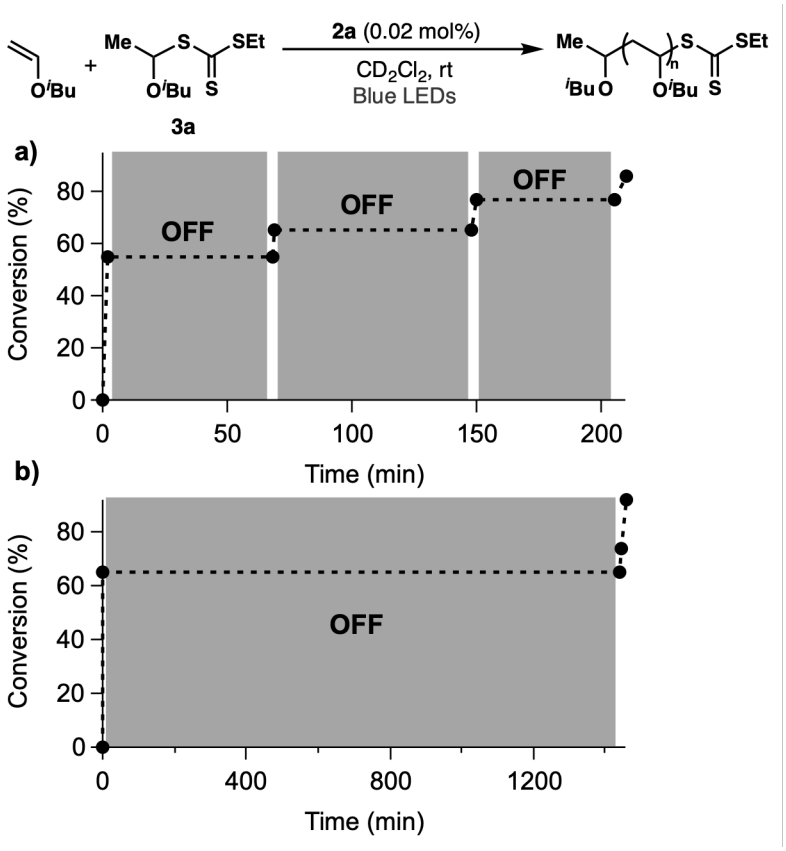

Figure 5.3. On/Off experiments with 0.02 mol % **2 a** in the presence of CTA **3 a**. a) Short off behavior, b) demonstration that no conversion occurs over long dark periods.

Notably, both catalysts maintained high activity after prolonged off stages and all the reactions were run to >70 % conversion. In all cases, the molecular weight distribution of the final polymer was monomodal, had comparable *Đ* values to polymers synthesized without intermittent light exposure, and the M_n values aligned well with the theoretical molar masses. These results clearly demonstrate that the improved stability of **2 a** and **2 b** enable highly efficient temporal control in these photocontrolled cationic polymerizations.

We next wanted to compare the quantum yields of our Ir complexes with the pyrylium-based catalysts. For typical photoinitiated cationic polymerizations, approximately 200 monomer additions occur per photon absorbed. In our previously reported photocontrolled polymerizations, pyrylium **1 a** and **1 b** yielded 35 and 6 monomer additions per photon absorbed, respectively.[13] Potassium ferrioxalate actinometry data of initial reaction rates when targeting a 5 kg mol^{-1} polymer revealed that polymerizations with **2 a** and **2 b** gave 4 and 3 monomer additions per photon absorbed, respectively (Figure 5.2). These results show that the quantum yields of **2 a** and **2 b** are similar to pyrylium **1 b**, which showed photogating in these polymerizations. Additionally, actinometry experiments with **2 c** showed significantly less than one monomer addition per photon absorbed, providing qualitative evidence that recapping is too fast to allow efficient chain propagation.

Next, we sought to take advantage of the stability of these Ir complexes for chain-end functionalization after polymerization. Specifically, **2 a** and **2 b** can be utilized in the presence of nucleophilic substrates, which we envisaged would

allow for the addition of an alcohol to the oxocarbenium chain end to form an acetal. To test this hypothesis, we synthesized pIBVE under our standard conditions and added 3 equiv of an alcohol at full monomer conversion. Additionally, 0.02 mol % of **2 a** and 1 equiv of base (2,6-di-*tert*-butylpyridine) relative to chain end were needed for successful functionalization (Scheme 5.1). The base was added to sequester any acid byproduct to ensure the stability of the acetal chain end and additional photocatalyst was needed to accelerate the reaction. Under polymerization conditions, activation of only a small fraction of the chain ends is necessary to give efficient propagation, whereas all of the trithiocarbonates need to be oxidized for efficient chain-end functionalization. Importantly, more than 90 % functionalization was achieved for three different alcohols, clearly illustrating the power of these systems to make polymers with functional and well-defined chain ends. It is worth noting that efficient acetal formation could not be achieved when the pyrylium catalyst **1 b** was used in place of Ir complex **2 a**.

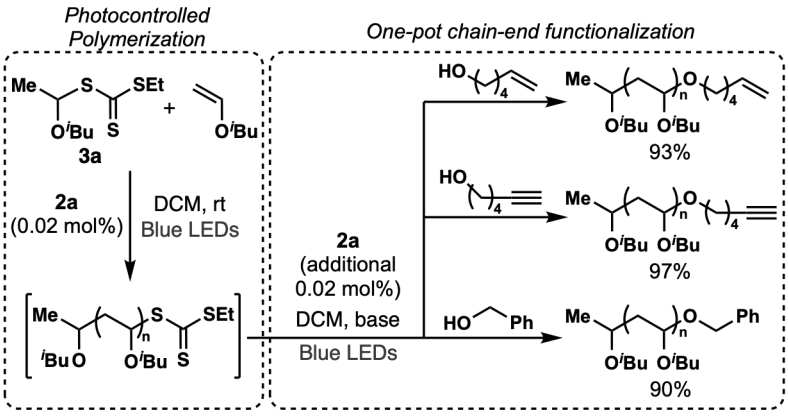

Scheme 5.1. Photocontrolled polymerization of isobutyl vinyl ether followed by chain-end functionalization with alcohols in a one-pot setup (base = 2,6-di-*tert*-butylpyridine).

5.4 Conclusion

In conclusion, we have described how to rationally design the ligand structure of a series of polypyridyl Ir complexes for the photocontrolled cationic polymerization of vinyl ethers. The enhanced stability of these complexes and the ability to precisely tune the redox potentials of these catalysts led to systems with outstanding temporal control. More specifically, **2 a** and **2 b** can be used to regulate chain growth at high conversion and for dark periods of several hours under the polymerization conditions. Even in the presence of nucleophiles, such as alcohols, the catalysts remain active and facilitate highly efficient chain-end functionalization in a one-pot setup. We envision that these findings will enable the directed synthesis of extremely potent catalysts tailored toward cationic photocontrolled polymerizations.

5.5 References

(1) R. B. Grubbs, R. H. Grubbs, *Macromolecules* **2017**, *50*, 6979.

(2) F. A. Leibfarth, K. M. Mattson, B. P. Fors, H. A. Collins, C. J. Hawker, *Angew. Chem. Int. Ed.* **2013**, *52*, 199; *Angew. Chem.* **2013**, *125*, 210.

(3) For selected examples of photo-ATRP, see: a) B. P. Fors, C. J. Hawker, *Angew. Chem. Int. Ed.* **2012**, *51*, 8850; *Angew. Chem.* **2012**, *124*, 8980; b) D. Konkolewicz, K. Schroder, J. Buback, S. Bernhard, K. Matyjaszewski, *ACS Macro Lett.* **2012**, *1*, 1219; c) G. R. Jones, R. Whitfield, A. Anastasaki, D. M. Haddleton, *J. Am. Chem. Soc.* **2016**, *138*,

7346; d) J. C. Theriot, C.-H. Lim, H. Yang, M. D. Ryan, C. B. Musgrave, G. M. Miyake, *Science* **2016**, *352*, 1082.

(4) For selected examples of photo-RAFT, see: a) J. Xu, K. Jung, A. Atme, S. Shanmugam, C. Boyer, *J. Am. Chem. Soc.* **2014**, *136*, 5508; b) M. Chen, M. J. MacLeod, J. A. Johnson, *ACS Macro Lett.* **2015**, *4*, 566; c) S. Shanmugam, J. Xu, C. Boyer, *J. Am Chem. Soc.* **2015**, *137*, 9174; d) S. Shanmugam, C. Boyer, *Chem. Sci.* **2015**, *6*, 1341; e) M. Chen, S. Deng, Y. Gu, J. Lin, M. J. MacLeod, J. A. Johnson, *J. Am. Chem. Soc.* **2017**, *139*, 2257

(5) For selected examples of photoinduced-TERP, see: a) S. Yamago, Y. Ukai, A. Matsumoto, Y. Nakamura, *J. Am Chem. Soc.* **2009**, *131*, 2100; b) Y. Nakamura, T. Arima, S. Tomita, S. Yamago, *J. Am. Chem. Soc.* **2012**, *134*, 5536.

(6) For selected examples of photo-ROMP, see: a) K. A. Ogawa, A. E. Goetz, A. J. Boydston, *J. Am. Chem. Soc.* **2015**, *137*, 1400; b) A. E. Goetz, L. M. M. Pascual, D. G. Dunford, K. A. Ogawa, D. B. Knorr, Jr, A. J. Boydston, *ACS. Macro Lett.* **2016**, *5*, 579; c) L. M. M. Pascual, A. E. Goetz, A. M. Roehrich, A. J. Boydston, *Macromol. Rapid Comm.* **2017**, *38*, 1600766 (1–6).

(7) For selected examples of electrochemically-mediated polymerizations: a) A. J. D. Magenau, N. C. Strandwitz, A. Gennaro, K. Matyjaszewski, *Science* **2011**, *332*, 81; b) M. Fantin, A. A. Isse, A. Venzo, A. Gennaro, K. Matyjaszewski, *J. Am. Chem. Soc.* **2016**, *138*, 7216; c) Y. Wang, M.

Fantin, S. Park, E. Gottlieb, L. Fu, K. Matyjaszewski, *Macromolecules* **2017**, *50*, 7872; d) B. M. Peterson, S. Lin, B. P. Fors, *J. Am. Chem. Soc*. **2018**, *140*, 2076.

(8) For selected examples of chemically-controlled polymerizations: a) E. M. Broderick, N. Guo, C. S. Vogel, C. Xu, J. Sutter, J. T. Miller, K. Meyer, P. Mehrkhodavandi, P. L. Diaconescu, *J. Am. Chem. Soc.* **2011**, *133*, 9278; b) A. B. Biernesser, B. Li, J. A. Byers, *J. Am. Chem. Soc*. **2013**, *135*, 16553; c) A. B. Biernesser, K. R. Delle Chiaie, J. B. Curley, J. A. Byers, *Angew. Chem. Int. Ed.* **2016**, *55*, 5251; *Angew. Chem.* **2016**, *128*, 5337.

(9) Example of photo-ROP: C. Fu, J. Xu, C. Boyer, *Chem. Commun.* **2016**, *52*, 7126.

(10) a) M. Chen, M. Zhong, J. A. Johnson, *Chem. Rev.* **2016**, *116*, 10167; b) Q. Michaudel, V. Kottisch, B. P. Fors, *Angew. Chem. Int. Ed.* **2017**, *56*, 9670; *Angew. Chem.* **2017**, *127*, 9798. c) N. Corrigan, S. Shanmugan, J. Xu, C. Boyer, *Chem. Soc. Rev.* **2016**, *45*, 6165; d) M. A. Tehfe, F. Louradour, J. Lalevee, J.-P. Fouassier, *Appl. Sci.* **2013**, *3*, 490; e) S. Dadashi-Silab, C. Aydogan, Y. Yagci, *Polym. Chem.* **2015**, *6*, 6595; f) J. T. Trotta, B. P. Fors, *Synlett* **2016**, *27*, 702.

(11) a) V. Kottisch, Q. Michaudel, B. P. Fors, *J. Am. Chem. Soc*. **2016**, *138*, 15535; b) V. Kottisch, Q. Michaudel, B. P. Fors, *J. Am. Chem. Soc.* **2017**, *139*, 10665.

(12) For examples of living cationic polymerization, see: a) M. Uchiyama, K. Satoh, M. Kamigaito, *Angew. Chem. Int. Ed.* **2015**, *54*, 1924; b) S.

Sugihara, N. Konegawa, Y. Maeda, *Macromolecules* **2015**, *48*, 5120; c) M. Uchiyama, K. Satoh, M. Kamigaito, *Macromolecules* **2015**, *48*, 5533; d) M. Ciftci, Y. Yoshigawa, Y. Yagci, *Angew. Chem. Int. Ed.* **2017**, *56*, 519–523; *Angew. Chem.* **2017**, *127*, 534–538.

(13) Q. Michaudel, T. Chauviré, V. Kottisch, M. J. Supej, K. J. Stawiasz, L. Shen, R. W. Zipfel, H. D. Abruña, J. H. Freed, B. P. Fors, *J. Am. Chem. Soc.* **2017**, *139*, 15530.

(14) a) E. V. Kuznetsov, I. V. Shcherbakova, A. T. Balaban in *Advances in Heterocyclic Chemistry, Vol. 50*. Academic Press, New York, **1990**, pp. 157–254; b) E. Alfonzo, F. S. Alfonso, A. B. Beeler, *Org. Lett.* **2017**, *19,* 2989.

(15) a) C. K. Prier, D. A. Rankic, D. W. C. MacMillan *Chem Rev.* **2013**, *113*, 5322; b) L. Marzo, S. K. Pagire, O. Reiser, B. König *Angew. Chem. Int. Ed.* 10.1002/anie.201709766; *Angew. Chem.* 10.1002/ange.201709766.

(16) a) G. J. Choi, Q. Zhu, D. C. Miller, C. J. Gu, R. R. Knowles, *Nature* **2016**, *539,* 268; b) Q. Zhu, E. C. Gentry, R. R. Knowles, *Angew. Chem. Int. Ed.* **2016**, *55*, 9969; *Angew. Chem.* **2016**, *128*, 10123; c) F. J. Coughlin, M. S. Westrol, K. D. Oyler, N. Byrne, C. Kraml, E. Zysman-Colman, M. S. Lowry, S. Bernhard, *Inorg. Chem*. **2008**, *47*, 2039; d) J. I. Goldsmith, W. R. Hudson, M. S. Lowry, T. H. Anderson, S. Bernhard, *J. Am. Chem. Soc*. **2005**, *127*, 7502.

(17) These cationic iridium catalysts have been previously synthesized and employed by Knowles and co-workers for a variety of small molecule transformations (see reference 15).

(18) P. J. Nichols, M. W. Grant, *Aust. J. Chem.* **1982**, *35*, 2455.

5.6 Appendix

General Reagent Information

All polymerizations were set up in an Unilab MBraun glovebox with a nitrogen atmosphere and irradiated with blue LED lights under nitrogen atmosphere outside the glovebox. Isobutyl vinyl ether (IBVE) (99%, TCI), 2-chloroethyl vinyl ether (2Cl-EVE) (97%, TCI), *n*-propyl vinyl ether (PVE) (99%, Sigma Aldrich), *n*-butyl vinyl ether (BVE) (98%, Sigma Aldrich), and benzene (Fischer Scientific) were dried over calcium hydride (CaH_2) (ACROS chemicals, 93% extra pure, 0–2 mm grain size) for 12 h, distilled under nitrogen and degassed by three freeze-pump-thaw cycles. d2-Dichloromethane (CD_2Cl_2) (99.8%, Cambridge Isotopes) was dried over CaH_2 for 12 h, vacuum transferred and degassed by three freeze-pump-thaw cycles. Ethanethiol (97%, Alfa Aesar) and carbon disulfide (99.9+%, Alfa Aesar) were distilled before use. $IrCl_3 \cdot H_2O$ (99.9%, Strem Chemicals), 2-bromo-5-(trifluoromethyl)pyridine (98%, Ark Pharm), 2-bromo-5-fluoropyridine (98%, Lancaster Synthesis), 2-bromo-4-(trifluoromethyl)pyridine (98%, Oakwood Chemicals), (2,4-difluorophenyl)boronic acid (Sigma Aldrich), palladium acetate (Pd(OAc)2) (98%, Sigma Aldrich), potassium carbonate (K_2CO_3) (Sigma Aldrich), lithium chloride (LiCl) (99%, Sigma Aldrich), ethanol (EtOH) (Anhydrous, KOPTEC USP), triphenylphosphine (99%, Aldrich), methanol (MeOH) (Fischer scientific), 2.0 M HCl in Et_2O (Sigma Aldrich), sodium hydride (60%, dispersion in mineral oil, Sigma Aldrich), and anhydrous benzyl alcohol (99.8%, Sigma Aldrich) were used as received. 5-hexyn-1-ol (97%, Alfa Aesar), 5-hexen-1-ol (95+%, TCI),

and 2,6-di-*tert*-butylpyridine (97%, Acros Organics) were dried by azeotroping with benzene (3 x 1 mL) under reduced pressure prior to use. Dichloromethane (DCM), diethylether (Et_2O) and dimethylformamide (DMF) were purchased from J.T. Baker and were purified by vigorous purging with argon for 2 h, followed by passing through two packed columns of neutral alumina under argon pressure. $[Ir(dF(CF_3)ppy)_2(5,5'dCF_3bpy)]PF_6$ **(2a)**,[1] $[Ir(dF(CF_3)ppy)_2(4,4'dCF_3bpy)]PF_6$ **(2b)**[1] and $[Ir(dF(CF_3)ppy)_2(5,5'dFbpy)]PF_6$ **(2c),**[1] *S*-1-isobutoxylethyl *S′*-ethyl trithiocarbonate **(3a)**[2] and *S*-1-isobutoxyethyl *N,N*-diethyl dithiocarbamate **(3b)**[2] were synthesized according to literature procedures.

General Analytical Information

All polymer samples were analyzed using a Tosoh EcoSec HLC 8320GPC system with two SuperHM-M columns in series at a flow rate of 0.350 mL/min. THF was used as the eluent and all number-average molecular weights (M_n), weight-average molecular weights (M_w), and dispersities ($Đ$) for all polymers were determined by light scattering using a Wyatt miniDawn Treos multi-angle light scattering detector. Nuclear magnetic resonance (NMR) spectra were recorded on a Mercury 300 MHz, Varian 400 MHz, Bruker 500 MHz, or a Varian 600 MHz instrument at room temperature using $CDCl_3$ or CD_2Cl_2 as a solvent. UV-vis spectra in DCM were recorded on a Varian Cary 50 Bio UV-Visible Spectrophotometer.

General Reaction Setup

Irradiation of photochemical reactions was done using blue diode led® BLAZE™ light strips (455 nm, 2.88 W/ft) or two H150-Bue KESSIL® lamps (465nm, 30W). Actinometry was performed with a Kobi Electric lamp 9W bulb (460–470nm). In the case of LED strips, the inside of a crystallization dish was lined with LED strips to irradiate the reaction vessel uniformly. The reaction was cooled by blowing compressed air over the reaction vial or J-Young NMR tube in the case of on-off experiments.

Procedure for "On-Off" Experiments with Catalyst 2a or 2b (Figure 5.3 and Figure 5.4)

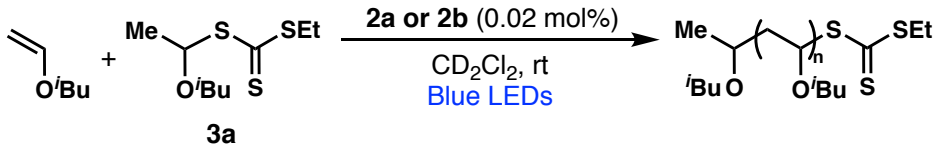

In a nitrogen filled glove box, an oven-dried one-dram vial was charged with IBVE (0.26 mL, 2.00 mmol, 50 equiv), 0.2 mL of a stock solution of either **2a** (Figure 3) or **2b** (Figure S1) in CD_2Cl_2 (2.0 mM, 0.20 µmol, 0.02 mol% relative to IBVE), and 0.04 mL of a stock solution of **3a** in DCM (1 M, 0.04 mmol, 1 equiv). Benzene (30 µL, 0.33 mmol, 8 equiv) was added as an internal standard for NMR. The total volume of the solution was equally divided into two oven-dried J-Young NMR tubes and each diluted with 0.2 mL of additional CD_2Cl_2. The tubes were sealed under an atmosphere of nitrogen, placed next to blue KESSIL® lamps outside of the glove box while cooling by blowing compressed

air over the tube. The lights were turned off during an off-period and the reaction was covered in aluminum foil to avoid irradiation. Conversion was measured by ^{1}H NMR before and after a dark period.

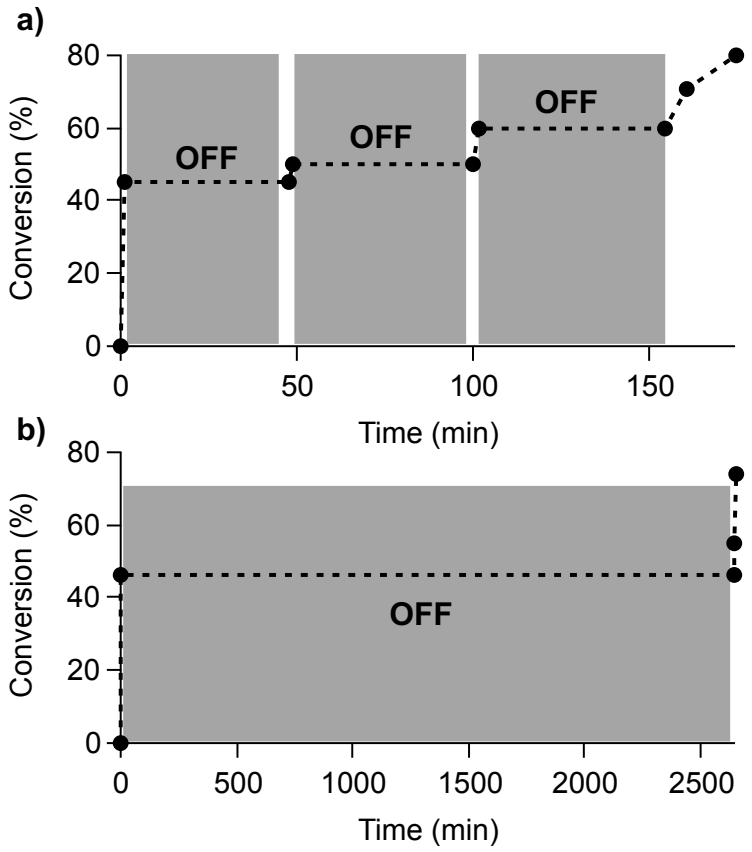

Figure 5.4. On/Off experiment with **2b** for a short (a) and long (b) off period.

Procedure for Isobutyl Vinyl Ether Homopolymerization (Table 5.1)

In a nitrogen filled glove box, an oven-dried one-dram vial was equipped with a stir bar and charged with IBVE (0.26 mL, 2.00 mmol, 100 equiv), 0.05–

0.2 mL of a stock solution of either **2a**, **2b**, or **2c** in DCM (2.0 mM, 0.05–0.20 μmol, 0.005–0.02 mol% relative to IBVE), and 0.02 mL of a stock solution of **3a** or **3b** in DCM (1 M, 0.02 mmol, 1 equiv). The vial was sealed with a cap equipped with a Teflon septum under an atmosphere of nitrogen, placed next to blue KESSIL® lamps or blue LED strips outside of the glove box, and stirred while cooling by blowing compressed air over the reaction vial. Following the desired amount of reaction time, benzene (89 μL, 1.0 mmol, 50 equiv) was added as an internal standard for NMR, and aliquots for NMR and GPC analysis were taken.

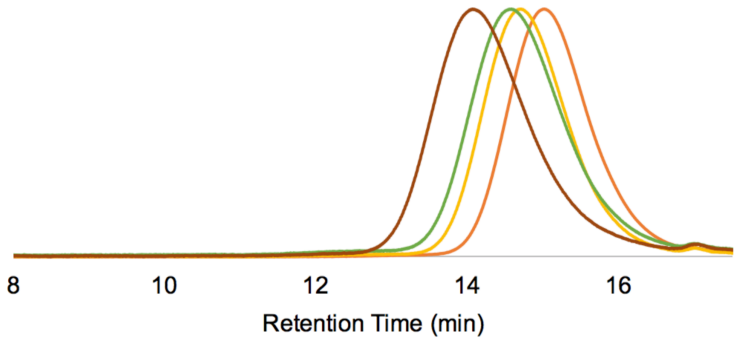

Figure 5.5. Representative GPC traces of poly(isobutyl vinyl ether) prepared by the general procedure above.

Procedure for Quantum Yield Determination of IBVE Polymerization (2a–2c)

General Procedure for Determination of Early Rate of IBVE polymerization (**2a** and **2b**)

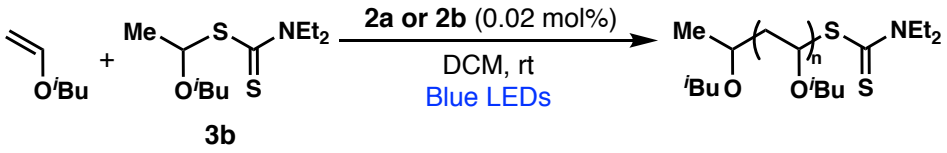

In a nitrogen filled glove box, an oven-dried one-dram vial was equipped with a stir bar and charged with IBVE (0.26 mL, 2.00 mmol, 50 equiv), 0.2 mL of a stock solution of either **2a** or **2b** in DCM (2.0 mM, 0.20 μmol, 0.02 mol% relative to IBVE), and 0.04 mL of a stock solution of **3b** in DCM (1 M, 0.04 mmol, 1 equiv). The vial was sealed with a cap equipped with a Teflon septum under an atmosphere of nitrogen, placed next to a 9W Kobi Electric lamp equipped with a 50% neutral density filter (460–470 nm) outside of the glove box, and stirred while cooling by blowing compressed air over the reaction vial. Following the desired amount of reaction time, benzene (89 μL, 1.0 mmol, 50 equiv) was added as an internal standard for NMR, and an aliquot for NMR analysis was taken. In each case, the average of two experiments was used to determine the quantum efficiency (Table 5.2). CTA **3b** was used in order to be able to directly compare quantum yields of **2a** and **2b** with previously reported data for **1a** and **1b**.[3]

General Procedure for Determination of Early Rate of IBVE polymerization (**2c**)

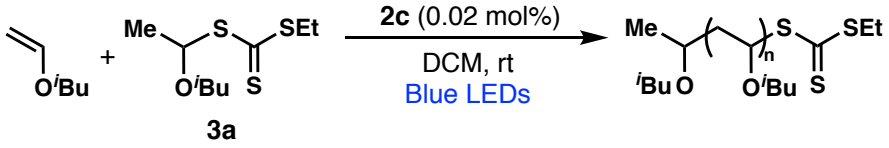

In a nitrogen filled glove box, an oven-dried one-dram vial was equipped with a stir bar and charged with IBVE (0.26 mL, 2.00 mmol, 50 equiv), 0.2 mL of a stock solution of **2c** in DCM (2.0 mM, 0.20 μmol, 0.02 mol% relative to IBVE), and 0.04 mL of a stock solution of **3a** in DCM (1 M, 0.04 mmol, 1 equiv). The vial was sealed with a cap equipped with a Teflon septum under an atmosphere of nitrogen, placed next to a 9W Kobi Electric lamp (460–470 nm) outside of the glove box, and stirred while cooling by blowing compressed air over the reaction vial. Following the desired amount of reaction time, benzene (89 μL, 1.0 mmol, 50 equiv) was added as an internal standard for NMR, and an aliquot for NMR analysis was taken. The reaction proceeded too slowly at 50% light intensity (as was used for **2a** and **2b**). An approximate rate constant at 50% light intensity was therefore determined by measuring the rate at 100% light intensity (i.e. without neutral density filter) and dividing the value by 2. Additionally, CTA **3a** was used rather than **3b** because of faster polymerization kinetics. Actinometry approximated less than one monomer addition per photon (3.0×10^{-7} mol.s^{-1} * 0.5 = 1.5×10^{-7} mol.s^{-1}).

Determination of the Quantum Yields of Polymerization Using Ferrioxalate Actinometry

Quantum yields were determined by following the procedure in reference 3. The quantum yield of polymerization for **2a**, **2b**, and **2c** was deduced by comparison of the early rate of IBVE polymerization and the rates of photodegradation of potassium ferrioxalate ([Fe(III)]), according to equation 5.1:

(5.1) $$\Phi_{\mathbf{1}} = \Phi_{[\mathrm{Fe(III)}]} * \frac{q(\mathbf{1})}{q([\mathrm{Fe(III)}])} * \frac{\left(1 - 10^{-A_{[\mathrm{Fe(III)}]}}\right)}{\left(1 - 10^{-A_{\mathbf{1}}}\right)}$$

where q(**1**) and q([Fe(III)]) are the conversion rate (in mol•s^{-1}) of IBVE during polymerization and of [Fe(III)] during photodegradation, respectively. The corrective factor accounts for the real flux of absorbed photon by the actinometer and photocatalysts **2a**, **2b**, and **2c** and therefore depends on the absorbance of both species at 455 nm. $\Phi_{[\mathrm{Fe(III)}]}$ is the known quantum yield of potassium ferrioxalate decomposition. A reported value of $\Phi_{[\mathrm{Fe(III)}]}$ of 0.86 at 457 nm was used in the calculations.[4]

The degradation rate q([Fe(III)]) was determined according to the protocol described by Kuhn *et al*.[5] A solution of potassium ferrioxalate (300 µl, 0.15 M) in aq. H_2SO_4 (0.05 M) in a 1 dram vial was irradiated with a 9W Kobi Electric (460–470 nm) bulb placed 2 cm away from the vial, with a 50% transmission neutral density filter placed in between the vial and the bulb. Aliquots (24 µl) were taken every 5 seconds and added to vials containing a solution of phenanthroline (96 µl, 0.01 % weight), sodium propionate buffer (12

μl, 0.6 M in aq. H_2SO_4 (0.19 M), and water (54 μl). After 1 h in the dark, the concentration of the resulting Fe(II) phenantroline complex present in each solution was measured by UV-visible spectroscopy (absorption at 510 nm, ε_{510} = 11100 L.mol.$^{-1}$cm^{-1}). The degradation rate q([Fe(III)]) was then determined by linear fitting to be 1.9x10^{-8} mol.s^{-1}.

The quantum yields of polymerization were estimated to be about four monomer additions per photon absorbed for photocatalyst **2a**, three monomer additions per photon for **2b** (Table 5.2) and less than one monomer addition per photon for **2c**.

Table 5.2. Compiled actinometry data of **2a** and **2b**.

	Transmission Filter	**Degradation rate (mmol*min^{-1})**	**A455[1] (Catalyst)**	**QY[2]**	
2a	50	–0.0049	0.7753036	4.3	
	50	–0.0044	0.7753036	3.8	
			Average50 =	**4.1**	
Total Point	50	–0.0045	0.7753036	3.9	**Standard Deviation 0.4**
2b	50	–0.0025	0.784487893	2.2	
	50	–0.0035	0.784487893	3.0	**Standard Deviation 0.6**
			Average50 =	**2.6**	
Total Point	50	–0.0030	0.784487893	2.6	

[1]**A455**: absorption at 455 nm; [2]**QY**: quantum yield = monomer additions per photon.

General Procedure for the In Situ Chain-End Functionalization of Poly(Vinyl Ethers)

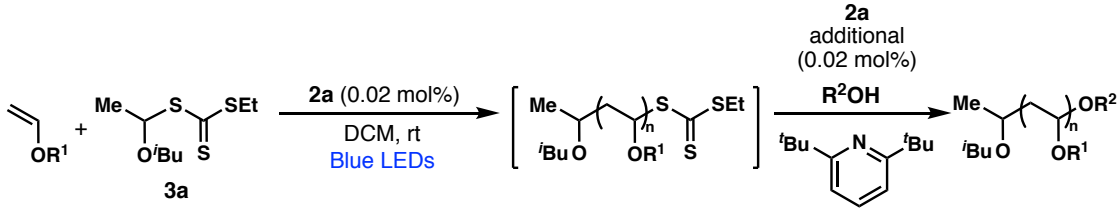

In a nitrogen filled glove box, an oven-dried one-dram vial was equipped with a stir bar and charged with vinyl ether (0.13 mL, 1.00 mmol, 100 equiv), 0.1 mL of a stock solution of **2a** in DCM (1.0 mM, 0.20 μmol, 0.02 mol % relative to IBVE), and 0.02 mL of a stock solution of **3a** in DCM (0.5 M, 0.02 mmol, 1 equiv), and 0.08 mL of DCM. The vial was sealed with a cap equipped with a Teflon septum under an atmosphere of nitrogen, placed 2 cm from two blue LED Kessil lamps outside of the glove box, and stirred while cooling by blowing compressed air over the reaction vial. After the desired reaction time (20–30 minutes), the reaction was removed from light and aliquots were taken for GPC and ^{1}H NMR. Solvent and residual monomer were removed *in vacuo* to yield the crude polymer.

Immediately following the polymerization, alcohol (0.03 mmol, 3 equiv), 0.1 mL of a stock solution of **2a** in DCM (1.0 mM, 0.20 μmol, additional 0.02 mol% to initial monomer concentration), 2,6-di-*tert*-butylpyridine (0.01 mmol, 1 equiv), and 0.2 mL of DCM were added. The vial was sealed with a cap equipped with a Teflon septum, degassed by three freeze-pump-thaw cycles, and put under an atmosphere of nitrogen. The reaction vessel was placed 2 cm from two blue LED Kessil lamps, and stirred while cooling by blowing

compressed air over the reaction vial. After 18h, the reaction was removed from the light and aliquots were taken for GPC and ^{1}H NMR. The polymer was then precipitated from cold methanol, washed three times with cold methanol to remove residual alcohol, and dried *in vacuo* to afford pure polymer. Respective ^{1}H NMRs for functionalized poly(isobutyl vinyl ethers) are shown in Figures 5.6–5.9. Representative GPC traces of the polymer before and after modification are shown in Figure 5.10.

To demonstrate that functionalization occurs readily on other poly(vinyl ethers) as well, the procedure above was performed with *n*-butyl vinyl ether. The functionalized polymer is depicted in Figure 5.9.

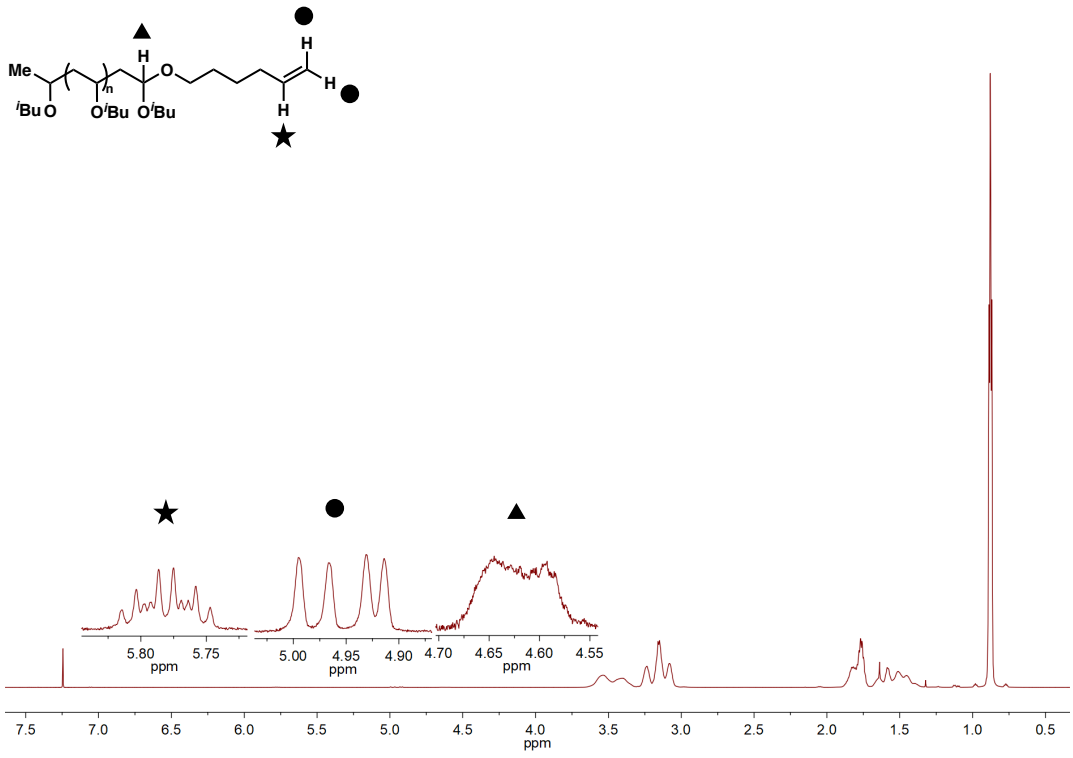

Figure 5.6. ^{1}H NMR of poly(isobutyl vinyl ether) functionalized with 5-hexen-1-ol.

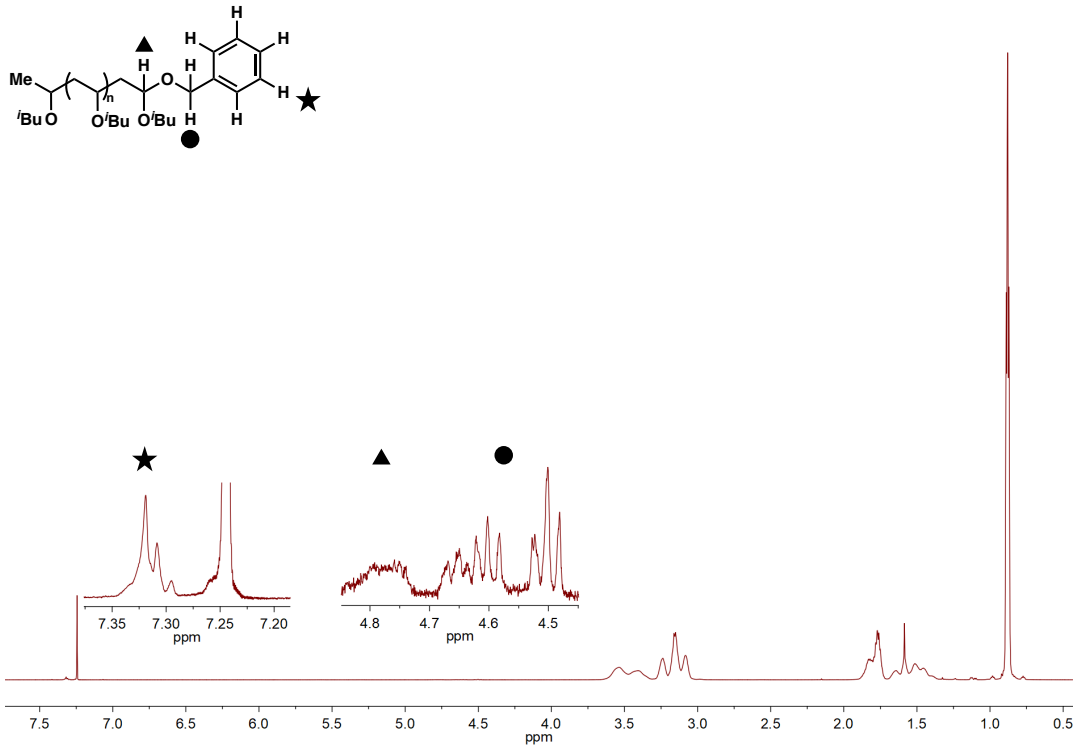

Figure 5.7. ^{1}H NMR of poly(isobutyl vinyl ether) functionalized with benzyl alcohol.

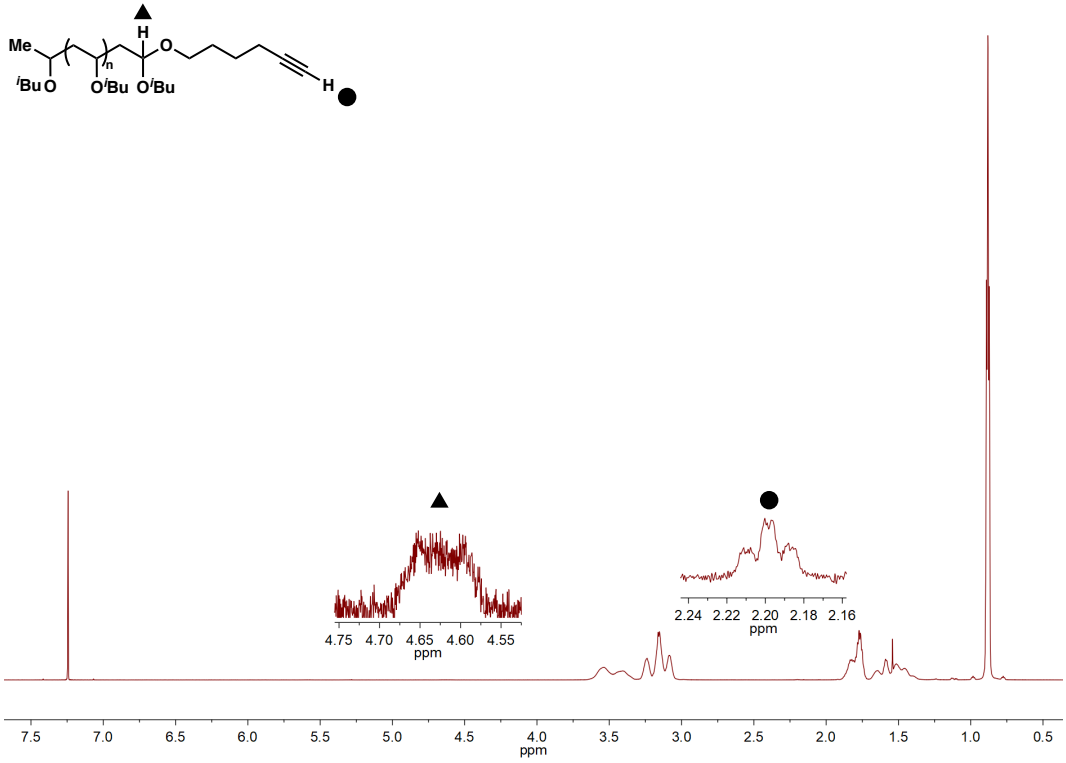

Figure 5.8. ^{1}H NMR of poly(isobutyl vinyl ether) functionalized with 5-hexyn-1-ol.

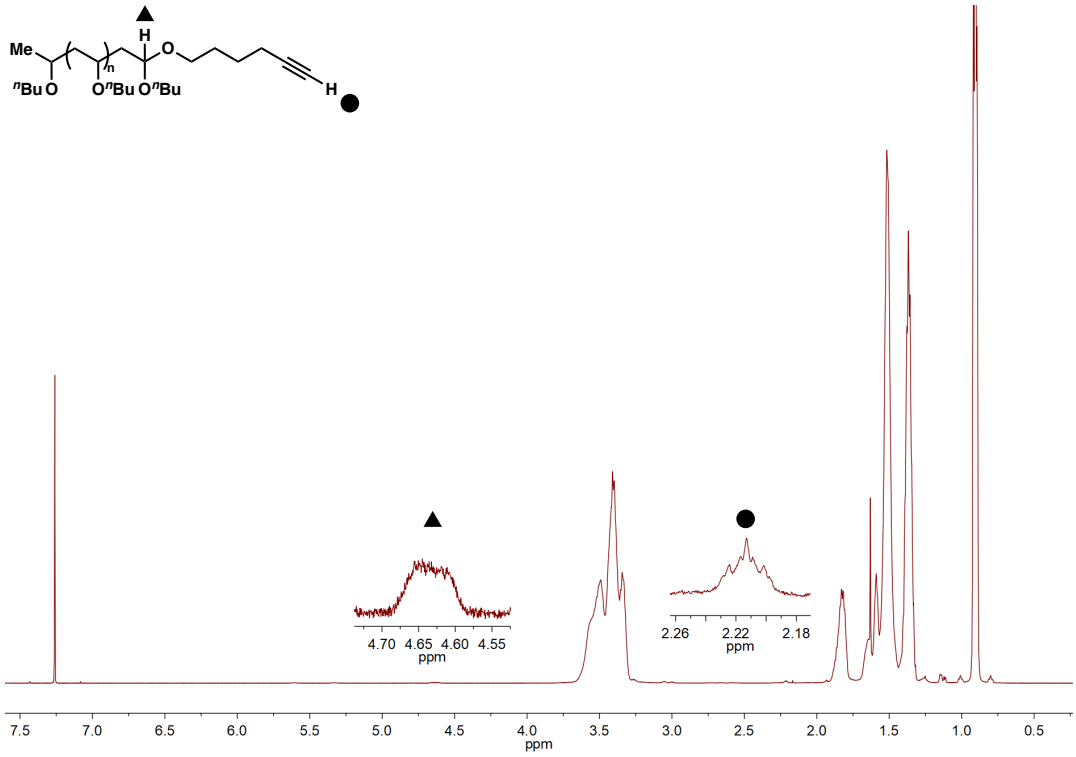

Figure 5.9. ^{1}H NMR of poly(*n*-butyl vinyl ether) functionalized with 5-hexyn-1-ol.

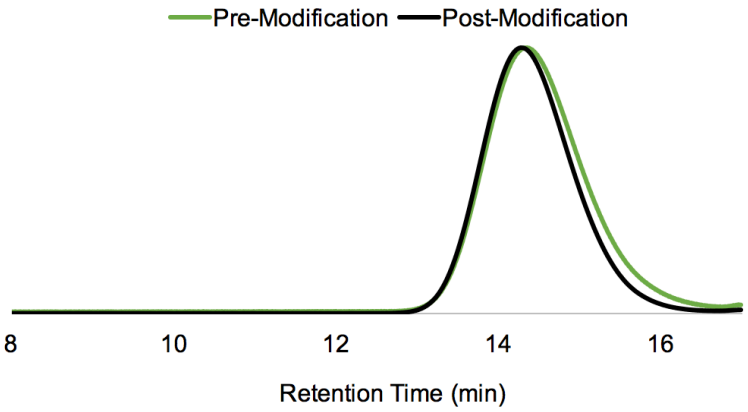

Figure 5.10. GPC traces of poly(isobutyl vinyl ether) before and after functionalization with 5-hexen-1-ol.

Table 5.3. Homopolymerization of other Vinyl Ethers Catalyzed by **2a**.

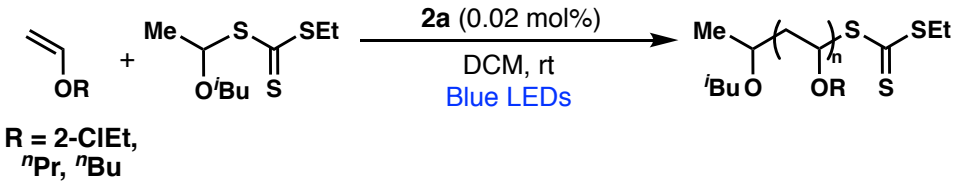

R = 2-ClEt, ^{n}Pr, ^{n}Bu

Entry	Monomer	Time (h)	Conv. (%)	$M_{n,theo}$ (kg/mol)	M_n (kg/mol)	$Đ$
1	2Cl-EVE	12.5	42	4.5	7.1	1.51
2	PVE	12.5	84	7.2	5.7	1.32
3	BVE	12.5	87	7.8	10.1	1.47

Appendix References

(1) G. J. Choi, Q. Zhu, D. C. Miller, C. J. Gu, R. R. Knowles, *Nature* **2016**, *539*, 268.

(2) V. Kottisch, Q. Michaudel, B. P. Fors, *J. Am. Chem. Soc.* **2016**, *138*, 15535.

(3) Q. Michaudel, T. Chauviré, V. Kottisch, M. J. Supej, K. J. Stawiasz, L. Shen, R. W. Zipfel, H. D. Abruña, J. H. Freed, B. P. Fors, *J. Am. Chem. Soc.* **2017**, *139*, 15530.

(4) J. N. Demas, W. D. Bowman, E. F. Zalewski, R. A. Velapoldi, *J. Phys. Chem.* **1981**, *85*, 2766.

(5) H. J. Kuhn, S. E. Braslavsky, R. Schmidt, *Pure Appl. Chem.* **2004**, *76*, 2105.

CHAPTER 6

CONTROLLED CATIONIC POLYMERIZATION: SINGLE-COMPONENT INITIATION UNDER AMBIENT CONDITIONS

6.1 Abstract

Cationic polymerizations provide a valuable strategy for preparing macromolecules with excellent control but are inherently sensitive to impurities and commonly require rigorous reagent purification, low temperatures, and strictly anhydrous reaction conditions. By using pentacarbomethoxycyclopentadiene (PCCP) as the single-component initiating organic acid, we found that a diverse library of vinyl ethers can be controllably polymerized under ambient conditions. Additionally, excellent chain-end fidelity is maintained even without rigorous monomer purification. We hypothesize that a tight ion complex between the PCCP anion and the oxocarbenium ion chain end prevents chain-transfer events and enables a polymerization with living characteristics. Furthermore, terminating the polymerization with functional nucleophiles allows for chain-end functionalization in high yields.

6.2 Introduction

Living ionic polymerizations are a powerful class of reactions that enable the synthesis of macromolecules with exquisite levels of control.[1,2] However, the utility of these processes is limited because of their sensitivity to impurities and requirement of stringent reaction conditions. Specifically, controlled cationic

polymerizations have to be run at low temperatures under highly inert atmospheres and require the use of monomers, solvents, and catalysts that have been rigorously purified.[2−14] These requirements inhibit the broader scientific community from fully taking advantage of these polymerizations to make well-defined polymeric materials for a variety of applications.

Over the past several years multiple research groups have reported cationic polymerization methods that use a single-component initiating species to make these processes more user-friendly; however, these reactions still mostly require low temperatures, inert atmospheres, and highly purified reagents.[15−18] Additionally, there have been a small number of methods published that can be run open to air or at elevated temperatures.[19] Unfortunately, these polymerizations open to air are not well controlled or afford only low molecular weights resulting from termination events.[20,21] On this basis, the development of a controlled cationic polymerization that can be run at ambient temperature without the need for purified reagents and the use of an inert atmosphere remains a grand challenge.

To overcome the limitations described above, we sought a cationic polymerization system where both the identity of the active chain-end and the mechanism of monomer addition were distinct from current systems. Specifically, we hypothesized that a process where the cationic chain end would tightly interact with a well-chosen counteranion would allow room-temperature propagation, as well as selective addition of the monomer over nucleophilic impurities to circumvent termination and chain-transfer events.

With this in mind, our attention was drawn to electron-deficient cyclopentadienes, such as 1,2,3,4,5-pentacarbomethoxycyclopentadiene (PCCP, **1**). This bench-stable, easily handled solid has an exceptionally low pK_a[22,23] and can be readily synthesized on scale from inexpensive, commercially available starting materials. The Lambert research group has recently leveraged the unique reactivity of these cyclopentadienes for small-molecule transformations.[24–26] Of particular relevance, we reported that PCCP-oxocarbenium complexes react with vinyl ethers. In collaboration with Vetticatt and co-workers, we found that this transformation proceeds via a transition state that involves non-covalent interactions between key reactant C–H bonds with both the cyclopentadienyl ring and carbonyl oxygens of the anion.[25] In regard to the current work, we hypothesized that this mechanism would enable cationic polymerization, in which selective addition of vinyl ethers over other nucleophilic impurities to a propagating oxocarbenium ion chain end would prevent termination and chain transfer events (Figure 6.1). Specifically, we propose that the propagating chain end would exist as an equilibrium between the cyclopentadienyl-oxocarbenium salt **2** and the covalent species **3** (Figure 6.1b), and that addition of monomers to **2** would occur via the transition state depicted in Figure 6.1c.[25,26] Given the reactive nature of the oxocarbenium ion, we speculate that the chain end would exist primarily in the covalent form and provide controlled polymerization at ambient temperature. This proposed

mechanism would eliminate the need for highly purified reagents, an inert atmosphere in order to exclude moisture, and low temperature conditions.

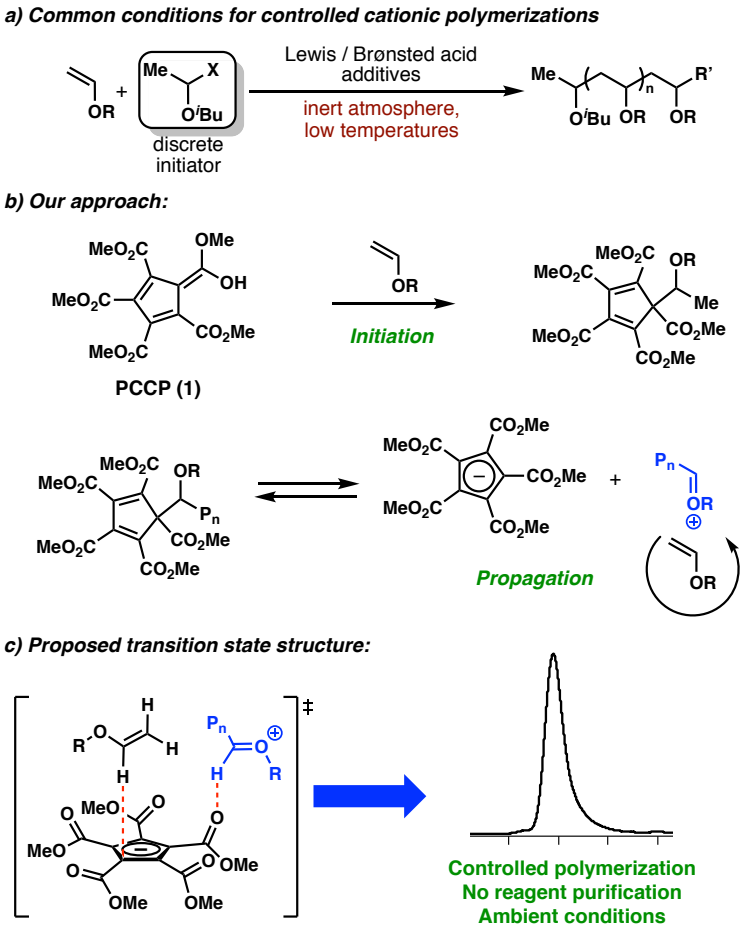

Figure 6.1. (a) Typical reaction conditions of cationic polymerizations. (b) PCCP is used in this work to controllably polymerize vinyl ethers. (c) Key H-bonding interactions lead to a controlled polymerization with narrow molecular weight distributions.

6.3 Results and Discussion

To test this hypothesis, we first examined the polymerization of isobutyl vinyl ether (IBVE) in the presence of PCCP. Importantly, all of the reactions were run open to air at room temperature. IBVE was simply passed through a plug of alumina to remove the KOH inhibitor prior to the reaction and was used

without further purification. We envisioned that **1** would efficiently initiate polymerization through protonation of IBVE (Figure 6.1b); acids with comparable pK_a values have been shown to readily protonate vinyl ethers to form Markovnikov adducts.[10] Stirring **1** with 50 equiv of IBVE led to complete consumption of the monomer after 16 h to give a 5.1 kg/mol polymer with a narrow dispersity ($Đ$) of 1.1 (Table 6.1, entry 1). Importantly, the experimental number-average molar mass (M_n) matched well with the theoretical value (M_n(theo) = 5.0 kg/mol), suggesting that each molecule of **1** is initiating a polymer chain. The narrow Đ value demonstrates that initiation with **1** through protonation of the IBVE is highly efficient (Figure 6.1b). Additionally, these data together provide strong evidence that termination and chain transfer events are not playing a major role in this reaction. Moreover, the relatively slow rate of polymerization and excellent control observed imply a strong interaction between the cyclopentadienyl anion and the oxocarbenium ion chain end, either as a tight ion pair or a dynamic covalent bond.[27] It is worth noting that the polymerization can be performed in a variety of solvents, including hexanes, toluene, and dichloromethane (DCM). The reaction rate is slightly higher in DCM, but proceeds with a minor loss of control (see Appendix).[28]

Table 6.1. Cationic Polymerization of Vinyl Ethers Promoted by **1**

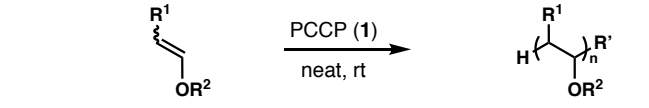

Monomers

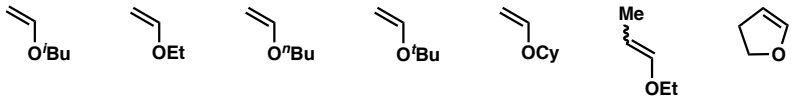

IBVE **EVE** **NBVE** **TBVE** **CyVE** **EPE** **DHF**

Entry[a]	**Monomer**	**Time (h)**	$M_{n,theo}$ **(kg/mol)**	$M_{n,exp}$ **(kg/mol)**	$Đ$
1	IBVE	16	5.0	5.1	1.11
2	IBVE	16	9.3	7.2	1.27
3	IBVE	16	23.0	18.1	1.15
4	EVE	3	3.4	2.5	1.06
5	EVE	5	6.6	6.5	1.08
6	EVE	20	13.5	12.8	1.06
7	NBVE	6	8.9	7.3	1.13
8	TBVE	0.1	8.1	6.2	1.25
9	CyVE	0.1	11.2	10.5	1.27
10[b]	EPE	6	4.0	5.4	1.24
11[c]	DHF	5	33.6	34.1	1.20
12[c,d]	DHF	3.5	44.9	49.9	1.33

[a]Vinyl ether (50–1300 equiv, filtered through basic alumina) and **1** (1 equiv, 0.014 mmol) were stirred under ambient atmosphere at room temperature unless otherwise noted; [b]performed at 0 °C; [c]performed under nitrogen atmosphere with distilled DHF; [d]diluted with equal volume of DCM.

To further probe the control in this system, we varied the ratio of **1** to IBVE and targeted polymers with higher molar mass. In all cases, polymers with narrow $Đ$ values were obtained and the experimental M_n's were slightly lower

than theoretical values but still in good agreement (Table 6.1, entries 2 and 3). These results suggest that, if chain transfer occurs, it has minimal effect on the polymerization process. When these same reactions were run under inert atmospheres with highly purified IBVE, almost identical results were obtained (see Appendix for details). This practical and robust new method eliminates the need for tedious purifications and the use of highly specialized moisture-free techniques. Targeting M_n's above 20 kg/mol with IBVE leads to increased chain transfer and lower experimental molar masses under both moisture-free and ambient conditions.

We further investigated the scope of these polymerizations using a diverse array of vinyl ether monomers. Ethyl vinyl ether (EVE) polymerized at a slightly faster rate than IBVE and gave polymers with $Đ$ values of <1.1 and excellent control over the M_n (Table 6.1, entries 4–6). The linear congener of IBVE, *n*-butyl vinyl ether (NBVE), also polymerized under our standard conditions to yield a well-defined material with a narrow $Đ$ of 1.13 (Table 6.1, entry 7). Additionally, more sterically challenging monomers such as *tert*-butyl vinyl ether (TBVE) and cyclohexyl vinyl ether (CyVE) polymerized within minutes in a controlled fashion (Table 6.1, entries 8 and 9); we postulated that the increased size of the monomers weakens the interaction between the cyclopentadienyl anion and the oxocarbenium ion and, therefore, results in an accelerated rate.

1,2-Disubstituted vinyl ethers that are more recalcitrant to controlled polymerization also polymerized in a controlled fashion using **1** as an initiator,

but modified conditions were required.[29,30] Under our standard conditions, ethyl-1-propenyl ether (EPE) only gave oligomerization. We posited that this could be due to a lower ceiling temperature of the poly(EPE). In support of this hypothesis, controlled polymerization was observed when the reaction was performed at 0 °C (Table 6.1, entry 10); it is worth noting the EPE reactions were still performed open to the air with unpurified monomer. Additionally, dihydrofuran (DHF), which is an interesting monomer because poly(DHF) has a high glass transition temperature of 126 °C,[30] polymerized under the standard conditions; however, the experimental M_n values of the formed polymer were lower than predicted and the molecular weight distributions were broad. We found that purification of the monomer and running the reaction under an inert atmosphere had a large influence in this case and led to a controlled polymerization process (Table 6.1, entries 11 and 12). These results indicate that the polymerization of DHF is much more sensitive to nucleophilic impurities than other monomers we have tested. We reasoned that this change in reactivity could be caused by a weakening of the interaction between the PCCP anion and the oxocarbenium ion, which we believe is responsible for the selectivity of vinyl ether addition over other nucleophiles.[31]

Next, we investigated the kinetics of the polymerization of IBVE initiated by **1**. When monitoring the reaction, we observed that M_n grew linearly with conversion, demonstrating that this polymerization was proceeding through a chain growth process (Figure 6.2a). Additionally, plotting the natural log of monomer depletion versus time showed a linear relationship (Figure 6.2b). This

result demonstrated that the polymerization showcases well-behaved first order kinetics and that the cation concentration remains constant throughout the polymerization, further supporting our hypothesis that termination was not playing a major role in these reactions.

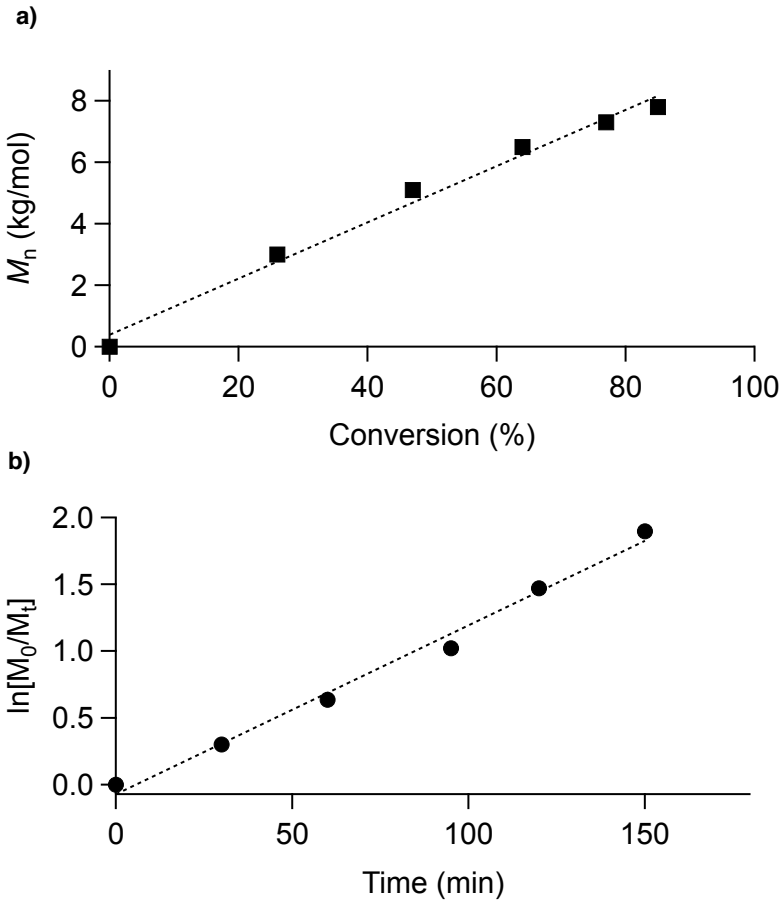

Figure 6.2. (a) The molecular weight of poly(IBVE) grows linearly with conversion. (b) A linear relationship of the change in monomer concentration with time indicates constant cation concentration throughout the polymerization of IBVE with **1**.

The living characteristics and the chain-end fidelity of this reaction were subsequently probed through the synthesis of diblock copolymers. In our initial studies we used purified monomers and an N_2 atmosphere. For the first block we grew a 4.0 kg/mol poly(EVE) and then after >95% conversion added IBVE

to furnish a well-defined 8.2 kg/mol poly(EVE-*b*-IBVE) diblock polymer. The size exclusion chromatography trace of the polymer after chain extension showed a clear shift to higher molecular weights, while maintaining a narrow *Đ* of 1.2 (Figure 6.3). It should be noted that when the reaction was allowed to sit at full conversion before the addition of the second monomer, termination events started to occur. Additionally, we found that when these same experiments were run with unpurified monomers and open to the air, some termination was observed at high conversion (see Appendix for details). Interestingly, in these cases if the second monomer was added before the first block reached 85% conversion efficient chain extension was observed with little to no termination to yield a tapered diblock copolymer. These results suggested that termination reactions with nucleophilic impurities started to become competitive when the reactions reach high conversion.

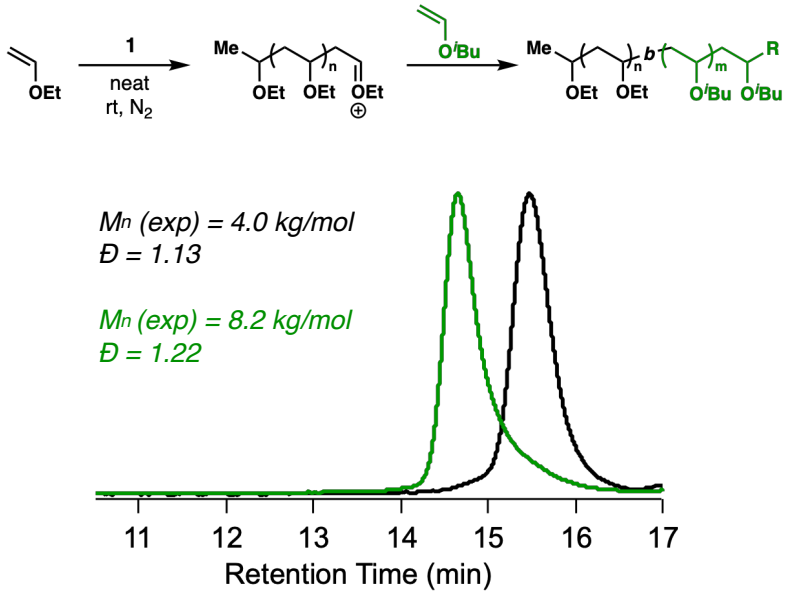

Figure 6.3. Synthesis of diblock copolymer demonstrates good chain-end fidelity.

To fully take advantage of these operationally simple polymerizations we looked to chain-end functionalize our polymers by quenching the propagating oxocarbenium ion with alcohols following full conversion of the monomer. Addition of 5 equiv of various alcohols and triethylamine to poly(IBVE) gave polymers with >95% of the desired acetals (Figure 6.4a). Additionally, we demonstrated that the oxocarbenium chain ends could efficiently be trapped with a dithiocarbamate salt to generate a poly(IBVE) macroinitiator, which provides access to multiblock materials via chain extension (Figure 6.4b).[7,8,13,32,33] Accordingly, using ferrocenium tetrafluoroborate ($FcBF_4$) as a chemical mediator as described in our previous study, poly(IBVE) was efficiently chain extended via a cationic reversible addition–fragmentation chain-transfer (RAFT) polymerization to provide poly(IBVE-*b*-IBVE) with excellent control. These results clearly demonstrate that we can effectively manipulate our chain ends after polymerization, as well as chain extend with other polymerization methods to make functional materials.

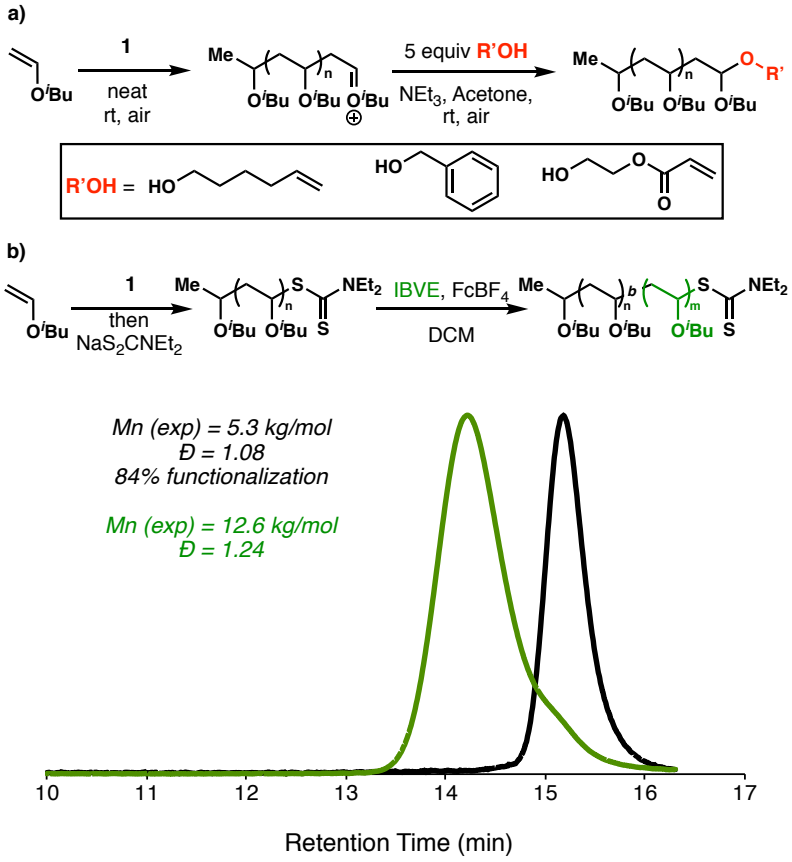

Figure 6.4. *In situ* chain-end functionalization of poly(IBVE) by quenching the polymerization (a) with functional alcohols and (b) with a dithiocarbamate salt, followed by chain extension with IBVE using ferrocenium tetrafluoroborate as the initiator.

6.4 Conclusion

In conclusion, we have developed a novel single-component acid-mediated polymerization of a variety of vinyl ethers under mild conditions. The polymerization is initiated by PCCP and controlled by the tight ion pair of the cyclopentadienyl anion and propagating cation. This interaction allows for good chain-end fidelity and the synthesis of block copolymers. Interestingly, the polymerization proceeds even under ambient atmosphere and does not require rigorous purification. We imagine that this method will induce a shift in how the

sensitivity of cationic polymerizations is conceptualized by the polymer community.

6.5 References

(1) Grubbs, R. B.; Grubbs, R. H. *Macromolecules* **2017**, *50*, 6979–6997,

(2) Ciftci, M.; Yilmaz, G.; Yagci, Y. *J. Photopolym. Sci. Technol.* **2017**, *30*, 385.

(3) Sawamoto, M. *Prog. Polym. Sci.* **1991**, *16*, 111.

(4) Goethals, E. J.; Du Prez, F. *Prog. Polym. Sci.* **2007**, *32*, 220.

(5) Aoshima, S.; Kanaoka, S. *Chem. Rev.* **2009**, *109*, 5245.

(6) Ouchi, M.; Kamigaito, M.; Sawamoto, M. *Macromolecules* **1999**, *32*, 6407.

(7) Uchiyama, M.; Satoh, K.; Kamigaito, M. *Angew. Chem. Int. Ed.* **2015**, *54*, 1924.

(8) Sugihara, S.; Konegawa, N.; Maeda, Y. *Macromolecules* **2015**, *48*, 5120.

(9) Uchiyama, M.; Satoh, K.; Kamigaito, M. *ACS Macro Lett.* **2016**, *5*, 1157.

(10) Treator, A. J.; Leibfarth, F. A. *Science* **2019**, *363*, 1439.

(11) Ciftci, M.; Yoshikawa, Y.; Yagci, Y. *Angew. Chem. Int. Ed.* **2017**, *56*, 519.

(12) Michaudel, Q.; Kottisch, V.; Fors, B. P. *Angew. Chem. Int. Ed.* **2017**, *56*, 9670.

(13) Kottisch, V.; Michaudel, Q.; Fors, B. P. *J. Am. Chem. Soc.* **2016**, *138*, 15535.

(14) Peterson, B. P.; Lin, S.; Fors, B. P. *J. Am. Chem. Soc.* **2018**, *140*, 2076.

(15) Sugihara, S.; Kitagawa, M.; Inagawa, Y.; Zaleska, I. M.; Ikeda, I. *Polym. Bull.* **2010**, *64*, 209.

(16) Song, J.; Xu, J.; Tang, D. *J. Polym. Sci., Part A: Polym. Chem.* **2016**, *54*, 1373.

(17) Yan, X.; Zhang, S.; Zhang, P.; Wu, X.; Liu, A.; Guo, G.; Dong, Y.; Li, X. *Angew. Chem. Int. Ed.* **2018**, *57*, 8947.

(18) Siu, P. W.; Hazin, K.; Gates, D. P. *Chem. Eur. J.* **2013**, *19*, 9005.

(19) Aoshima, S.; Higashimura, T. *Macromolecules* **1989**, *22*, 1009.

(20) Radchenko, A. V.; Kostjuk, S. V.; Ganachaud, F. *Polym. Chem*. **2013**, *4*, 1883.

(21) Vijayaraghavan, R.; MacFarlane, D. R. *Macromolecules* **2007**, *40*, 6515.

(22) Diels, O. *Ber. Dtsch. Chem. Ges.* **1942**, *75*, 1452.

(23) Diels, O.; Kock, U. *Liebigs Ann. Chem.* **1944**, *556*, 38.

(24) Gheewala, C. D.; Collins, B. E.; Lambert, T. H. *Science* **2016**, *351*, 961.

(25) Gheewala, C.; Hirschi, J. S.; Lee, W.-H.; Paley, D. W.; Vetticatt, M. J.; Lambert, T. H. *J. Am Chem. Soc.* **2018**, *140*, 3523.

(26) Radtke, M. A.; Dudley, C. C.; O'Leary, J. M.; Lambert, T. H. *Synthesis* **2019**, *51*, 1135.

(27) Jefferson, E. A.; Warkentin, J. *J. Org. Chem.* **1994**, *59*, 463.

(28) The polymerization results of IBVE in different solvents as well as the percentage of meso diads are highlighted in Table 6.4.

(29) Ishido, Y.; Kanazawa, A.; Kanaoka, S.; Aoshima, S. *J. Polym. Sci. Part A: Polym. Chem.* **2014**, *52*, 1334.

(30) Yonezumi, M.; Kanaoka, S.; Aoshima, S. *J. Polym. Sci. Part A: Polym. Chem.* **2008**, *46*, 4495.

(31) Monomers without α-Hs, i.e. 2-methoxypropene and α-methylstyrene, did not give controlled polymerization.

(32) Peterson, B. M.; Kottisch, V.; Supej, M. J.; Fors, B.P. *ACS Cent. Sci.* **2018**, *4*, 1228.

(33) Michaudel, Q.; Chauviré, T.; Kottisch, V.; Supej, M. J.; Stawiasz, K. J.; Shen, L.; Zipfel, W. R.; Abruña, H. D.; Freed, J. H.; Fors, B. P. *J. Am. Chem. Soc.* **2017**, *139*, 15530.

6.6 Appendix

General Reagent Information

Isobutyl vinyl ether (IBVE) (99%, TCI), *tert*-butyl vinyl ether (TBVE) (98%, Alfa Aesar), ethyl vinyl ether (EVE) (99%, Sigma Aldrich), cyclohexyl vinyl ether (CyVE), (>95%, TCI), ethyl-1-propenyl ether (EPE) (98%, Sigma Aldrich), and 2-hydroxy ethyl acrylate (96%, Sigma Aldrich) were filtered through a plug of activated basic aluminum oxide to remove inhibitors prior to use. Additionally, EVE for diblock copolymer synthesis, and dihydrofuran (DHF) (99%, Sigma Aldrich) were dried over calcium hydride (CaH_2) (ACROS chemicals, 93% extra pure, 0–2 mm grain size) for 12 h, distilled under nitrogen and degassed by three freeze-pump-thaw cycles. IBVE was distilled from CaH_2 onto *n*-butyllithium, followed by distillation under nitrogen and degassing by three freeze-pump-thaw cycles for the use in diblock copolymer synthesis. Anhydrous benzyl alcohol (99.8%, Sigma Aldrich), 5-hexen-1-ol (95+%, TCI) and alumina (activated, basic, Brockmann Grade I, 58 Ångstroms, Alfa Aesar) were used as received. Sodium *N,N*-diethylcarbamate trihydrate (98%, Alfa Aesar) was azeotropically dried with benzene. Dichloromethane (DCM) was purchased from Honeywell and was purified by vigorous purging with argon for 2 h, followed by passing through two packed columns of neutral alumina under argon pressure. 1,2,3,4,5-Pentacarbomethoxycyclopentadiene (PCCP, **1**) was synthesized according to a reported literature procedure.[1]

General Analytical Information

All polymer samples were analyzed using a Tosoh EcoSEC HLC 8320 GPC system with two SuperHM-M columns in series at a flow rate of 0.350 mL/min. Tetrahydrofuran was used as the eluent and number-average molecular weights (M_n), weight-average molecular weights (M_w), and dispersities ($Đ$) for all homopolymers were determined by light scattering using a Wyatt miniDawn Treos multi-angle light scattering detector. Number-average molecular weights (M_n), weight-average molecular weights (M_w), and dispersities ($Đ$) for diblock copolymers and aliquots of kinetic experiments were determined against polystyrene standards. Nuclear magnetic resonance (NMR) spectra were recorded on a Mercury 300 MHz, Varian 400 MHz, Bruker 500 MHz, or a Varian 600 MHz instrument at room temperature using $CDCl_3$ as a solvent unless otherwise noted.

General Procedure for Homopolymerization of Vinyl Ethers (Table 6.1) excluding DHF

Under ambient atmosphere, a one-dram vial was charged with PCCP (**1**) (typically 0.014 mmol, 5 mg, 1 equiv) and a stir bar. The respective monomer was filtered through a short plug of basic alumina and subsequently added to the vial. The reaction was sealed with a cap equipped with a Teflon septum and stirred at room temperature (unless otherwise noted in table 6.2) for the reported time. The polymerization was terminated by the addition of 50 μL of 5% triethylamine/methanol and aliquots for GPC and ^{1}H NMR analysis were taken

(Figure 6.5). Volatiles were removed *in vacuo* and the polymer could be further purified by precipitation from cold methanol. ^{1}H and ^{13}C NMR spectra of the pure polymers are shown in Figure 6.6–6.17.

Table 6.2. Results of Vinyl Ether Homopolymerization Including Conversion

Entry[a]	**Monomer**	**Time (h)**	**Conv (%)**	$M_{n,theo}$ **(kg/mol)**	$M_{n,exp}$ **(kg/mol)**	$Đ$
1	IBVE	16	100	5.0	5.1	1.11
2	IBVE	16	93	9.3	7.2	1.27
3	IBVE	16	58	23.0	18.1	1.15
4	EVE	3	95	3.4	2.5	1.06
5	EVE	5	91	6.6	6.5	1.08
6	EVE	20	94	13.5	12.8	1.06
7	NBVE	6	89	8.9	7.3	1.13
8	TBVE	0.1	81	8.1	6.2	1.25
9	CyVE	0.1	89	11.2	10.5	1.27
10[b]	EPE	5	47	4.0	5.4	1.24
11[c]	DHF	3.5	64	33.6	34.1	1.20
12[c,d]	DHF	6	50	44.9	49.9	1.33

[a]Vinyl ether (50–1300 equiv, filtered through basic alumina) and **1** (1 equiv, 0.014 mmol) were stirred under ambient atmosphere at room temperature unless otherwise noted; [b]performed at 0 °C; [c]performed under nitrogen atmosphere with distilled DHF; [d]diluted with equal volume of DCM.

Table 6.3. Results of Vinyl Ether Homopolymerization under an Inert Atmosphere

Entry[a]	Monomer	Time (h)	Conv (%)	$M_{n,theo}$ (kg/mol)	$M_{n,exp}$ (kg/mol)	$Đ$
1	IBVE	5	73	7.3	7.1	1.14
2	IBVE	16	90	18.0	16.0	1.17
3	IBVE[b]	23	60	24.0	21.1	1.21
4	IBVE	20	79	31.4	18.9	1.24
5	EVE	<1	94	3.4	2.9	1.34
6	EVE	5	95	6.8	6.4	1.01
7	TBVE	<1	76	7.6	10.0	1.20
8	DHF	3	58	14.8	17.0	1.11

[a]Vinyl ether (50–1300 equiv) and **1** (1 equiv, 0.014 mmol) were stirred under nitrogen atmosphere at room temperature unless otherwise noted; [b]performed at 0 °C with equal volume of DCM and warmed to rt overnight

General Procedure for Homopolymerizations under Inert Atmosphere

Under ambient atmosphere, an oven-dried one-dram vial was charged with PCCP (**1**) (0.014 mmol, 5 mg, 1 equiv) and an oven-dried stir bar. The vial was then transferred to a nitrogen-filled glovebox and charged with distilled monomer (50–400 equiv). The reaction vial was sealed with a cap equipped with a Teflon septum and stirred at room temperature under an inert atmosphere for the reported time unless otherwise noted (see Table 6.3). The resulting polymer was analyzed by GPC and ^{1}H NMR analysis.

Procedure for Homopolymerizations of DHF (Table 6.1, entries 11 and 12)

Under ambient atmosphere, an oven-dried one-dram vial was charged with PCCP (**1**) (0.0033 or 0.0056 mmol, 1.2 or 2 mg, 1 equiv) and an oven-dried stir bar. The vial was then transferred to a nitrogen-filled glovebox and charged

with distilled DHF (4.2 mmol, 330 μL, 1270 or 750 equiv). When targeting higher molecular weights, an equal volume of dry DCM was added to solubilize the polymer. The reaction vial was sealed with a cap equipped with a Teflon septum and stirred at room temperature for the reported time. The polymerization was terminated by the addition of 50 μL of 5% triethylamine/methanol outside of the glovebox and aliquots for GPC and ^{1}H NMR analysis were taken. The polymer was purified by precipitation from cold methanol. ^{1}H and ^{13}C NMR spectra are depicted in Figures 6.18 and 6.19, respectively.

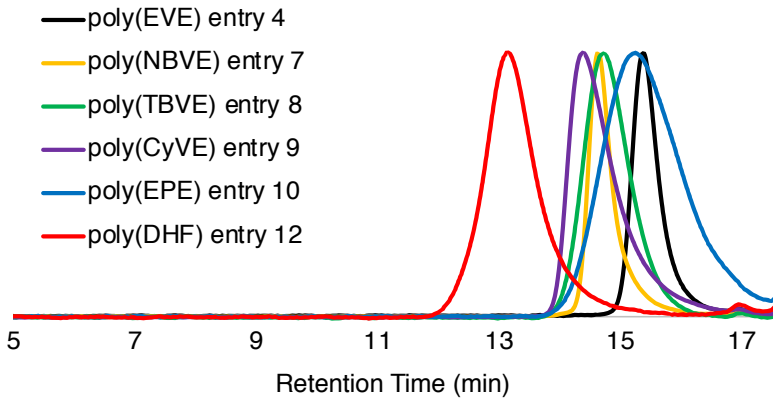

Figure 6.5. Representative GPC traces of polymers from Table 6.1.

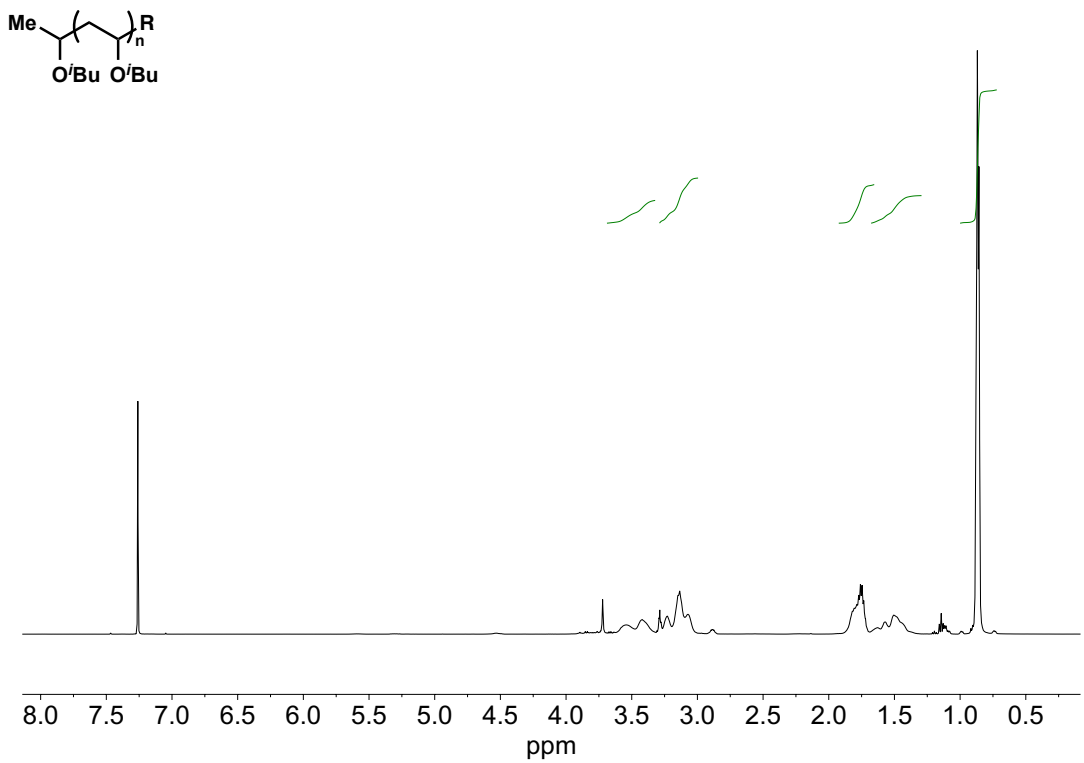

Figure 6.6. ^{1}H NMR of poly(IBVE) in $CDCl_3$ (Table 6.1, entry 1).

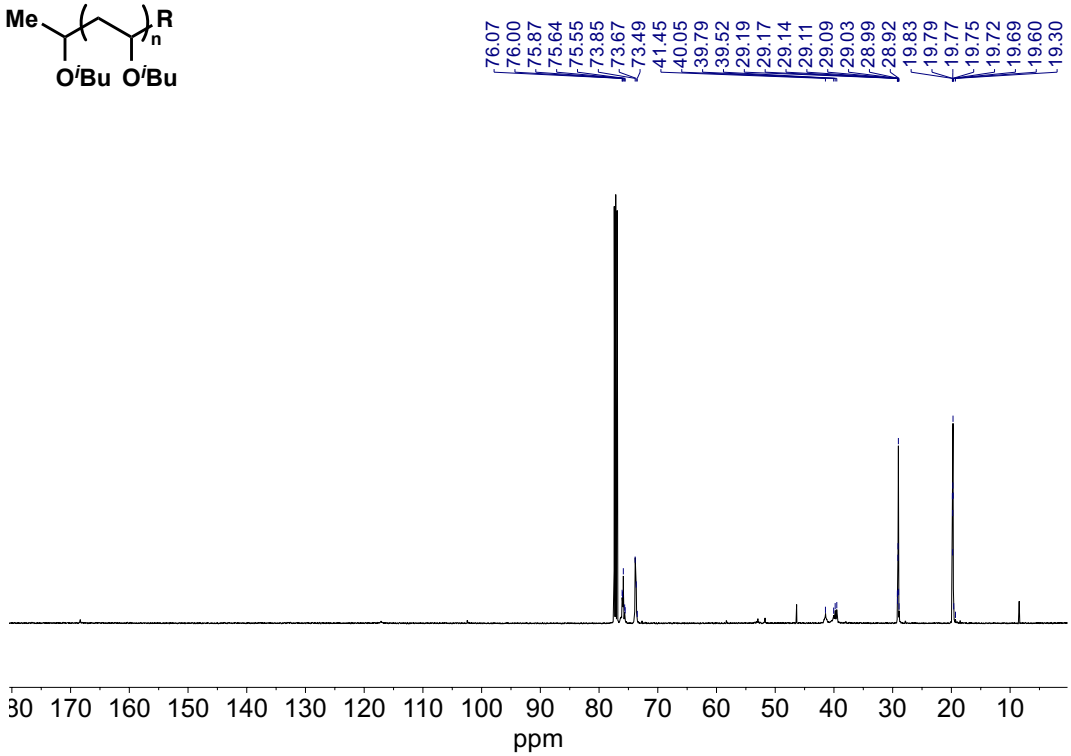

Figure 6.7. ^{13}C NMR of poly(IBVE) in $CDCl_3$ (Table 6.1, entry 1).

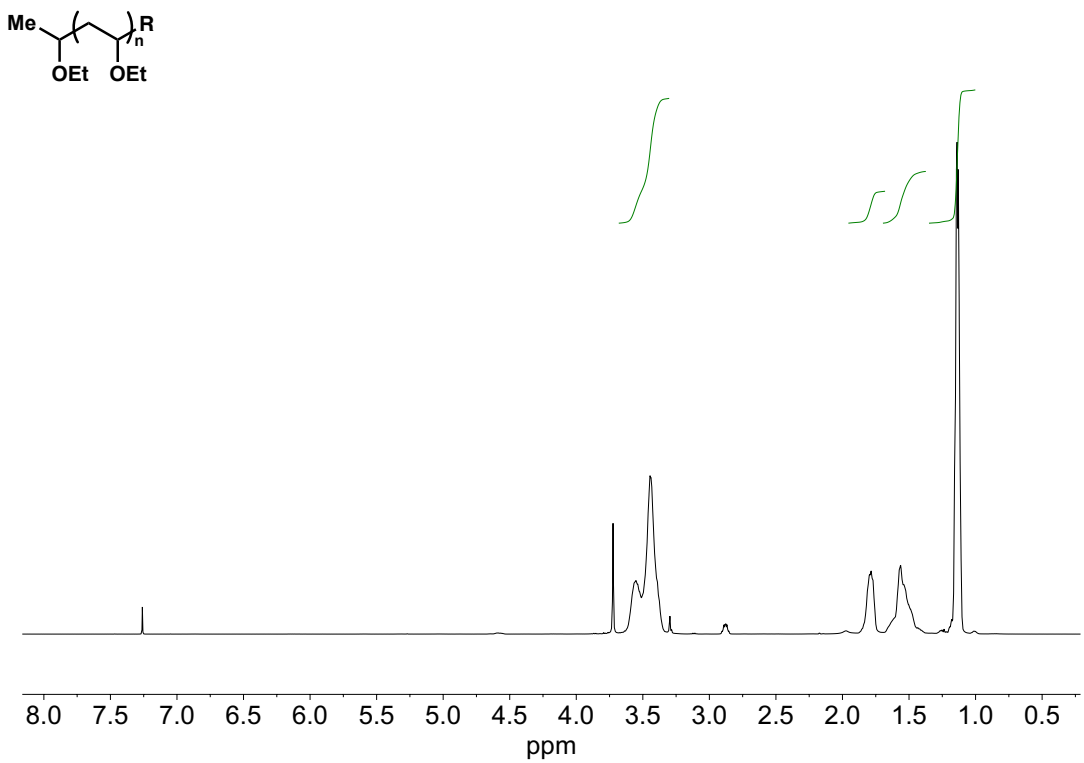

Figure 6.8. ^{1}H NMR of poly(EVE) in $CDCl_3$ (Table 6.1, entry 5).

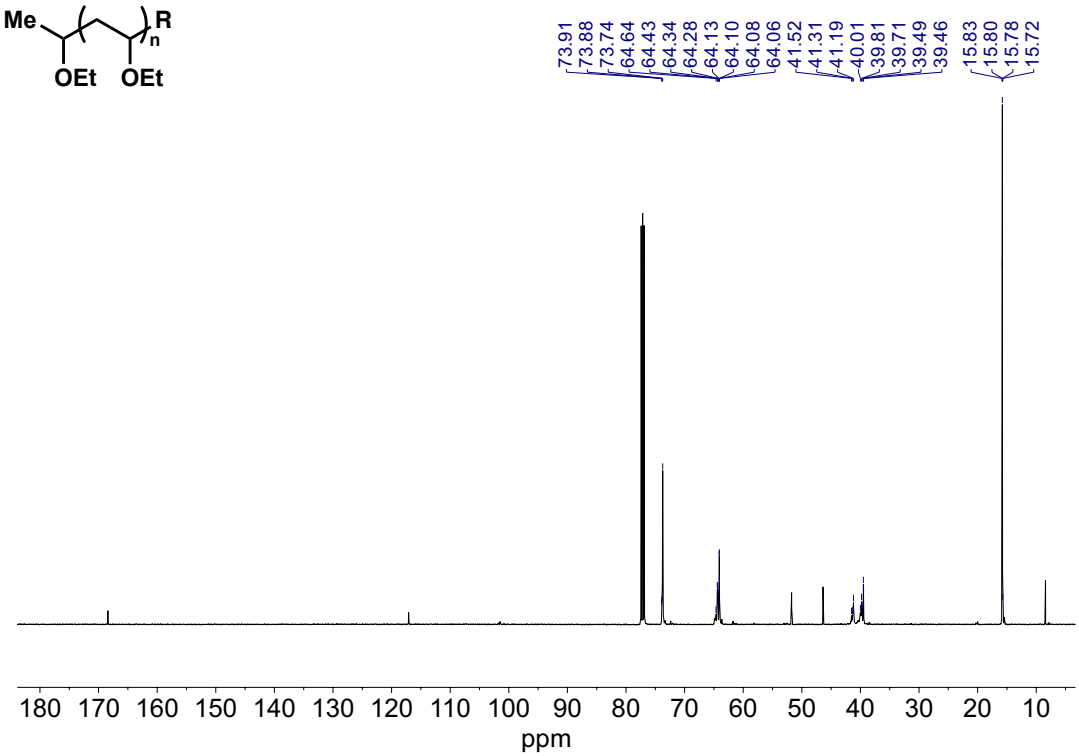

Figure 6.9. ^{13}C NMR of poly(EVE) in $CDCl_3$ (Table 6.1, entry 5).

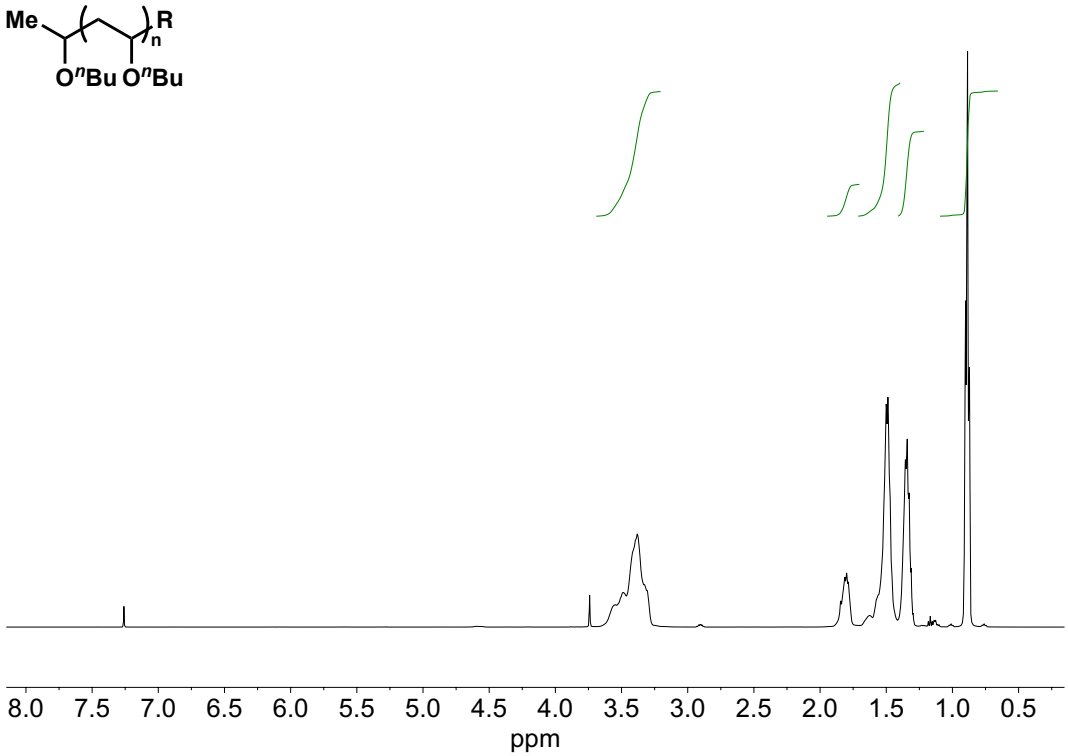

Figure 6.10. ^{1}H NMR of poly(NBVE) in $CDCl_3$ (Table 6.1, entry 7).

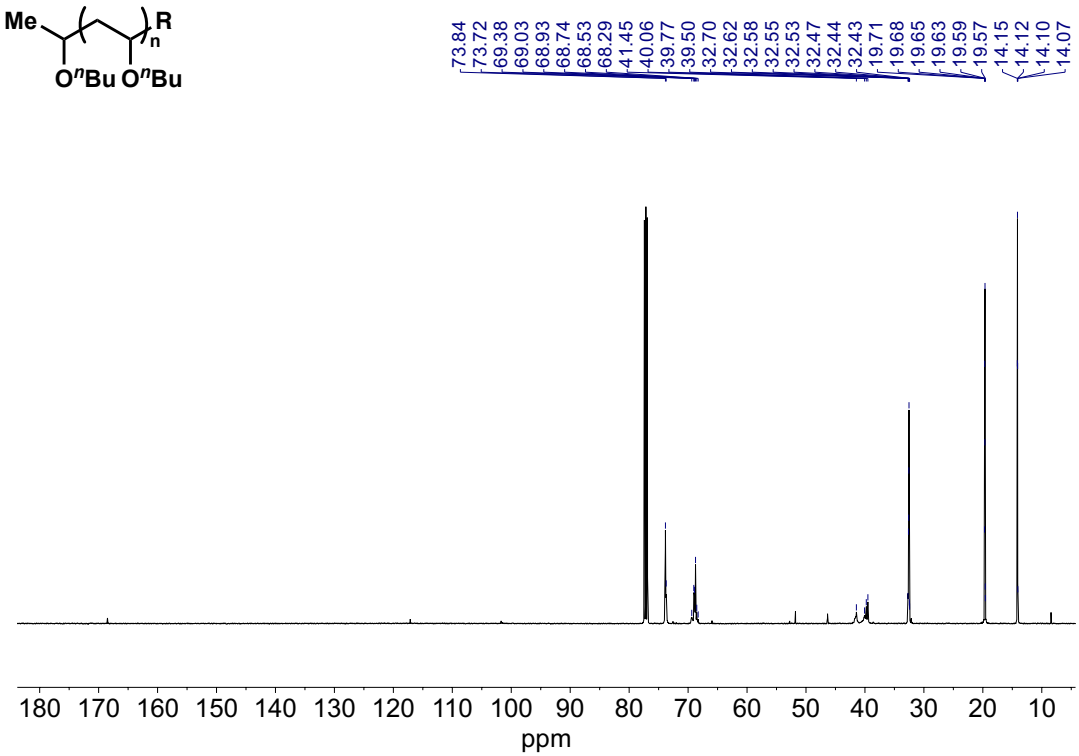

Figure 6.11. ^{13}C NMR of poly(NBVE) in $CDCl_3$ (Table 6.1, entry 7).

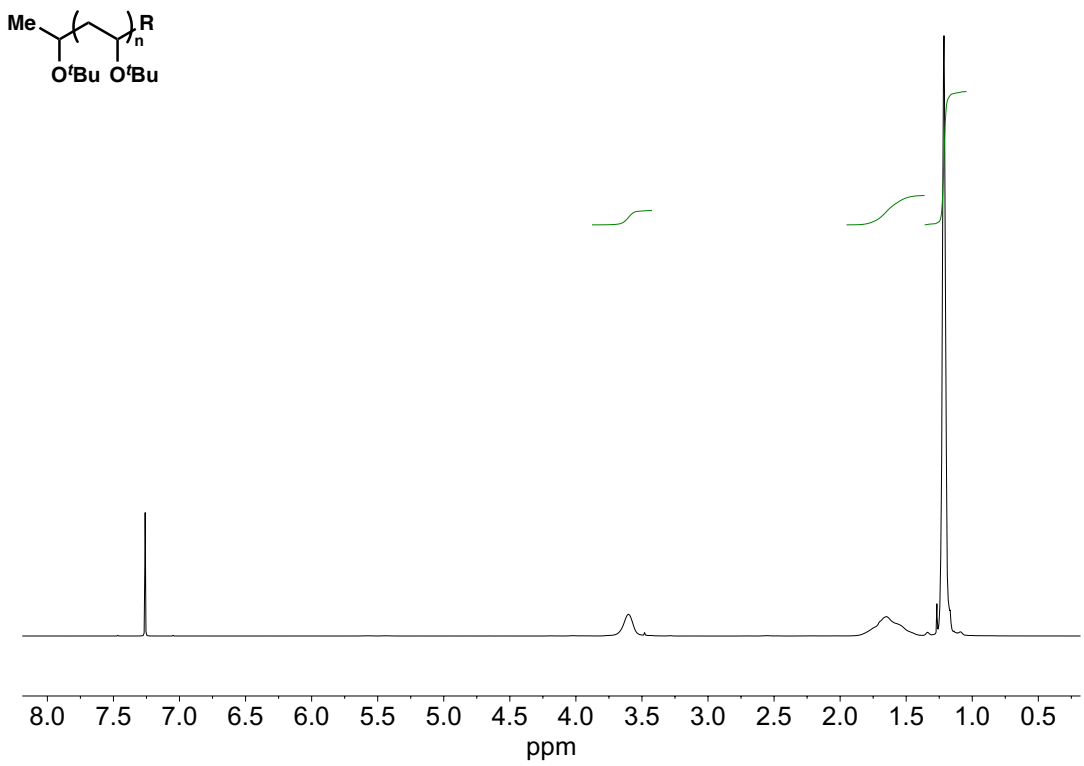

Figure 6.12. ^{1}H NMR of poly(TBVE) in $CDCl_3$ (Table 6.1, entry 8).

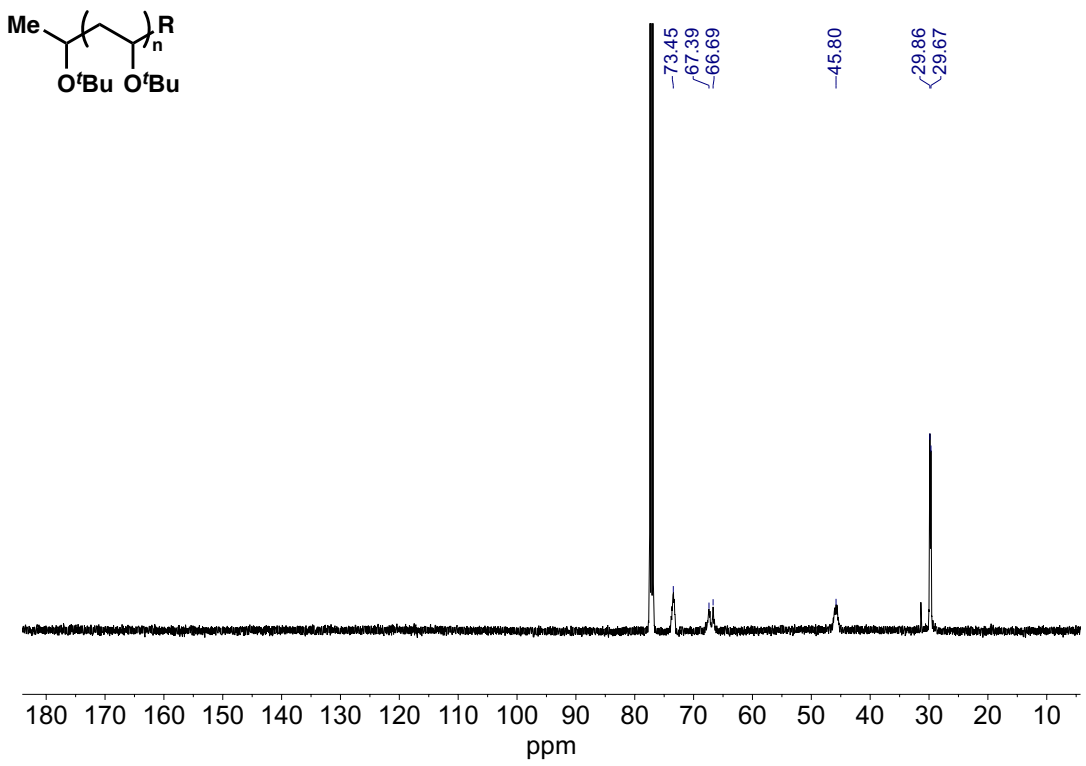

Figure 6.13. ^{13}C NMR of poly(TBVE) in $CDCl_3$ (Table 6.1, entry 8).

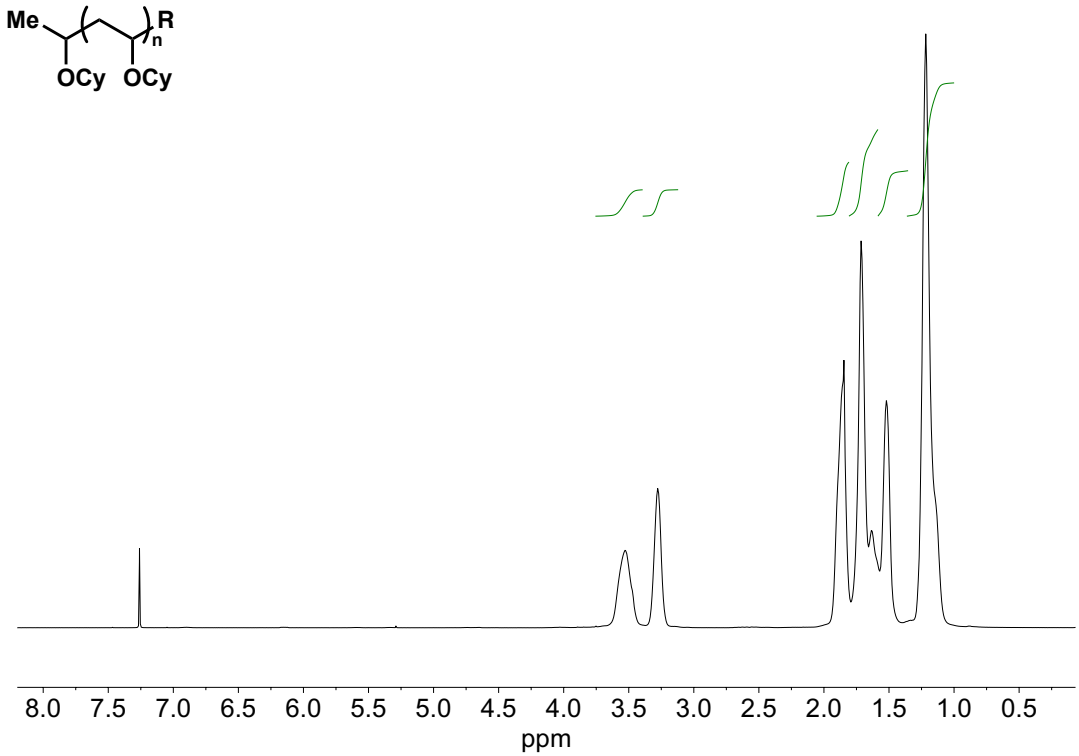

Figure 6.14. ^{1}H NMR of poly(CyVE) in $CDCl_3$ (Table 6.1, entry 9).

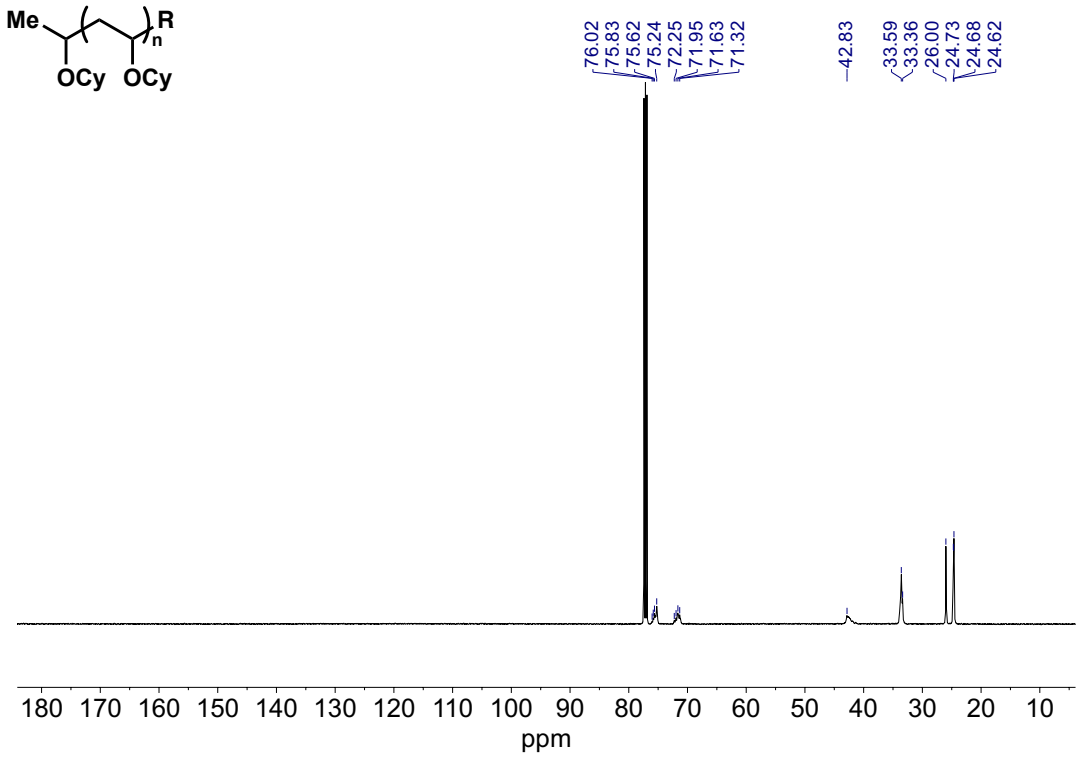

Figure 6.15. ^{13}C NMR of poly(CyVE) in $CDCl_3$ (Table 6.1, entry 9).

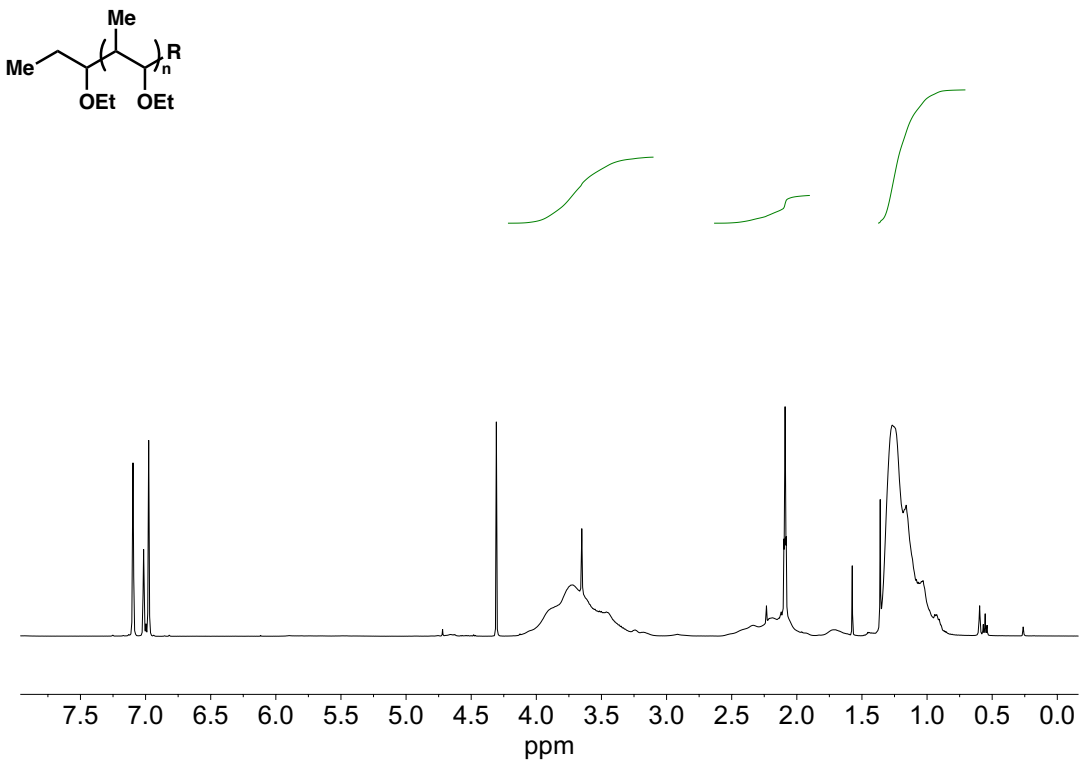

Figure 6.16. ^{1}H NMR of poly(EPE) in d8-toluene (Table 6.1, entry 10).

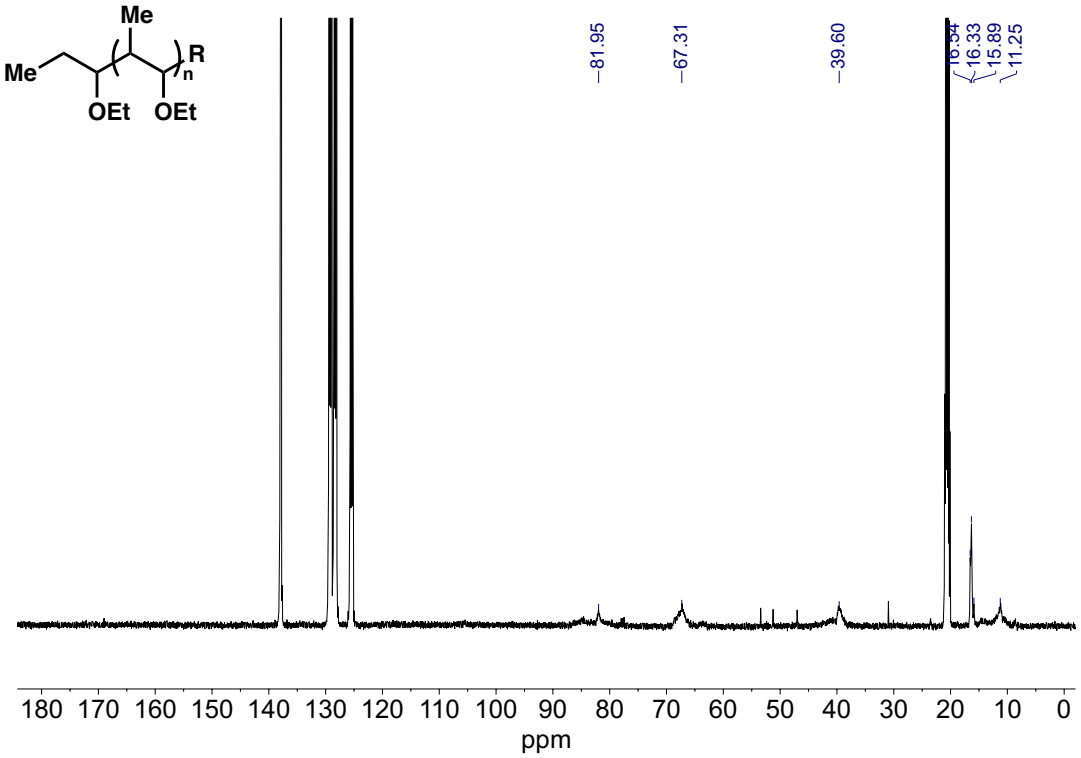

Figure 6.17. ^{13}C NMR of poly(EPE) in d8-toluene at 80 °C (Table 6.1, entry 10).

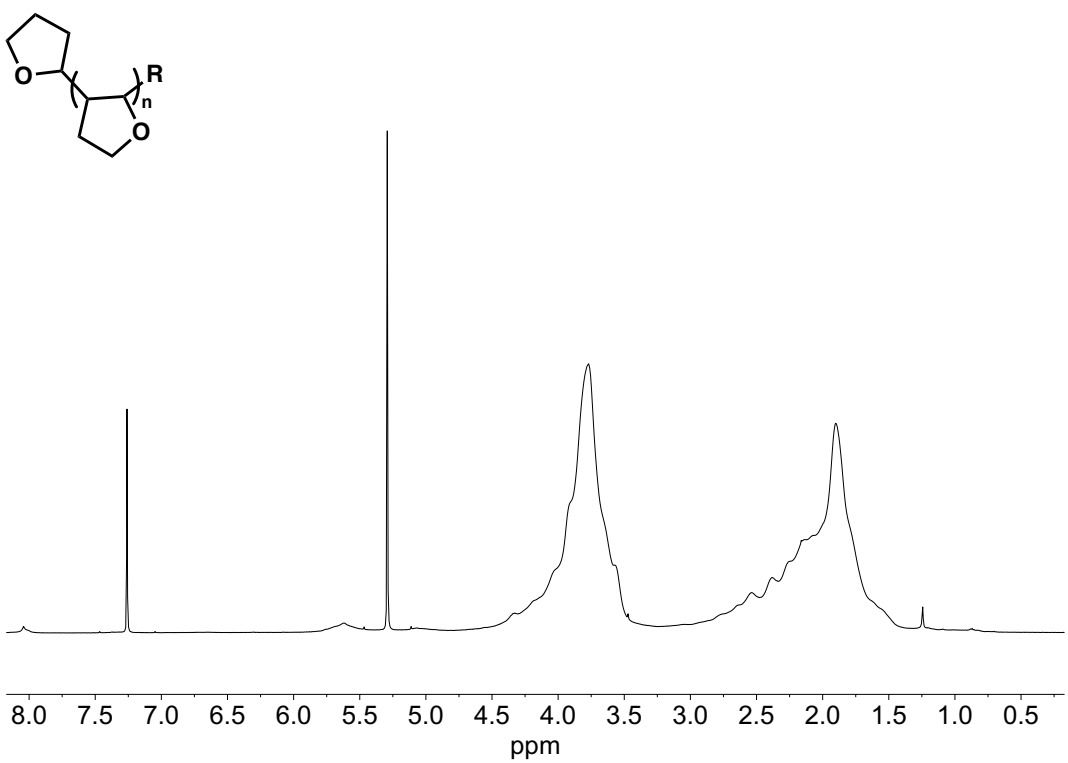

Figure 6.18. ^{1}H NMR of poly(DHF) in $CDCl_3$ (Table 6.1, entry 12).

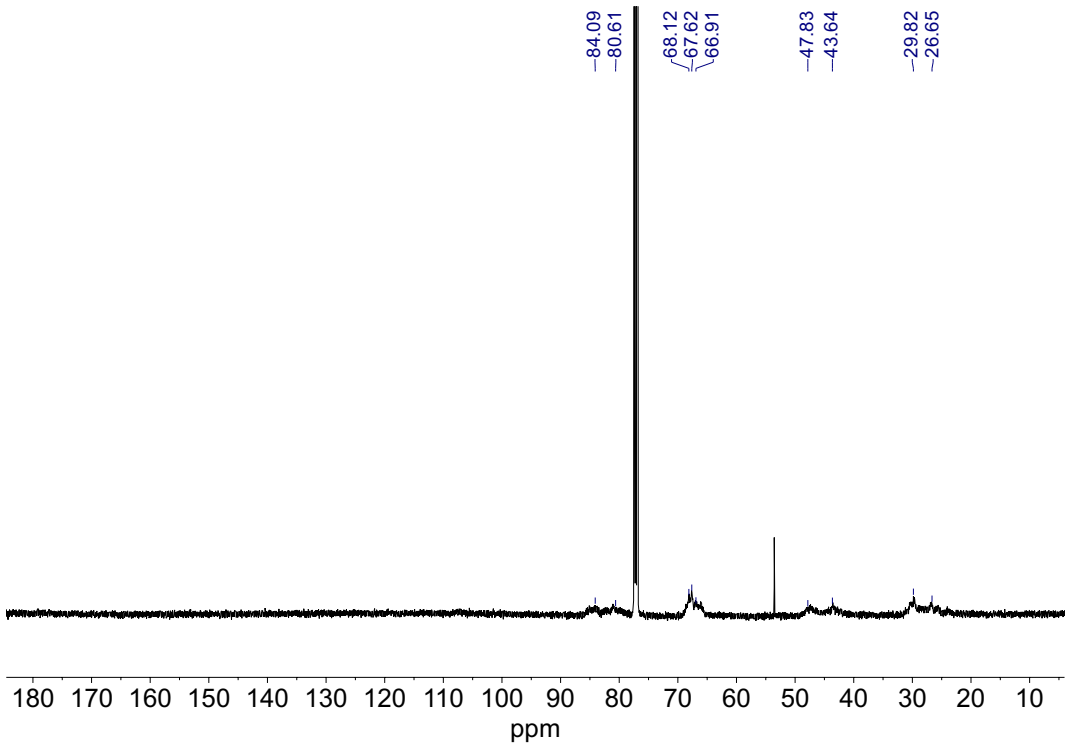

Figure 6.19. ^{13}C NMR of poly(DHF) in $CDCl_3$ (Table 6.1, entry 12).

Procedure for Kinetic Investigation of PCCP-Mediated Polymerization of IBVE (Figure 6.2)

Under ambient atmosphere, an oven-dried one-dram vial was charged with PCCP (**1**) (0.042 mmol, 15 mg, 1 equiv) and an oven-dried stir bar. The vial was then transferred to a nitrogen-filled glovebox. **1** was dissolved in 150 µL of dry DCM, after which distilled IBVE (4.2 mmol, 540 µL, 100 equiv) was added. The reaction vial was sealed with a cap equipped with a Teflon septum and stirred at room temperature. Aliquots for GPC and ^{1}H NMR were taken after 30 min, 60 min, 95 min, 120 min, and 150 min.

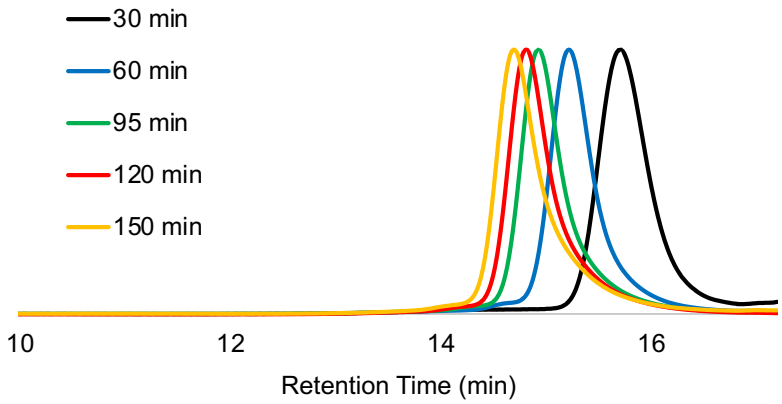

Figure 6.20. GPC traces of kinetic experiment (Figure 6.2).

Procedure for Diblock Copolymer Synthesis under Inert Atmosphere (Figure 6.3)

Under ambient atmosphere, a one-dram vial was charged with PCCP (**1**) (0.015 mmol, 5.5 mg, 1 equiv) and an oven-dried stir bar. The vial was then transferred to a nitrogen-filled glovebox, charged with distilled EVE (0.7 mmol, 70 µL, 45 equiv), and sealed with a cap equipped with a Teflon septum. The

reaction was stirred at room temperature for 2 h until it gelled up. An aliquot for GPC was taken prior to the addition of distilled IBVE (1 mmol, 130 μL, 65 equiv). The polymerization was terminated by the addition of 50 μL of 5% triethylamine/methanol after an additional 5 h of reaction time. An aliquot for GPC and ^{1}H NMR of the final diblock polymer was taken. IBVE conversion had reached 75% after 5 h of reaction time. The final diblock copolymer was concentrated *in vacuo* to yield the pure polymer. ^{1}H and ^{13}C NMR spectra are shown in Figures 6.21 and 6.22, respectively.

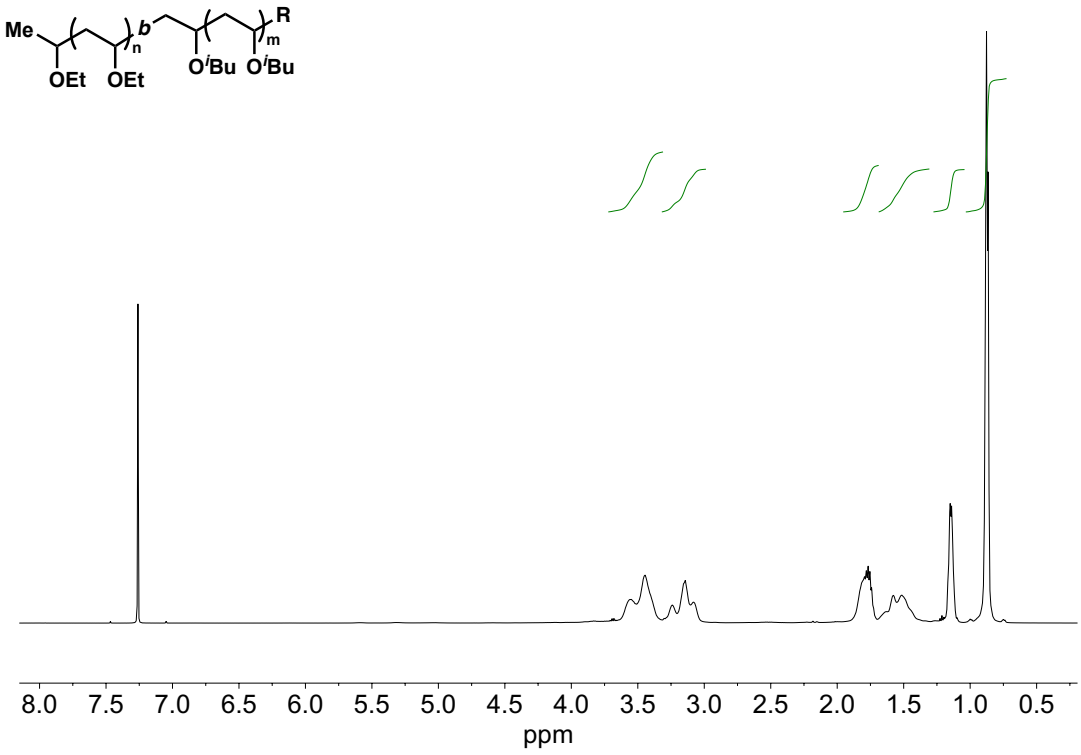

Figure 6.21. ^{1}H NMR of poly(EVE-*b*-IBVE) in $CDCl_3$ (Figure 6.3).

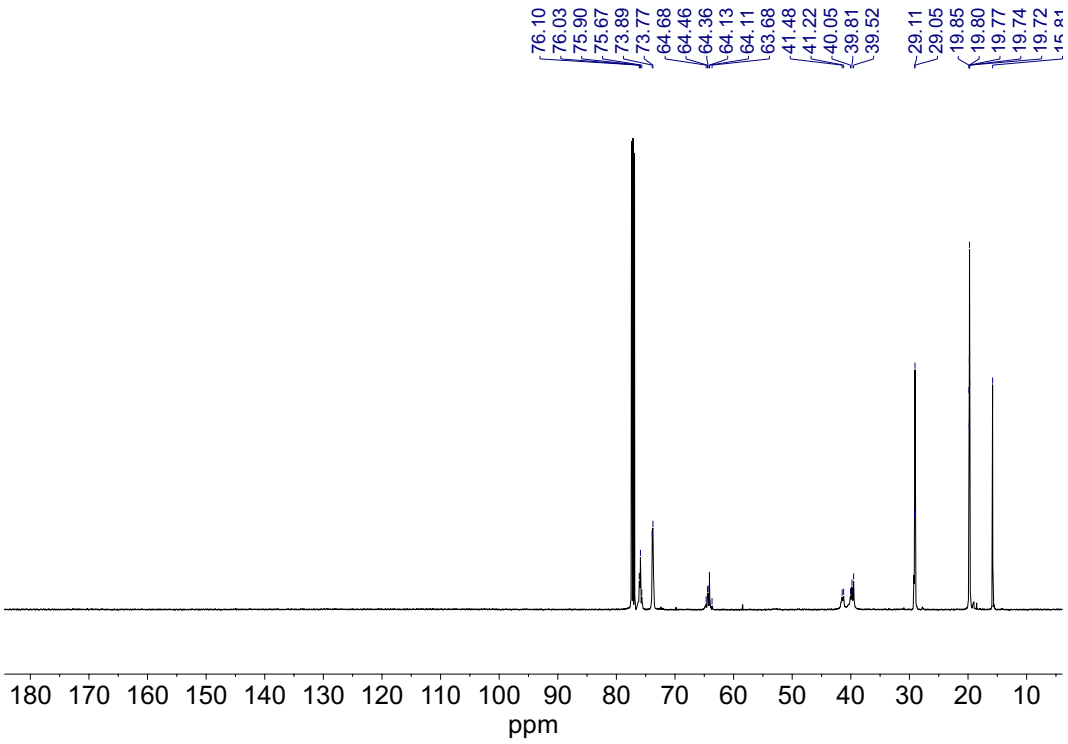

Figure 6.22. ^{13}C NMR of poly(EVE-*b*-IBVE) in $CDCl_3$ (Figure 6.3).

Procedure for Diblock Copolymer Synthesis under Ambient Conditions

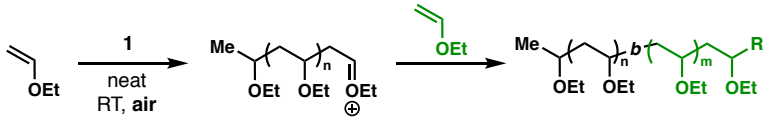

Under ambient atmosphere, a one-dram vial was charged with PCCP (**1**) (0.028 mmol, 10 mg, 1 equiv) and a stir bar. EVE (1.4 mmol, 140 µL, 50 equiv) was filtered through a short plug of basic alumina and subsequently added to the vial. The reaction was sealed with a cap equipped with a Teflon septum and stirred at room temperature for 50 min. An aliquot for GPC and ^{1}H NMR was taken prior to the addition of a fresh batch of EVE (1.4 mmol, 140 µL, 50 equiv). The polymerization was terminated by the addition of 50 µL of 5% triethylamine/methanol after an additional 100 min of reaction time. An aliquot for GPC and ^{1}H NMR of the final diblock polymer was taken. EVE had reached 69% conversion for the first block, while the final conversion of EVE was 86%. GPC traces are shown in Figure 6.23.

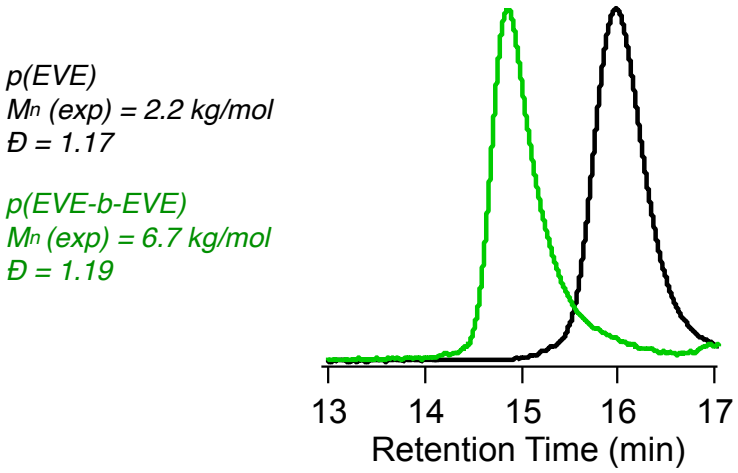

Figure 6.23. SEC traces of poly(EVE) and poly(EVE-*b*-EVE) synthesized under ambient conditions.

General Procedure for Chain-End Functionalization with Alcohols (Figure 6.4a)

Under ambient atmosphere, a one-dram vial was charged with PCCP (**1**) (0.042 mmol, 15 mg, 1 equiv), IBVE (4.2 mmol, 540 μL, 100 equiv), and a stir bar. IBVE was filtered through a plug of basic alumina prior to use. The reaction was sealed with a cap equipped with a Teflon septum and stirred at room temperature until IBVE had reached ~60% conversion. An aliquot for GPC and ^{1}H NMR was taken. The reaction was quenched by the addition of the respective alcohol (0.21 mmol, 5 equiv, 3.1 M in acetone, containing 1 equiv of triethylamine) and stirred for an additional 2 h. The polymer was then precipitated upon the addition of cold methanol and dried *in vacuo* prior to GPC and ^{1}H NMR analysis. ^{1}H NMRs of the functionalized polymers reported in Figure 4a are shown in Figures 6.24–6.26.

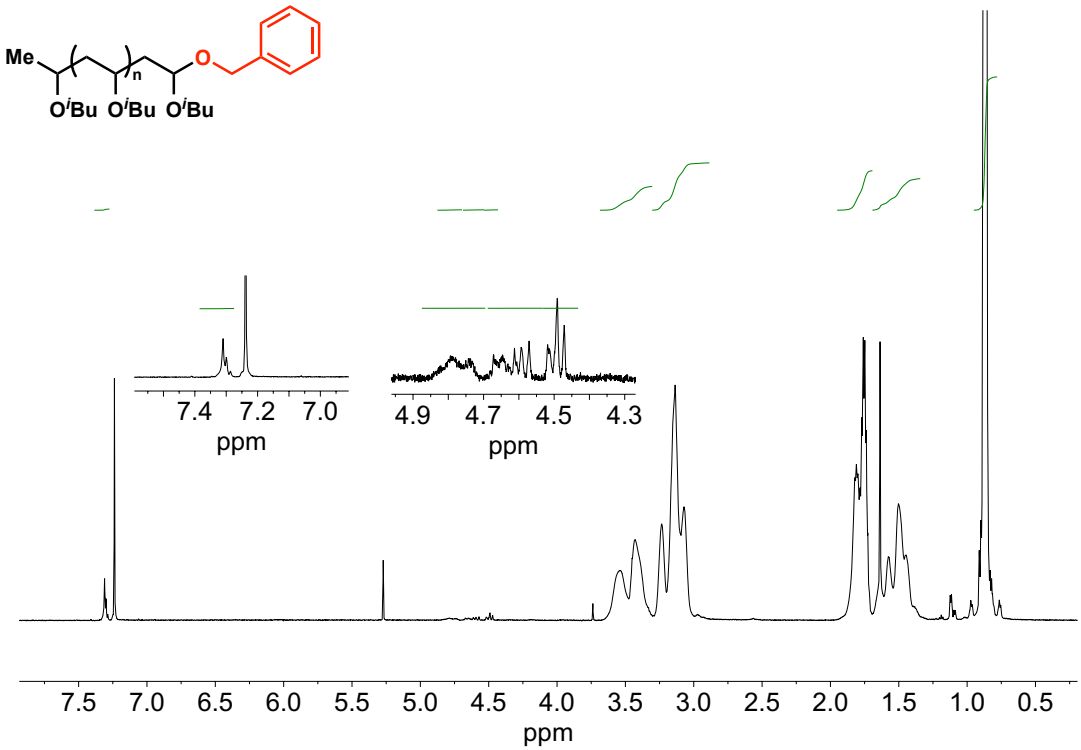

Figure 6.24. ^{1}H NMR of poly(IBVE) functionalized with 5-hexen-1-ol; M_n (GPC) = 5.4 kg/mol; M_n (NMR) = 6.6 kg/mol.

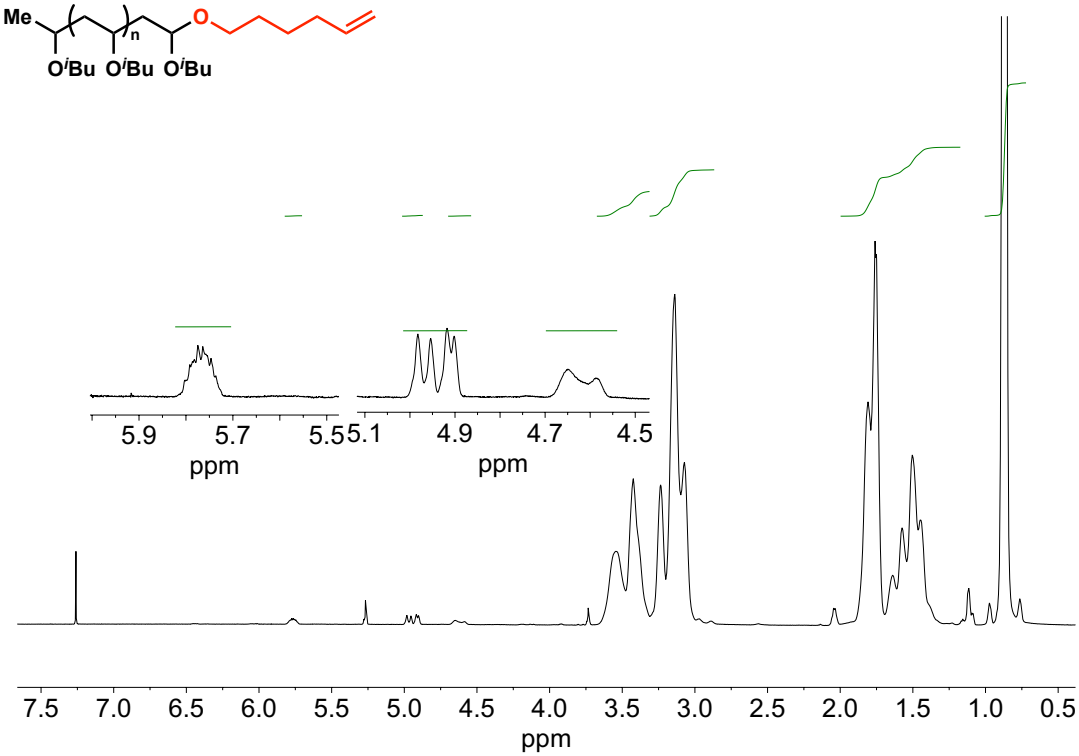

Figure 6.25. ^{1}H NMR of poly(IBVE) functionalized with benzyl alcohol; M_n (GPC) = 7.5 kg/mol; M_n (NMR) = 8.8 kg/mol.

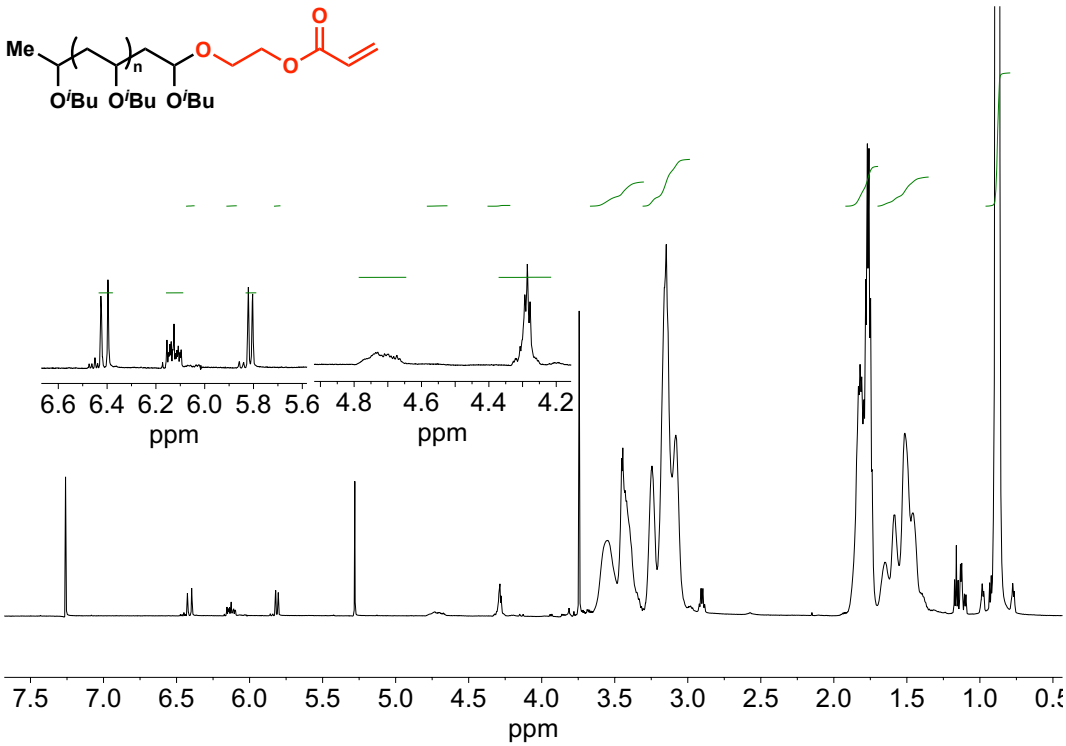

Figure 6.26. ^{1}H NMR of poly(IBVE) functionalized with 2-hydroxy ethyl acrylate; M_n (GPC) = 6.2 kg/mol; M_n (NMR) = 6.1 kg/mol.

Procedure for Chain-End Functionalization with Dithiocarbamate Salt and Chain Extension Using Ferrocenium (Figure 6.4b)

An oven-dried vial was charged with an oven-dried stir bar and PCCP (**1**) (0.042 mmol, 15.0 mg, 1.0 equiv). Then IBVE (4.2 mmol, 540 μL, 100 equiv) (previously filtered through two plugs of basic alumina) was added and the vial sealed with a cap and Teflon septum and stirred for 3 h at room temperature (~40% conversion). Sodium *N,N*-diethyl dithiocarbamate (0.84 mmol, 144 mg, 20 equiv) was added to the reaction and the suspension was stirred for an additional 2 h at room temperature. The reaction mixture was transferred with DCM (5 mL) to a scintillation vial containing basic alumina (500 mg) and the slurry was stirred an additional 10 minutes. The solids were filtered, and the filtrate concentrated *in vacuo*. The residue was taken up in a minimal amount of DCM and precipitated twice from MeOH at –78 °C. The sticky residue was dried under high vacuum before being transferred into a nitrogen-filled glove box. M_n(GPC) = 5.3 kg/mol, $Đ$ = 1.08.

In a nitrogen-filled glove box, an oven-dried one-dram vial was equipped with a stir bar and charged with poly(IBVE) (0.0109 mmol, 58 mg, 1.0 equiv), IBVE (0.14 mL, 1.09 mmol, 100 equiv), and then 0.10 mL of a stock solution of $FcBF_4$ in DCM (5.5 mM, 0.55 μmol, 0.05 mol% relative to IBVE). The vial was sealed with a cap equipped with a Teflon septum under an atmosphere of nitrogen and left to stir. The reaction was run for 5 h to reach full conversion and quenched by the addition of sodium *N,N*-diethyl dithiocarbamate, then an aliquot was removed for ^{1}H NMR and GPC analysis (M_n = 12.6 kg/mol, $Đ$ = 1.24). ^{1}H NMR

spectra of the functionalized polymer before and after chain extension are depicted in Figures 6.27 and 6.28, respectively.

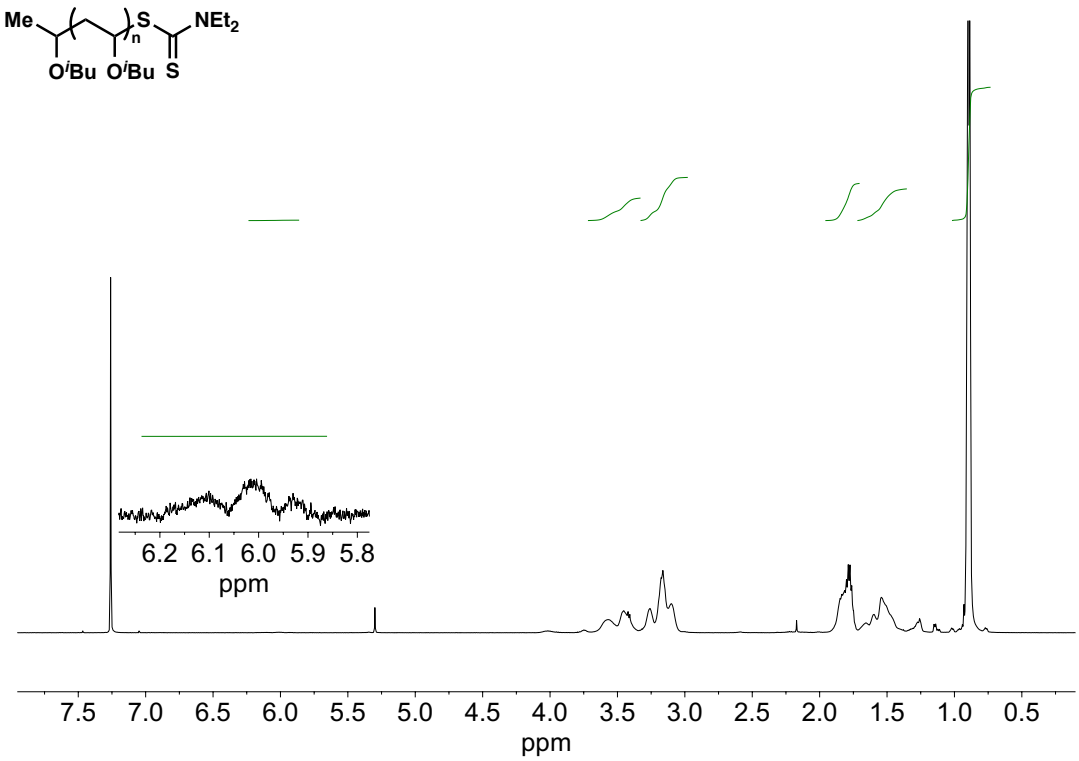

Figure 6.27. ^{1}H NMR of poly(IBVE) functionalized with dithiocarbamate prior to chain extension (Figure 6.4b).

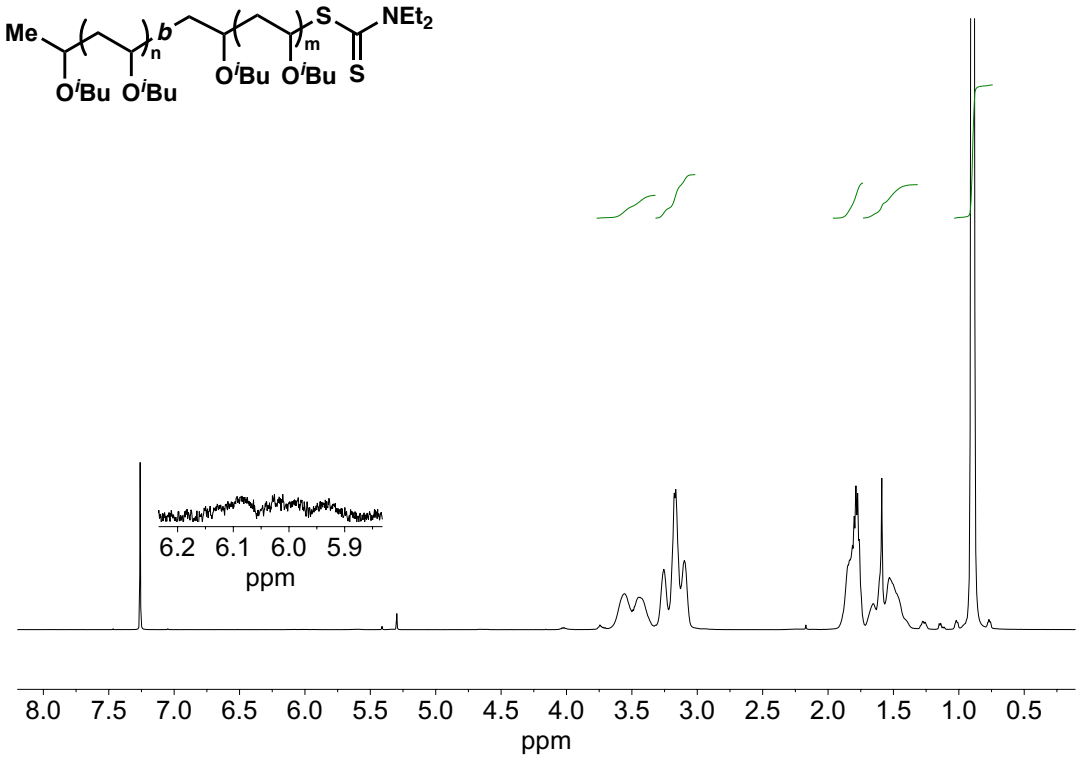

Figure 6.28. ^{1}H NMR of poly(IBVE-*b*-IBVE) functionalized with dithiocarbamate after chain extension using ferrocenium (Figure 6.4b).

Procedure for IBVE Homopolymerization with Varying Amounts of Water

Under ambient atmosphere, a one-dram vial was charged with PCCP (**1**) (0.014 mmol, 5.0 mg, 1 equiv) and a stir bar. Deionized water (1–100 equiv, 0.014–1.4 mmol, 0.25–25 μL) was added to the reaction vial, followed by IBVE (1.4 mmol, 180 μL, 100 equiv), which was filtered through a plug of basic alumina prior to use. The vial was sealed with a cap equipped with a Teflon septum and stirred at room temperature for 19 h. An aliquot for GPC and ^{1}H NMR analysis was taken. Reactions with 40 and 100 equiv of water did not yield any polymer. The GPC traces of polymerizations performed under inert

conditions, ambient conditions, in the presence of 1 equiv, and 10 equiv of water are depicted in Figure 6.29.

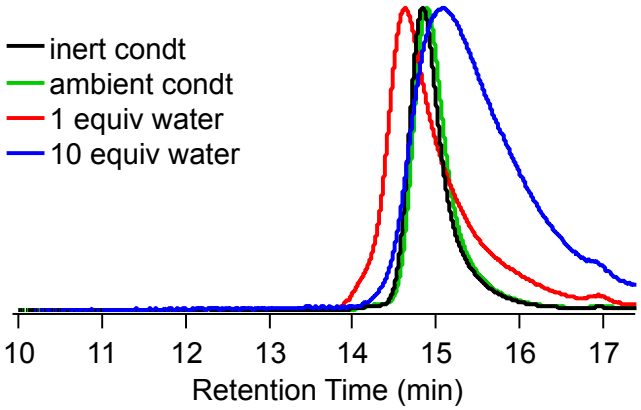

Figure 6.29. SEC traces of poly(IBVE) synthesized in the presence of different amounts of water.

Procedure for Active Chain-End Analysis by ^{1}H NMR Analysis

In a nitrogen-filled glove box, a J-Young NMR tube was charged IBVE (2 mmol, 260 µL, 50 equiv) and 120 µL of $CDCl_3$. PCCP (**1**) (0.04 mmol, 14.4 mg, 1 equiv) was dissolved in 150 µL of $CDCl_3$ in a one-dram vial and sealed under a nitrogen atmosphere. In a separate J-Young Tube, the same amount of **1** was dissolved in 530 µL $CDCl_3$ and used for the reference ^{1}H NMR spectrum. The ^{1}H NMR spectra of pure IBVE and **1** were recorded at room temperature. Subsequently, dissolved **1** was quickly added to the tube containing IBVE and shaken before recording ^{1}H NMR spectra of the active polymerization ~8 min of reaction time. The spectra are depicted in Figures 6.30–6.33. Specifically, Figure 6.31 highlights the appearance of several new methyl-ester resonances

of **1** upon reaction with IBVE, which we attribute to the IBVE-PCCP adduct. The insert in Figure 6.32 depicts three new resonances at 4.5–5.0 ppm. These can tentatively be assigned to the methine of a covalent IBVE-PCCP adduct. Figure 6.33 shows the absence of aldehyde and olefin resonances, which have been previously assigned to poly vinyl ether chain ends.[2]

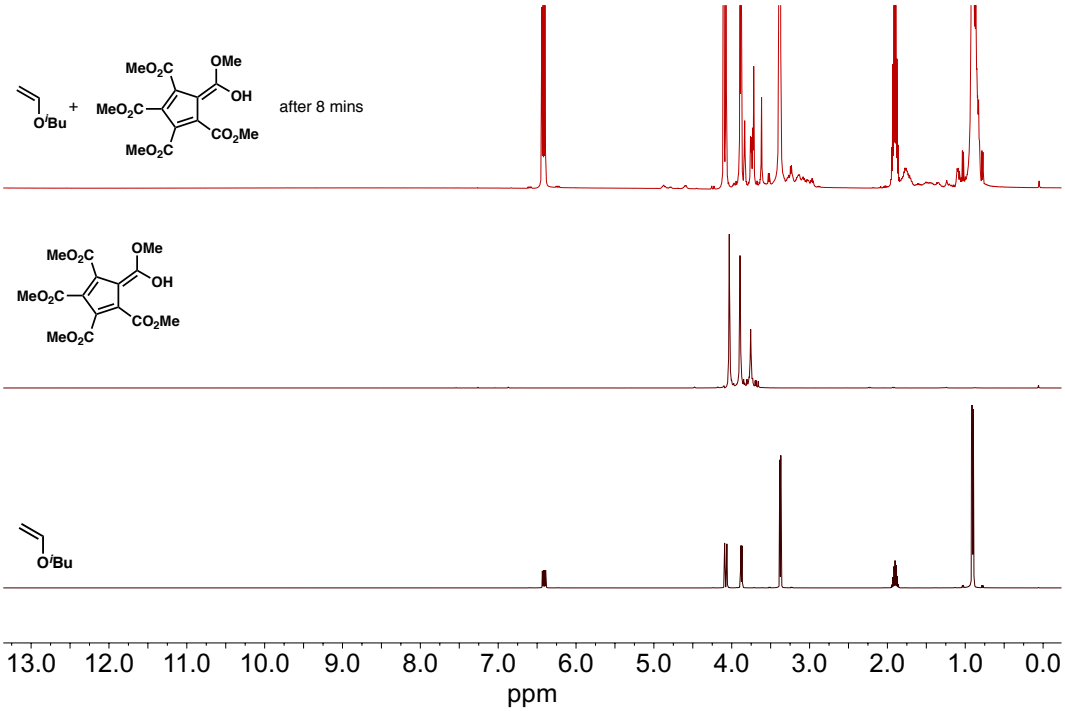

Figure 6.30. Stacked ^{1}H NMR spectra of IBVE, PCCP (**1**), IBVE and PCCP mixture after eight minutes of reaction time (bottom to top).

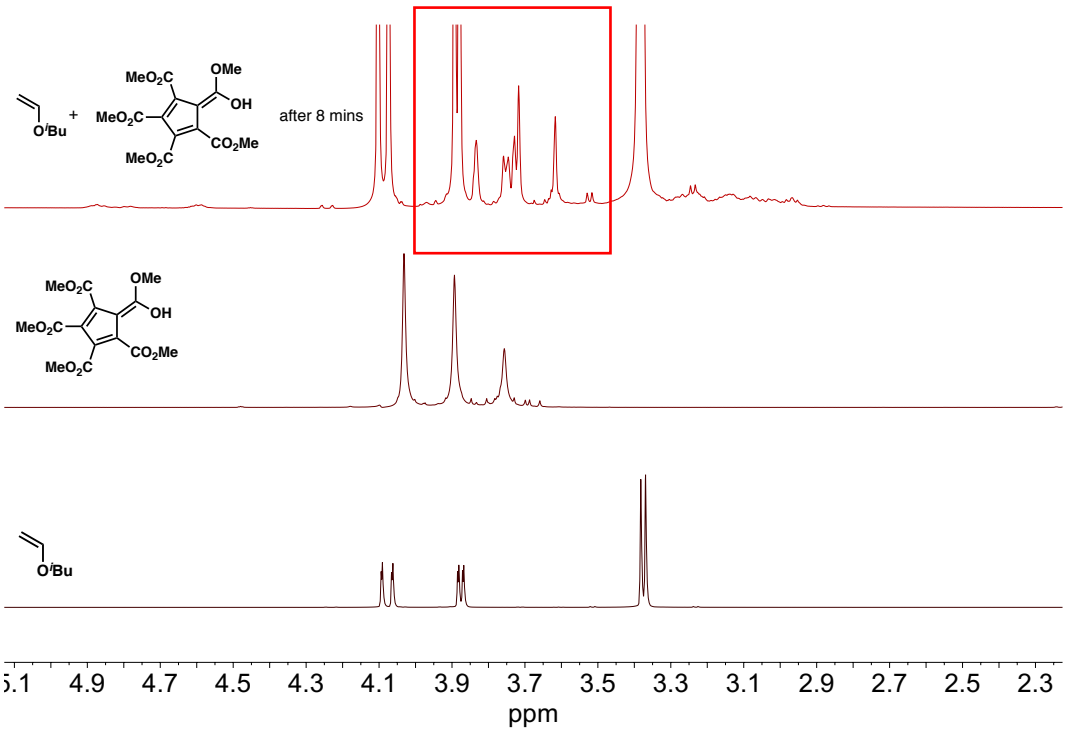

Figure 6.31. Zoom of stacked ^{1}H NMR spectra of IBVE, PCCP (**1**), IBVE and PCCP mixture after eight minutes of reaction time (bottom to top). Red box highlights new methyl-ester resonances of **1** upon reaction with IBVE.

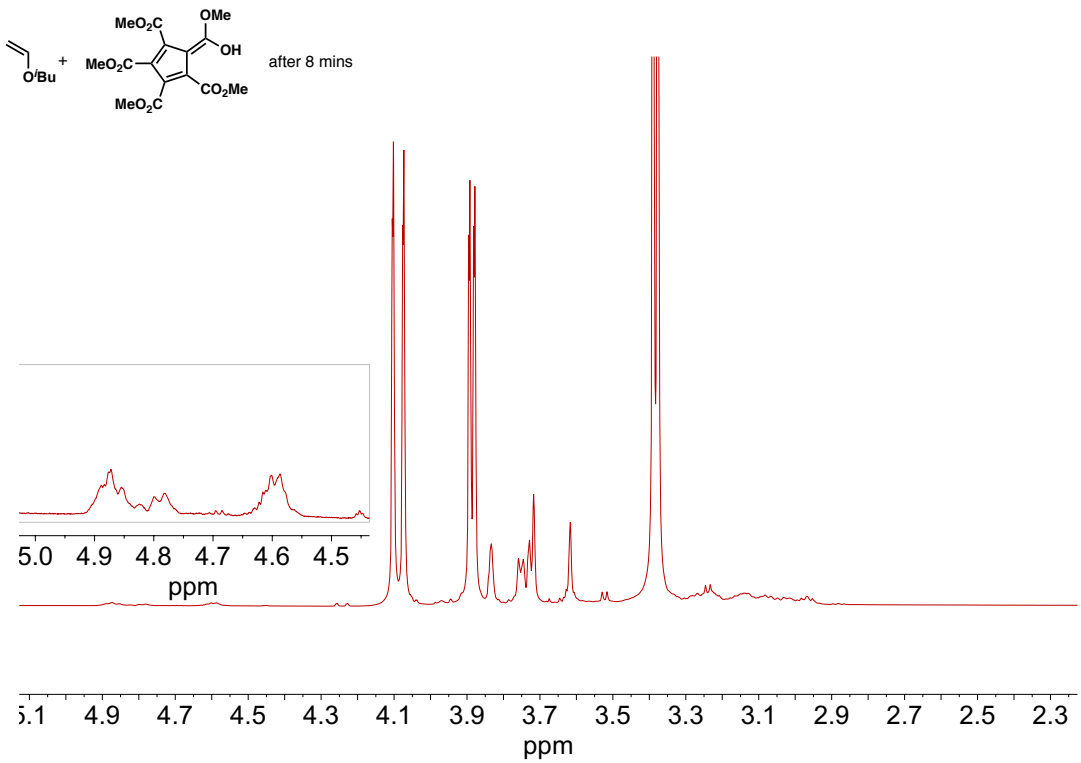

Figure 6.32. Zoom of ^{1}H NMR spectrum of the IBVE and PCCP mixture after eight minutes of reaction time; Insert highlights the appearance of new resonances between 4.5 and 5.0 ppm.

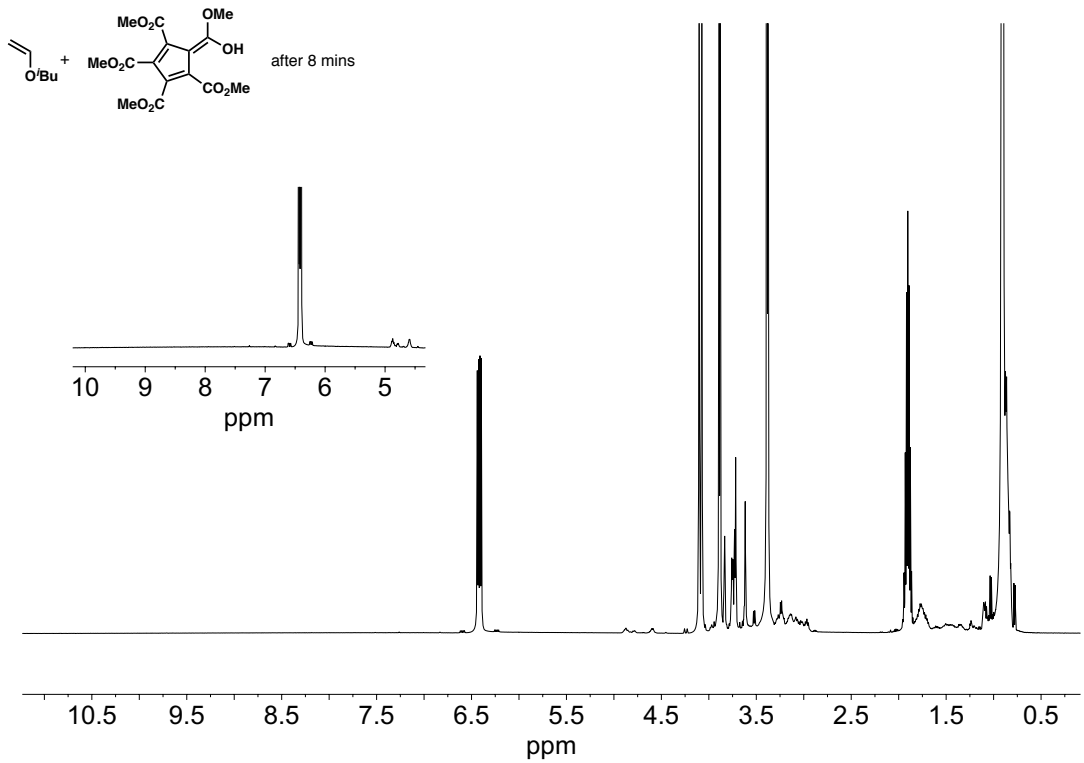

Figure 6.33. ^{1}H NMR spectrum of the IBVE and PCCP mixture after eight minutes of reaction time. Insert highlights the appearance of new resonances between 4.5 and 5.0 ppm and the absence of aldehyde and olefin resonances at the polymer chain end.

Table 6.4. Polymerization of IBVE in different solvents.

Entry[a]	**solvent**	$M_{n,theo}$ **(kg/mol)**	[b]$M_{n,exp}$ **(kg/mol)**	[b]$Đ$	**Meso (%)**
1	-	5.0	4.87	1.15	71
2	DCM	11.0	7.6	1.30	65
3	hexane	11.0	6.7	1.21	70
4	cyclohexane	11.0	6.2	1.18	73
5	toluene	11.0	5.4	1.20	69

[a]Vinyl ether (50–1300 equiv), solvent (volume ratio 1:1) and **1** (1 equiv, 0.014 mmol) were stirred under a nitrogen atmosphere at room temperature; [b]determined against polystyrene standards.

Appendix References

(1) Bruce, M.I.; Walton, J. K.; Williams, M. L.; Hall, S. R.; Skelton, B. W.; White, A. H. *J. Chem. Soc., Dalton Trans.* **1982**, 2209.

(2) Kanazawa, A.; Kanaoka, S.; Aoshima, S. *J. Polym. Sci. Part A: Polym. Chem.* **2010**, *48*, 3702.

CHAPTER 7

"SHAPING" THE FUTURE OF MOLECULAR WEIGHT DISTRIBUTIONS IN ANIONIC POLYMERIZATION

7.1 Abstract

Varying molecular weight distributions (MWDs) have the potential to precisely tune polymer properties, but this approach remains relatively unexplored owing to a lack of synthetic methods that provide control over the exact makeup of a distribution. Herein, we report a simple and highly efficient strategy for addressing this challenge through temporal regulation of initiation in the anionic polymerization of styrene. This method yields unprecedented control over the shape of the polymer MWD and facilitates the synthesis of diblock copolymers with controlled MWD compositions. Importantly, we show that the MWD symmetry has a marked influence on the stiffness of poly(styrene-*block*-isoprene) copolymers, which demonstrates that varying MWD shape is an effective method for altering polymer properties.

7.2 Introduction

The dispersity (*Đ*) of a polymer sample is a key parameter in the control of material properties such as viscosity, processability, and all facets of block copolymer self-assembly.[1−14] However, *Đ* is the normalized standard deviation of the molecular weights in a polymer sample and, therefore, describes only the relative breadth of the molecular weight distribution (MWD).[15] Theoretical

studies have looked beyond the breadth of MWD and suggested that distribution shape has a marked influence on polymer physical properties.[16,17] Therefore, synthetic methods that enable deterministic control over the exact distribution of chain lengths in a sample are needed to understand the full influence of MWD composition on polymer properties; these methods have the potential to facilitate the implementation of polymer distribution as a means to develop improved materials. shape has a marked influence on polymer physical properties. Therefore, synthetic methods that enable deterministic control over the exact distribution of chain lengths in a sample are needed to understand the full influence of MWD composition on polymer properties; these methods have the potential to facilitate the implementation of polymer distribution as a means to develop improved materials.

On this basis, multiple methods have been developed to modify MWDs in controlled polymerizations. The majority of these processes only give control over the relative breadth of the distribution;[9–13] however, a limited number have taken a step toward changing MWD shape. Specifically, Meira and co-workers have demonstrated that variation of monomer and initiator flow rates in continuous flow reactors imparted partial control over MWD shape.[18–21] Further, methods have been developed using pulsed initiation through photolysis or monomer/initiator feeds to give multimodal distributions.[22–24] Additionally, Aoshima and co-workers have tuned polymer composition through controlled termination processes.[25] Although these methods give partial control, new

strategies are still needed to give precise regulation of MWD shape in living polymerization processes.

In an effort to realize deterministic control of MWD symmetry, we recently reported a method in which we used temporally controlled initiation in nitroxide-mediated polymerization (NMP) reactions.[26] Specifically, by controlling the addition of an alkyl nitroxide initiator to the polymerization of styrene, we predictably modulated polymer MWD shape while maintaining excellent control over number-average molecular weight (M_n) and $Đ$. Although this protocol afforded robust command of the MWD, several challenges need to be addressed to make this strategy more powerful and practical. For example, NMP processes inherently produce polymers with broader distributions, which limits how precisely the MWD can be defined through temporally controlled initiation.[27,28] Moreover, these radical polymerizations have limited substrate scopes and can be run only to partial conversions to get reasonable chain-end fidelities. Therefore, we sought a polymerization method that gives more precise control over MWD shape, is applicable to a wider array of monomer types, and provides higher-molecular-weight polymers. Additionally, we wanted a truly living polymerization process that would enable reactions to be run to full conversion, thereby providing access to the one-pot synthesis of block copolymers.

We hypothesized that anionic polymerization would be the ideal reaction class with which to address the above challenges owing to its capacity to give narrow $Đ$s, truly living nature and broad monomer scope.[29–35] Furthermore, for

the anionic polymerization of styrene, Lynd and Hillmyer have successfully broadened polymer *Đ* up to 1.3 through a combination of metered initiator addition and temperature control.[9] BASF also patented a method that enabled the synthesis of broad polystyrene samples through controlled addition of monomer, initiator, and rate-retarding agents.[36] Although both of these reports did not control the MWD shape, they provided evidence that anionic polymerization would work well in our temporally controlled initiation strategy. Herein, we report the deterministic control of polymer MWDs for the anionic polymerization of styrene (Figure 7.1). This method imparts unprecedented control over MWD shape and opens the door to better understand the relationship between polymer chain-length composition and material properties. Using our new method, we demonstrate that the shape of the MWD in block copolymers has a significant influence on their physical properties, which clearly illustrates that MWD composition can be used to tune polymer function.

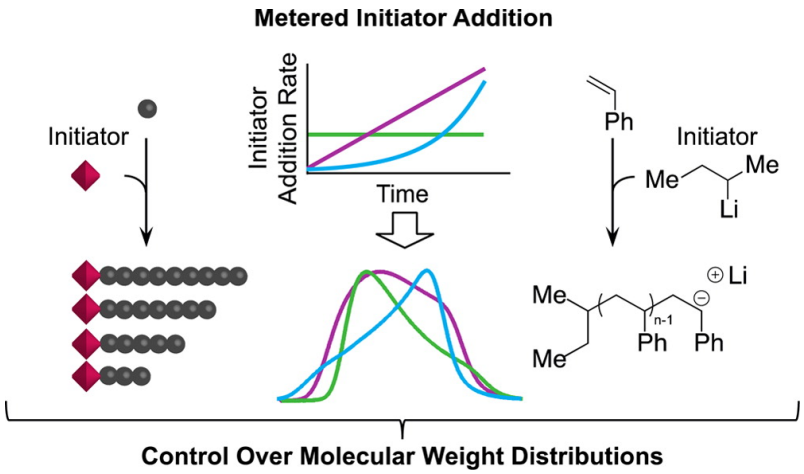

Figure 7.1. Metered addition of *sec*-butyllithium in the anionic polymerization of styrene to tailor the shape and composition of the molecular weight distribution (MWD).

7.3 Results and Discussion

We began our studies by looking at the temporally controlled initiation of anionic polymerizations of styrene. Metering in a fixed amount of the initiator, *sec*-butyllithium (*s*-BuLi), at a constant rate to a solution of styrene in cyclohexane, we expected to observe the MWD broadening with increasing addition time while M_n remained unchanged (Figure 7.2a). Traditional reaction conditions, in which the full amount of the initiator is added at the beginning of the reaction, yielded a 14.6 kg/mol polystyrene (PS) sample with a narrow $Đ$ of 1.07. In support of our hypothesis, the addition of the same molar quantity of *s*-BuLi at constant rates from 20 to 120 min broadened the $Đ$ from 1.16 to 2.47 without changing M_n (Figure 7.2b). Size exclusion chromatography (SEC) traces of these reactions showed a shift in the peak maximum (M_p) to higher molecular weights and a clear broadening of the distribution as addition time increased (Figure 7.2c). Moreover, a linear relationship between initiator

addition time and $Đ$ was observed (Figure 7.2d). These results illustrate that temporally controlled initiation in the anionic polymerization of styrene enables predictable control over polymer $Đ$ and M_n.

Next, we efficiently achieved our goal of controlling the shape of the distribution by modulating the initiator addition rate profile. Compared with polymer samples synthesized with constant rates of initiator addition, those produced with linearly increasing addition rates gave distributions that had less tailing and were significantly broader at 50% peak height (Figure 7.2e–h). Furthermore, drastically different peak shapes were obtained when exponentially increasing rates were used (Figure 7.2i–l). For these addition profiles, the SEC traces showed a decrease in M_p at longer addition times, with a tailing into higher molecular weights. These shapes are the antithesis of the polymer samples prepared with constant rates of addition and demonstrate that our method can be used to achieve drastically different MWD compositions. Notably, for both the linearly and exponentially increasing addition rates,

excellent control over M_n was obtained and a linear relationship between $Đ$ and addition time was observed.

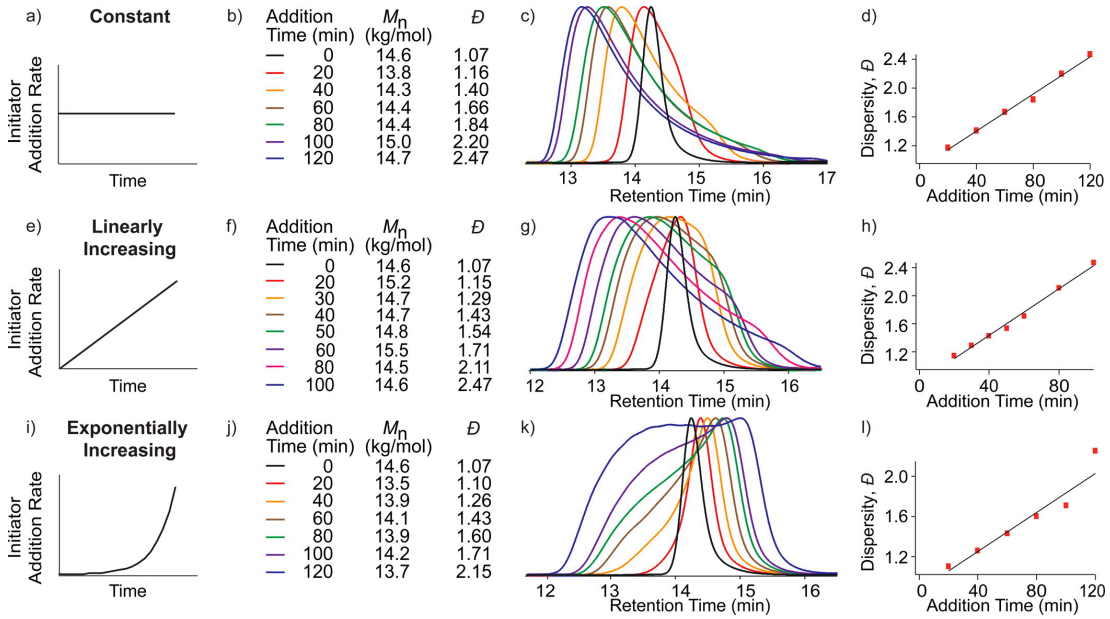

Figure 7.2. Controlling the breadth and shape of polystyrene MWD distributions with constant (a–d), linearly ramped (e–h), and exponentially ramped (i–l) rates of initiator addition (a, e, and i are representative initiator addition profiles).

A major advantage of using temporally controlled initiation in anionic polymerizations is that vastly different MWD shapes are accessible even at relatively low $Đ$s. We highlight this in Figure 7.3, which shows three SEC curves of PS samples that have $Đ$s of ~1.4 and M_ns of ~14.5 kg/mol but were made with different initiator addition profiles. According to only M_n and $Đ$, these materials would be considered almost identical; however, there is little resemblance among these traces, which have asymmetry factor (A_s) values of 3.6, 1.6, and 0.3 corresponding to polymers made with constant, linearly increasing, and exponentially increasing addition rates, respectively (see Figure

7.3).[37] The overlay of these SEC traces illustrates the drastically variable shapes that can be accessed with our method.

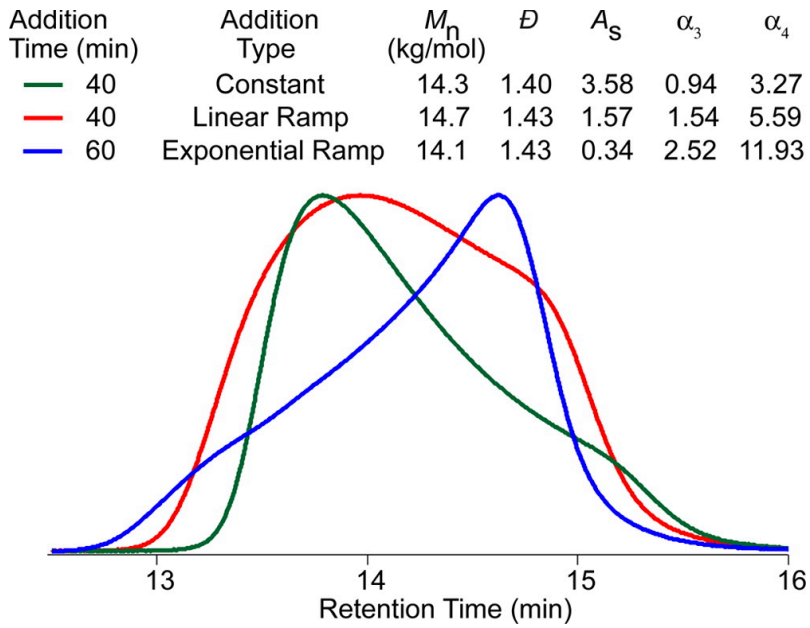

Figure 7.3. Three polymer samples with similar M_n and dispersity ($Đ$) values but drastically variable MWD compositions. α_3, skewness; α_4, kurtosis; A_s, asymmetry factor.

These MWDs can be further described by going beyond M_n and $Đ$ values to the third (skewness, α_3) and fourth (kurtosis, α_4) moments of the distribution function.[38] Skewness describes the symmetry of the curve, whereas kurtosis indicates the amount of tailing on either side of the MWD around M_p. Both of these parameters, which further describe the shape of the distribution, are significantly different among the polymers made with the three initiator addition profiles.

Compared with temporally controlled initiation in NMP reactions, the anionic polymerizations permitted significantly higher levels of control over the shape of the distribution. For example, for PS polymers with *Đ* values of ~1.4 made with NMP, A_s values ranged from 0.6 to 1.0 (compared with values of 0.3 to 3.6 for anionic polymerizations).[26] These results demonstrate that the inherently narrow MWDs afforded by anionic polymerization enable markedly better command of MWD shape, especially when *Đ* is below 1.7.

During our studies, we noticed that the majority of the constant and linearly increasing initiator addition rates afforded polymers for which SEC traces showed precipitous peak edges at low molecular weights. We postulated that this outcome was a result of abrupt stops in initiator addition, which caused the distribution to decline sharply to baseline with shorter addition times. To investigate this hypothesis, we monitored one of the polymerizations in which the initiator was added at a constant rate over 40 min. The SEC curves of the polymer before the end of the addition showed a smooth return to baseline (Figure 7.4). However, time points after the addition showed the emergence of the peak edge, which grew as the polymerization proceeded. This experiment provided straightforward evidence to support our hypothesis.

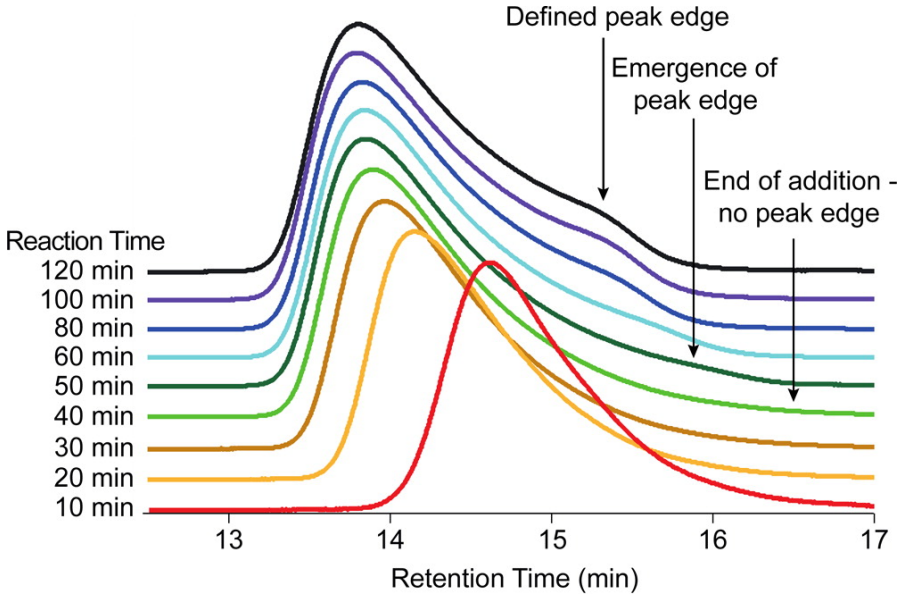

Figure 7.4. Size exclusion chromatography curves at indicated time points with a 40 min constant rate addition.

We reasoned that the observed peak edge could be removed by gradually decreasing the initiator addition rate at the end of the process. Using bell-shaped addition profiles, we obtained nearly symmetrical PS distributions that had no discernible peak edges (Figure 7.5). These data further demonstrate that MWD shape and composition can be precisely tuned by simply modulating the addition profile of the initiator.

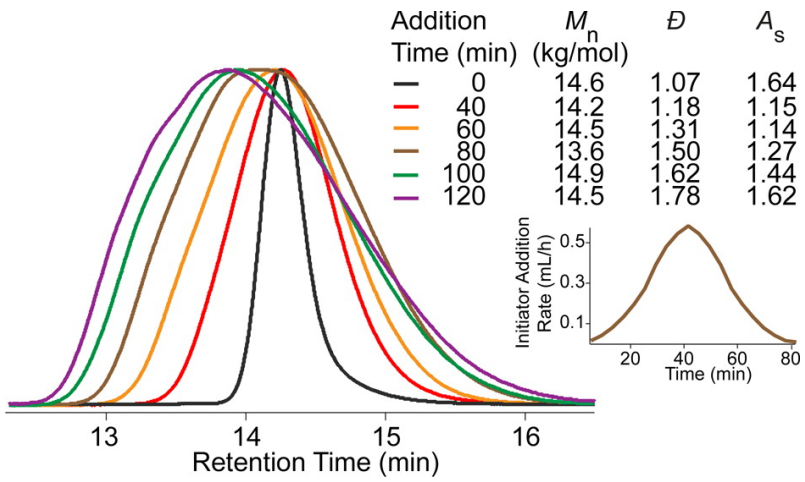

Figure 7.5. Size exclusion chromatography curves of a bell-shaped initiator addition profile. Inset: rate (mL/h) vs time (min) of an 80 min addition profile.

The living nature of anionic polymerizations allows these reactions to run to full conversion and enables the one-pot synthesis of diblock copolymers.[9,39] Taking advantage of these features, we synthesized a series of poly(styrene-*block*-isoprene) copolymers (PS-*b*-PI) in which both the shape and the *Đ* of the PS block varied (Figure 7.6a).[40] In all cases, efficient chain extension of our compositionally controlled PS samples with isoprene gave well-defined PS-*b*-PI copolymers.

a)

Entry	M_n (S) (kg/mol)	$Đ$ (S)	A_S	M_n (SI) (kg/mol)	$Đ$ (SI)	E (MPa)
1a	14.1	1.19	1.85	35.6	1.14	460
1b	14.2	1.22	0.52	35.1	1.16	560
2a	14.9	1.42	3.52	36.8	1.21	450
2b	14.1	1.39	0.37	33.6	1.22	530
3a	15.2	1.69	4.48	36.3	1.25	220
3b	14.1	1.71	0.31	36.5	1.28	440
4a	14.4	2.01	4.97	37.2	1.28	85
4b	13.8	1.97	0.26	34.4	1.29	300

b)

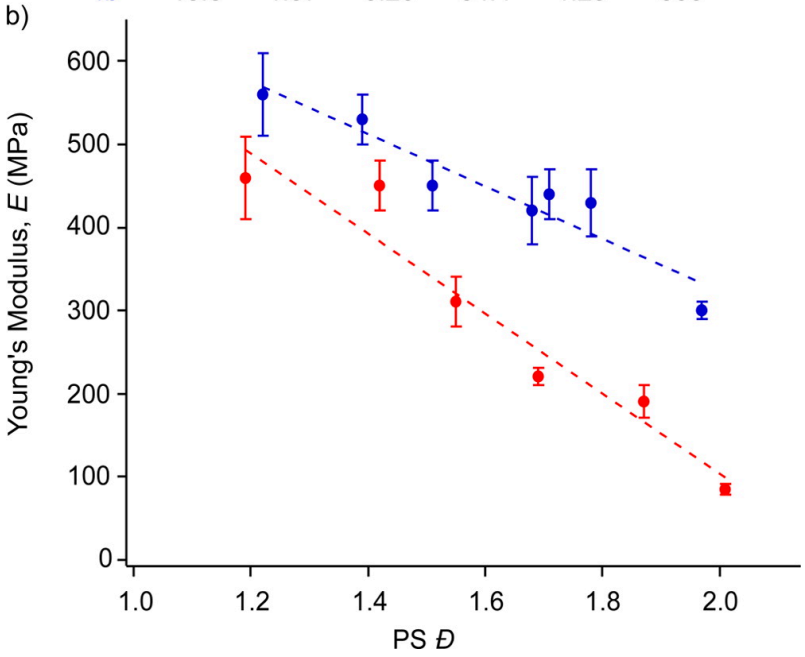

Figure 7.6. (a) Poly(styrene-block-isoprene) block copolymers with varying polystyrene (PS) MWD shapes and Young's moduli (E) determined with dynamic mechanical analysis. (b) Plot of PS $Đ$ vs E (MPa): blue circles indicate PS blocks with asymmetry factor (A_s) values of <1; red circles indicate PS blocks with A_s values of > 1; S = PS; SI = poly(styrene-*block*-isoprene). Each E value is an average of at least four measurements.

With the above series of copolymers in hand, we set out to investigate the influence of MWD shape and breadth on the Young's modulus (E) of the material (Figure 7.6b).[41–44] For all samples, materials in which the PS MWD shape was tailing to higher molecular weights (A_s < 1) had E values that were

consistently higher than those of samples with shapes tailing to lower molecular weights (A_s > 1). This difference in E between the two MWD shapes increased as $Đ$ increased or as the difference in A_s values widened between the samples. For example, two samples in which the $Đ$ of the PS block was ~1.2 with A_s values of 1.9 and 0.5 gave E values of 460 and 560 MPa, respectively; a moderate 1.2-fold increase in E. Remarkably, when we switched to two samples that had PS $Đ$s of ~2.0 with A_s values of 5.0 and 0.3, we observed E values of 300 and 85 MPa, respectively. In this case, the change in E was 3.5-fold between the samples, which clearly shows that the MWD shape and composition have a significant influence. Moreover, these results demonstrate that the MWD shape is just as important, if not more important, than the breadth of the distribution and can effectively be used as a parameter for tuning material function.

7.4 Conclusion

In summary, we have developed a robust method for precisely tailoring MWD shape by temporally regulating initiation in the anionic polymerization of styrene. The truly living nature of this anionic polymerization allows the synthesis of materials with similar M_n and $Đ$ values but drastically different polymer compositions and provides facile access to block polymers. Taking advantage of our new method, we synthesized a library of PS-*b*-PI copolymers with various PS MWD shapes. Significantly, we found that MWD symmetry had a considerable influence on the stiffness of the material, which shows that MWD

shape is a key parameter influencing polymer properties. This simple and modular approach offers unparalleled levels of control and gives access to a wide array of functional materials with systematically deviating polymer compositions. It also provides a platform for further fundamental studies of the influence of MWD shape on polymer properties.

7.5 References

(1) Nichetti, D.; Manas-Zloczower, I. *Polym. Eng. Sci*. **1999**, *39*, 887.

(2) Collis, M. W.; Mackley, M. R. *J. Non-Newtonian Fluid Mech*. **2005**, *128*, 29.

(3) Lynd, N. A.; Meuler, A. J.; Hillmyer, M. A. *Prog. Polym. Sci*. **2008**, *33*, 875.

(4) Sides, S. W.; Fredrickson, G. H. *J. Chem. Phys*. **2004**, *121*, 4974.

(5) Bates, F. S.; Hillmyer, M. A.; Lodge, T. P.; Bates, C. M.; Delaney, K. T.; Fredrickson, G. H. *Science* **2012**, *336*, 434.

(6) Hillmyer, M. A. *J. Polym. Sci., Part B: Polym. Phys*. **2007**, *45*, 3249.

(7) Schmitt, A. K.; Mahanthappa, M. K. *Macromolecules* **2014**, *47*, 4346.

(8) Bendejacq, D.; Ponsinet, V.; Joanicot, M.; Loo, Y. L.; Register, R. A. *Macromolecules* **2002**, *35*, 6645.

(9) Lynd, N. A.; Hillmyer, M. A. *Macromolecules* **2007**, *40*, 8050.

(10) Widin, J. M.; Schmitt, A. K.; Schmitt, A. L.; Im, K.; Mahanthappa, M. K. *J. Am. Chem. Soc*. **2012**, *134*, 3834.

(11) Hustad, P. D.; Marchand, G. R.; Garcia-Meitin, E. I.; Roberts, P. L.; Weinhold, J. D. *Macromolecules* **2009**, *42*, 3788.

(12) Listak, J.; Jakubowski, W.; Mueller, L.; Plichta, A.; Matyjaszewski, K.; Bockstaller, M. R. *Macromolecules* **2008**, *41*, 5919.

(13) Lynd, N. A.; Hillmyer, M. A. *Macromolecules* **2005**, *38*, 8803.

(14) Meuler, A. J.; Ellison, C. J.; Evans, C. M.; Hillmyer, M. A.; Bates, F. S. *Macromolecules* **2007**, *40*, 7072.

(15) Rane, S. S.; Choi, P. *Chem. Mater*. **2005**, *17*, 926.

(16) Lynd, N. A.; Hillmyer, M. A.; Matsen, M. W. *Macromolecules* **2008**, *41*, 4531.

(17) Cooke, D. M.; Shi, A.-C. *Macromolecules* **2006**, *39*, 6661.

(18) Meira, G. R.; Johnson, A. F. *Polym. Eng. Sci*. **1981**, *21*, 415.

(19) Alassia, L. M.; Couso, D. A.; Meira, G. R. *J. Appl. Polym. Sci*. **1988**, *36*, 481.

(20) Couso, D. A.; Alassia, L. M.; Meira, G. R. *J. Appl. Polym. Sci*. **1985**, *30*, 3249.

(21) Laurence, R. L.; Vasudevan, G. *Ind. Eng. Chem. Process Des. Dev*. **1968**, *7*, 427.

(22) Hungenberg, K. D.; Knoll, K.; Wulkow, M. *Macromol. Theory Simul*. **1997**, *6*, 393.

(23) Farkas, E.; Meszena, Z. G.; Johnson, A. F. *Ind. Eng. Chem. Res*. **2004**, *43*, 7356.

(24) Gosden, R. G.; Meszena, Z. G.; Mohsin, M. A.; Auguste, S.; Johnson, A. F. *Polym. React. Eng*. **1997**, *5*, 45.

(25) Seno, K. I.; Kanaoka, S.; Aoshima, S. *J. Polym. Sci., Part A: Polym*. *Chem*. **2008**, *46*, 2212.

(26) Gentekos, D. T.; Dupuis, L. N.; Fors, B. P. *J. Am. Chem. Soc*. **2016**, *138*, 1848.

(27) Hawker, C. J.; Bosman, A. W.; Harth, E. *Chem. Rev*. **2001**, *101*, 3661.

(28) Grubbs, R. B. *Polym. Rev*. **2011**, *51*, 104.

(29) Baskaran, D.; Müller, A. H. E. *Prog. Polym. Sci*. **2007**, 32, 173.

(30) Bywater, S. In Comprehensive Chemical Kinetics; Bamford, C. H., Tipper, C. F. H., Eds.; Elsevier, 1976; Vol. 15, pp 1−65.

(31) Young, R. N.; Quirk, R. P.; Fetters, L. J. In Anionic Polymerization; Springer: Berlin; Heidelberg, 1984; pp 1−90.

(32) Hadjichristidis, N.; Pitsikalis, M.; Pispas, S.; Iatrou, H. *Chem. Rev*. **2001**, *101*, 3747.

(33) Hadjichristidis, N.; Iatrou, H.; Pitsikalis, M.; Pispas, S.; Avgeropoulos, A. *Prog. Polym. Sci*. **2005**, 30, 725.

(34) Hirao, A.; Hayashi, M.; Loykulnant, S.; Sugiyama, K.; Ryu, S.; Haraguchi, N.; Matsuo, A.; Higashihara, T. *Prog. Polym. Sci*. **2005**, *30*, 111.

(35) Higashihara, T.; Hayashi, M.; Hirao, A. *Prog. Polym. Sci*. **2011**, *36*, 323.

(36) Fischer, W.; Knoll, K.; Loth, W.; Warzelhan, V.; Deffieux, A.; Desbois, P.; Fontanille, M.; Latsch, S.; Schade, C.; Gausepohl, H. Anionic Polymerization Process. US6444762 B1, August 18, 1997.

(37) Asymmetry factors (A_s) > 1 describe polymer MWDs tailing into low molecular weights, A_s < 1 describes polymer MWDs tailing into high molecular weights; A_s = 1 indicates a symmetric distribution; see Appendix for details;. Kirkland, J. J.; Yau, W. W.; Stoklosa, H. J.; Dilks, C. H. J. *J. Chromatogr. Sci*. **1977**, *15*, 303.

(38) Rudin, A. *J. Chem. Educ*. **1969**, *46*, 595.

(39) Khandpur, A. K.; Foerster, S.; Bates, F. S.; Hamley, I. W.; Ryan, A. J.; Bras, W.; Almdal, K.; Mortensen, K. *Macromolecules* **1995**, *28*, 8796.

(40) Roovers, J. E. L.; Bywater, S. *Macromolecules* **1968**, *1*, 328.

(41) Oral, I.; Guzel, H.; Ahmetli, G. *Polym. Bull*. **2011**, *67*, 1893.

(42) Nielsen, L. E. *Rheol. Acta* **1974**, *13*, 86.

(43) Kenney, J. F. *Polym. Eng. Sci*. **1968**, *8*, 216.

(44) Lach, R.; Weidisch, R.; Knoll, K. *J. Polym. Sci., Part B: Polym. Phys*. **2005**, *43*, 429.

7.6 Appendix

General Reagent Information

All reactions were performed in an Unilab MBraun Glovebox with a nitrogen atmosphere. Styrene (99+%, Sigma Aldrich), isoprene (>99+%, Sigma Aldrich), and cyclohexane (Fischer Scientific, ACS Grade) were dried over calcium hydride (CaH_2) (ACROS organics, 93% extra pure, 0-2 mm grain size) for 12 h. Styrene was vacuum transferred degassed by three freeze-pump-thaw cycles. Cyclohexane and isoprene were distilled under nitrogen and degassed by vigorously sparging with nitrogen for 30 minutes or three freeze-pump-thaw cycles, respectively. *Sec*-butyllithium (Sigma Aldrich, 1.4 M in cyclohexane) and isopropanol (anhydrous, 99.5%) were used as received.

General Analytical Information

All polymer samples were analyzed using a Tosoh EcoSEC HLC 8320GPC system with two SuperHM-M columns in series at a flow rate of 0.350 mL/min. THF was used as the eluent and all number-average molecular weights (M_n), weight-average molecular weights (M_w), dispersities ($Đ$), asymmetry factors (A_s), M_z and M_{z+1} were calculated from refractive index chromatograms against TSKgel polystyrene standards. Conversions were determined on a Varian 400 MHz NMR spectrometer in $CDCl_3$. Tensile properties of compression molded block copolymer samples were analyzed by dynamic mechanical analysis using a TA Instruments DMA Q800 Dynamic Mechanical Thermal Analysis (DMTA) instrument.

General Procedure for Styrene Polymerizations

A 20 mL scintillation vial equipped with a magnetic stirrer was flame dried, brought into the glove box, and charged with 6.9 mL of cyclohexane and 0.8 mL of styrene (6.98 mmol). A *sec*-butyllithium stock solution in cyclohexane (0.16 M) was prepared for the reactions and a total volume of 360 μL of the solution was drawn into a 1mL syringe and then mounted onto a New Era NE-4000 Double Syringe Pump. The pump was programmed according to the appropriate rate profile, which would dispense a total volume of 320 μL (0.0512 mmol of *s*BuLi) of the initiator solution. Once the needle was submerged into the reaction mixture, the addition program was started. The reaction turned slowly bright orange over the course of the addition due to the formation of the polystyryl anion. The reaction was allowed to reach full conversion and was quenched with excess isopropanol until the solution was clear and colorless. The polymer was isolated by removing the solvent under vacuum overnight to afford a white solid.

For the 80 min, 100 min, and 120 min additions of exponentially increasing rates a 0.0533 M initiator solution was prepared. The total initiator solution volume and cyclohexane volume were adjusted to 960 μL (0.0512 mmol) and 6.1 mL, respectively.

Procedure for Figure 7.2a–c: Constant Addition Rate Profiles

The synthesis was performed according to the general procedure and the New Era NE-4000 Double Syringe Pump was programmed to the following addition rate profiles for the constant rates shown in Table 7.1.

Table 7.1. Constant Rate Addition Profiles

Addition Time (min)	**Rate (μL/h)**	**Total Volume (μL)**
20	960	320
40	480	320
60	320	320
80	240	320
100	192	320
120	160	320

Procedure for Figure 7.2d–f: Linearly Ramped Addition Rate Profiles

The synthesis was performed according to the general procedure. All linearly increasing addition rate profiles were programmed as a sequence of 20 step increments with each step corresponding to a phase in the New Era NE-4000 Double Syringe Pump program. See Table 7.2 for detailed rates and volumes.

Table 7.2. Linearly Ramped Rate Addition Profile

Step #	Rate (µL/h)							Volume per Step (µL)
	20min	30min	40min	50min	60min	80min	100min	
1	167	111	83	67	56	42	33	2.8
2	250	167	125	100	83	62	50	4.2
3	334	223	167	134	111	83	67	5.6
4	417	278	209	167	139	104	84	7.0
5	501	334	250	200	167	125	100	8.3
6	584	390	292	234	195	146	117	9.7
7	668	445	334	267	223	167	134	11.1
8	751	501	376	301	250	188	150	12.5
9	835	557	417	334	278	209	167	13.9
10	918	612	459	367	306	230	184	15.3
11	1002	668	501	401	334	250	200	16.7
12	1085	724	543	434	362	271	217	18.1
13	1169	779	584	468	390	292	234	19.5
14	1252	835	626	501	417	313	250	20.9
15	1336	890	668	534	445	334	267	22.3
16	1419	946	710	568	473	355	284	23.7
17	1503	1002	751	601	501	376	301	25.0
18	1586	1057	793	634	529	397	317	26.4
19	1670	1113	835	668	557	417	334	27.8
20	1753	1169	877	701	584	438	351	29.2

Procedure for Figure 7.2g–i: Exponentially Ramped Addition Rate Profiles

The synthesis was performed according to the general procedure. All exponentially increasing addition profiles were programmed as a sequence of 20 step increments with each step corresponding to a phase in the New Era NE-4000 Double Syringe Pump program. See Table 7.3 for detailed rates and

volumes. For 80, 100, and 120 min long exponentially ramped additions, the total addition volume had to adjusted to 960 µL due to a more dilute initiator solution (0.0533 M) (Table 7.4).

Table 7.3. Exponentially Ramped Rate Addition Profile for 20–60 min

Step #	**Rate (µL/h)**			**Volume per Step (µL)**
	20min	40min	60min	
1	9.2	4.6	3.1	0.2
2	12.9	6.4	4.3	0.2
3	18.0	9.0	6.0	0.3
4	25.2	12.6	8.4	0.4
5	35.3	17.7	11.8	0.6
6	49.4	24.7	16.5	0.8
7	69.2	34.6	23.1	1.2
8	96.9	48.5	32.3	1.6
9	135.6	67.8	45.2	2.3
10	189.9	95.0	63.3	3.2
11	265.9	132.9	88.6	4.4
12	372.2	186.1	124.1	6.2
13	521.1	260.6	173.7	8.7
14	729.5	364.8	243.2	12.2
15	1021	510.7	340.4	17.0
16	1430	715.0	476.6	23.8
17	2002	1001	667.3	33.4
18	2803	1401	934.2	46.7
19	3924	1962	1308	65.4
20	5493	2747	1831	91.6

Table 7.4. Exponentially Ramped Rate Addition Profile for 80–120 min

Step #	Rate (µL/h)			Volume per Step (µL)
	80min	100min	120min	
1	6.9	5.5	4.6	0.5
2	9.7	7.7	6.4	0.6
3	13.5	10.8	9.0	0.9
4	18.9	15.1	12.6	1.3
5	26.5	21.1	17.7	1.8
6	37.1	29.7	24.7	2.5
7	51.9	41.5	34.6	3.5
8	72.7	58.1	48.4	4.8
9	101.7	81.4	67.8	6.8
10	142.4	113.9	95.0	9.5
11	199.4	159.5	132.9	13.3
12	279.1	223.3	186.1	18.6
13	390.8	312.6	260.6	26.1
14	547.1	437.7	364.8	36.5
15	765.9	612.7	510.7	51.1
16	1072	857.8	715.0	71.5
17	1501	1201	1001	100.1
18	2102	1681	1401	140.1
19	2942	2354	1962	196.2
20	4119	3295	2747	274.6

Procedure for Figure 7.4: Bell-Shaped Addition Rate Profiles

The synthesis was performed according to the general procedure. All bell-shaped addition profiles were programmed as a sequence of 20 step increments with each step corresponding to a phase in the New Era NE-4000 Double Syringe Pump program. See Table 7.5 for detailed rates and volumes.

Table 7.5. Bell-Shaped Rate Addition Profile

Step #	Rate (μL/h)					Volume per Step (μL)
	20min	40min	60min	80min	100min	
1	25.6	17.0	12.8	10.2	8.5	0.9
2	76.7	51.1	38.3	30.7	25.6	2.6
3	153.4	102.2	76.7	61.3	51.1	5.1
4	255.6	170.4	127.8	102.2	85.2	8.5
5	383.4	255.6	127.8	153.4	127.8	12.8
6	536.8	357.8	191.7	214.7	178.9	17.9
7	766.8	511.2	268.4	306.7	255.6	25.6
8	945.7	630.5	383.4	378.3	315.2	31.5
9	1074	715.7	472.9	429.4	357.8	35.8
10	1150	766.8	536.8	460.1	383.4	38.3
11	1074	715.7	575.1	429.4	357.8	35.8
12	945.7	630.5	536.8	378.3	315.2	31.5
13	766.8	511.2	472.9	306.7	255.6	25.6
14	536.8	357.8	383.4	214.7	178.9	17.9
15	383.4	255.6	268.4	153.4	127.8	12.8
16	255.6	170.4	191.7	102.2	85.2	8.5
17	153.4	102.2	76.7	61.3	51.1	5.1
18	76.7	51.1	38.3	30.7	25.6	2.6
19	25.6	17.0	12.8	10.2	8.5	0.9
20	12.8	8.5	6.4	5.1	4.3	0.4

Description of MWD shape by asymmetry factor (A_s), skewness (α_3) and kurtosis (α_4)

The asymmetry factors (A_s) of our MWDs were calculated using the ECOSEC Analysis program. A_s is defined as the ratio of the distance from the

peak maximum to the right edge of the peak and the distance from the peak maximum to the left edge of the peak at 10 % peak height. A graphical description is provided in Figure 7.7.

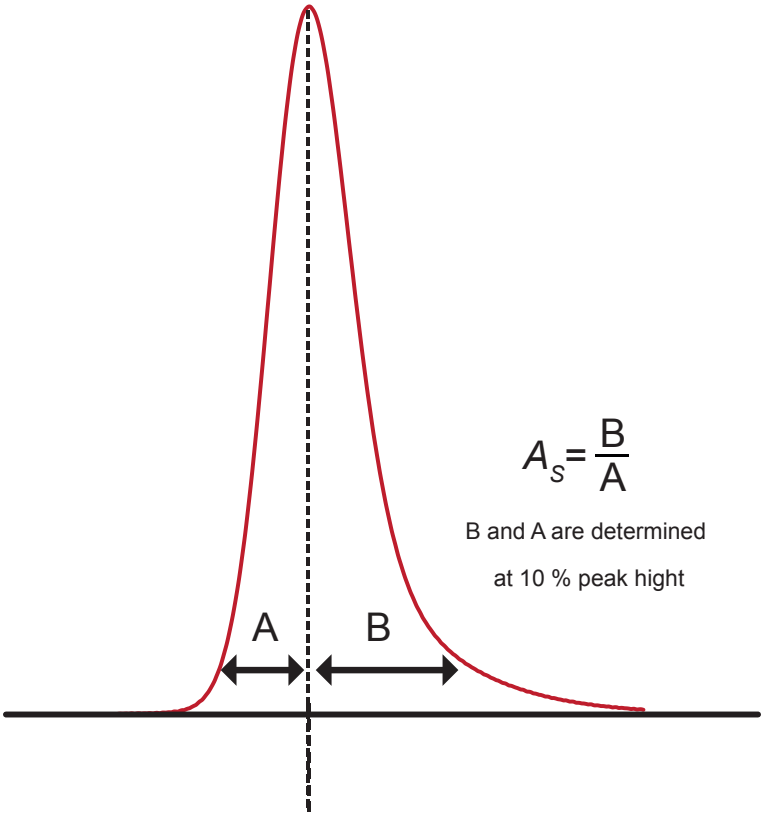

Figure 7.7. Graphical Illustration of the Calculation of Asymmetry Factor A_s.

The third and fourth moments about the mean, skewness (α_3) and kurtosis (α_4), respectively, were calculated according to the method described by Rudin.[1] The equations are shown below:

$$\alpha_3 = \frac{M_z M_w M_n - 3M_n^2 M_w + 2M_n^2}{(M_w M_n - M_n^2)^{3/2}} \quad (7.1)$$

$$\alpha_4 = \frac{M_{z+1}M_z M_w M_n - 4M_n^2 M_z M_w + 6M_n^3 M_w - 3M_n^4}{(M_w M_n - M_n^2)^2} \quad (7.2)$$

General Procedure for Poly(styrene-*b*-isoprene) (PS-*b*-PI) Polymerizations and Sample Preparation for Dynamic Mechanical Analysis

Polystyryllithium was prepared according to the general procedure. After approximately 5 hours, 1 mL (9.99 mmol) of isoprene was added to the stirring reaction mixture. The solution turned colorless. The reaction was allowed to stir for 6 hours to allow for full conversion according to ^{1}H NMR. See Table 7.6 from details on block polymer compositions.

Preparation of PS-*b*-PI samples for Dynamic Mechanical Analysis

0.2 wt% BHT as a stabilizer was added as a solution in DCM followed by concentrating on a rotary evaporator and vacuum overnight. After densifying at 120 °C and 2000 lbs. for 5 min using a Carver Press, samples were compression molded into dog bones (16 mm, 2.5 mm, 0.6 mm) at the same temperature and pressure for 5 minutes.

Table 7.6. PS-*b*-PI samples for dynamic mechanical analysis; f_{PI} indicates the weight fraction of polyisoprene

Entry	PS M_n	PS $Đ$	PS A_s	PSPI M_n	PS-PI $Đ$	f_{PI}
1a	14.1	1.19	1.85	35.6	1.14	0.60
1b	14.2	1.22	0.52	35.1	1.16	0.60
2a	14.9	1.42	3.52	36.8	1.21	0.60
2b	14.1	1.39	0.37	33.6	1.22	0.58
3a	15.2	1.69	4.48	36.3	1.25	0.58
3b	14.1	1.71	0.31	36.5	1.28	0.61
4a	14.4	2.01	4.97	37.2	1.28	0.61
4b	13.8	1.97	0.26	34.4	1.29	0.60
5a	15.1	1.55	4.14	37.7	1.21	0.60
5b	14.9	1.51	0.33	35.5	1.23	0.60
6a	14.2	1.87	4.71	34.8	1.30	0.59
6b	15.5	1.78	0.29	36.3	1.32	0.57
7a	14.5	1.68	0.32	35.9	1.27	0.60

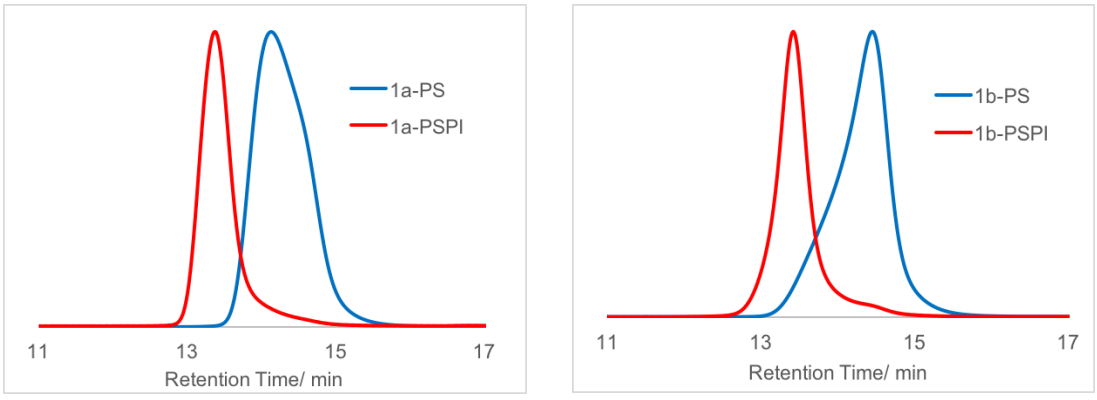

Figure 7.8. Size-exclusion chromatograms of polydisperse PS block and the corresponding PS-*b*-PI block copolymers corresponding to entries 1a,b in Figure 7.6.

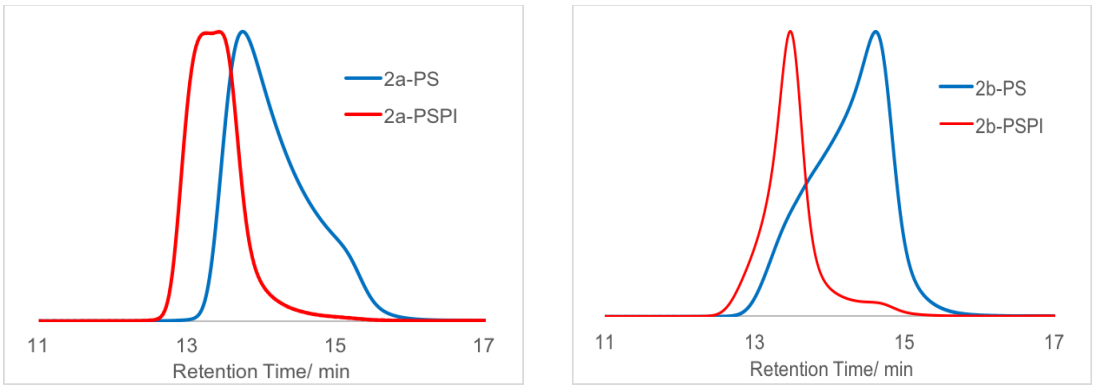

Figure 7.9. Size-exclusion chromatograms of polydisperse PS block and the corresponding PS-*b*-PI block copolymers corresponding to entries 2a,b in Figure 7.6.

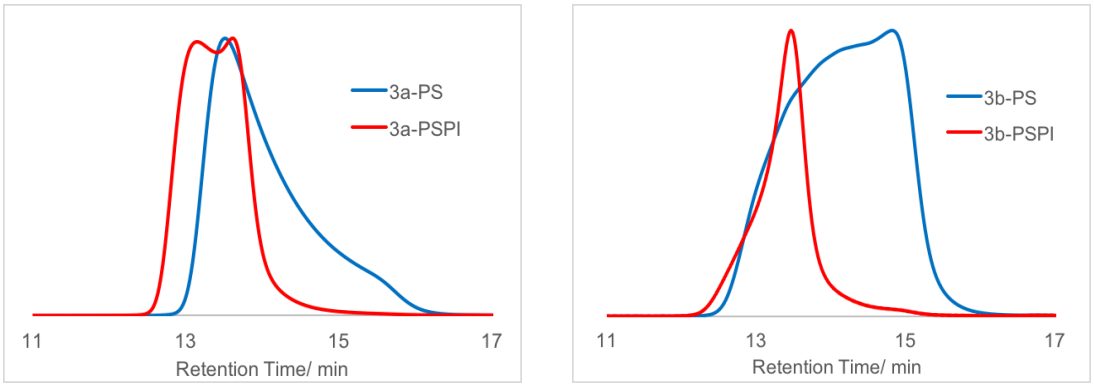

Figure 7.10. Size-exclusion chromatograms of polydisperse PS block and the corresponding PS-*b*-PI block copolymers corresponding to entries 3a,b in Figure 7.6.

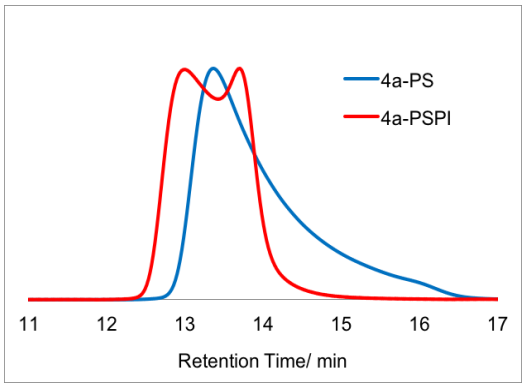

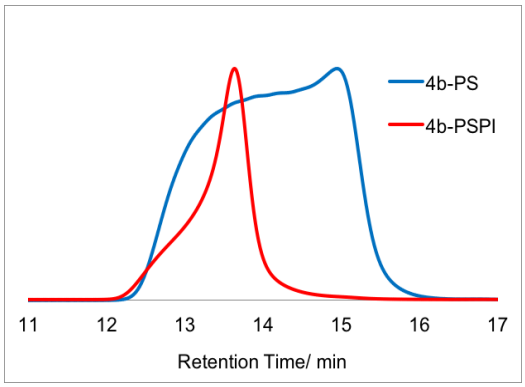

Figure 7.11. Size-exclusion chromatograms of polydisperse PS block and the corresponding PS-*b*-PI block copolymers corresponding to entries 4a,b in Figure 7.6.

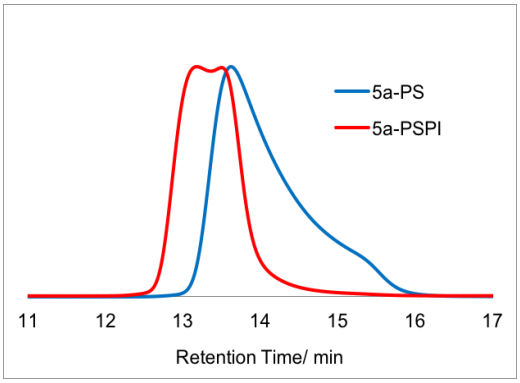

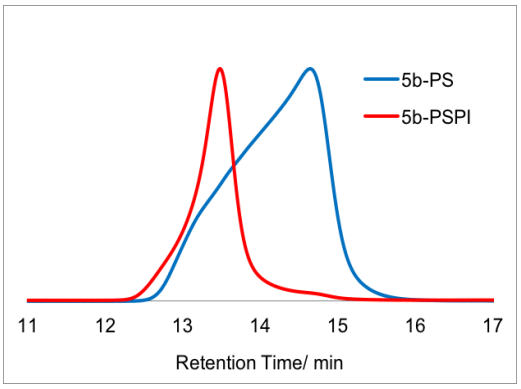

Figure 7.12. Size-exclusion chromatograms of polydisperse PS block and the corresponding PS-*b*-PI block copolymers corresponding to entries 5a,b in Figure 7.6.

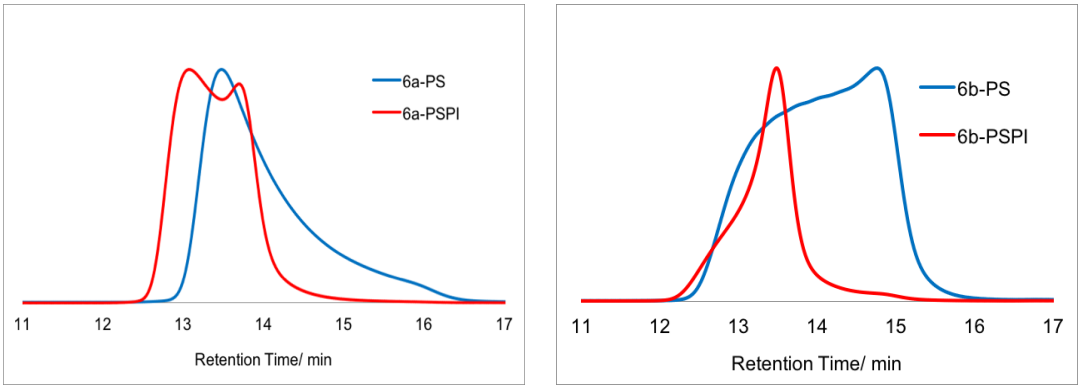

Figure 7.13. Size-exclusion chromatograms of polydisperse PS block and the corresponding PS-*b*-PI block copolymers corresponding to entries 6a,b in Figure 7.6.

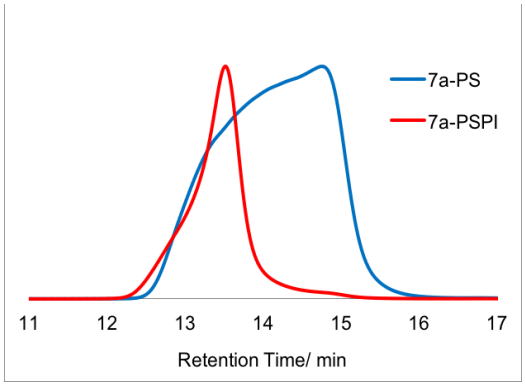

Figure 7.14. Size-exclusion chromatograms of polydisperse PS block and the corresponding PS-*b*-PI block copolymers corresponding to entry 7a in Figure 7.6.

Measurement of Young's Moduli of PS-b-PI samples

Stress/strain curves were obtained in tension with force control of 1.0 N/min and Young's moduli were obtained by evaluating the slope of the stress/strain curve at low strain values.

Appendix References

(1) Rudin, A. *J. Chem. Ed*. **1969**, *46*, 595.